

**FORMULATION, DEVELOPMENT AND ASSESSMENT OF
TENOFIVIR DISOPROXIL FUMARATE-LOADED PELLETS**

By

TAWANDA DUBE

*A thesis submitted to Rhodes University in
Fulfillment of the Requirements for a Degree of*

MASTER OF SCIENCE (PHARMACY)

APRIL 2014

Faculty of Pharmacy
RHODES UNIVERSITY
Grahamstown
South Africa

ABSTRACT

Tenofovir disoproxil fumarate (TDF) is a novel nucleotide analog reverse transcriptase inhibitor that is recommended by the WHO for use in first line treatment of HIV infections. Due to the high dose of TDF for anti-retroviral treatment the formulation of a pellet dosage form may improve patient adherence by incorporation of a large dose in a relatively small dosage form. TDF is currently only available in tablet form.

A simple, sensitive, selective, rapid, accurate, precise, stability indicating reversed-phase HPLC method was developed and validated in accordance with ICH guidelines and was successfully used for the analysis of TDF raw material and pharmaceutical dosage forms.

Preformulation studies included an investigation of TDF-excipient and excipient-excipient interactions with all materials that could potentially be used to produce extruded and spheronized pellets. Nuclear Magnetic Resonance spectroscopy (NMR), Infrared Spectroscopy (IR), Differential Scanning Colorimetry (DSC) and Thermogravimetric analysis were used for identification and purity testing of TDF and all excipients. DSC data revealed that no potential interactions between TDF and the excipients occurred suggesting that incompatibility reactions were unlikely during manufacture and storage. These findings were confirmed by IR analysis that revealed that no physical interaction was likely between any of the excipients used and TDF. DSC data also reveal the existence of the α and β -polymorphs of TDF as evidenced by two enthalpy changes observed on the resultant thermograms. The existence of two polymorphs is unlikely to result in incompatibility and was confirmed by IR analysis. The IR spectra reveal that all characteristic peaks for TDF were present in 1:1 binary mixtures. Therefore TDF is compatible with all excipients tested and thermal analysis confirmed the stability of TDF under manufacturing conditions. The temperature of degradation temperature established through DSC analysis confirmed that degradation during manufacture is unlikely as the temperature of manufacture is lower than that at which degradation occurs.

Extrusion and spheronization were the processes used to manufacture TDF pellets as it is a simple and economic approach for production. The effects of extruder and spheronizer speed, amount of spheronization aid and diluents on the pellet size, shape, flow properties and TDF release characteristics were examined. In order to decrease the complexity of analysis and reduce

the cost of development a Taguchi orthogonal array design of experiments was successfully applied to evaluate the impact of formulation variables on product characteristics and predict an optimized formulation with a minimum number of experiments.

The use of Response Surface Methodology for the development and optimization of pharmaceutical systems, including the optimization of formulation composition, manufacturing processes and/or analytical methods is well established. However the application of RSM requires that accurate, precise and reproducible experimental conditions are used for the generation of reliable data and RSM use is limited due to sensitivity to experimental variability.

The benefits of using RSM for formulation optimization include the fact that more than one variable can be investigated at a time and large amounts of information can be generated at the same time ensuring a more efficient process with respect to time and cost. An added advantage of this approach is that mathematical relationships can be generated for the models that are produced and provide formulation scientists with an indication of whether the effect(s) between factors are synergistic or antagonistic. There are several statistical design approaches that use RSM and a Taguchi orthogonal array design was selected for use in this optimization process as fewer experiments are required to generate data for the same number of factors to be investigated when compared to other statistical designs such as Central Composite (CCD) and Box-Behnken designs.

The use of RSM clearly demonstrates the impact of different input variables on the % TDF released at 45 min and % TDF loaded into the particles. The amount of sorbitol and Kollidon[®] CL-M were the only significant variables that affected the % TDF released at 45 min and both excipients had an overall synergistic effect on the *in vitro* release of TDF. The prediction and manufacture of an optimized formulation led to the production of pellets that met predetermined specifications which was successfully achieved using RSM.

The development of a TDF containing pellet dosage form has been achieved and the formulation, manufacture and characterization of the dosage form reveal that the product has the potential to be further developed.

ACKNOWLEDGEMENTS

I would like to express my sincere gratitude to the following people:

My supervisor, Professor R. B. Walker, for his continued patience and assistance throughout the course of this research, I am truly grateful,

Dr S.M.M Khamanga, who took time off his busy schedule to assist with core aspects of this research,

The Head and Dean of Faculty of Pharmacy, Rhodes University, Professor R. B. Walker, for the opportunity to conduct this research as well as the provision of lab space, equipment and facilities during the course of this research,

Dr K. WaKasongo, who helped tremendously with structuring this research,

Mr T. Samkange, Mr L. Purdon, Mr C. Nontyi, Mr D. Morley and Ms. S. Morley for their technical assistance during my studies,

My colleagues and friends in the Faculty of Pharmacy for their academic assistance, and moral support for the duration of my project: Ms. Ayesha Fauzee, Ms. Ashmita Ramanah, Ms. Samantha Mukozhiwa, Mr. Pedzisai Makoni, Mr. Chiluba Mwila, Mr. Tendai Chanakira, Ms. Chiedza Zindove, Mr. F Mhaka,

My parents Mrs R. Dube and the late Mr M. Dube for making me what I am and for the sacrifices made, I cannot thank you enough, Doreen, Maynard and Givemore, siblings that made me,

My extended family Mr and Mrs L.K.C Dube for being like a father and mother to me, for all the support given, Tanaka, Mwazvita, Danai, Nyasha, Tariro, Violet, Mike, Tatenda M, my team.

Special Thanks to Ms S.V Kutukwa for being a pillar I could lean on when times got tough during this research.

Most of all to the Lord God Almighty, for whom without this would all have been just a dream, I am truly grateful.

STUDY OBJECTIVES

Tenofovir disoproxil fumarate (TDF) is a pro-drug and is a novel nucleotide analog that exhibits activity against HIV type-1 (HIV-1) and the hepatitis B virus. Tenofovir diphosphate (PMPApp), the active moiety is a potent inhibitor of retroviral reverse transcriptase and is a DNA chain terminator.

Nucleoside analogs are normally converted to nucleotide analogs *in vivo* and administration of nucleotide analog reverse-transcriptase inhibitors (NtARTI or NtRTI) avoids this conversion step making NtRTI more effective than the precursor. In 2010 the World Health Organisation (WHO) released new recommendations for antiretroviral treatment for adults and adolescents and the new recommendations advise health authorities to phase out the use of stavudine (d4T) based regimens, since they exhibit long-term irreversible side-effects. The recommendation suggests that zidovudine (AZT) or TDF based first-line regimens are better. Consequently research into the safety and efficacy of TDF has increased and its use in first world and resource limited settings has increased substantially. Viread[®] 300 mg tablets are the only TDF formulation that is commercially available and is manufactured by Gilead Sciences. Inc., USA. The high dose requirement results in the manufacture of a large dosage form that is expensive to manufacture. Therefore a cost effective formulation and manufacturing process is needed to reduce the size of the dosage form size and reduce the cost of production.

The objectives of this study were:

- i. To develop and validate a high performance liquid chromatographic method of analysis for TDF as a raw material and in pharmaceutical dosage forms.
- ii. To conduct preformulation studies to select appropriate excipients for the production of TDF pellets and establish whether interactions between TDF and the excipients are evident.
- iii. To develop and optimize a suitable method of manufacture for TDF pellets.
- iv. To use experimental design to establish relationships between independent formulation and manufacturing variables and formulation responses.
- v. To use experimental design to optimize TDF pellets to conform to target specifications.
- vi. To evaluate and ensure the quality of TDF pellets by evaluation of *in vitro* release, pellet size, shape, flow properties and loading efficiency.

TABLE OF CONTENTS

CHAPTER ONE.....	1
TENOFOVIR DISOPROXIL FUMARATE	1
1.1 INTRODUCTION.....	1
1.2 PHYSICOCHEMICAL PROPERTIES OF TDF.....	2
1.2.1 Description	2
1.2.2 Solubility.....	3
1.2.3 pH of solution	3
1.2.4 pK_a	3
1.2.5 Melting range	3
1.2.6 Specific optical rotation.....	4
1.2.7 Stability.....	4
1.2.8 Ultraviolet absorption spectrum.....	4
1.2.9 Infrared absorption spectrum	5
1.2.10 Synthesis of TDF.....	6
1.3 CLINICAL PHARMACOLOGY	7
1.3.1 Mechanism of action.....	7
1.3.2 Indications and clinical use.....	9
1.3.3 Contraindications	9
1.3.4 Side effects and interactions	10
1.3.5 Resistance	11
1.3.6 Cross-resistance	11
1.3.7 Drug Interactions	11
1.3.8 High risk groups	13
1.3.8.1 Geriatric patients	13
1.3.8.2 Patients with renal impairment.....	13
1.3.8.3 Pregnancy	13
1.4 PHARMACOKINETICS	14
1.4.1 Dose and administration.....	14
1.4.1.2 Missed dose and overdosing	15
1.4.2 Absorption.....	15
1.4.3 Distribution.....	15
1.4.4 Metabolism	16
1.4.5 Elimination	16
1.5 CONCLUSIONS	16
CHAPTER TWO.....	18
DEVELOPMENT AND VALIDATION OF AN HPLC METHOD FOR THE ANALYSIS OF TENOFOVIR DISOPROXIL FUMARATE.....	18

2.1	INTRODUCTION.....	18
2.1.1	<i>Historical background.....</i>	18
2.1.2	<i>Principles of HPLC.....</i>	18
2.1.3	<i>Overview.....</i>	20
2.2	ANALYTICAL METHODS FOR THE ANALYSIS OF TDF.....	20
2.3	EXPERIMENTAL.....	22
2.3.1	<i>Materials and reagents.....</i>	22
2.3.2	<i>HPLC system.....</i>	23
2.3.3	<i>Column selection.....</i>	23
2.3.4	<i>Internal standard (IS).....</i>	24
2.3.5	<i>Preparation of Stock Solutions.....</i>	25
2.3.6	<i>Selection of mobile phase and flow rate.....</i>	25
2.3.7	<i>Preparation of mobile phase.....</i>	25
2.4	RESULTS AND DISCUSSION.....	26
2.4.1	<i>Effect of ACN composition on retention time.....</i>	26
2.4.2	<i>Effect of flow rate.....</i>	27
2.4.3	<i>Chromatographic conditions.....</i>	27
2.5	METHOD VALIDATION.....	30
2.5.1	<i>Introduction.....</i>	30
2.5.2	<i>Linearity and range.....</i>	30
2.5.3	<i>Precision.....</i>	32
2.5.3.1	<i>Repeatability.....</i>	32
2.5.3.1.2	<i>Intermediate precision.....</i>	32
2.5.3.3	<i>Reproducibility.....</i>	33
2.5.4	<i>Accuracy.....</i>	33
2.5.5	<i>Limits of quantitation (LOQ) and detection (LOD).....</i>	34
2.5.6	<i>Specificity.....</i>	36
2.5.7	<i>Forced Degradation Studies.....</i>	36
2.5.7.1	<i>Method.....</i>	37
2.5.7.1.1	<i>Sample preparation.....</i>	37
2.5.7.1.1.1	<i>Acid degradation.....</i>	37
2.5.7.1.1.2	<i>Alkali degradation studies.....</i>	38
2.5.7.1.1.3	<i>Oxidative degradation.....</i>	38
2.5.7.1.1.4	<i>Photolytic degradation.....</i>	38
2.5.7.2	<i>Results and Discussion.....</i>	39
2.5.7.2.1	<i>Acid degradation.....</i>	39
2.5.7.2.2	<i>Alkali degradation.....</i>	40
2.5.7.2.3	<i>Oxidative degradation.....</i>	41
2.5.7.2.4	<i>Photolytic degradation.....</i>	42
2.6	CONCLUSIONS.....	43

CHAPTER THREE	44
PREFORMULATION	44
3.1 INTRODUCTION.....	44
3.1.1 <i>Physicochemical properties</i>	45
3.1.1.1 Particle size and shape.....	45
3.1.1.2 Powder density	46
3.1.1.2.2 Tapped density	48
3.1.1.2.3 True density.....	48
3.1.2 <i>Molecular properties of powders</i>	49
3.1.2.1 Polymorphism	49
3.1.3 <i>Drug-excipient compatibility</i>	50
3.2 EXPERIMENTAL METHODS.....	51
3.2.1 <i>SEM</i>	51
3.2.2 <i>Powder density</i>	51
3.2.3 <i>IR spectroscopy</i>	52
3.2.4 <i>Thermogravimetric analysis (TGA) and Differential thermal analysis (DTA)</i>	52
3.2.5 <i>Differential scanning calorimetry (DSC)</i>	52
3.3 RESULTS AND DISCUSSION.....	53
3.3.1 <i>SEM</i>	53
3.3.2 <i>Density</i>	58
3.3.2.1 Bulk and tapped density	58
3.3.3 <i>Polymorphism</i>	60
3.3.3.1 DSC	60
3.3.3.2 IR spectroscopy	67
3.4 CONCLUSIONS	74
CHAPTER FOUR	75
FORMULATION DEVELOPMENT AND MANUFACTURE OF TENOFOVIR DISOPROXIL FUMARATE PELLETS.....	75
4.1 INTRODUCTION.....	75
4.1.1 <i>Overview</i>	75
4.1.2 <i>Manufacture of multi-unit particulate systems (MUPS)</i>	76
4.1.2.1 Pelletization by solution layering.....	76
4.1.2.2 Direct pelletization	76
4.1.2.3 Spray congealing	77
4.1.2.4 Extrusion and spheronization	77
4.1.3 <i>Method of manufacture</i>	82
4.1.4 <i>Excipients</i>	82
4.1.4.1 Binders	82

4.1.4.2	Diluents	83
4.1.4.3	Disintegrants.....	83
4.1.4.4	Surfactants.....	84
4.1.4.5	Spheronization aids	84
4.1.4.6	Separating agents.....	85
4.1.4.7	Solvents	85
4.1.5	<i>Wet granulation</i>	85
4.1.6	<i>Capsules</i>	87
4.2	METHODS.....	88
4.2.1	<i>Materials</i>	88
4.2.2	<i>Manufacturing equipment</i>	88
4.2.3	<i>Method of Manufacture</i>	89
4.2.3.1	Manufacturing Procedure.....	89
4.2.3.2	Capsule filling.....	91
4.2.4	<i>Physical characterization of pellets</i>	93
4.2.4.1	Size Analysis.....	93
4.2.4.2	Sphericity	93
4.2.4.3	TDF release	94
4.2.4.4	Density	96
4.2.4.5	Flow Properties	97
4.2.4.6	Assay.....	97
4.3	RESULTS AND DISCUSSION	98
4.3.1	<i>Physical properties of the pellets</i>	98
4.3.2	<i>Physico-mechanical properties of the pellets</i>	99
4.3.3	<i>In vitro release of TDF</i>	100
4.4	CONCLUSIONS.....	102
CHAPTER FIVE.....	104
OPTIMIZATION OF A TDF PELLETT FORMULATION USING RESPONSE SURFACE METHODOLOGY.	104
5.1	INTRODUCTION.....	104
5.2	EXPERIMENTAL DESIGN.....	107
5.2.1	<i>Quantitative factors and the factor space</i>	107
5.2.2	<i>Mathematical models</i>	108
5.2.3	<i>Optimization and validation</i>	109
5.2.4	<i>Response Surface Design</i>	110
5.2.4.1	Taguchi orthogonal array	110
5.3	EXPERIMENTAL	112
5.3.1	<i>Proposed design</i>	112
5.3.2	<i>Statistical analysis</i>	114

5.4 RESULTS AND DISCUSSION.....	114
5.4.1 <i>Formulation Development.....</i>	114
5.4.2 <i>Model fitting and statistical analysis.....</i>	115
5.5 RESPONSE SURFACE MODELING	116
5.5.1 <i>% TDF released at 45 min.....</i>	116
5.5.2 <i>% TDF loaded</i>	125
5.5.3 <i>Formulation optimization.....</i>	126
5.6 CONCLUSIONS.....	130
CHAPTER SIX	132
CONCLUSIONS	132
APPENDIX 1	138
BATCH RECORD SUMMARIES	138
APPENDIX 2	166
RESPONSE SURFACE METHODOLOGY STATISTICS.....	166
REFERENCES.....	176

LIST OF FIGURES

Figure 1.1 Molecular structure of TDF, $C_{19}H_{30}N_5O_{10}P \cdot C_4H_4O_4$ (MW = 635.52).....	13
Figure 1.2 UV absorption spectrum of 30 μ g/ml TDF in ACN:water(40:60).....	15
Figure 1.3 IR absorption spectrum of TDF.....	16
Figure 1.4 Reaction scheme for the synthesis of TDF.....	17
Figure 1.5 Intermediate metabolites involved in pro-drug metabolism to active PMPApp.....	18
Figure 2.1 Effect of organic solvent composition on R_t of TDF and NVP.....	36
Figure 2.2 Effect of flow rate on R_t of TDF and NVP.....	37
Figure 2.3 Typical chromatogram of the separation of TDF (180 μ g/ml) and NVP (44 μ g/ml) using the conditions described in Table 2.2.....	39
Figure 2.4 Typical calibration curve for TDF over the concentration range 1 – 180 μ g/ml (n=5).....	42
Figure 2.5 Chromatogram of a standard solution of TDF 30 μ g/ml (I) and a sample following exposure to acid for 24 h (II).....	50
Figure 2.6 Chromatogram of a standard solution of TDF 30 μ g/ml (I) and following exposure to alkali conditions for 24 h (II).....	51
Figure 2.7 Chromatogram of a standard solution of TDF 30 μ g/ml (I) and following exposure to oxidative conditions for 8 hr (II).....	52
Figure 2.8 Chromatogram of a standard solution of TDF 30 μ g/ml (I) and following exposure to photolytic conditions for 24 h (II).....	53
Figure 3.1 Typical SEM showing particle morphology of TDF (A), CCS (B), Kollidon [®] 30 (C), sorbitol (D), MCC (E) and Kollidon [®] CL-M (F).....	66
Figure 3.2 Typical SEM showing particle size range of TDF (A), CCS (B), Kollidon [®] 30 (C), sorbitol (D), MCC (E), Kollidon [®] CL-M (F).....	68
Figure 3.4 Typical DSC thermogram for TDF generated at a heating rate of 10 [°] C/min.....	72
Figure 3.5 Typical DSC thermogram for sorbitol generated at a heating rate of 10 [°] C/min.....	73
Figure 3.6 Typical DSC thermogram for Kollidon [®] CL-M generated at a heating rate of 10 [°] C/min.....	74
Figure 3.7 Typical DSC thermogram for Kollidon [®] 30 generated at a heating rate of 10 [°] C/min.....	74
Figure 3.8 Typical DSC thermogram for croscarmellose sodium generated at heating rate of 10 [°] C/min.....	75
Figure 3.9 Typical DSC thermogram for a 1:1 binary mixture of TDF and croscarmellose sodium generated at a heating rate of 10 [°] C/min.....	76
Figure 3.10 Typical DSC thermogram for a 1:1 binary mixture of TDF and Kollidon [®] CL-M generated at a heating rate of 10 [°] C/min.....	76
Figure 3.11 Typical DSC thermogram for a 1:1 binary mixture of TDF and Kollidon [®] 30 generated at a heating rate of 10 [°] C/min.....	77
Figure 3.12 Typical DSC thermogram for a 1:1 binary mixture of TDF and sorbitol generated at a heating rate of 10 [°] C/min.....	78
Figure 3.13 Typical IR spectrum of TDF.....	79
Figure 3.14 Typical IR spectrum of CCS (I) and a 1:1 binary mixture of TDF and CCS (II).	80
Figure 3.15 Typical IR spectrum of Kollidon [®] 30 (I) and a 1:1 binary mixture of TDF and Kollidon [®] (II).	81
Figure 3.16 Typical IR spectrum of Kollidon [®] CL-M (I) and a 1:1 binary mixture of TDF and Kollidon [®] CL-M (II).	82

Figure 3.17 Typical IR spectrum of sorbitol (I) and 1:1 binary mixture of TDF and sorbitol (II).	83
Figure 3.18 Typical IR spectrum of MCC (I) and a 1:1 binary mixture of TDF and MCC (II).	84
Figure 4.1 Schematic depicting the different stages of direct pelletization.....	87
Figure 4.2 Extruders used for pellet manufacture.....	89
Figure 4.3 SEM images showing examples of a smooth extrudate (A) and an extrudate exhibiting shark skinning (B).....	90
Figure 4.4 Two examples of spheronizer disk patterns viz., cross-hatched (A) and radial (B)	90
Figure 4.5 Characteristic rope-like formation observed during spheronization of extrudate	91
Figure 4.6 Graphic representation of the two models proposed to describe spheronization	92
Figure 4.7 Schematic representation of granule formation	98
Figure 4.8 Method of manufacture of TDF pellets.....	101
Figure 4.9 Schematic representation of capsule filling.....	103
Figure 4.10 SEM image of the surface of a pellet from batch TDF-001 collected after 45 min of dissolution testing	112
Figure 5.1 Process flow in DOE	117
Figure 5.2 Quantitative factors and factor space for extruder speed and time.....	118
Figure 5.3 Half-normal plot depicting input variable effects on response R6	128
Figure 5.4 Normal plot of residuals for % TDF released at 45 min	130
Figure 5.5 Box-Cox Plot for Power Transformation for % TDF released at 45 min	131
Figure 5.6 Plot of externally studentized residuals vs. predicted responses for % TDF released at 45 min	132
Figure 5.7 One Factor Effects Plot for % TDF released at 45 minutes vs. % w/w sorbitol	133
Figure 5.8 One Factor Effects Plot for % TDF released at 45 minutes vs. %w/w Kollidon [®] CL-M.....	133
Figure 5.9 3-D plot of the effect of % w/w Kollidon [®] CL-M on % TDF released at 45 min.....	134
Figure 5.10 3-D plot of the effect of % w/w sorbitol on % TDF released at 45 min.....	135
Figure 5.11 One Factor Effects Plot for % TDF loaded vs. % w/w sorbitol	137
Figure 5.12 Ramp plots used for numerical optimization of input variables and target responses.....	139
Figure 5.13 Dissolution profile of TDF from the optimized formulation and innovator tablets.....	140
Figure 5.14 SEM image showing pellet shape (I) and pellet surface morphology (II)	141

LIST OF TABLES

<i>Table 1.1 Solubility of TDF</i>	15
<i>Table 1.2 Side effects and associated symptoms of TDF</i>	21
<i>Table 1.3 Pharmacokinetic effects of co-administered drugs on the pharmacokinetics of TDF</i>	23
<i>Table 1.4 Dosage adjustments for TDF in patients with altered creatinine clearance</i>	25
<i>Table 2.1 Summary of analytical methods developed for the analysis of TDF in different matrices</i>	32
<i>Table 2.2 Chromatographic conditions for analysis of TDF</i>	39
<i>Table 2.3 Peak height ratio of TDF and NVP as a function of concentration</i>	42
<i>Table 2.4 Repeatability and Intermediate precision data for HPLC analysis of TDF</i>	44
<i>Table 2.5 Accuracy of TDF analysis</i>	46
<i>Table 2.6 LOQ data for the analysis of TDF</i>	47
<i>Table 3.1 Carr's index</i>	59
<i>Table 3.2 Bulk and tapped density of materials</i>	70
<i>Table 3.3 Carr's index and Hausner ratio for raw materials</i>	70
<i>Table 4.1 Formulae used for the manufacture of TDF pellets</i>	103
<i>Table 4.2 Capsule fill weight and assay results</i>	105
<i>Table 4.3 Flow properties of batches TDF 001 - 010</i>	110
<i>Table 4.4 Physico-mechanical properties of batches TDF 001-008</i>	111
<i>Table 4.5 Dissolution data for Batches TDF 001-008</i>	112
<i>Table 4.6 Mass balance analysis of non-disintegrating pellets</i>	114
<i>Table 5.1 L9(3⁴) orthogonal array</i>	122
<i>Table 5.2 Independent variables and levels investigated</i>	124
<i>Table 5.3 Actual values used for experimental design</i>	125
<i>Table 5.4 Response values measured and constraints of response used for experimental design</i>	125
<i>Table 5.5 Responses observed following use of the Taguchi design</i>	127
<i>Table 5.6 ANOVA data at 5% level of significance</i>	128
<i>Table 5.7 ANOVA results for % TDF released at 45 min</i>	129
<i>Table 5.8 ANOVA results for % TDF loaded</i>	137
<i>Table 5.9 Input variables and predicted responses</i>	138
<i>Table 5.10 Experimental and predicted responses for prediction of the optimized formulation</i>	139

LIST OF ACRONYMS

ACN	Acetonitrile
AIDS	Acquired Immune Deficiency Syndrome
ANOVA	Analysis of variance
AOR	Angle of repose
API	Active pharmaceutical ingredient
ARV	Antiretroviral
ATR	Attenuated total reflectance
AUC	Area under curve
AZT	Zidovudine
BB	Box Behnken Design
BCS	Biopharmaceutics classification system
BP	British pharmacopeia
CCD	Central Composite design
CCS	Croscarmellose sodium
CI	Carr's index
CrCL	Creatinine clearance
d4T	Stavudine
dATP	Deoxyadenosine triphosphate
DNA	Deoxyribonucleic acid
DOE	Design of experiments
DSC	Differential Scanning Calorimetry
DTA	Differential thermal analysis
ESRD	End stage renal disease
FDA	Food and drug administration
FDC	Fixed dose combination
FTIR	Fourier transform infrared
GIT	Gastrointestinal tract
HAART	Highly active antiretroviral therapy

HIV	Human Immunodeficiency Virus
HPLC	High Performance Liquid Chromatography
HR	Hausner ratio
ICH	International Conference on Harmonization
IS	Internal standard
IST	Isothermal stress testing
LOD	Limit of detection
LOQ	Limit of quantitation
LSD	Least significant difference
MCC	Microcrystalline cellulose
MeOH	Methanol
MUPS	Multi-unit pellet systems
NP-HPLC	Normal phase-HPLC
NtRTI	Nucleotide reverse transcriptase inhibitor
NVP	Nevirapine
OA	Orthogonal array
ODS	Octadecylsilane
PMPA	Tenofovir
PMPApp	Tenofovir diphosphate
PRESS	Predicted residual error sum of squares
QbD	Quality by design
RNA	Ribonucleic acid
RP-HPLC	Reversed phase-HPLC
RSD	Relative standard deviation
RSM	Response surface methodology
SEM	Scanning electron microscopy
TDF	Tenofovir Disoproxil Fumarate
TGA	Thermogravimetric analysis
USP	United States Pharmacopeia
UV	Ultraviolet
WHO	World Health Organization

XRPD

X-ray powder diffraction

CHAPTER ONE

TENOFOVIR DISOPROXIL FUMARATE

1.1 INTRODUCTION

Acquired immune deficiency syndrome (AIDS) is a disease of the human immune system caused by the human immunodeficiency virus (HIV). Infection with HIV results in a progressive, viral disease that eventually presents as AIDS[1]. HIV is transmitted to humans via sexual oral and anal intercourse, contaminated blood through transfusion, used hypodermic needles, mother to foetus transmission, at childbirth and during breastfeeding. HIV can also be transmitted through contact of mucous membranes or the systemic circulation with fluids such as blood, semen, vaginal fluids, pre-seminal fluids or breast milk that are contaminated with the virus [2, 3].

The lifecycle of HIV in humans commences when it binds to the CD4 receptor and one of two co-receptors on the surface of a CD4+ T-lymphocyte. The virus then fuses with the host cell after which viral RNA is released into the host cell. The HIV reverse transcriptase enzyme converts single-stranded HIV RNA into double-stranded HIV DNA [4]. It is at this stage of the lifecycle that most antiretroviral agents act by inhibiting the reverse transcriptase enzyme thereby preventing the replication of the single strand viral RNA genome into viral DNA.

Tenofovir disoproxil fumarate (TDF) is a pro-drug that is a novel nucleotide analog that exhibits activity against HIV type-1 (HIV-1) and hepatitis B viruses. Tenofovir diphosphate (PMPApp), the active intracellular moiety, is a potent inhibitor of retroviral reverse transcriptase and acts as a DNA chain terminator [5-7].

Nucleoside analogs are normally converted to nucleotide analogs *in vivo* and administration of nucleotide analog reverse-transcriptase inhibitors (NtARTI or NtRTI) directly avoids the conversion step. In 2010 the World Health Organization (WHO) released new recommendations for antiretroviral treatment in adults and adolescents and the new recommendations advise health authorities to phase out the use of stavudine (d4T) based regimens since they exhibit long-term irreversible side effects. The recommendation suggests that zidovudine (AZT) or TDF become the base for first-line HIV regimens [8, 9]. Consequently research into the safety and efficacy of TDF has increased and its use in the first world and resource limited settings has increased

significantly. Viread[®] is the only TDF formulation that is commercially available in South Africa and is a 300 mg tablet manufactured by Gilead Sciences. Inc., USA.

1.2 PHYSICOCHEMICAL PROPERTIES OF TDF

1.2.1 Description

TDF is known as 9-[(R)-2-[[bis[[isopropoxycarbonyl]oxy]methoxy]phosphinyl]methoxy]propyl] adenine fumarate 1:1 and the chemical structure is depicted in Figure 1.1. It has a molecular formula of $C_{19}H_{30}N_5O_{10}P \cdot C_4H_4O_4$ and a molecular weight of 635.52. TDF occurs as a white to off-white crystalline powder with little or no odour.

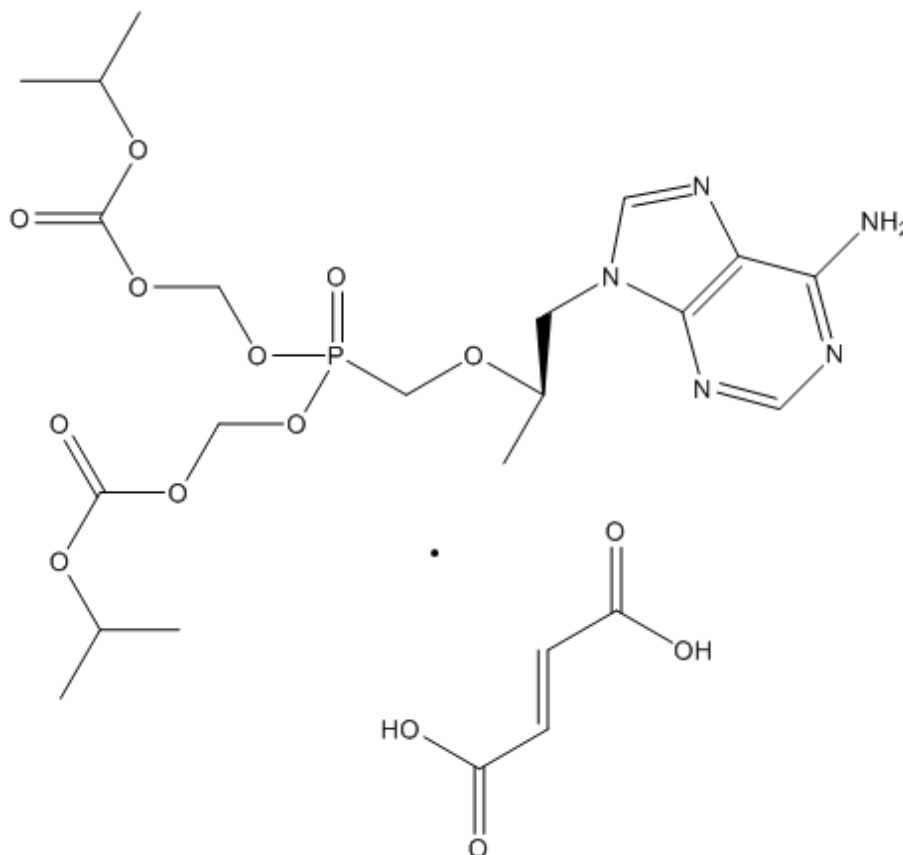


Figure 1.1 Molecular structure of TDF, $C_{19}H_{30}N_5O_{10}P \cdot C_4H_4O_4$ (MW = 635.52)

1.2.2 Solubility

TDF is sparingly soluble in water and is freely soluble in dimethyl-formamide, is soluble in methanol, 0.1 N HCl, ethanol, is sparingly soluble in acetone, isopropanol and is slightly soluble in acetonitrile, ethyl acetate, insoluble in dichloromethane, hexane, diethyl ether, di-n-butyl ether and isopropylether [5-7, 10, 11]. The solubility of TDF in different solvents is summarized in Table 1.1.

Table 1.1 Solubility of TDF

Solvent	Solubility
Water	Sparingly soluble
Methanol	Soluble
Dimethyl-formamide	Freely soluble
Acetone	Sparingly soluble
Methylene chloride	Very slightly soluble

1.2.3 pH of solution

The pH of a 1% w/v solution of TDF is 3.92.

1.2.4 pK_a

The dissociation constant of TDF determined by potentiometric titration at 25°C was 7.91 [6] indicating that TDF is weakly acidic. This characteristic may affect the analysis and formulation approach for a dosage form and stability studies would be necessary to establish whether there is an influence on performance of the analytical procedure.

1.2.5 Melting range

TDF occurs in two polymorphic forms that have been identified by X-ray powder diffraction and DSC. The α polymorph has a melting range of 115-118°C and the β polymorph a melting range of 112-114°C [6, 7].

1.2.6 Specific optical rotation

The specific optical rotation of a 10.0 mg/ml TDF solution in 0.1M HCl is -20° to -26° established with respect to an anhydrous reference standard[6].

1.2.7 Stability

Exposure of TDF to acidic conditions (1.0M HCl) for 5 min resulted in the formation of tenofovir (PMPA) and tenofovir diphosphate (PMPApp) via hydrolysis. Following heating for 15 minutes almost 100% had degraded with a corresponding increase in the concentration of PMPA and a decreased concentration of PMPApp. TDF was found to be susceptible to alkaline hydrolysis when exposed to 0.1M NaOH with complete decomposition of TDF without heating. The primary degradation products of TDF were PMPA and PMPApp. Under neutral hydrolytic conditions TDF degrades to form PMPApp and to a lesser extent PMPA [6]. TDF should be stored at temperatures between 4°C and 8°C .

1.2.8 Ultraviolet absorption spectrum

An ultraviolet scan of a 10 $\mu\text{g/ml}$ solution of TDF is depicted in Figure 1.2 and shows that maximal absorption occurs at a wavelength (λ_{max}) of 259.5 nm. The scan was generated using a Model-GBC 916 UV-VIS Double Beam Spectrophotometer (GBC Scientific Equipment Pty. Ltd, Melbourne, Victoria, Australia) over a scanning range of 230-300 nm.

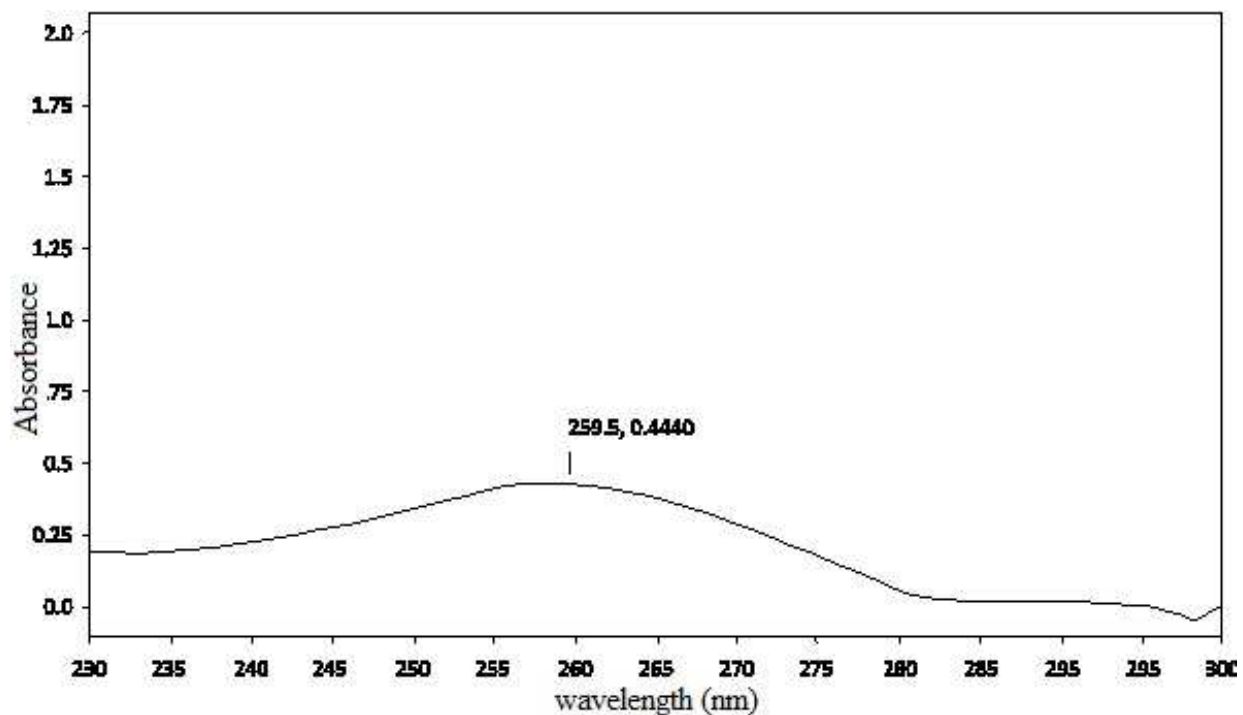


Figure 1.2 UV absorption spectrum of 30µg/ml TDF in ACN:water(40:60)

1.2.9 Infrared absorption spectrum

The infrared (IR) absorption spectrum of TDF powder generated using a Spectrum 100 Fourier Transform Infrared (FTIR) Attenuated Total Reflectance (ATR) spectrophotometer (Perkin Elmer® Ltd Beaconsfield, England) is depicted in Figure 1.3. The main absorbance bands in the spectrum of TDF reveal the presence of an aromatic C-H stretch at 2985 cm^{-1} , two weak intensity broad O-H bands at 3051 cm^{-1} and 3208 cm^{-1} , a P=O stretch at 1674 cm^{-1} , an aromatic C=N stretch in pairs at 1376 cm^{-1} and 1421 cm^{-1} , a medium stretch of NH_2 scissoring band at 1504 cm^{-1} and 1622 cm^{-1} , N-H wagging bands between 670-950 cm^{-1} and C-H out of plane deformation between 950-650 cm^{-1} [12].

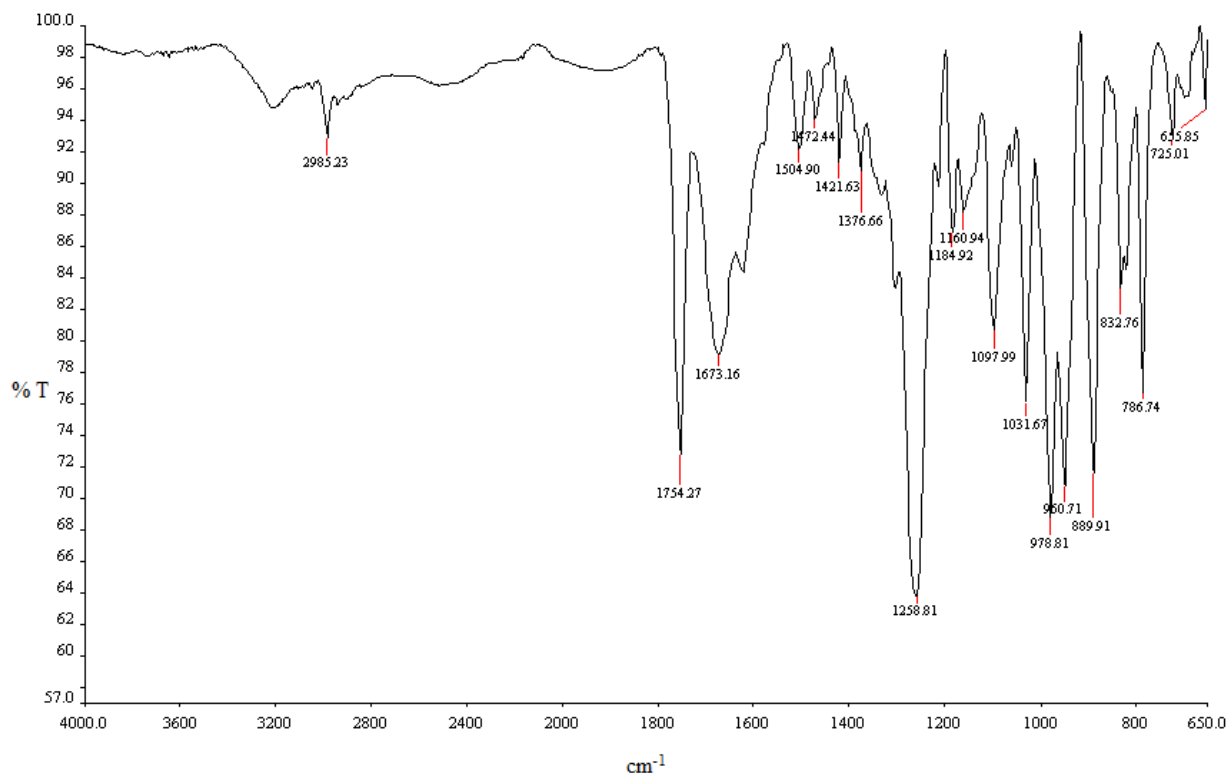


Figure 1.3 IR absorption spectrum of TDF

1.2.10 Synthesis of TDF

TDF is manufactured using a three-stage, four-reaction process that is depicted in Figure 1.4. Initially adenine (3) is reacted with *R*-propylene carbonate (4) that is followed by alkylation of the secondary alcohol with a tosylated hydroxymethylphosphonate diester (6). Hydrolysis of the diethyl phosphonate ester results in the formation of tenofovir (2). The synthesis is completed using an alkylative esterification process to produce crude free base (9) that is subsequently treated with fumaric acid to form crystalline TDF. The yields for this process are fair with an overall yield from adenine of approximately 13%. The third stage of the synthetic process is particularly challenging with isolated yield of TDF of only 35% that is based on the amount of tenofovir produced from the stage 2b reaction [7].

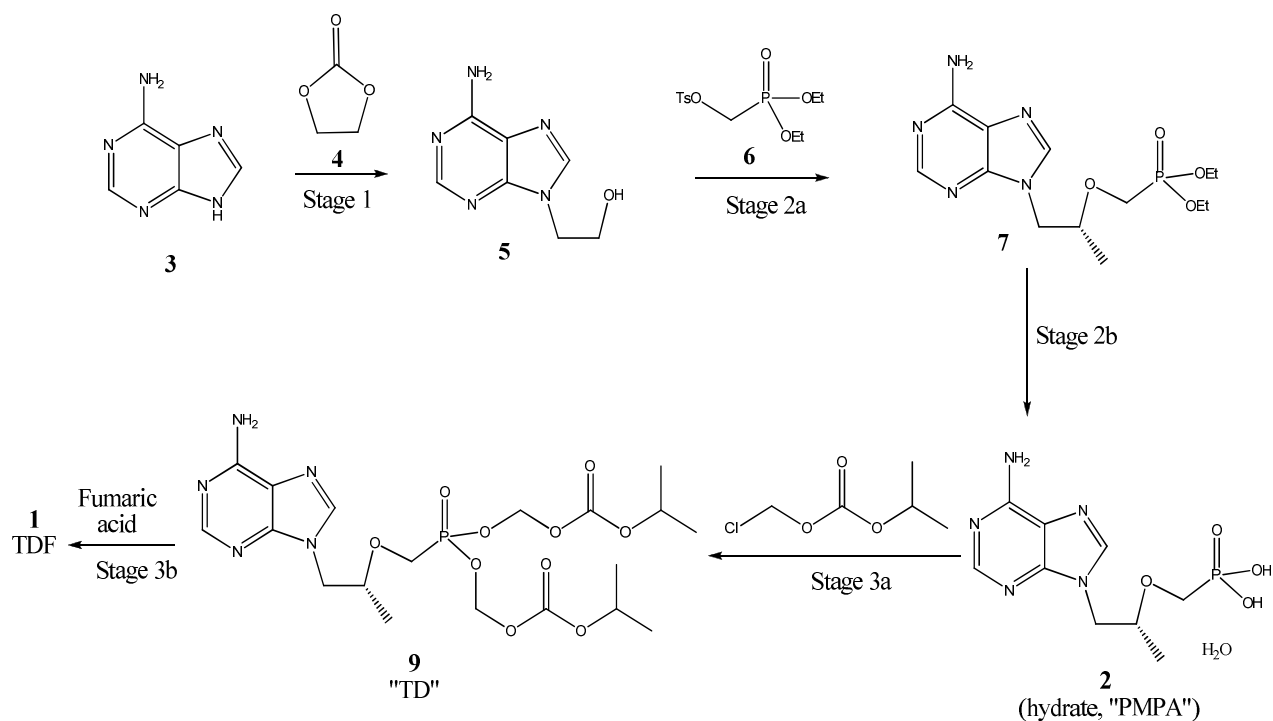


Figure 1.4 Reaction scheme for the synthesis of TDF

1.3 CLINICAL PHARMACOLOGY

1.3.1 Mechanism of action

TDF is an acyclic nucleoside phosphonate diester analogue of adenosine monophosphate. Initially as shown in Figure 1.5 hydrolysis of the TDF diester is necessary for the conversion of TDF to tenofovir (PMPA) (**I**) that is subsequently absorbed by cells in which the molecule undergoes phosphorylation by AMP-kinase and nucleoside diphosphate kinase to produce the active metabolite tenofovir diphosphate (PMPApp) (**II**). PMPApp is a competitive inhibitor and substrate of HIV-1 reverse transcriptase that competes with deoxyadenosine triphosphate (dATP) (**III**) for incorporation into DNA. Since PMPApp lacks a 3'hydroxyl functional group premature chain termination of DNA is achieved thus inhibiting proliferation of HIV [5, 6].

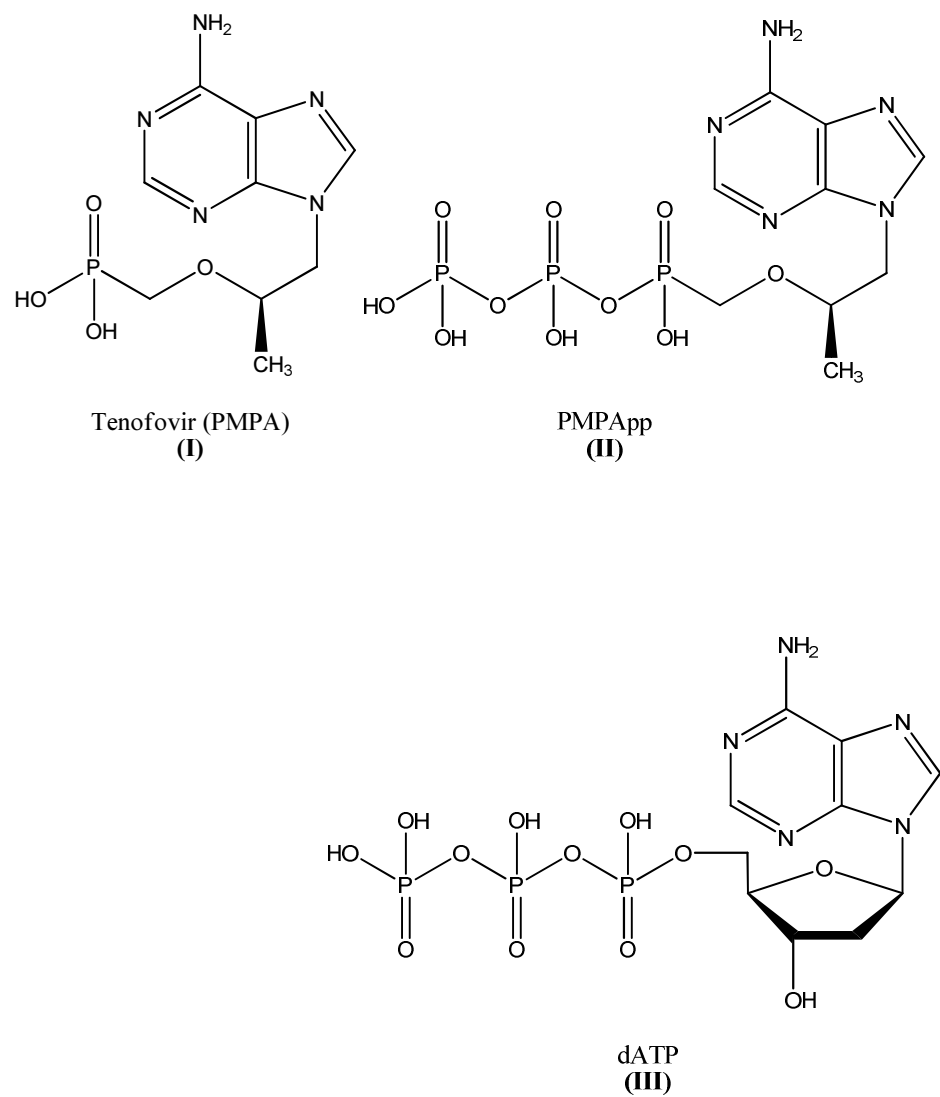


Figure 1.5 Intermediate metabolites involved in pro-drug metabolism to active PMPApp[5].

1.3.2 Indications and clinical use

TDF is indicated for the treatment of HIV-1 infection in combination with other antiretroviral agents in patients that are 12 years of age or older. The safety and efficacy of TDF in pediatric patients younger than 12 years of age has not yet been established. TDF is also indicated for the treatment of chronic hepatitis B infection in patients 18 years of age and older [5, 13, 14].

TDF is commonly prescribed as part of first-line antiretroviral (ARV) treatment in the USA and Europe and has been used increasingly for patients that are naïve to ARV therapy as it exhibits fewer side effects than other commonly used ARV agents. TDF is useful for treating patients that have been on therapy for several years [8, 9].

1.3.3 Contraindications

TDF is principally eliminated via the kidney and renal impairment, including acute renal failure or Fanconi syndrome, renal tubular injury with severe hypophosphatemia have been reported following TDF use in clinical practice. The majority of these cases occurred in patients with underlying systemic or renal disease or those that had been treated with nephrotoxic agents. However renal injury has also been reported in patients that did not present with the identified risk factors [15]. It has been recommended that the creatinine clearance (CrCL) should be calculated for all patients prior to the initiation of therapy and during treatment with TDF [16-19].

Due to the risk of development of resistance, TDF should only be used in HIV and HBV co-infected patients as part of appropriate ARV combination therapy[19, 20]. HIV antibody testing should be offered to all HBV-infected patients prior to initiating therapy with TDF. It has also been recommended that all patients with HIV be tested for the presence of chronic hepatitis B infection prior to commencing TDF therapy [20-22].

1.3.4 Side effects and interactions

The most common side effects associated with TDF use include nausea, vomiting, diarrhoea and asthenia. Less frequent side effects that have been reported include hepatotoxicity, abdominal pain and flatulence. TDF has also been implicated in precipitating renal toxicity, particularly when elevated concentrations of the compound are reached [14, 23-25]. The side effects occur due to accumulation of TDF in the proximal tubules of the kidney. Allergic reactions, including angioedema with symptoms such as skin rash, redness, swelling of the hands, legs, feet, face, lips, tongue and/or throat with difficulty in breathing have been reported [26, 27]. A summary of severe side effects, rank and associated symptoms are listed in Table 1.2.

Table 1.2 Side effects and associated symptoms of TDF

RARE	VERY RARE
<p>Renal toxicity <u>Symptoms</u></p> <p>Polyuria and polydipsia Swelling of legs and feet Feeling listless and tired</p>	<p>Hepatotoxicity <u>Symptoms</u></p> <p>Jaundice Urine pigmentation Stool discolouration Loss of appetite for several days or longer Nausea Lower abdominal pain</p>
<p>Lactic acidosis <u>Symptoms</u></p> <p>Extreme weakness or tiredness Unusual muscle pain Stomach pain with nausea and vomiting Feeling cold especially in arms and legs Dizziness or lightheadedness Irregular heartbeat</p>	<p>Flare-ups of hepatitis B virus infection</p>

1.3.5 Resistance

HIV-1 isolates with reduced susceptibility to TDF have been observed *in vitro*. Reduction in HIV susceptibility to TDF occurs due to expression of the K65R mutation in reverse transcriptase of the virus and has been reported [28]. TDF resistant isolates of HIV-1 have also been recovered from patients treated with TDF in combination with certain ARV agents. There have been reports of a high rate of virological failure and of emergence of resistance at an early stage in HIV patients when TDF was used in combination with lamivudine and abacavir or lamivudine and didanosine as a once daily regimen.

1.3.6 Cross-resistance

Cross-resistance of HIV-1 by certain reverse transcriptase inhibitors has also been reported. The K65R mutation has been observed in some HIV-1 infected patients that had been treated with abacavir and/or didanosine [28, 29]. HIV isolates with this mutation also revealed a reduced susceptibility to emtricitabine and lamivudine. Therefore cross-resistance may occur in patients that are infected with the virus that is host to the K65R mutation [23].

1.3.7 Drug Interactions

TDF concentrations substantially higher (~300-fold) than those observed *in vivo* do not inhibit *in vitro* metabolism mediated by any of the following human cytochrome P450 (CYP450) isoforms *viz.*, CYP3A4, CYP2D6, CYP2C9 or CYP2E1. However a 6% statistically significant reduction in metabolism of CYP1A substrate has been observed [28, 30]. Based on the results of *in vitro* experiments and the elimination pathway of TDF the potential for CYP450 mediated interactions involving TDF with other therapeutic compounds is low [6, 31, 32].

TDF may increase the serum levels of didanosine necessitating a dose reduction for that ARV. The use of didanosine and TDF should be avoided in all patients. TDF serum levels may increase if co-administered with Kaletra[®] that contains lopinavir and ritonavir [33]. Use of this combination requires that the patient be monitored closely for adverse effects and dose adjustment should be made if required. Co-administration of TDF with molecules that are eliminated by active tubular secretion may increase serum concentrations of TDF or co-administered drugs due to competition for the elimination pathway. Drugs that decrease renal

function may also increase serum concentrations of TDF. No clinically significant drug interactions have been observed in healthy volunteers between TDF and abacavir, efavirenz, emtricitabine, entecavir, indinavir, lamivudine, methadone, nelfinavir, oral contraceptives, ribavirin, saquinavir, ritonavir and tacrolimus [6, 34-36].

A summary of the pharmacokinetic effects of co-administered drugs on the pharmacokinetics of TDF are summarized in Table 1.3.

Table 1.3 Pharmacokinetic effects of co-administered drugs on the pharmacokinetics of TDF [28]

Drug	Dose mg	% Change in TDF parameters 90% CI		
		C _{max}	AUC	C _{min}
Abacavir	300 once	↔	↔	↔
adefovir/dipivoxil	10 once	↔	↔	↔
atazanavir	400 once daily x 14 days	↑14	↑24	↑22
didanosine (enteric coated)	400 once	↔	↔	↔
didanosine (buffered)	250 or 400 once daily x 7 days	↔	↔	↔
Efavirenz	600 once daily x 7 days	↔	↔	↔
emtricitabine	200 once daily x 7 days	↔	↔	↔
Indinavir	800 three times daily x 7 days	↑14	↔	↔
lamivudine	150 twice daily x 7 days	↔	↔	↔
lopinavir/ritonavir	400/100 twice daily x 14 days	↔	↑32	↑29

1.3.8 High risk groups

1.3.8.1 Geriatric patients

TDF has not yet been studied in patients over the age of 65. As elderly patients are more likely to present with a decreased renal function, caution should be exercised when treating geriatric individuals with TDF.

1.3.8.2 Patients with renal impairment

Since TDF can cause renal toxicity, close monitoring of renal function is recommended in any patient with pre-existing renal impairment being treated with TDF. The pharmacokinetics of TDF are altered in patients with renal impairment and patients with a creatinine clearance of < 50 ml/min or with end stage renal disease (ESRD) requiring dialysis. The concentration of tenofovir increases substantially over 48 hours achieving a mean C_{max} of 1,032 ng/ml and a mean AUC_{0-48h} of 42,857 ng·h/ml. It is recommended that the dosing interval for TDF be modified to 300mg TDF every 48 hours in patients with a creatinine clearance of <50 ml/min or in patients with ESRD who require dialysis [6, 34, 37].

1.3.8.3 Pregnancy

Currently there is a paucity of well controlled TDF use studies in pregnant women and since animal reproduction studies are not always predictive of human response TDF should not be used during pregnancy. TDF is only recommended for use in pregnancy when the benefits of treatment outweigh the risk of therapy. In a study in which fifteen HIV infected women with limited treatment options were prescribed HAART containing TDF during 16 pregnancies the *in utero* exposure to TDF was 127 days (range 6– 259 days), TDF was well tolerated by all women throughout their pregnancies. There were 15 successful deliveries occurring at a median of 36 weeks (30-40) and the median birth weight was 3255g (1135-3610). Complications including one spontaneous abortion occurred in nine of the pregnancies, however the complications were not attributed to TDF [38, 39]. Eleven or 73% of the women had abnormal laboratory results, including six that experienced grade one haemoglobin abnormalities and four of whom also had pre-existing anemia. The glomerular filtration rate, calculated using the Modification of Diet in Renal Disease equation remained >90 mL/min in all women, except for one who responded with

a transient decline [40, 41]. Fourteen of the infants demonstrated normal growth and development for weight and height at birth in addition to during the 12-month follow-up period with no congenital malformations being documented. Mother-to-child transmission of HIV was not observed in this cohort of patients. TDF was found to be a well-tolerated component of HAART in this small patient cohort. A longer-term assessment of the effects of TDF on childhood growth and larger prospective studies of TDF use in pregnant women are therefore necessary [39, 40, 42].

1.4 PHARMACOKINETICS

1.4.1 Dose and administration

TDF can be administered to adolescent patients that are 12 years of age and older with a body weight ≥ 35 kg infected with HIV-1. The treatment of HIV or chronic hepatitis B requires a dose of TDF of 300 mg orally taken once daily. Food does not appear to affect the absorption of TDF. For the treatment of chronic Hepatitis B the optimal duration of treatment is unknown. The only dosage forms of TDF commercially available are tablets. Significantly increased TDF exposure has been reported when TDF was administered to patients with moderate to severe renal impairment, therefore the dosing interval for TDF should be adjusted in patients with a baseline creatinine clearance of < 50 mL/min [6, 14, 37]. The recommended dosage adjustments have been summarized in Table 1.4. The pharmacokinetics of TDF has not been evaluated in patients undergoing haemodialysis with a creatinine clearance of < 10 mL/min and therefore no dosing recommendations for these patients are available.

Table 1.4 Dosage adjustments for TDF in patients with altered creatinine clearance.

	Creatinine Clearance (mL/min)			Hemodialysis Patients
	≥ 50	30–49	10–29	
Recommended Dosing Interval	Every 24 hours	Every 48 hours	Every 72 to 96 hours	Every 7 days or after 12 hours of dialysis.

1.4.1.2 Missed dose and overdosing

If a patient misses a dose at the scheduled administration time the patient should take the missed dose immediately if the dose is taken on the same day it was missed. The next dose should then be taken at the scheduled time the following day and patients should not take two doses of TDF at the same time to make up for a missed dose. If an overdose with TDF occurs patients must be monitored for evidence of toxicity and standard supportive treatment implemented, if and when necessary. Administration of activated charcoal may also be used to facilitate the removal of any unabsorbed TDF remaining in the gastrointestinal (GIT) tract. TDF is efficiently removed by hemodialysis with an extraction coefficient of approximately 54% and a four hour hemodialysis session has been reported to remove approximately 10% of a single 300mg dose of TDF [34].

1.4.2 Absorption

TDF is a sparingly soluble diester pro-drug of tenofovir. In fasted patients the oral bioavailability of TDF is approximately 25% which increases to approximately 40% when administered with a high fat meal of approximately 700 to 1000kCal containing 40-50% fats[5]. The maximum serum concentration or C_{max} occurs 1.0 ± 0.4 hours following administration. The C_{max} and AUC values were 296 ± 90 ng/ml and 2287 ± 685 ng.hr/ml, respectively following administration of 300 mg TDF once daily in the fasted state. Food is reported to delay the time to C_{max} by approximately 1 hour. The C_{max} and AUC of TDF were 326 ± 119 ng/mL and 3324 ± 1370 ng.hr/mL following administration of 300 mg TDF once daily in the fed state for 7 days, when the content of meal was not controlled [6, 14, 28, 43].

1.4.3 Distribution

Following oral administration of TDF, tenofovir is distributed to most tissues with the highest levels observed in the kidney, liver and intestinal contents. *In vitro* protein binding of PMPA to plasma or serum proteins was less than 0.7 and 7.2%, respectively over a concentration range of 0.01 - 25 µg/ml PMPA. The volume of distribution at steady state was 1.3 ± 0.6 L/kg and 1.2 ± 0.4 L/kg following intravenous administration of 1.0 mg/kg and 3.0 mg/kg PMPA[6, 28].

1.4.4 Metabolism

In vitro studies have established that neither TDF nor tenofovir are substrates for CYP450 enzymes. Moreover at substantially higher concentrations (approximately 300-fold) than those observed *in vivo* PMPA did not inhibit *in vitro* drug metabolism mediated by any of the major human CYP450 isoforms involved in drug metabolism *viz.*, CYP3A4, CYP2D6, CYP2C9, CYP2E1, or CYP1A1/2. Based on these data it is unlikely that clinically significant interactions involving TDF and other compounds that undergo CYP450 metabolism are likely to occur [28, 29].

1.4.5 Elimination

The plasma half-life of TDF has been reported to be approximately 17 hours. Tenofovir (PMPA) is primarily excreted through the kidney by filtration and active tubular transport with approximately 70 – 80% of the dose excreted unchanged in the urine within 72 hours following intravenous administration. Approximately $32 \pm 10\%$ of the administered dose is recovered in the urine 24 hours following administration of multiple oral doses for 7 days. Total body clearance has been estimated to be approximately 300ml/min. Renal clearance has been estimated to be approximately 210ml/min which is in excess of the glomerular filtration rate thereby indicating that active tubular secretion is an important contributor to the elimination of PMPA [5, 6, 28].

1.5 CONCLUSIONS

There are currently approximately 40 million people living with HIV-1 and/or AIDS worldwide. The goal of antiretroviral therapy for patients with HIV-1 infection is to delay progression of the disease and increase survival by achieving maximal and prolonged suppression of HIV-1 replication [44, 45]. The standard of care for treatment of these patients involves the use of combinations, typically using at least three ARV agents, including an NNRTI or a protease inhibitor (PI) and two active substances from the NRTI or NtRTI class of drugs [46-49].

ARV regimens imply that a high tablet burden and frequency of administration are necessary and this is not likely to be compatible in the daily life of a patient possibly resulting in a reduction in adherence. Furthermore the achievement of successful long-term therapy and prevention of

resistance has become a significant challenge. Incomplete adherence to ARV regimens is an important factor contributing to the development of viral resistance and treatment failure. Therefore there continues to be a need for new treatments that combine potent and sustained efficacy with acceptable tolerability and minimal long-term toxicity in addition to ensuring that a practical and convenient dosing regimen is available for use [9].

TDF has been used in fixed dose combinations (FDC) and has also been administered on its own as a once daily tablet. TDF has proven to be an effective compound with an acceptable safety profile for the treatment of HIV-1 infections. Recent research has focused on attempting to improve the bioavailability of TDF and to reduce potential side-effects in an effort to increase patient adherence and avoid treatment failure. In tandem with WHO goals for access to more affordable medications for all, research into developing cheaper formulations has become essential to help combat HIV/AIDS in poor nations. This research project focused on the use of a delivery approach that would reduce production costs and ultimately may provide access to cheaper medicines to combat HIV/AIDS.

CHAPTER TWO

DEVELOPMENT AND VALIDATION OF AN HPLC METHOD FOR THE ANALYSIS OF TENOFOVIR DISOPROXIL FUMARATE

2.1 INTRODUCTION

2.1.1 Historical background

Chromatography is the most frequently used analytical technique for pharmaceutical analysis. An understanding of the parameters that govern chromatographic performance has given rise to improvements in chromatographic systems and therefore improvements continually increase the ability of an analyst to achieve high-resolution, rapid and efficient separations [50]. Analysis of pharmaceuticals by chromatography can be traced back to 1922. Liquid chromatography in the form of descending and ascending paper, thin layer, ion-exchange and exclusion chromatography were described in the United States Pharmacopeia (USP) as a method for use in the identification of drug products as early as 1955 [51]. Poor efficiency and long analysis times due to low mobile phase flow rates resulted in the subsequent introduction of gas chromatography and in 1975 high performance liquid chromatographic (HPLC) method was reported in the USP [52]. By 1985 the USP had listed in excess of 700 chromatographic methods for drug product identification [53]. HPLC has proved to be the method of choice over other forms of liquid chromatography since HPLC stationary phases can be used for long periods of time without the need for regeneration and the resolution achieved with these stationary phases is far better than that of older chromatographic methods. Furthermore HPLC instrumentation is readily automated and the separation is not as dependent on the skills of the operator as other modes of analysis, therefore the method is reproducible and in general analysis times are shorter than with other techniques [54, 55].

2.1.2 Principles of HPLC

Simply put, HPLC involves passing a liquid phase under pressure through a stainless steel column containing particles of a stationary phase with a mean particle size varying between 3 and 10 μm and is usually silica based when operated in the reversed-phase chromatographic mode. The analyte of interest is loaded into the column via an injection valve and separation of the sample mixture occurs according to the relative residence time of each component within

column [50]. Monitoring of the eluent is undertaken using one of a variety of detectors and the response is recorded on a suitable data capture system.

The selection of HPLC as the method for a particular separation requires classification of the sample to be analyzed. A regular sample would be defined as a matrix that contains mixtures of small molecules of <2000 Da and that can also be further sub-classified as either neutral or ionic. Ionic samples include acids, bases, amphoteric compounds and organic salts. Reversed-phase columns are recommended for this class of sample and when developing an analytical method, initial exploratory runs would be performed to establish separation parameters after which it can be systematically improved and optimized in order to achieve a suitable separation[55].

Reversed-phase HPLC (RP-HPLC) is more convenient and rugged than other forms of liquid chromatography and yields better sample separations. RP-HPLC is more efficient, stable, reproducible and detection is readily achieved with UV detection the most commonly used form of detection for pharmaceutical analysis.

RP-HPLC stationary phases are silica based that are modified by attaching long hydrocarbon chains of 8 or 18 carbon atoms to the surface of the silica to produce a non-polar surface. A polar solvent is used as the mobile-phase and may for example be a mixture of water and an alcohol such as methanol. A strong attraction between the polar solvent and polar molecules in the mixture to be analyzed as the sample moves through the column will result in the polar molecules in the solution migrating with the solvent. However no such attraction would exist between polar molecules and the hydrocarbon chains attached to the silica backbone of the stationary phase and therefore non-polar components in the sample mixture will tend to be attracted to the hydrocarbon functional groups due to Van Der Waal's forces and will be less soluble in the solvent and therefore spend less time in solution resulting in retention of these compounds for a longtime. Consequently polar molecules travel more rapidly through a reversed-phase column than non-polar solutes and the retention characteristics of analytes of interest can be adjusted by changing the composition or solvent strength of the mobile phase [50, 53, 55].

In NP-HPLC the stationary phase is more polar than the mobile phase that is usually a mixture of organic solvents without water. The column packing is either an inorganic adsorbent such as

silica, alumina or a polar bonded phase on a silica based support. Regardless of the type of mobile or stationary phase used sample retention in NP-HPLC increases as the polarity of the mobile phase decreases which is in contrast to RP-HPLC [55].

NP-HPLC is most useful for the separation of compounds of moderate to strong polarity since non-polar solutes elute near the solvent front. NP-HPLC is normally restricted to the separation of stereochemical isomers, diastereomers, low molecular weight aromatic compounds and long chain aliphatic compounds [55].

RP-HPLC is usually the technique of choice for most pharmaceutical applications, particularly for the analysis of neutral or non-polar compounds that dissolve in aqueous-organic solvent mixtures. Since the majority of pharmaceutical compounds of interest are relatively non-polar most HPLC analyses in pharmaceutical research are performed using RP-HPLC.

2.1.3 Overview

Very few analytical methods have been reported for the analysis of TDF in pharmaceutical dosage forms or biological fluids. Most of the methods that have been reported use UV based detection systems, however they tend to have long analyses times and no stability indicating studies have been reported. Despite the rapid advancement in analytical technology and techniques HPLC is still the preferred tool for the analyses of active pharmaceutical ingredients (API) and products in most official compendia [52, 56, 57]. The objective of this study was to develop and validate an HPLC method for the determination of TDF in pharmaceutical solid dosage forms.

2.2 ANALYTICAL METHODS FOR THE ANALYSIS OF TDF

Prior to the development of an HPLC method for the analysis of TDF a review of the literature was undertaken and relevant aspects of HPLC methods that have been published for the analysis of TDF are summarized in Table 2.1.

Table 2.1 Summary of analytical methods developed for the analysis of TDF in different matrices

Column	Mobile phase	Flow rate ml/min	Detection method	Reference
Symmetry shield [®] 5µm RP ₁₈ column (250x4.6 mm I.D.)	pH 6 buffer (15 mM Na ₂ HPO ₄ and 10 mM TBA (A) and acetonitrile (B). (A-B, 94:6)	1.0	DAD-259nm	[58]
Inertsil [®] C ₈ 5 µm(250 x 3 mm I.D.) with column heater at 35°C	phosphate buffer (5 mM, pH 6) containing 5 mM tetrabutylammonium chloride:acetonitrile (85:15, v/v)	0.5	Fluorimetric Excitation, emission wavelengths at 236 and 420 nm.	[59]
Atlantis [™] 5.0 µm dC-18 analytical column (150 x 3.9 mm I.D.)	phosphate buffer (pH 5.7) : methanol (15:85 % v/v)	1.0	DAD-259nm	[60]
Inertsil [®] ODS 3V (250 x 4.6 mm, 5µm)	0.02M Sodium dihydrogen orthophosphate monohydrate (A), Methanol and water in the ratio of (85:15) (B). (A-B) 35:65 % v/v	1.5	DAD-265nm	[61]
Camag Linomat [®] 5 semiautomatic spotting device (Camag, Muttenz, Switzerland), Camag twin-trough chamber (10 cm × 10 cm) (HPTLC)	chloroform : methanol (9 : 1 % v/v)	-	UV-260nm (HPTLC)	[62]

The majority of methods reported for the analysis of TDF make use of UV based diode array detection systems with a wavelength range of 259 to 265 nm. The mobile phase systems used were comprised of complex tri-phasic solvent mixtures with the most commonly used organic modifier and buffer solution used of tetrabutylammonium chloride, acetonitrile and mono-basic potassium phosphate buffer of pH between 5.1 and 7.0 [61]. The stationary phases for most of the methods were housed in long columns resulting in long sample analysis times.

These studies provided sufficient data for identifying chromatographic conditions to be used as a starting point for the development and selection of an appropriate HPLC method for the analysis of TDF in raw material, powder blends and dosage form. A RP-HPLC method using UV detection was selected as the preferred analytical tool for the quantitation of TDF during formulation development and assessment studies.

2.3 EXPERIMENTAL

2.3.1 Materials and reagents

TDF was purchased from Hetero Labs Limited (Jinnaram Mandal, India). Nevirapine (NVP) was purchased from Sigma Aldrich (St Louis, Missouri, USA). Acetonitrile (ACN) and methanol (MeOH) were purchased from Romil Ltd (Waterbeach, Cambridge, UK). Sodium hydroxide pellets and hydrochloric acid were purchased from Merck Chemicals Ltd (Modderfontein, Gauteng, South Africa). Viread[®] tablets (Gilead Sciences Inc (Pty) Ltd, Foster city, California, USA) were purchased from Wallaces Pharmacy (Grahamstown, Eastern Cape, RSA).

HPLC grade water was prepared using a Milli-RO[®] 15 water purification system (Millipore Co., Bedford, Massachusetts, USA) that consisted of a Super-C[®] carbon cartridge, two Ion-X[®] ion exchange cartridges and an Organex-Q[®] cartridge. The HPLC grade water was filtered through a 0.45µm Millipak[®] 40 sterile filter (Millipore Co., Milford, Massachusetts, USA) prior to use.

2.3.2 HPLC system

The modular HPLC system as comprised of a Spectra-Physics[®] Iso-Chrom solvent delivery module (Spectra-Physics, San Jose, California, USA), a Waters[®] Associates WISP[®] 712 auto-sampler (Waters Chromatography Division, Milford, Massachusetts, USA), a Linear[®] UVIS 200 spectrophotometer (Linear Instruments Co., Irvine, California, USA) and a Spectra-Physics[®] SP 4290 integrator (Spectra-Physics, San Jose, California, USA). Separation was achieved using a 5 μ m Phenomenex[®] Luna[®] C₁₈ (2)150 x 4.60mm i.d. column (Phenomenex[®] Torrance, California, USA).

2.3.3 Column selection

The selection of a suitable column for RP-HPLC analyses is essential when developing a rugged and reproducible analytical method. The physicochemical properties of the analyte of interest are important when selecting a suitable column for use as these parameters give a clear picture of the potential interactive forces that may be involved between the analyte and stationary phase when developing the separation [55, 56].

Different bonded stationary phases are prepared by reacting organo-alkoxysilane or organo-chlorosilane with silanol functional groups of the silica gel backbone used to manufacture. Octadecylsilane (ODS) is the most popular commercially available sorbent, however it has limited pH stability thus mobile phases of pH > 7 are not recommended as the silica backbone is soluble in solutions of alkali pH. As reported in § 1.2 *vide infra* TDF is a weak acid and the physicochemical properties of this molecule have been described in detail in Chapter One. Following evaluation of the physicochemical properties of TDF and a review of the relevant literature a RP-C₁₈ column was selected for this study [53, 56]

The optimum diameter of the column to be used will depend on the volume of the peak and the quality of the column packing process. At the interface of the column wall and column packing solute band broadening is generally increased and negatively affects column performance [54]. In order to ensure that wall effects do not significantly affect the performance of the column a minimum internal diameter for a column should be used and manufacturers have established that

an internal diameter of 4.6 mm reduces the impact of band broadening and facilitates optimization of column performance. Generally the column length for analytical columns is between 100 and 1000 mm. Most manufacturers have standardized on a column length of 250 mm as these columns are capable of generating high plate counts. The use of shorter columns however gives rise to smaller pressure drops and shorter analysis times and therefore these are rapidly becoming columns of choice for developing separations. Therefore a column of 4.6 mm id and 150 mm in length was selected for use to develop a method for the analysis of TDF [53, 54, 56].

Following evaluation of the factors likely to affect column performance and a review of literature a 5 μ M Phenomenex[®] Luna[®] C₁₈ (2)150 x 4.60mm i.d. analytical column (Phenomenex[®] Torrance, California, USA) was selected for the development of a RP-HPLC UV method for the analysis of TDF in pharmaceutical dosage forms.

2.3.4 Internal standard (IS)

The quantitative analysis of pharmaceutical products usually requires some sample preparation that may result in sample loss due to extensive manipulation prior to analysis. Furthermore instrumental responses can vary from run to run for reasons that are difficult to control, such as for example flow rate or injection volume variability that may result in imprecise detector responses when monitoring samples of the same concentration of analyte. To compensate for this eventuality an internal standard (IS) may be added to calibration and sample solutions to reduce variability. The IS should be well resolved from all components or analytes during separation and must not be present in the original sample. Furthermore the IS should be stable and unreactive with the analyte of interest and/or mobile phase. To facilitate analysis an IS with a similar chemical structure to the analyte of interest is normally selected for use. Furthermore the response factor for the IS should have a similar response to the analyte of interest for the concentration used.

A review of the literature reveals that an IS is frequently used for the analyses of TDF and metaxalone, piroxicam and tegafur have been used. For the purposes of this study nevirapine was

selected as the preferred IS as it did not elute close to TDF and it is stable and unreactive with the sample or mobile phase and was readily available as a high purity standard.

2.3.5 Preparation of Stock Solutions

Standard stock solutions of TDF of 300 µg/ml and NVP of 300 µg/ml were prepared by accurately weighing approximately 30 mg of TDF and NVP separately using a Model AG-135 Mettler Toledo top-loading analytical balance (Mettler Instruments, Zurich, Switzerland) into 100 ml A-grade volumetric flasks and dissolving the powders in mobile phase. The stock solutions were sonicated using a Model 8845-30 ultrasonic bath (Cole-Parmer Instrument Comp. Chicago, Illinois, USA) for 3 minutes in-order to ensure complete dissolution of the compounds after which the samples were made up to volume with mobile phase. Calibration standards of TDF were prepared by serial dilution with mobile phase to produce solutions of concentration 1,3,6,15,90 and 180µg/ml. All stock and standard solutions were prepared daily prior to analysis.

2.3.6 Selection of mobile phase and flow rate

The preferred mobile phase was identified by varying the concentration of ACN and monitoring the retention times for TDF and the IS. A retention time of ≤ 10 minutes was considered appropriate for this separation. The flow rate was also varied between 0.8 ml/min to 1.8 ml/min to establish a separation with adequate peak resolution, symmetry and retention time.

2.3.7 Preparation of mobile phase

The appropriate volume of ACN was measured using an A-grade measuring cylinder. The required volume was then made up to volume with HPLC grade water in a 1000 ml Schott® Duran bottle (Schott Duran GmbH, Wertheim, Germany). The mobile phase was mixed and then filtered and degassed under vacuum using an Eyela Aspirator A-2S vacuum pump (Rikakikai Co., Ltd, Tokyo, Japan) and a Millipore® HVLP 0.45µm filter (Millipore, Bedford, MA, USA). The mobile phase was prepared daily and was not recycled during analysis.

2.4 RESULTS AND DISCUSSION

2.4.1 Effect of ACN composition on retention time

The retention time of TDF and NVP was significantly influenced by the ACN content of the mobile phase as depicted in Figure 2.1.

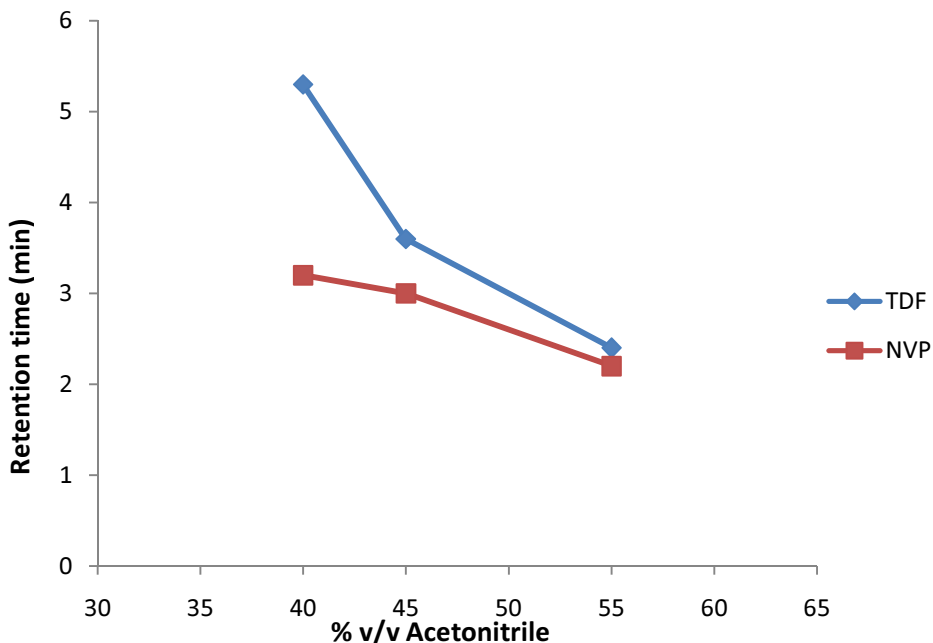


Figure 2.1 Effect of organic solvent composition on R_t of TDF and NVP

The R_t of TDF and NVP were 5.3 and 3.2 minutes respectively when the ACN content was 40% v/v in HPLC grade water. An increase in the amount of ACN to 45% v/v resulted in a decrease in R_t for both TDF and NVP to 3.6 and 3.0 minutes respectively. A further increase in ACN content resulted in a further decrease in R_t for TDF and NVP due to an enhanced solute-solvent interaction and a diminished solute-stationary phase interaction. The aim of conducting these studies was to establish an optimal amount of ACN to use in the mobile phase that would produce a separation with acceptable retention times for TDF and NVP. The FDA guideline recommends that the resolution factor between the peaks of interest should not be < 2 [63]. The resolution for the peaks of interest when 40% v/v ACN was used was 2.1 and combined with our aim to produce a rapid method of analysis the optimal conditions for the separation would be achieved by using a mobile phase with 40% v/v ACN in HPLC grade water.

2.4.2 Effect of flow rate

In general flow rate has an effect on the analytical run time and the effect of changes in mobile phase flow rate on analytical run time is depicted in Figure 2.2.

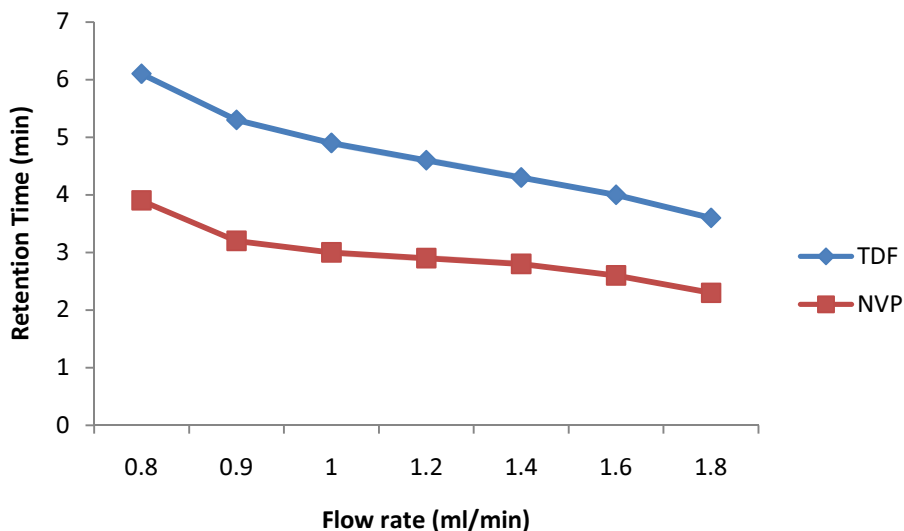


Figure 2.2 Effect of flow rate on R_t of TDF and NVP

An increase in the flow rate of the mobile phase results in shorter analytical run times and increasing the flow rate of the mobile phase from 0.8 to 1.8 ml/min resulted in a reduction in the analytical run time from 6 to 2 minutes. Higher flow rates were not tested in order to safeguard the integrity of the column and pump. Despite the short analytical run time observed at 1.8 ml/min the resolution between the peak for fumaric acid and TDF was not suitable to permit reliable quantitation of TDF and therefore a flow rate of 0.9 ml/min was selected for use, as an optimal analytical run time was achieved using this flow rate.

2.4.3 Chromatographic conditions

The ultimate chromatographic conditions selected for the analysis of TDF using NVP as internal standard are summarized in Table 2.2 and a typical chromatogram obtained using these conditions is depicted in Figure 2.3.

Table 2.2 Chromatographic conditions for analysis of TDF

Column	5 μ mPhenomenex [®] Luna [®] , C ₁₈ (2)150 x 4.60 mm i.d.
Detection wavelength	259 nm
Detector sensitivity	0.1 AUFS
Integrator speed	2.5 mm min ⁻¹
Flow rate	0.9 ml min ⁻¹
Injection volume	10 μ l
Temperature	Ambient, 22 \pm 0.5°C
Column pressure	700 – 1000 psi
Mobile phase composition	ACN:H ₂ O (40:60) % v/v

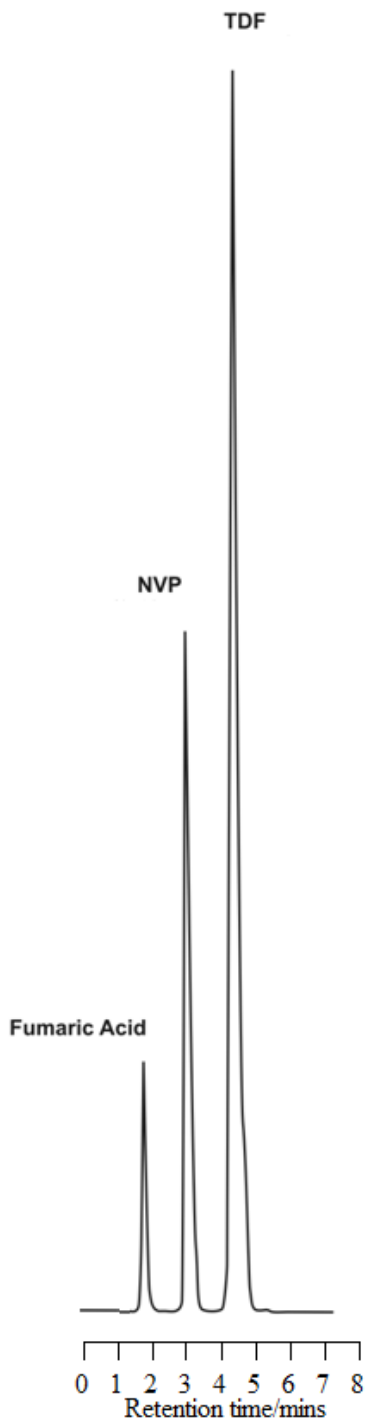


Figure 2.3 Typical chromatogram of the separation of TDF (180 µg/ml) and NVP (44µg/ml) using the conditions described in Table 2.2

2.5 METHOD VALIDATION

2.5.1 Introduction

Method validation is a process that is used to confirm that an analytical procedure that is used for a specific analysis is suitable for its intended purpose. Results from method validation studies can be used to judge the quality, reliability and consistency of analytical results and are an integral part of good analytical practice [55, 64]. However in practice, many analytical methods fail to produce expected results when different environmental conditions, instrumentation, equipment and/or different analysts are used thereby affirming the importance of undertaking method validation studies [65].

Analytical methods must be validated or revalidated prior to introduction into routine use or whenever conditions for which the method has been validated change, such as for example when an instrument with different performance characteristics is used or whenever the method is changed and the change is outside the original scope of the method [50, 55, 64]. The USP, FDA, and BP have published specific guidelines for method validation for compound evaluation and defines eight steps for validation that includes an assessment of accuracy, precision, specificity, limits of detection and quantitation, linearity, range, ruggedness and robustness [57, 66, 67]. The validation of analytical methods is an integral part of the requirements for submission of analytical methods to regulatory authorities such as the Medicine Control Council (MCC) in South Africa and Food and Drug Administration (FDA) amongst others [57, 68-70].

2.5.2 Linearity and range

The ICH defines linearity of an analytical procedure as the ability of that procedure within a given range to produce test results that are directly proportional to the concentration or amount of analyte in a sample [70, 71]. The data that can be used for the quantitation of an analyte include peak area, peak height or the ratio of peak area/height of the analyte of interest to that of the internal standard. The reliable quantitation of an analyte is dependent on adherence to the Beer-Lambert law for UV detection over the concentration range under investigation [57, 72, 73].

Linearity is best evaluated by visual inspection of a plot of a signal as a function of analyte concentration and the data are used to calculate a least squares linear regression line. At least five concentration levels should be used and the linearity of a method is considered acceptable if the coefficient of determination, R^2 is ≥ 0.999 . The linearity and range for the HPLC analysis of TDF were established by plotting the peak height ratio of TDF/NVP versus the concentration of TDF and these data are summarized in Table 2.3.

Table 2.3 Peak height ratio of TDF and NVP as a function of concentration.

Concentration $\mu\text{g/ml}$ (n=5)	Average peak height ratio	%RSD
1	0.01 ± 0.001	2.14
3	0.03 ± 0.001	1.19
6	0.05 ± 0.001	0.44
15	0.17 ± 0.001	0.52
90	0.92 ± 0.002	0.17
180	1.82 ± 0.015	0.85

The equation of the line and R^2 value for TDF were $y = 0.0101x + 0.0023$ and 0.9998, respectively. A typical calibration curve for TDF is depicted in Figure 2.4 and the resultant curve was linear for the range 1 - 180 $\mu\text{g/ml}$.

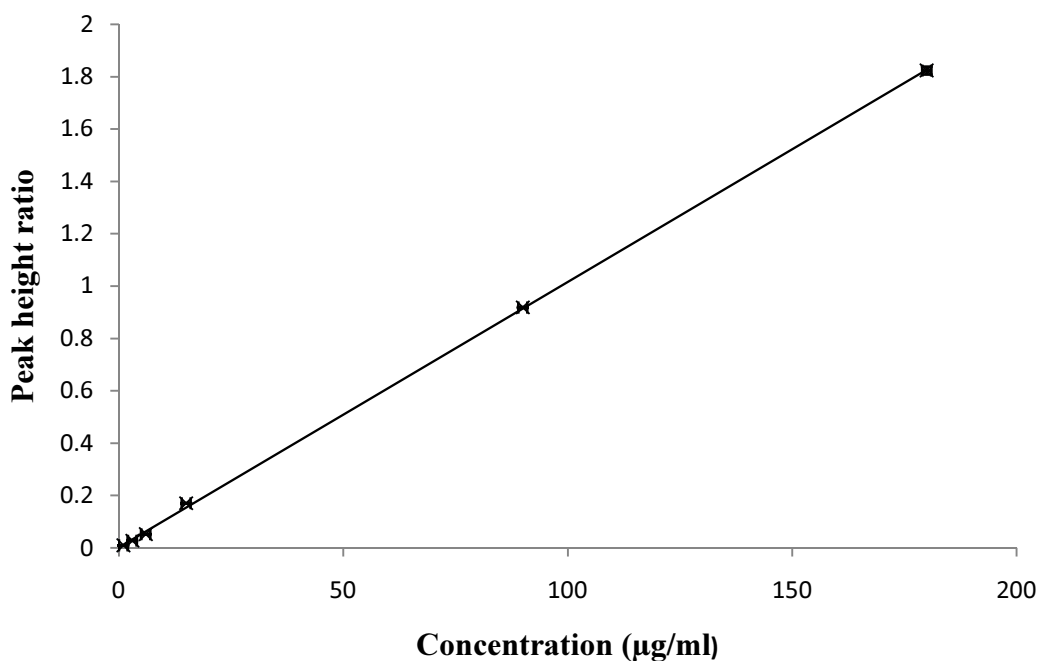


Figure 2.4 Typical calibration curve for TDF over the concentration range 1 – 180 $\mu\text{g/ml}$ (n=5)

2.5.3 Precision

The precision of an analytical procedure expresses the closeness of agreement between a series of measurements obtained from multiple testing of the same homogeneous sample under prescribed conditions. Precision includes an investigation of three defined parameters *viz.*, repeatability, intermediate precision and reproducibility [72]. The precision of an analytical method is usually expressed as a coefficient of variation or percent relative standard deviation (% RSD) of a series of measurements. The acceptance criterion for precision studies in our laboratory was set at $\leq 5\%$ RSD at each concentration level.

2.5.3.1 Repeatability

Repeatability is commonly known as intra-assay precision and involves multiple measurements of the same sample prepared independently by the same analyst under the same conditions. Repeatability is also used to evaluate instrumental precision that is measured by sequential, repetitive analysis of the same homogenous sample and establishing the % RSD for all samples [55]. The ICH guidelines recommend that repeatability be assessed using a minimum of nine determinations covering the range of the analytical method or using at least six determinations at 100% of the test concentration. Repeatability was established following replicate (n=3) analysis of three samples of different concentration that covered the calibration range at low, medium and high levels. The repeatability data for TDF analysis revealed % RSD $\leq 5\%$ for all analyses indicating that the method was precise. The results of analysis for Day 1 are summarized in Table 2.4 [65, 72].

2.5.3.1.2 Intermediate precision

Intermediate precision is an indication of the agreement of measurements when the same method is used repeatedly in the same laboratory on different days. These studies test the impact of analyzing samples on different days or by different analysts using different equipment on the results of the analytical method [55]. Intermediate precision was investigated by replicate analysis (n=6) of samples of concentration 3, 90 and 180 $\mu\text{g/ml}$ that were performed on three different days. These data from intermediate precision studies are summarized in Table 2.4 and reveal that the method has the necessary intermediate precision for the analysis of TDF.

Table 2.4 Repeatability and Intermediate precision data for HPLC analysis of TDF

Day	Concentration µg/ml	Peak height ratio (n=6)	Standard deviation	% RSD
1	3	0.0331	0.0003	0.95
	90	1.0480	0.0017	0.16
	180	2.0779	0.0084	0.40
2	3	0.0336	0.0002	0.52
	90	1.0295	0.0022	0.21
	180	2.0404	0.0051	0.25
3	3	0.0316	0.0003	0.99
	90	0.9685	0.0015	0.16
	180	1.9205	0.0037	0.19

2.5.3.3 Reproducibility

The reproducibility of a method examines the precision of analysis when samples are tested in different laboratories and this parameter is often determined in collaborative studies or through method transfer studies [55, 74]. The assessment of precision during initial method validation often applies to repeatability and intermediate precision and reproducibility is determined during method transfer to another laboratory [55, 65]. Since no crossover studies were to be conducted in these studies reproducibility was not investigated and repeatability and intermediate precision were considered sufficient to indicate the precision of the method and appropriateness for its intended purpose.

2.5.4 Accuracy

Accuracy is a measure of the closeness of test results generated by a method to the true value for a sample. For a particular API, accuracy may be determined by application of the analytical method to testing a sample of known purity. The ICH also recommends that accuracy be assessed by testing a minimum of nine samples over a minimum of three concentration levels covering the specified range for the method [65, 66]. Accuracy is usually reported as percent recovery of a known amount of an analyte that was added to a sample or as the difference between the mean and accepted true value with confidence intervals. The range for the limit of

accuracy should be within the linear range of the method. Typically the accuracy of recovery of an API is expected to be approximately 99 – 101% and the accuracy of recovery of an API from a drug product is expected to be approximately 98 – 102% [65, 66, 72]. The accuracy of the analytical method was established by replicate analysis of samples containing known amounts of TDF. Three samples representing low (12 µg/ml), medium (30 µg/ml) and high (60 µg/ml) concentrations were analyzed (n=6). The accuracy was reported as the percent recovery, % RSD and % Bias. The Bias of a method is the difference between the mean value determined for an API and the accepted true value for that sample and Bias assesses the influence of an analyst on method performance [13]. In addition accuracy measurements are designed to establish the effectiveness of sample preparation prior to analysis [72]. A tolerance of 5% was set for the % RSD and % bias and the resultant % RSD values were < 5% thereby indicating that the method was accurate [75]. The results of accuracy studies are summarized in Table 2.5.

Table 2.5 Accuracy of TDF analysis

Theoretical Concentration µg/ml	Actual Concentration µg/ml	Standard Deviation	RSD %	Bias %	Recovery %
12	11.64	0.3522	3.02	3.05	97.04
30	29.60	0.1572	0.53	1.34	98.68
60	59.52	0.3026	0.51	0.81	99.19

2.5.5 Limits of quantitation (LOQ) and detection (LOD)

The limit of quantitation (LOQ) is the lowest concentration of an analyte that can be quantitated with acceptable precision and accuracy under the stated operational conditions of an analytical method [55, 74]. The limit of detection (LOD) is defined as the lowest concentration of a sample that can be detected but not necessarily quantitated under the stated experimental conditions of an analytical method [55, 66, 76].

The limit of detection is important for impurity testing and for the assay of low API content technologies or placebo dosage forms. The LOD is generally established as the concentration yielding a signal-to-noise ratio of 3:1 and is confirmed by analyzing a number of samples near this value and is confirmed using Equation 2.1.

$$s = H/h$$

Equation 2.1

Where,

H = height of the peak corresponding to the component,

h = absolute value of the largest noise fluctuation from the baseline of the chromatogram of a blank solution.

Since the establishment of the LOD is dependent on the signal-to-noise ratio it can be improved by enhancing the signal for the analyte of interest and simultaneously reducing the noise associated with the detector [72]. The signal or peak height can be increased by selecting the optimum wavelength to monitor the eluent, increasing the injection volume or sample mass, increasing the sharpness of the peak through the use of high efficiency columns or by optimizing the mobile phase composition. For absorbance detectors longer flow cell path lengths enhance sensitivity although this compromises post column dispersion. Noise can be reduced by using high sensitivity detectors with low noise and drift characteristics, slower detector response times, mobile phases with low absorbance and pumps with a low pulsation potential [65, 66, 72].

The equipment used for this analytical method did not produce or exhibit any baseline noise and therefore the use of methods incorporating the signal to noise ratio were not deemed appropriate to establish the LOD for this separation. The LOQ was determined by evaluating the lowest concentration of analyte that produced precision data of <5 % RSD. By convention the LOD value was taken as 30% of the LOQ value. Six different concentrations of TDF were evaluated as the potential LOQ and the data generated in these studies are reported in Table 2.6.

Table 2.6 LOQ data for the analysis of TDF

Concentration µg/ml	Peak height ratio (n=6)	Standard Deviation	% RSD
3	0.03363	0.00017	0.517
2	0.02315	0.00007	0.301
1	0.01261	0.00011	0.849
0.8	0.00923	0.00031	3.41
0.6	0.00692	0.00032	4.67
0.5	0.00583	0.00043	7.30

Based on the results for the determination of the LOQ for this analytical method the LOQ was found to be 1.0 µg/ml with a % RSD of 0.86% and by convention the LOD was taken as 0.3 µg/ml which when injected onto the HPLC resulted in a detectable but non-quantifiable peak.

2.5.6 Specificity

The specificity of an analytical method is the ability of the method to be able to accurately quantitate an analyte in the presence of compounds such as impurities and/or excipients that may interfere with the analysis. The specificity of an analytical method is tested by comparing results of the analysis of samples containing impurities with the results obtained following the analysis of samples without impurities [53].

The chromatographic procedure that is developed must resolve the API of interest from any possible excipients or contaminants that may be present in samples prepared from a dosage form during analysis of that dosage form. A commercially available oral tablet dosage form containing TDF *viz.*, Viread[®] was crushed and dissolved in mobile phase and on following analysis no interfering peaks were observed for the API and internal standard (NVP) that eluted at 5.3 min and 3.2 min, respectively.

2.5.7 Forced Degradation Studies

HPLC is an analytical tool that is also used to assess drug product stability. HPLC methods should separate, detect and facilitate the quantitation of an API and related degradation products that can form during storage or manufacture, in addition to detecting and quantitating any drug related impurities that may be present as a result of the synthesis of an API. Forced degradation studies or chemical and physical stress testing of an API and dosage forms are essential to facilitate the development of a method and to demonstrate the specificity of stability indicating analytical methods[54, 55]. In addition to demonstrating specificity, forced degradation studies can be used to elucidate degradation pathways and products of an API that may form during storage, thereby facilitating formulation development, manufacturing and packaging approaches. Furthermore the ICH guidelines recommend that forced degradation studies should be performed under a variety of conditions including light, oxidative, acidic, basic and heat [70, 71]. In

addition the ICH guidelines require analysis of individual degradation products be undertaken qualitatively and quantitatively, however only qualitative analysis of degradation products were undertaken in this project [71, 73, 77].

2.5.7.1 Method

The analysis of results of degradation studies was undertaken by comparing the chromatograms generated from samples during forced degradation studies and those following analysis of freshly prepared standard solutions of TDF.

2.5.7.1.1 Sample preparation

Approximately 30 mg of TDF was accurately weighed and transferred into a 100 ml A-grade volumetric flask. The TDF was dissolved and made up to volume in a medium specific for that degradation study to yield solutions of approximately 30 µg/ml. The degradation studies were performed using acidic, basic, oxidative and photolytic conditions.

2.5.7.1.1.1 Acid degradation

A 0.1M HCl solution was prepared by transferring 833 µl HCl into an A-grade volumetric flask and making up to volume with distilled water. A 0.1M NaOH solution was also prepared by weighing 0.4g NaOH pellets that were transferred to an A-grade 100ml volumetric flask and dissolved in distilled water. The solution was sonicated for 10 minutes to ensure that all pellets had dissolved and then made up to volume with distilled water. A 1ml aliquot of the primary stock solution was added into a 10 ml A-grade volumetric flask and making up to volume with 0.1M HCl to produce a solution of TDF with a final concentration of 30 µg/ml. A 1 ml aliquot of the sample was withdrawn at 2, 4, 8, 12 and 24 hours after exposure and was diluted with 5 ml of mobile phase in a 10 ml A-grade volumetric flask and the pH adjusted to between 3-7 using 0.1M NaOH. The solution was then made up volume with mobile phase and analyzed using the HPLC method described in § 2.4.3 *vide infra*.

2.5.7.1.1.2 Alkali degradation studies

A 1 ml aliquot of the primary TDF stock solution was added to a 10 ml A-grade volumetric flask and made up to volume with 0.1M NaOH to produce a solution of final concentration of 30 µg/ml of TDF. A 1 ml aliquot of the sample was withdrawn at 2, 4, 8, 12 and 24 hours and diluted with 5 ml of mobile phase in a 10 ml A-grade volumetric flask and the pH adjusted to between 3-7 using 0.1M HCl. The solution was then made up volume with mobile phase and analyzed using the HPLC method described in § 2.4.3, *vide infra*.

2.5.7.1.1.3 Oxidative degradation

A 1 ml aliquot of the primary TDF stock solution was added to a 10 ml A-grade volumetric flask and made up to volume with 3% v/v H₂O₂ solution to produce a solution of final concentration of 30 µg/ml. The sample was then refluxed for 8 h and sample aliquots (10µL) were harvested at 2, 4 and 8 hour marks and transferred into a volumetric flask followed by the addition of IS solution prepared as described in § 2.3.5. The solution was then made up volume with mobile phase and analyzed using the HPLC method described in § 2.4.3, *vide infra*.

2.5.7.1.1.4 Photolytic degradation

A 1 ml aliquot of the primary TDF stock solution was added to a 10 ml A-grade volumetric flask and made up to volume with HPLC grade water. The resultant solution was exposed to 500W/m² light for 24 hours in a photo-stability chamber. A 1 ml sample of the exposed sample was withdrawn at 2, 4, 8, 12 and 24 hours and made up to up volume with mobile phase and analyzed using the HPLC method described in §2.4.3, *vide infra*.

2.5.7.2 Results and Discussion

2.5.7.2.1 Acid degradation

Analyses performed following acid hydrolysis of TDF revealed mild degradation had occurred under these conditions. The R_t of TDF was similar to that of a standard solution and two additional peaks were observed at an R_t of 1.43 and 7.99 min as depicted in Figure 2.5 (II) as A and B. These peaks are more than likely degradation products of TDF produced following exposure to acidic conditions for 24 hr. The percentage recovery of TDF calculated following exposure to acidic conditions for 24 hr was 95.7%.

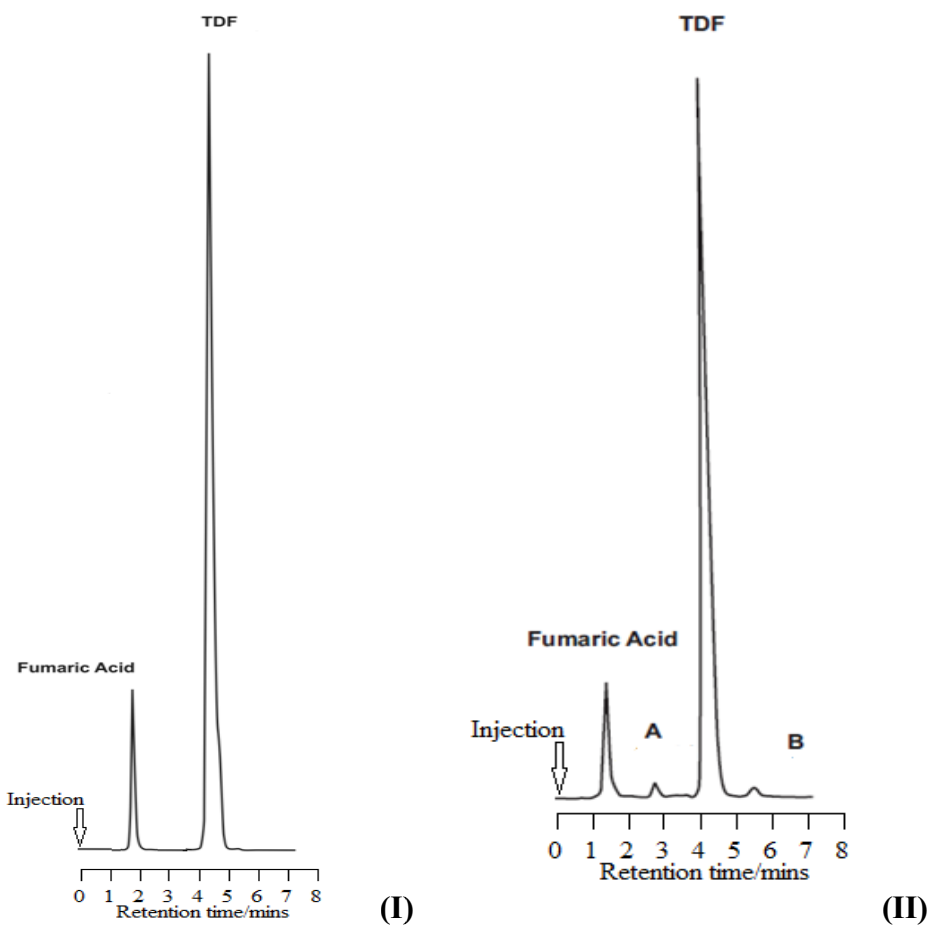


Figure 2.5 Chromatogram of a standard solution of TDF 30 µg/ml (I) and a sample following exposure to acid for 24 h (II)

2.5.7.2.2 Alkali degradation

TDF was observed to degrade rapidly when exposed to alkaline conditions and the chromatograms observed following exposure of TDF to these conditions revealed complete degradation of TDF (Figure 2.6). Total degradation of TDF was observed after 24 hr of exposure with a percent recovery of 0 % TDF confirming the 100 % degradation of TDF observed following incubation of the drug in 0.1 M NaOH at 50°C [62, 78].

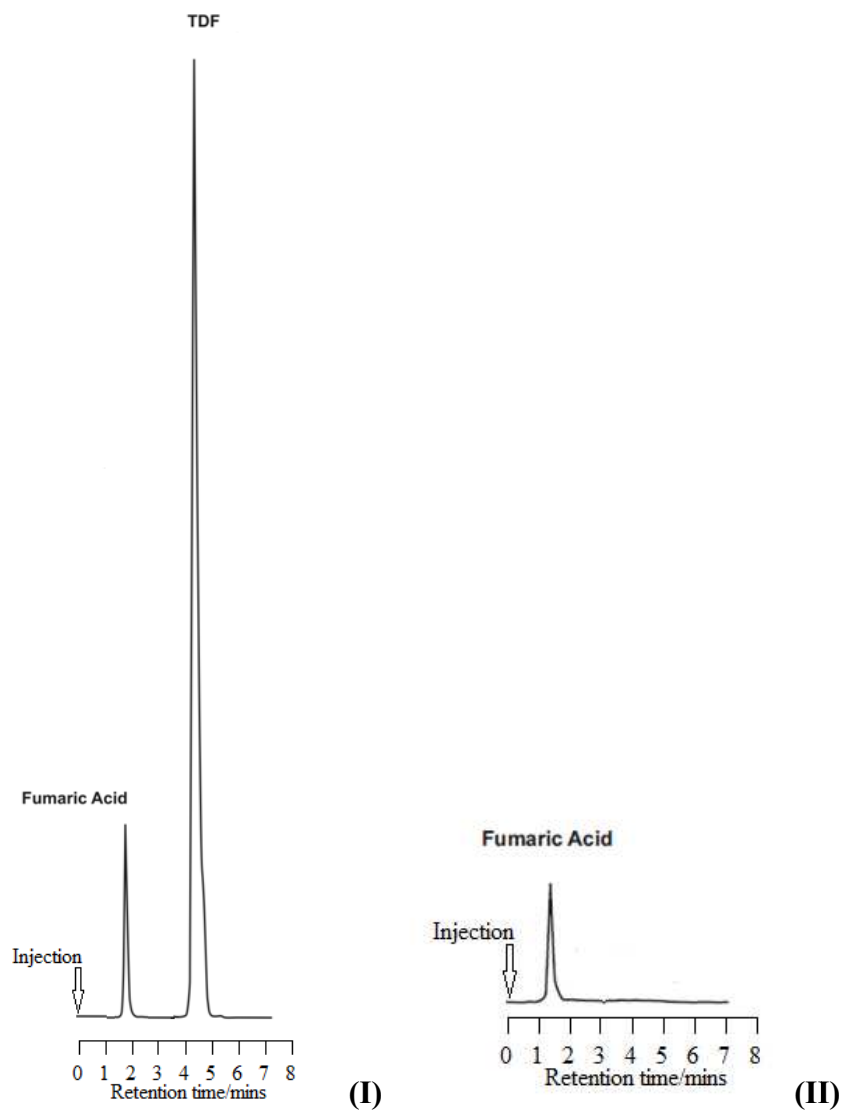


Figure 2.6 Chromatogram of a standard solution of TDF 30 µg/ml (I) and following exposure to alkali conditions for 24 h (II)

2.5.7.2.3 Oxidative degradation

TDF did not exhibit appreciable degradation when incubated in a 3% v/v H₂O₂ solution at room temperature (25°C). No new degradation peaks were observed but analysis of samples revealed a decrease in the peak height for TDF with a resultant total percentage recovery of 92.7% (Figure 2.7). The degradation products could not be qualitatively or quantitatively analyzed and similar results following 8 hr incubation of TDF in 3% v/v H₂O₂ solution have been reported[62, 79, 80].

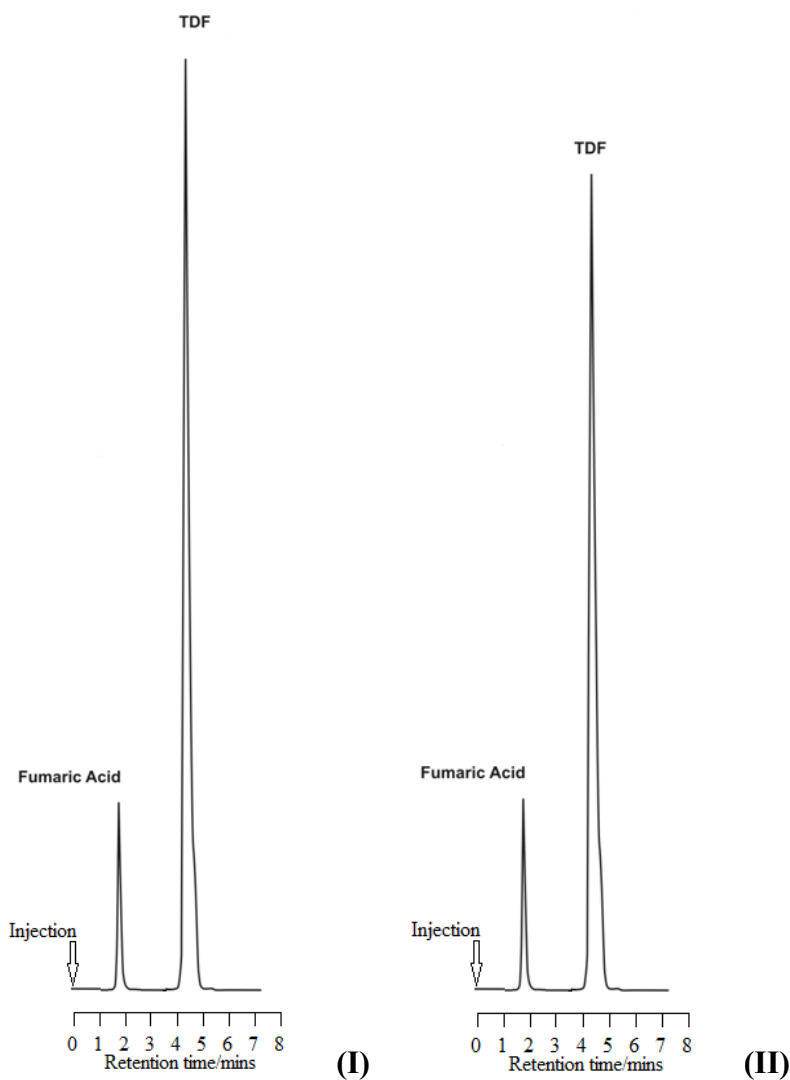


Figure 2.7 Chromatogram of a standard solution of TDF 30 µg/ml (I) and following exposure to oxidative conditions for 8 hr (II)

2.5.7.2.4 Photolytic degradation

The chromatograms generated following injection of samples subjected to light revealed no evidence of degradation and no corresponding decrease in the peak height for TDF suggesting that TDF is stable in the presence of light (Figure 2.8). Similar results following exposure of TDF to UV light for 24 h have also been reported [61, 62, 79].

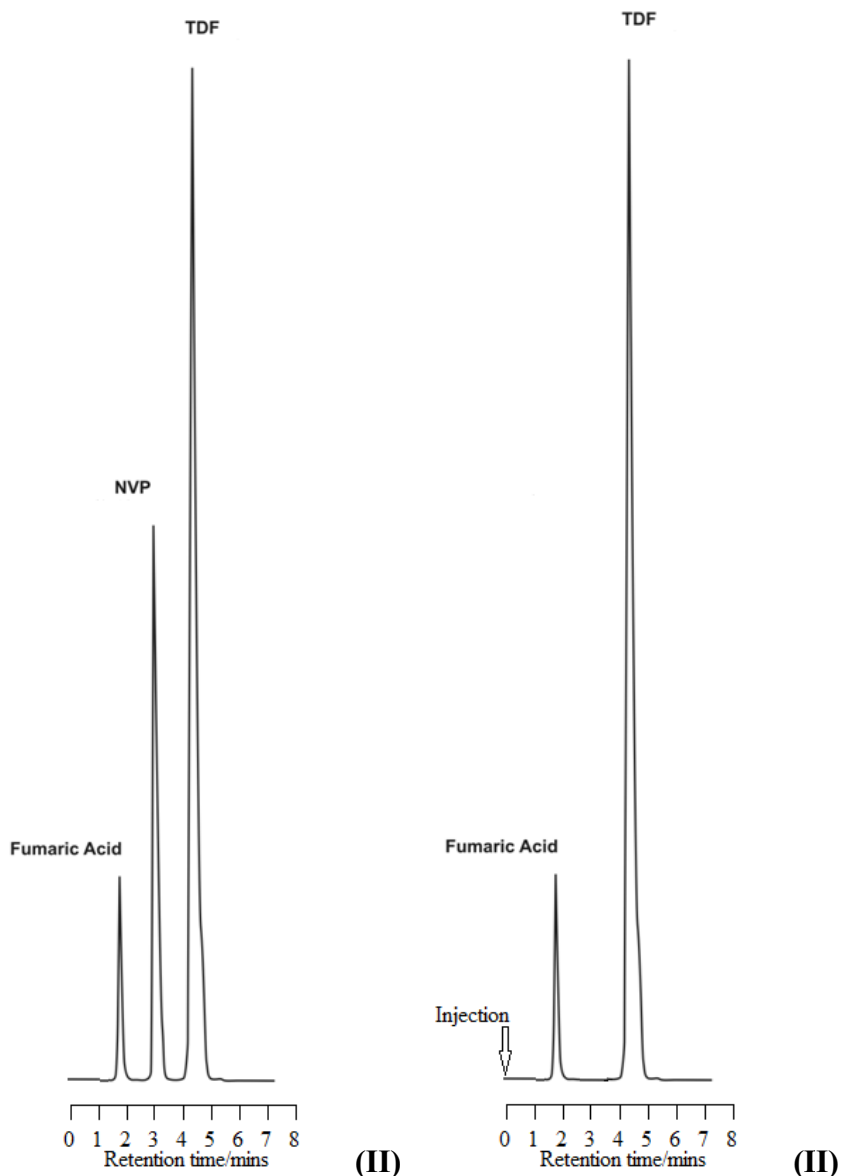


Figure 2.8 Chromatogram of a standard solution of TDF 30 µg/ml (I) and following exposure to photolytic conditions for 24 h (II)

2.6 CONCLUSIONS

A RP-HPLC analytical method with UV detection at 259 nm has been developed and validated for the *in vitro* analysis of TDF in pharmaceutical dosage forms. Method development studies included an investigation into the selection of a suitable wavelength for detection, analytical column, IS and the mobile phase composition. An IS method was used in order to eliminate the introduction of potential variability thereby generating more accurate data.

The use of an appropriate and validated analytical method is essential for the generation of reliable data for the analysis of raw materials, intermediate and finished pharmaceutical products. The method was validated to ensure that the analyte of interest was well resolved and free from interference from excipients that may be used in a formulation and the IS.

An HPLC method for the analysis of TDF has been developed and has the necessary specificity, precision and accuracy for the quantitation of TDF during formulation development studies. The method that was developed was linear over the range 1 – 180 µg/ml and the equation for the line and R² for TDF was $y = 0.0101x + 0.0023$ and 0.9998, respectively. Furthermore the method can be used for the assessment of TDF in solid dosage forms. In addition the separation of degradation products has been achieved using the validated chromatographic conditions. Suitability parameter tests were also performed during method validation to ensure that the results produced were accurate.

The method that was developed is rapid with a run time of <6 minutes allowing for shorter analysis times and high sample throughput which is appropriate for quality control purposes. The method is stability indicating. However further investigation is necessary to identify and analyze the degradation products using instrumentation such as NMR and/or mass spectrometry.

CHAPTER THREE

PREFORMULATION

3.1 INTRODUCTION

Up to the mid-1950's the general emphasis in pharmaceutical product development was to develop elegant dosage forms for which organoleptic considerations outweighed considerations of potential API-excipient interactions, stability challenges or bioavailability issues [81]. The pharmacokinetics and biopharmaceutics of dosage forms were not prioritized or were considered less important than stability; however decomposition of formulations were often undetected. An improvement in analytical technology and the requirement for stability indicating analytical methods revealed that dosage forms that were previously considered stable were susceptible to degradation. Consequently many products originally thought to be adequate required urgent reformulation [81, 82].

The role and activity of excipients is well understood and as each excipient contributes specific functionality to the total performance of a dosage form it is vital that an evaluation of excipients is undertaken to achieve a successful formulation. The choice and use of an excipient in a dosage form depends on the type of dosage form to be produced in addition to understanding and/or investigating the physicochemical and mechanical properties of the API. Research to elucidate relevant scientific data that describe the effect(s) of excipients in a formulation are necessary for the formulation scientist to select the most appropriate composition to use for a particular technology. Consequently experiments, known as preformulation analyses, are undertaken to generate relevant data in respect of the API and potential excipients [83].

A number of experiments are performed during preformulation studies to identify the physicochemical properties of the API, kinetic rate profiles and compatibility with commonly used excipients. The specific tests to be conducted include but are not limited to establishing the particle size, pK_a , aqueous solubility, pH solubility profile, intrinsic dissolution rate, polymorphism and excipient compatibility of the API [81, 84].

The physicochemical properties were reported in Chapter 1 *vide infra* and the physicochemical and molecular properties of the API and potential excipients for use in the manufacture of a TDF

dosage form were investigated to facilitate the successful development and manufacture of pellets of TDF for inclusion in a capsule dosage form.

3.1.1 Physicochemical properties

3.1.1.1 Particle size and shape

Powder blend uniformity is in part affected by the size and in part the shape of an API and those of the excipients to be included in a dosage form. The shape of a particle is defined by the exterior morphology of the material and has a significant impact on the distribution of particles in a powder blend [85]. A qualitative description of the shape of powder particles can be made through the use of descriptive terms such as spherical, granular, crystalline, fibrous and/or flaky amongst others [86, 87]

The shape of a particle is an important consideration when undertaking preformulation studies as the shape may influence critical properties of a blend such as flowability, compatibility, content uniformity and dissolution rate [84]. The flow properties of a powder forms an integral part of preformulation studies and the design of oral dosage forms, since quality control parameters for raw materials and product uniformity must be established to ensure the production of high quality products [88]. Particle shape plays a crucial role in blending, granulation and other manufacturing processes. Irregularly shaped particles generally exhibit or contribute to poor flow whereas spherical powder particles tend to flow adequately.

Particle size has a significant impact on the dissolution rate of materials. Small particles exhibit better dissolution rates than larger particles as a consequence of their larger apparent surface area and the effect of surface area on dissolution has been documented [89]. The interrelationship of other contributing factors on the dissolution rate of an API can be described mathematically using Equation 3.1.

$$\frac{dC}{dt} = A \cdot \frac{D}{h} \cdot \frac{(C_s - C)}{V}$$

Equation 3.1

Where,

- $\frac{dC}{dt}$ = Dissolution rate
- A = Surface area of dissolving particles
- D = Diffusion coefficient of a solute
- h = Thickness of the hydrodynamic layer
- C_s = Equilibrium solubility
- C = Solute concentration in the bulk solution
- V = Volume of dissolution medium

It is evident that an increase in the surface area of particles results in an increase in the dissolution rate of the API (Equation 3.1); however an increase in the surface area of materials may also result in blend heterogeneity. The mixing properties of powders may be compromised as particle size decreases, since smaller particles have the potential to acquire surface charges and consequently adhere to other particles that have an opposite charge [90]. In addition segregation resulting in poor blend uniformity is inevitable when powders of different particle size are mixed. Therefore the determination of properties of powders and particles is essential to generate preliminary data that can be used to guide formulation scientists during the selection of an appropriate composition and manufacturing process [91].

3.1.1.2 Powder density

The density of the individual components of a powder and blends of a powder may contribute to the ultimate processing characteristics of a material. The compressibility, compactability and flow properties of powders depend on or are closely associated with the density of the individual materials and/or the properties exhibited when the material is added to a blend. When developing solid dosage forms the true, bulk and tapped densities of the individual powders are important characteristics that must be evaluated [81, 83].

The bulk density of a powder is defined as the mass of powder particles that occupies a specific total volume. The total volume of a powder includes consideration of the particle volume, inter-particle void volume and internal pore volume of the material [87]. The bulk density of a powder is an important parameter as it is used to establish the necessary requirements for equipment selection and appropriate batch size for manufacture in specific blenders and/or granulators.

Furthermore the bulk density of a powder is usually used to establish Carr's compressibility index (CI) that may be used to describe the flow properties of a powder blend. Carr's index can be calculated using Equation 3.2.

$$CI = 100 \left(1 - \frac{\rho_B}{\rho_T} \right) \quad \text{Equation 3.2}$$

Where,

ρ_B = Bulk density

ρ_T = Tapped density

In general a low CI is indicative of excellent flow properties whereas a high index of >40 is indicative of extremely poor flow characteristics. The interpretation of the value for CI is summarized in Table 3.1.

Table 3.1 Carr's index

Carr's index (%)	Description of flow
5 – 15	Excellent
12 – 16	Good
18 – 21	Fair
23 – 35	Poor
33 – 38	Very poor
> 40	Extremely poor

Carr's index is related to the Hausner ratio that is another indication of the flow properties as shown in Equation 3.3.

$$CI = 100 \left(1 - \frac{1}{H} \right) \quad \text{Equation 3.3}$$

Where,

H = Hausner ratio

A Hausner ratio of < 1.25 is indicative of powder flow that is free flowing whereas a value > 1.25 reflects poor flow [56]. The Hausner ratio and Carr's index are sometimes criticized as not being based on a strong theoretical basis despite a relationship to powder flow having been established empirically. However their use to define the flow properties of powder persists since the equipment required to perform density analysis is relatively cheap and simple to use [92].

3.1.1.2.2 Tapped density

The tapped density of a powder is the apparent bulk density of the material after it has been tapped or agitated in a specific manner for a set period of time. The tapped density is measured by mechanically tapping a measuring cylinder containing the powder sample at a set rate for a set period of time [93]. The initial mass and volume of a powder are recorded after which the measuring cylinder is mechanically tapped for a specified period of time and the volume of the powder is recorded. Mechanical tapping is achieved by raising the cylinder and allowing it to drop under its own weight over a specified distance for that time. Devices that rotate the cylinder during tapping may be preferred to minimize any possible separation of the powder mass during tapping. The tapped density and the bulk density are used to define the Hausner ratio that can be calculated using Equation 3.4.

$$H = \left(\frac{\rho_T}{\rho_B} \right) \quad \text{Equation 3.4}$$

Where,

H = Hausner ratio

ρ_B = Bulk density

ρ_T = Tapped density

3.1.1.2.3 True density

The true density of a substance is the density of the solid material excluding the volume of any open and/or closed pores. Depending on the molecular arrangement of the material the true density maybe equivalent to the theoretical density and therefore could be indicative of the crystalline state of the powder [94]. The true density of powders has been used to calculate the porosity of solid dosage forms, parameters on which hardness and strength of the dosage form are dependent. The true density of a material is measured using high precision gas pycnometers that are commonly helium based devices [93, 95, 95].

3.1.2 Molecular properties of powders

3.1.2.1 Polymorphism

Most API exist in different solid-state forms that are known as polymorphic forms and exhibit different physical and chemical properties such as solubility, dissolution rate, chemical reactivity and mechanical properties in the solid state [81, 84]. Differences in these properties may influence the bioavailability, stability and ability to process and manufacture the API into a product. However when determining the effect of polymorphism on bioavailability, the concept of the Biopharmaceutics Classification System (BCS) should be considered. In the case of BCS Class II molecules where the rate of absorption is dissolution rate limited, large differences in the solubility of polymorphs are likely to affect the bioavailability of the compound. However in the case of BCS Class III drugs where the rate of absorption is intestinal permeability dependent differences in the solubility of polymorphic forms is unlikely to have a significant effect on the bioavailability of the API, as is the case for TDF.

The identification of polymorphic forms of a compound is usually achieved using X-Ray Powder Diffraction (XRPD) in combination with techniques that include differential scanning calorimetry (DSC), thermogravimetric analysis coupled with differential thermal analysis (TGA/DTA) and IR spectroscopy [96, 97]. Thermal analysis is one of the core analytical techniques used for solid-state characterization of API, medicines and excipients. Thermal analysis investigates and measures physical stability such as weight loss, loss of hydration/solvation, degradation and/or decomposition. Furthermore phase transitions such as melting, sublimation, polymorphic conversion and other complex phenomena in solids when exposed to heat can be monitored [97-100]. Thermal analysis can also be used for pre-formulation screening studies to identify potential API-excipient and/or excipient-excipient interactions. In addition spectroscopic techniques offer a broad range of approaches to gather information about the molecular structure and the nature of chemical bonds present in a molecule whilst in the solid state [101-103].

3.1.3 Drug-excipient compatibility

Studies of API-excipient compatibility are vitally important during the preformulation stages of development of all dosage forms. The potential physical and chemical interactions between API and excipients can affect the chemical nature, stability and bioavailability of an API and consequently have an impact on therapeutic efficacy and safety. The successful formulation of a stable and effective solid dosage form depends on careful selection of all excipients that are to be added. Excipients can be defined as enabling substances that facilitate the production of dosage forms, enhance API stability and absorption and/or improve taste and other sensory requirements for patients. The interaction between API and excipients can be classified as physical, chemical and physiological and are furthermore classed as either detrimental or beneficial [104].

Beneficial API excipient interactions are defined as those particular interactions that positively contribute to the manufacture of drug delivery technologies. Such interactions include for example the use of fine croscopvidone as an effective extrusion and spheronization aid in the production of pellets. Fine croscopvidone adsorbs and releases water for lubrication during the extrusion process and offers enhanced API release characteristics through pellet disintegration and solubility enhancement by croscopvidone. This property is highly desirable when formulating dosage forms of poorly soluble drugs.

Detrimental API excipient interactions are defined as those particular interactions that contribute negatively to the manufacture and systemic delivery of particular dosage forms. Examples of API excipient interactions such as transacylation, Maillard reactions, acid base reactions and physical changes have been reported for different API from different therapeutic categories including antiviral, anti-inflammatory, antidiabetic, antihypertensive, anti-convulsant, antibiotic, bronchodilators, antimalarial, antiemetic, antiamoebic, antipsychotic, antidepressant, anticancer, anticoagulant, sedative/hypnotic molecules and vitamins [105, 106]. Once the solid state reactions of a pharmaceutical system are understood the necessary steps can be taken to avoid reactivity and improve the stability of API and products.

Several approaches have been proposed that satisfy the requirements of API-excipient chemical compatibility screening. The most resource sparing of these approaches is computational for which API-excipient chemical compatibility may possibly be predicted. This approach requires a

comprehensive database of reactive functional groups for API and excipients combined with an in depth knowledge of excipients and their potential impurities. Such an approach provides for rapid analysis and requires no bulk raw material. However there are inherent risks with using only a computational approach as the sole source of information. Isothermal stress testing (IST) and DSC are frequently used to screen for physical or chemical reactions associated with API-excipient interactions. Although DSC is unquestionably a valuable technique the interpretation of data may not be straight forward. A sample is exposed to high temperatures (up to 300°C or more), which in reality is not likely to be reached during conventional handling of dosage forms. Therefore DSC results should be carefully interpreted as the conclusions based on DSC results alone may be misleading and inconclusive. Therefore results obtained from DSC studies should always be confirmed using IST. FT-IR spectroscopy has also been successfully used to screen for physical or chemical reactions associated with API-excipient interactions. FTIR analysis results in the generation of peaks that occur due to energy shifts as a consequence of bond vibration in molecules [107-109].

3.2 EXPERIMENTAL METHODS

3.2.1 SEM

Particle size and surface morphology of TDF was evaluated using a Vega[®] Scanning Electron Microscope (Tescan, Vega LMU, Czechoslovakia Republic). A small amount of TDF, Kollidon[®] 30, croscarmellose sodium, Kollidon[®] CL-M and sorbitol were individually dusted onto a graphite plate and sputter coated with gold under vacuum for 30 minutes. The samples were visualized using SEM at an accelerated voltage of 20 kV.

3.2.2 Powder density

The tapped density of the raw powder materials was determined using a Model SVM 203 tapped density tester (Erweka GmbH, Heuseastamm, Germany) at a rate of 220 taps per minute for 2 minutes. Approximately 15 g TDF and each excipient were separately filled into individual tared 100ml A-grade graduated measuring cylinders. The bulk and tapped volume, V_b and V_t were recorded. The density of the materials was assessed in triplicate and the bulk and tapped density were calculated using Equation 3.5.

$$\rho = \frac{m}{v}$$

Equation 3.5

Where,

ρ = true density (where bulk density $\rho = \rho_b$, tapped density $\rho = \rho_t$)

v = volume (where bulk density $v = V_b$, tapped density $v = V_t$)

Carr's index was calculated using Equation 3.2 to provide an indication of the flow characteristics of each raw material.

3.2.3 IR spectroscopy

The IR spectra of individual components and 1:1 mixtures of API and excipients were generated using a Spectrum 100 Fourier transform-infrared (FT-IR) attenuated total reflectance (ATR) spectrophotometer (Perkin Elmer[®] Ltd, Beaconsfield, England). The powder blends were prepared by mixing the individual components in 1:1 ratio using a mortar and pestle. Aggressive mixing was avoided in order to avoid particle fracture leading to polymorphic shifts. Analysis was performed between the 4000-650 cm^{-1} wave number range at a resolution of 4 cm^{-1} (n=5).

3.2.4 Thermogravimetric analysis (TGA) and Differential thermal analysis (DTA)

TGA and DTA analyses were performed using a Model TGA 7 Thermogravimetric analyzer (Perkin Elmer[®] Norwalk, Connecticut, USA). Mass loss due to solvent or water liberation from the powders was monitored by recording the sample weight during heating and plotting a weight versus temperature curve. The TGA/DTA instrument was calibrated for temperature using indium and platinum. Approximately 2.5 mg of TDF was used and the measurements were performed in a nitrogen atmosphere using a flow rate of 20ml/min over the temperature range of 50°C to 650°C at a heating rate of 10°C/min.

3.2.5 Differential scanning calorimetry (DSC)

The heat transition properties of materials were evaluated from DSC thermograms and recorded with a Model DSC 7 (Perkin Elmer[®], Norwalk, Connecticut, USA) equipped with a TAC 7 PC control unit (Perkin Elmer[®], Norwalk, Connecticut, USA). The instrument was calibrated for temperature and enthalpy with a small piece of indium (mp=156.6° C, $\Delta H = 28.45 \text{ J/g}$). Samples were sealed in standard 40 μL aluminum pans and heated from 50° C to 250° C at a heating rate

of 10° C/min. Dry Nitrogen gas set at a flow rate of 20 ml/min was used to purge the DSC during analysis. Data analysis was performed using Pyris™ Manager (Perkin Elmer, Waltham, Massachusetts, USA) software.

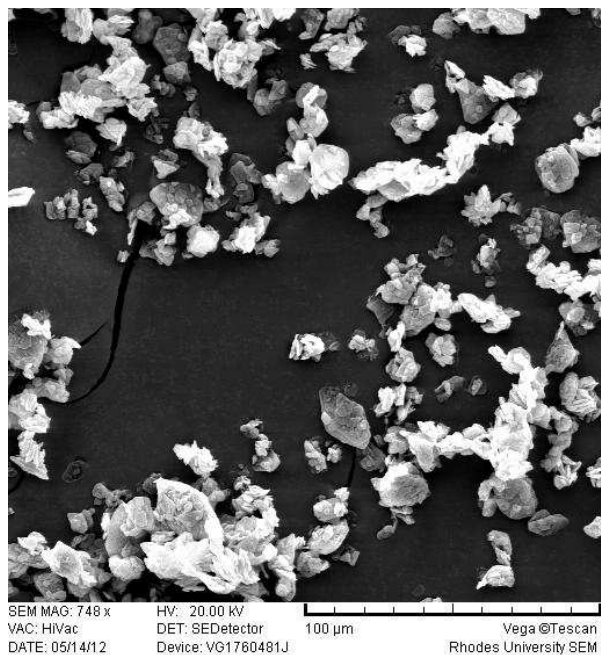
3.3 RESULTS AND DISCUSSION

3.3.1 SEM

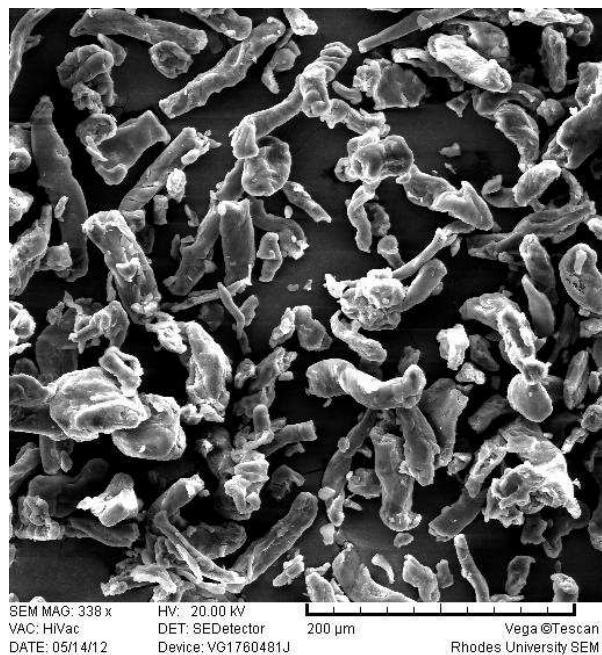
SEM imaging was used to obtain information relating to the particle size and shape of TDF and excipients. This approach provides additional information about the potential flow and properties of powder blends. SEM was used as it is a relatively simple approach and high resolution images are generated rapidly.

Excipients are added to pharmaceutical dosage forms to ensure that the API is delivered to the intended site of absorption, to impart characteristics to the dosage forms that ensure stability and to facilitate the manufacture of products. The selection of appropriate excipients is vital since these materials facilitate the formation of delivery technologies such as pellets of suitable strength and integrity. The excipients not only affect the interplay between the physical and mechanical forces during pellet formation but also influence the rate and extent of growth of pellets manufactured by different processes. Consequently pellet hardness, friability, size, shape and dissolution characteristics often depend on the properties of the excipients used.

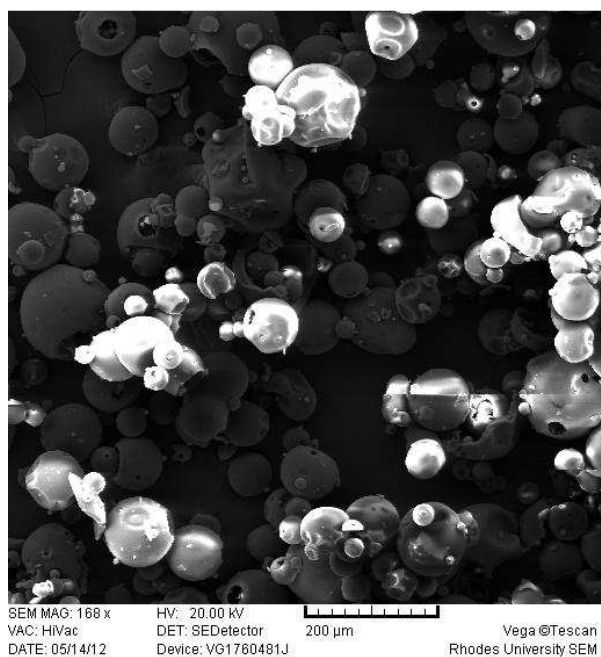
SEM images of TDF, croscarmellose sodium (CCS), Kollidon® CL-M, sorbitol, MCC PH102 (MCC) and Kollidon® 30 are depicted in Figures 3.1 and 3.2.



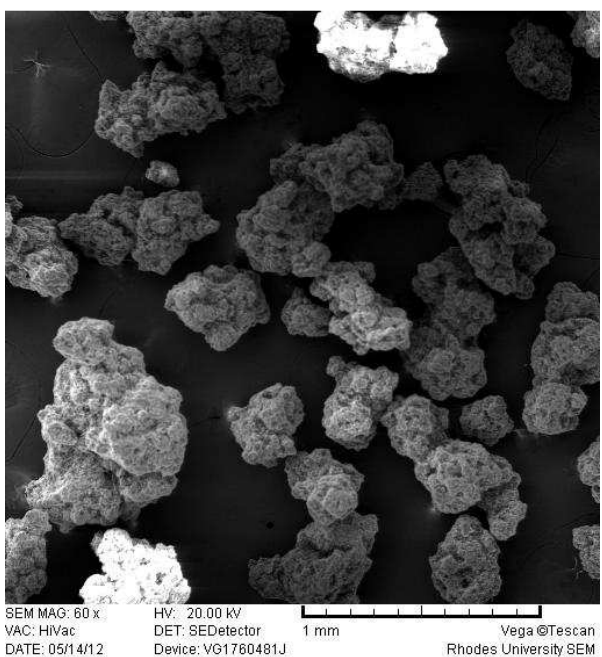
A



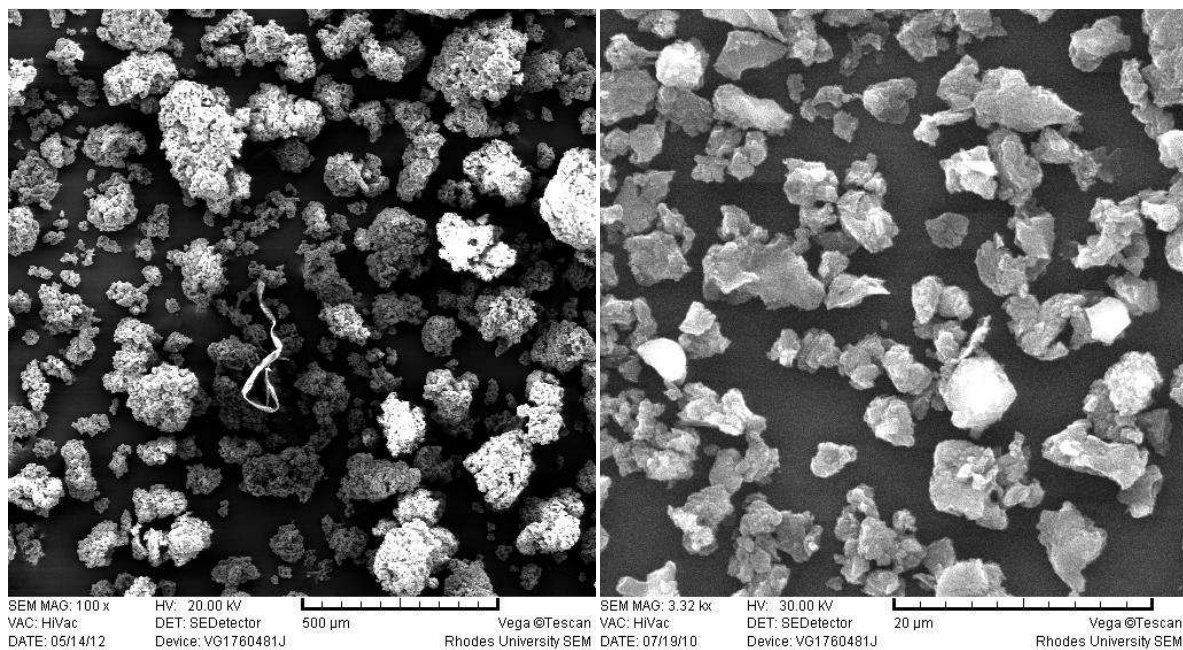
B



C



D

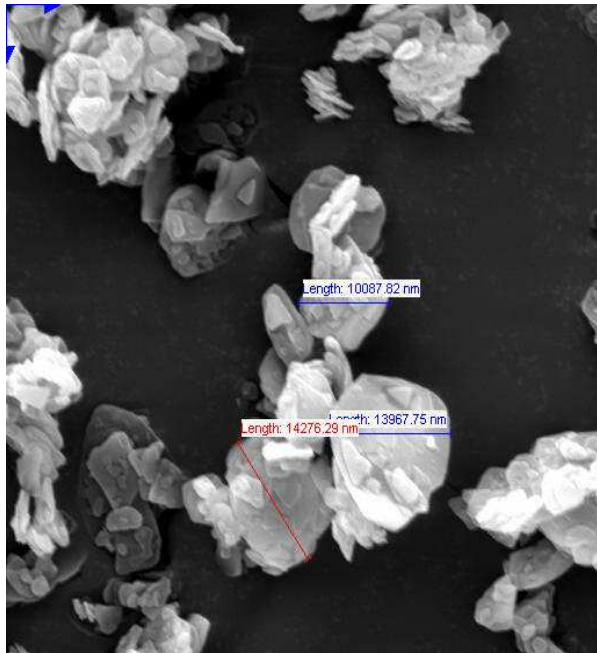


E

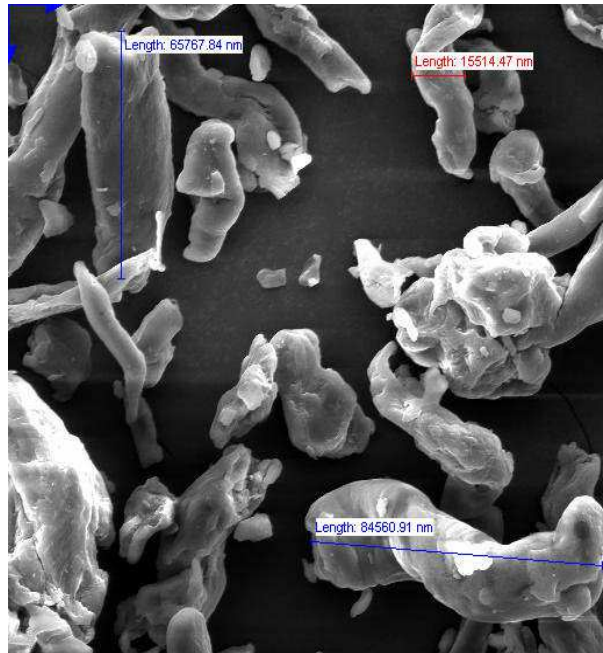
F

Figure 3.1 Typical SEM showing particle morphology of TDF (A), CCS (B), Kollidon[®] 30 (C), sorbitol (D), MCC (E) and Kollidon[®] CL-M (F)

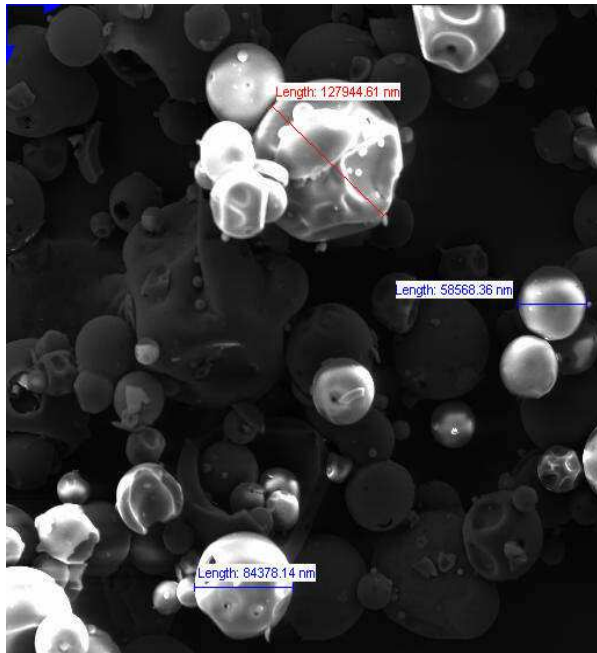
SEM images of dry MCC powder reveal that the particles are granular and highly porous (Figures 3.1 E and 3.2 E). The porosity facilitates rapid liquid uptake by capillary action. MCC swells in contact with water and the ability to absorb water permits release during extrusion that provides lubrication for extrusion to be successful. Furthermore extrudate containing MCC have good plastic characteristics that lead to easier rounding of the pellets during spheronization. The smaller the particle size of MCC used the larger surface area that facilitates greater interaction with water leading to an improvement in API release. SEM images for Kollidon[®] CL-M (Figures 3.1 F and 3.2 F) reveal that the particles have a small particle size and therefore a large surface area. Kollidon[®] CL-M particles are also porous and aid lubrication of extrudate surfaces during extrusion. SEM images of CCS (Figures 3.1 B and 3.2 B) reveal rod shaped particles that swell when in contact with water and this accounts for the disintegrant activity of this material. SEM images of sorbitol (Figures 3.1 D and 3.2 D) show the popcorn crystalline particles that absorb water during dissolution thus enhancing dissolution rate.



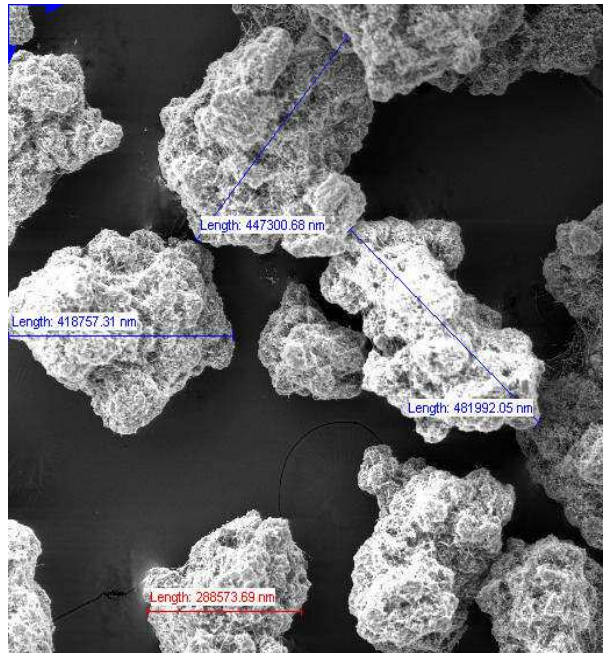
A



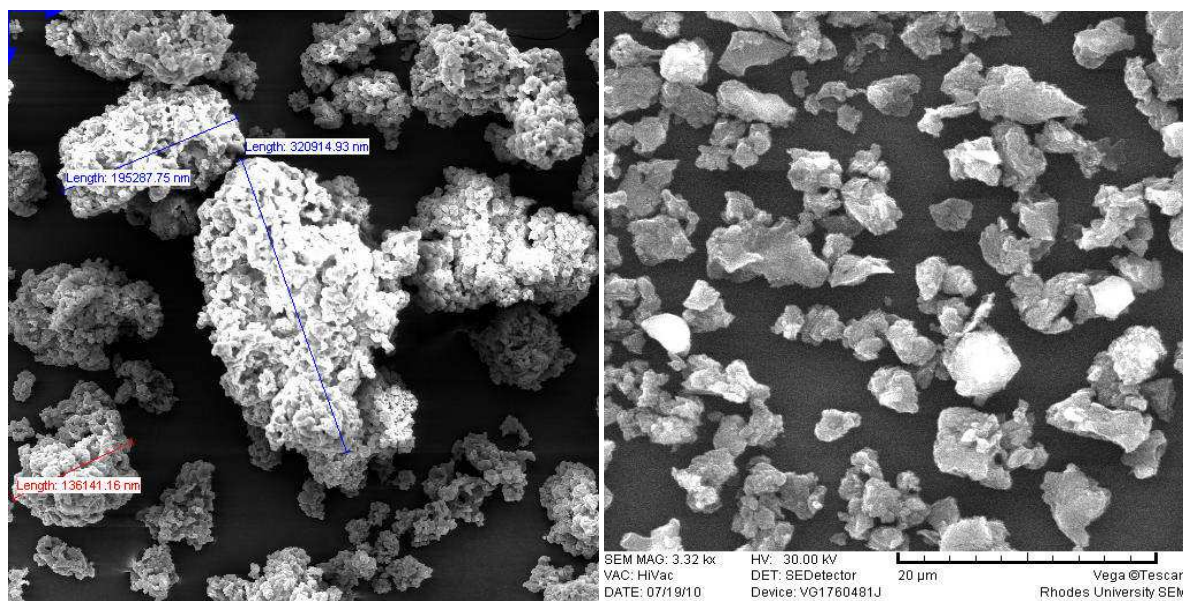
B



C



D



E **F**
Figure 3.2 Typical SEM showing particle size range of TDF (A), CCS (B), Kollidon[®] 30 (C), sorbitol (D), MCC (E), Kollidon[®] CL-M (F).

3.3.2 Density

3.3.2.1 Bulk and tapped density

The data from bulk and tapped density testing of TDF, MCC, CCS, Kollidon[®] CL-M, Kollidon[®] 30 and sorbitol are summarized in Table 3.2.

Table 3.2 Bulk and tapped density of materials

Material	Bulk density (g/ml)		Tapped density (g/ml)		Reference
	Actual	Literature	Actual	Literature	
TDF	0.312±0.015	0.300	0.450±0.014	Not stated	-
MCC	0.273±0.016	0.320	0.320±0.015	0.450	[110]
CCS	0.531±0.013	0.529	0.610±0.015	0.819	[111]
Kollidon [®] CL-M	0.322±0.020	0.250	0.411±0.154	0.500	[112]
Kollidon [®] 30	0.478±0.015	0.390	0.500±0.013	0.540	[112]
Sorbitol	0.516±0.019	0.448	0.710±0.011	0.400	[113]

The calculated values for CI and HR for all raw materials are summarized in Table 3.3

Table 3.3 Carr's index and Hausner ratio for raw materials.

Material	CI	HR
TDF	31.23±1.27	1.51±0.02
MCC	15.13±1.10	1.22±0.03
CCS	12.43±1.70	1.18±0.05
Kollidon [®] CL-M	19.92±3.10	1.32±0.07
Kollidon [®] 30	4.10±1.08	1.11±0.02
Sorbitol	25.32±2.89	1.54±0.16

The true density value of a powder provides useful information that can be applied to the characterization of the mechanical properties of powders on which properties of pellets such as hardness, flowability and shape are reliant. Due to the fact that powders flow under the influence of gravity, dense particles are generally less cohesive than low density particles of similar size and shape. Determination of the true density of the API and potential excipients is a vital part of preformulation studies with regard to pellets as these data are used to determine the porosity and flowability of a powder.

The data summarized in Tables 3.2 and 3.3 reveal that experimentally determined values for density generally deviate from those reported in the literature. This is most likely due to the fact that true densities are typically calculated using a helium pycnometer an instrument that was not accessible for the purposes of this research. The data was generated empirically by measuring the weight and volume. The deviations noted may therefore be attributed to the use of this approach and variations in machined tooling.

Microcrystalline cellulose has been extensively studied as an extrusion-spheronization aid. It has been proposed that MCC enhances the tensile strength of a wet mass through auto-adhesion that in turn imparts strength to pellets manufactured with MCC thereby resulting in the production of a hard, non-compressible and non-disintegrating product. When mixtures of an API and MCC are extruded and spheronized, the MCC acts as a matrix from which the API can slowly dissolve and be released. The void volume and packing properties of MCC play an important role in determining water retention and release characteristics during extrusion-spheronization that in turn has an impact on the grade of MCC to use and subsequently the ultimate qualities of the pellets produced.

Koo and Heng reported that an increase in density of the MCC used results in a decrease in the sphericity of the resultant pellets as MCC has an impact on shaping forces during extrusion-spheronization[56]. MCC grades with higher tapped densities produced pellets with poorer flow properties whereas grades with high packing densities produce pellets of higher bulk and tapped densities with low water content. Therefore at low water content the packing and void volumes of MCC play a vital role in determining the packing density of the resultant pellets. However as the size of the pellets increase with higher water content, the influence of the tapped density of MCC on the packing properties of pellets is larger.

The tapped and bulk densities of the MCC grade used was low (Table 3.2) thereby allowing the formation and shaping forces involved during the extrusion-spheronization process to produce pellets of the desired shape and size.

The calculated CI indicate that CCS, Kollidon[®] CL-M, Kollidon[®] 30 and sorbitol are likely to exhibit good flow and compressibility properties whereas TDF is likely to exhibit poor flow and compressibility properties. The HR data listed in Table 3.3 are < 1.25. These values are generally

considered to indicate that materials are likely to exhibit good flow properties. Most of the excipients to be used for pellet manufacture exhibit good flow characteristics making dry powder blending easier, thereby ensuring powder blend homogeneity.

The data generated in these studies are valuable as the intended method of manufacture of TDF pellets was through an extrusion-spheronization process. It was therefore important to assess the flowability and powder density of raw materials to ensure that content uniformity would be achieved during wet granulation and deformation during the extrusion process. These data reveal that the extrusion-spheronization approach may be an appropriate and successful method for the manufacture of TDF pellets using the excipients listed in Table 3.2.

3.3.3 Polymorphism

3.3.3.1 DSC

The DSC thermogram for TDF is depicted in Figure 3.4. The thermogram exhibits an endothermic peak at 117.17°C ($\Delta H = 82.3437$ J/g) which is associated with the melting phase transition of the α -polymorph of TDF. Another thermal event is observed at a lower temperature as a small endothermic transition at 114°C ($\Delta H = 12.0220$ J/g) which is associated with the melting of the β -polymorph (112 - 114°C). The melting enthalpies, intrinsic dissolution rates and solubility of crystal forms of TDF are indistinguishable and therefore these solid-state differences are unlikely to result in undesirable formulation or clinical consequences.

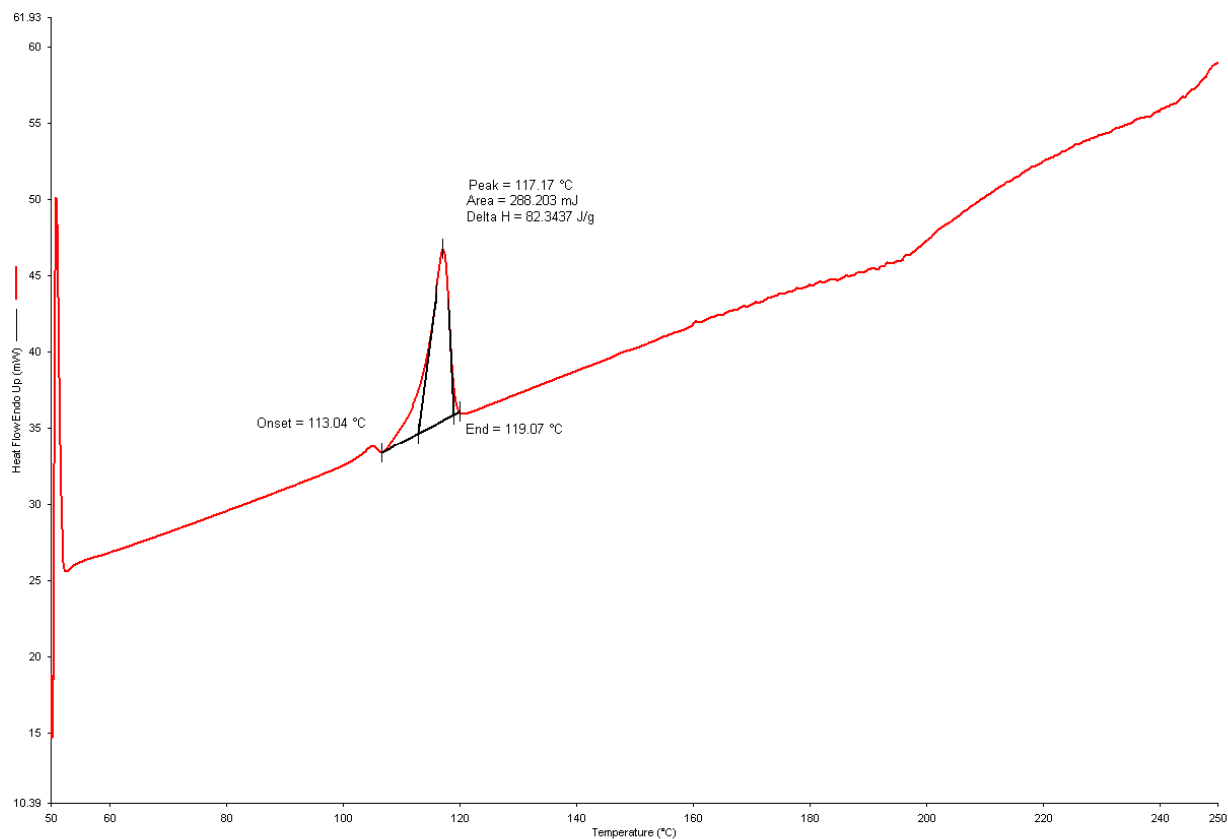


Figure 3.4 Typical DSC thermogram for TDF generated at a heating rate of 10°C/min

The DSC thermogram for sorbitol (Figure 3.5) exhibits a melting point endotherm at 99.17°C ($\Delta H = 158.6913$ J/g) and this data is in close agreement with the reported melting point of anhydrous sorbitol of 99°C[83].

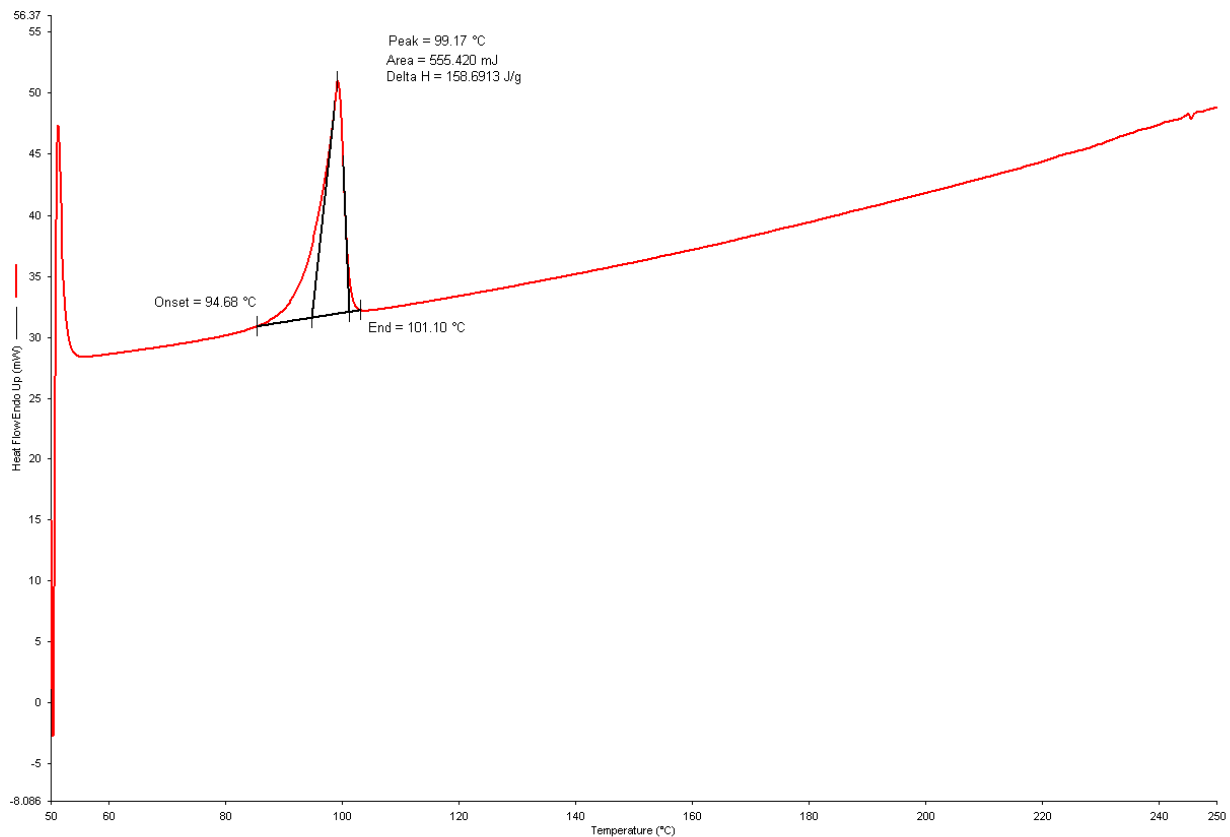


Figure 3.5 Typical DSC thermogram for sorbitol generated at a heating rate of 10°C/min

The thermograms for Kollidon[®] CL-M, Kollidon[®] 30 and croscarmellose sodium revealed no significant thermal events within the temperature ranges studied and the thermograms are depicted in Figures 3.6 – 3.8.

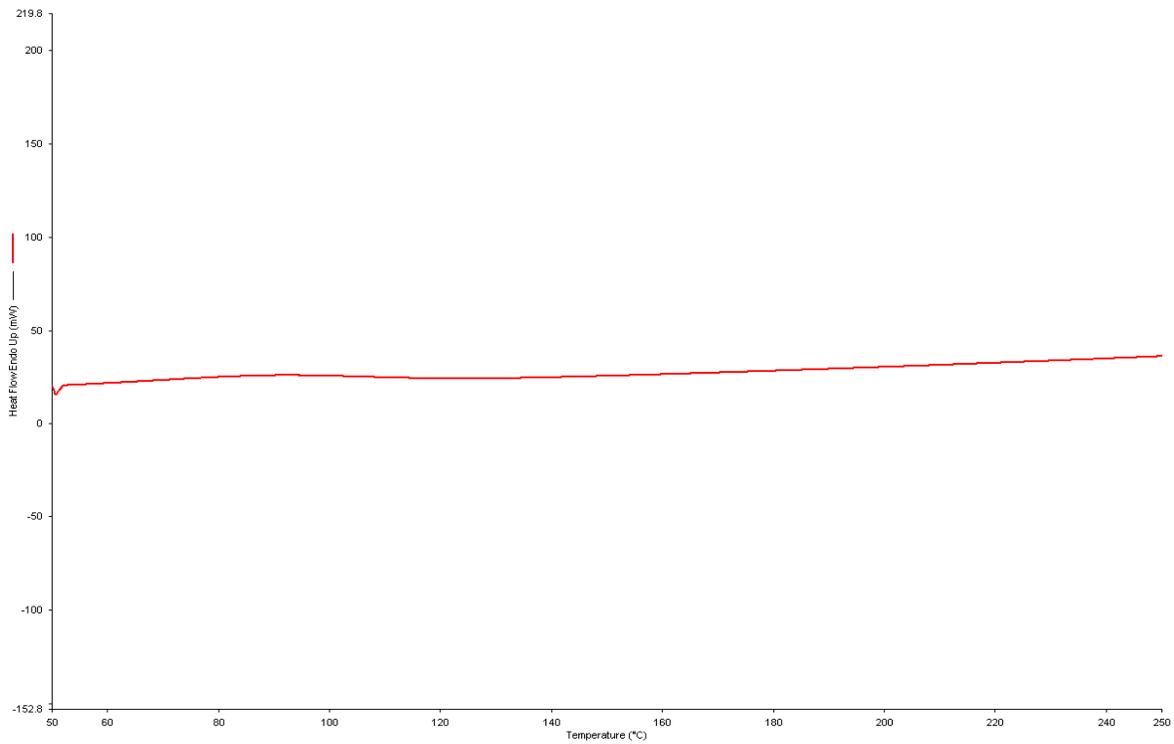


Figure 3.6 Typical DSC thermogram for Kollidon[®] CL-M generated at a heating rate of 10°C/min

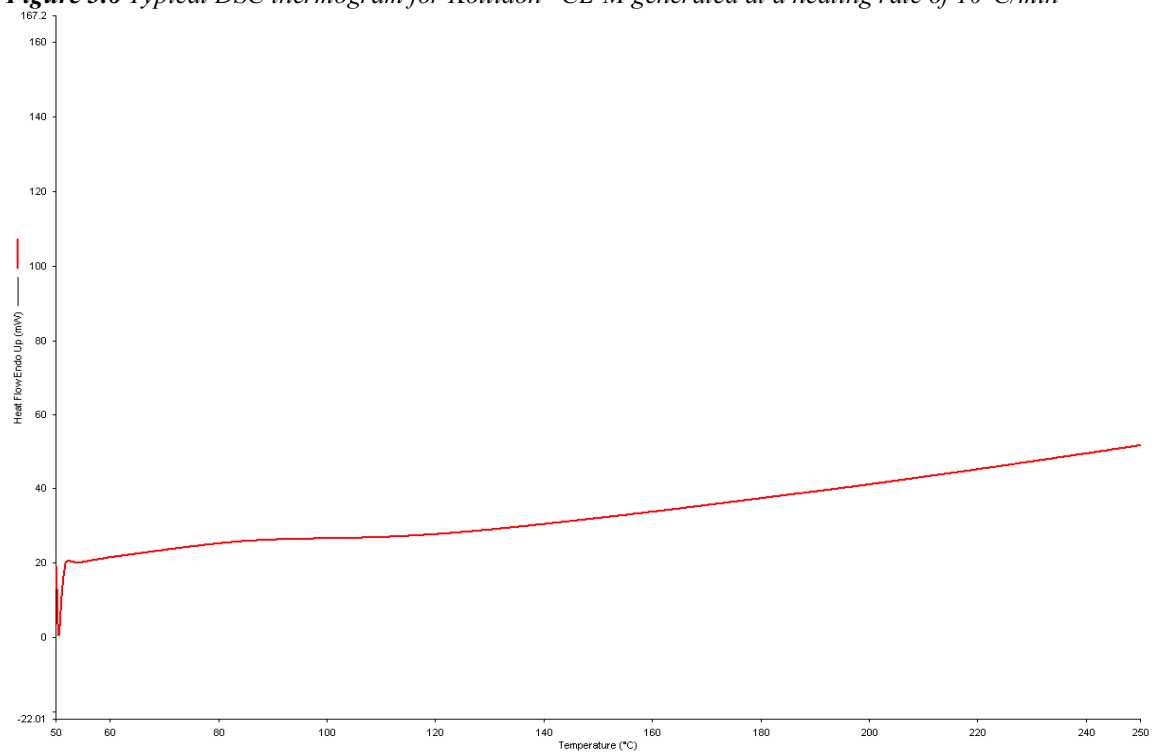


Figure 3.7 Typical DSC thermogram for Kollidon[®] 30 generated at a heating rate of 10°C/min

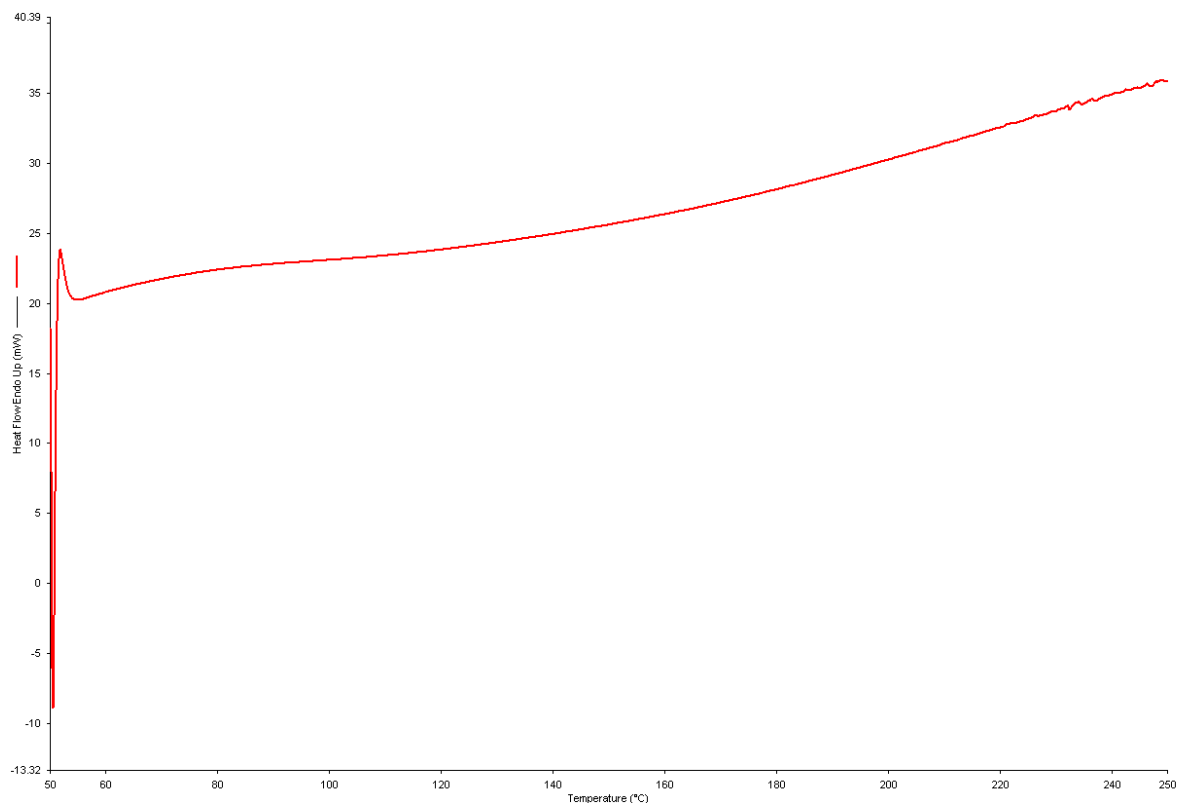


Figure 3.8 Typical DSC thermogram for croscarmellose sodium generated at heating rate of 10°C/min

The DSC thermograms of binary mixtures of TDF in a 1:1 ratio with croscarmellose sodium, Kollidon[®] CL-M and Kollidon[®] 30 are depicted in Figures 3.9 – 3.11 and reveal transition endothermic peaks at temperatures of 118°C ($\Delta H = 24.3772$ J/g), 117.83°C ($\Delta H = 24.2020$ J/g) and 118.50°C ($\Delta H = 15.9490$ J/g), respectively. The peaks are due to melting of the stable α -polymorph of TDF which is the primary composition of TDF. The minor melting point changes with reference to pure TDF were not considered significant and do not support a conclusion relating to the likely occurrence of incompatibility between TDF and the excipients. The peak height decrease observed in the thermogram may be attributed to the use of a low sample mass and a change in reaction kinetics as a consequence of dilution of TDF with the relevant excipient.

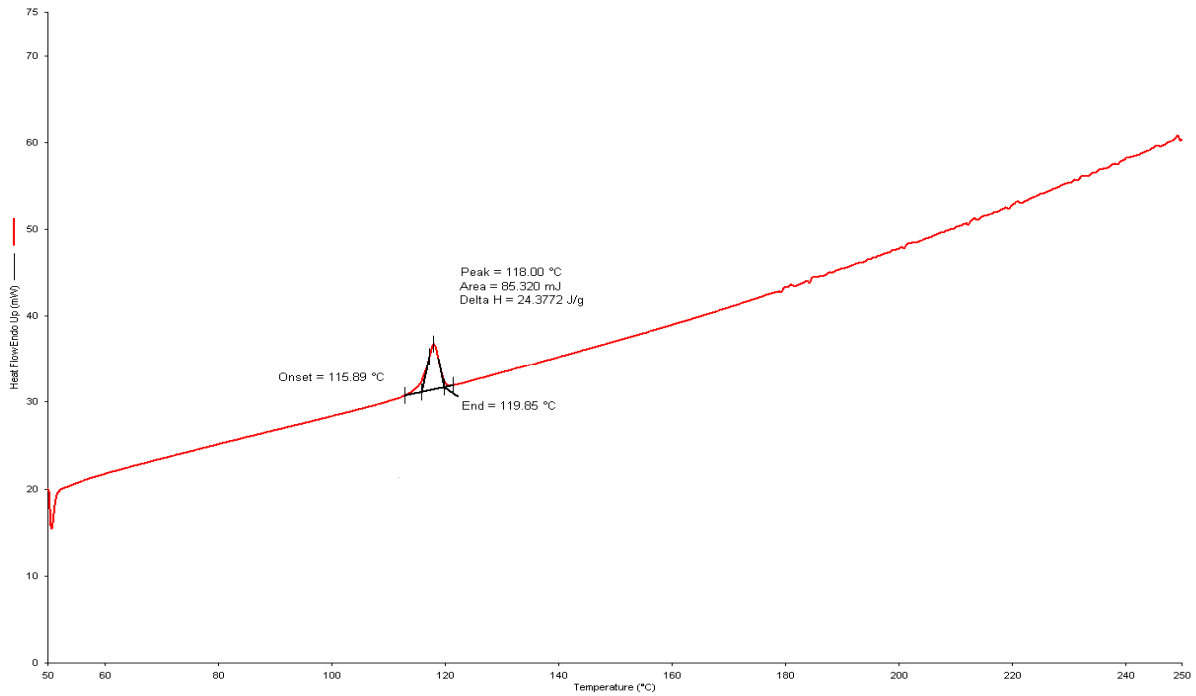


Figure 3.9 Typical DSC thermogram for a 1:1 binary mixture of TDF and croscarmellose sodium generated at a heating rate of 10°C/min

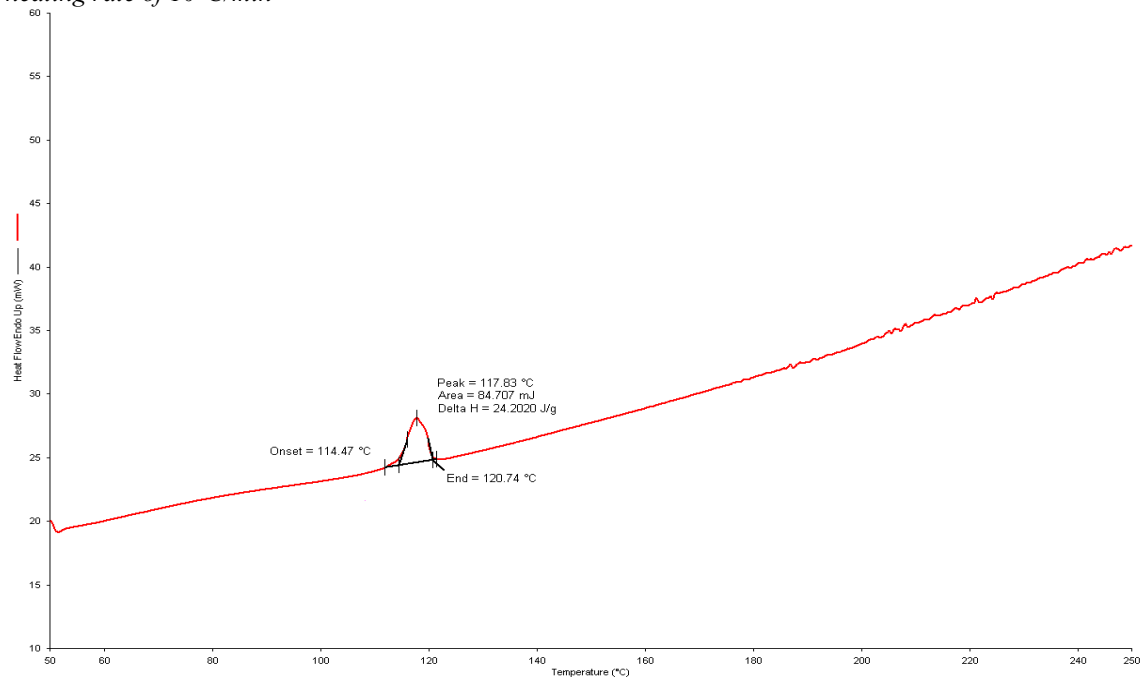


Figure 3.10 Typical DSC thermogram for a 1:1 binary mixture of TDF and Kollidon[®] CL-M generated at a heating rate of 10°C/min

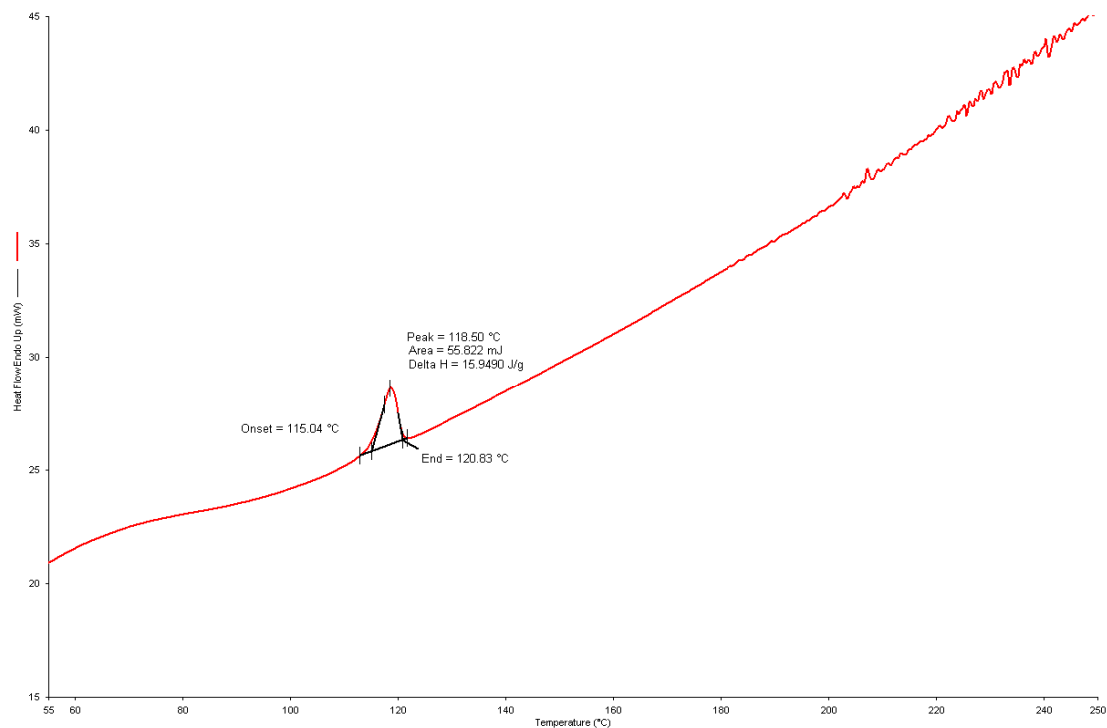


Figure 3.11 Typical DSC thermogram for a 1:1 binary mixture of TDF and Kollidon[®] 30 generated at a heating rate of 10°C/min

The thermogram following analysis of a 1:1 binary mixture of TDF and sorbitol is depicted in Figure 3.12 and reveals the presence of two transition endotherms at temperatures of 98.83°C ($\Delta H = 179.3903$ J/g) and 115.33°C ($\Delta H = 54.3230$ J/g) which are due to melting of sorbitol and TDF respectively. The melting point of TDF was lowered by 3°C and the resultant melting point is within the melting point range of 115 - 118°C which is attributed to the stable α -polymorph. This finding confirms that there is no evidence to support a conclusion relating to potential incompatibility of TDF and the excipients to be used.

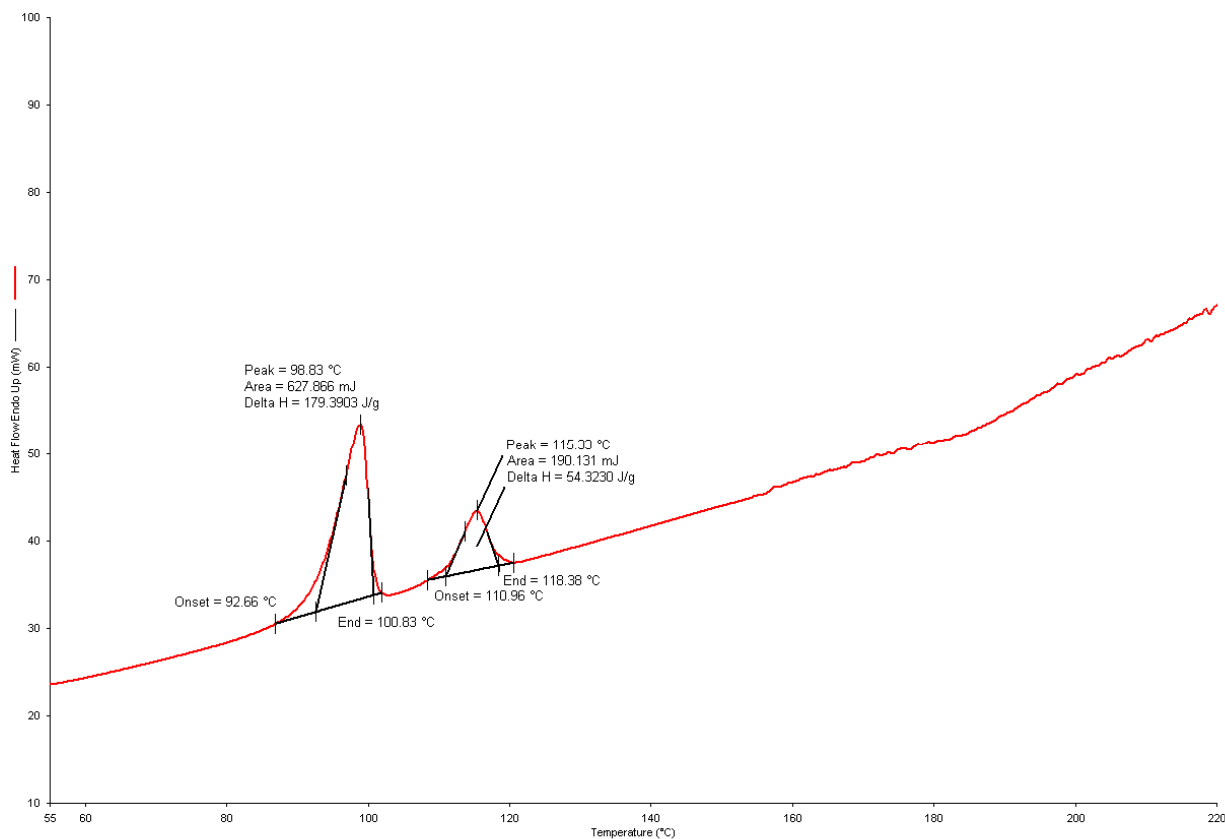


Figure 3.12 Typical DSC thermogram for a 1:1 binary mixture of TDF and sorbitol generated at a heating rate of 10°C/min.

3.3.3.2 IR spectroscopy

A typical IR spectrum for TDF is depicted in Figure 3.12. The main absorbance bands in the spectrum of TDF show an aromatic C-H stretch at 2985 cm^{-1} , two weak intensity broad O-H bands at 3051 cm^{-1} and 3208 cm^{-1} , P=O stretch at 1674 cm^{-1} , an aromatic C=N stretch in pairs at 1376 cm^{-1} and 1421 cm^{-1} , a medium stretch of NH_2 scissoring band at 1504 cm^{-1} and 1622 cm^{-1} , various N-H wagging bands at 670-950 cm^{-1} and various C-H out of plan deformations at 950-650 cm^{-1} [12]. These characteristic bands were also observed when IR spectra of 1:1 physical mixtures of excipients and TDF were evaluated and revealed the same absorbance bands obtained from a pure sample of TDF. The individual IR spectra of excipients and 1:1 TDF and excipient mixtures are depicted in Figures 3.13 – 3.17 and clearly indicate that no obvious physical interactions occurred between TDF and any of the excipients to be used.

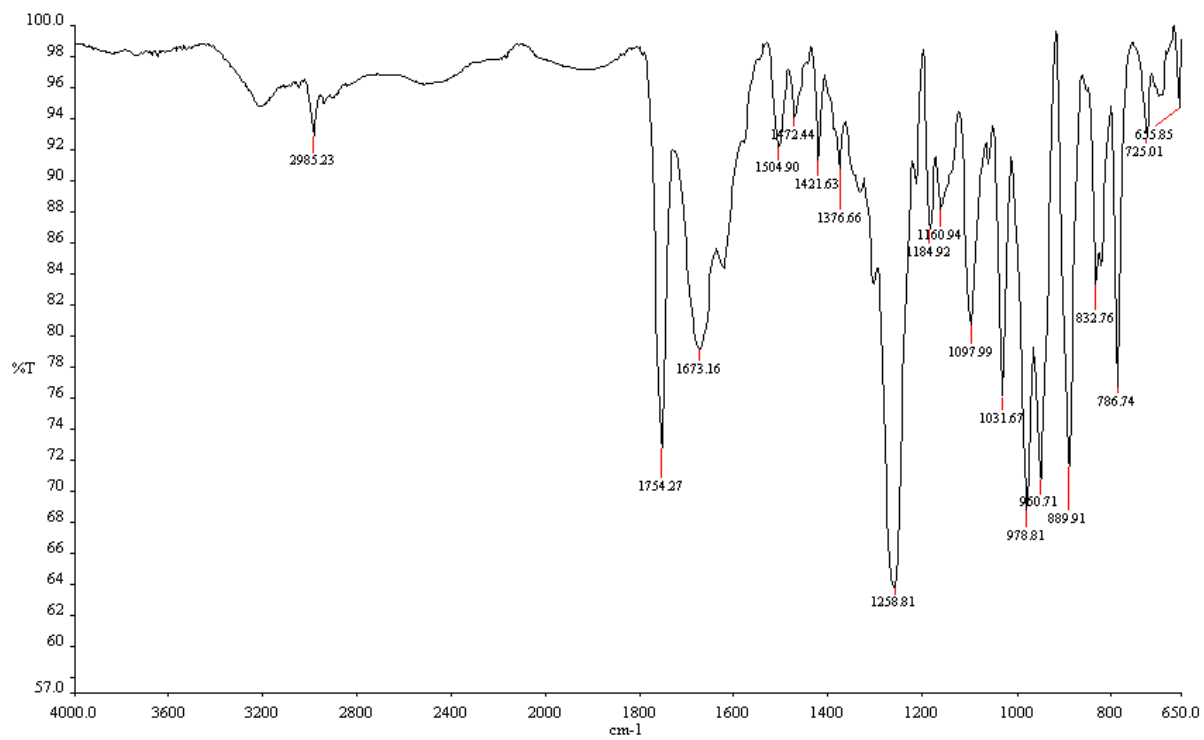


Figure 3.13 Typical IR spectrum of TDF.

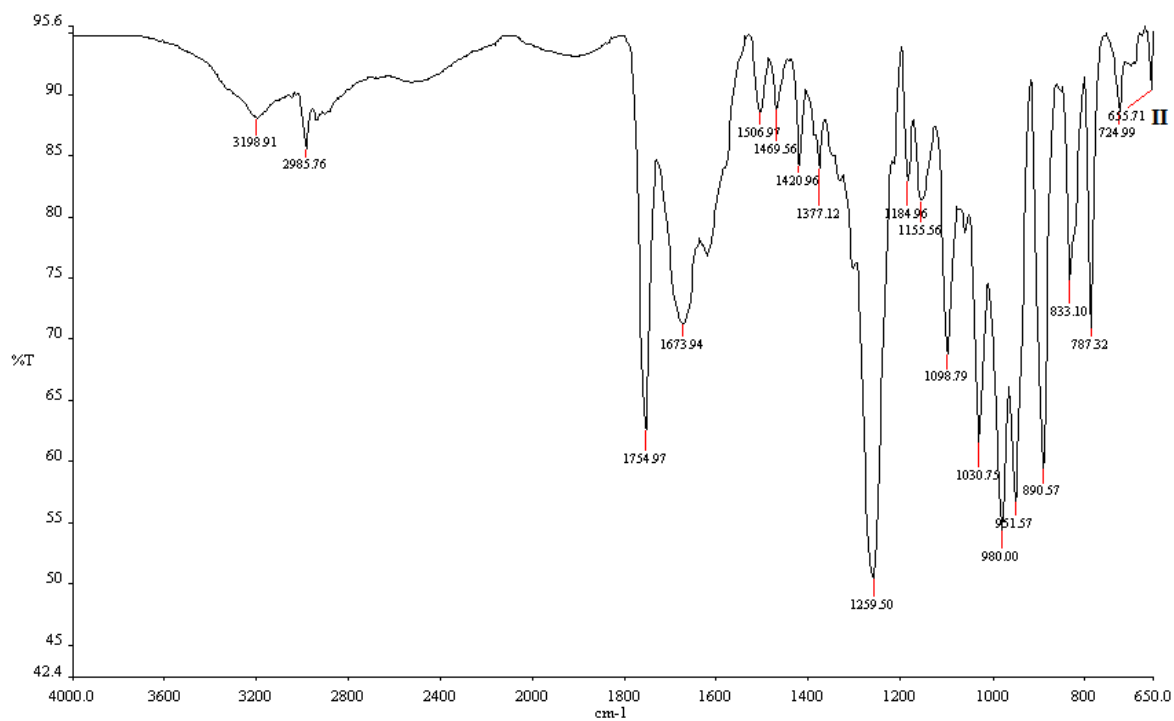
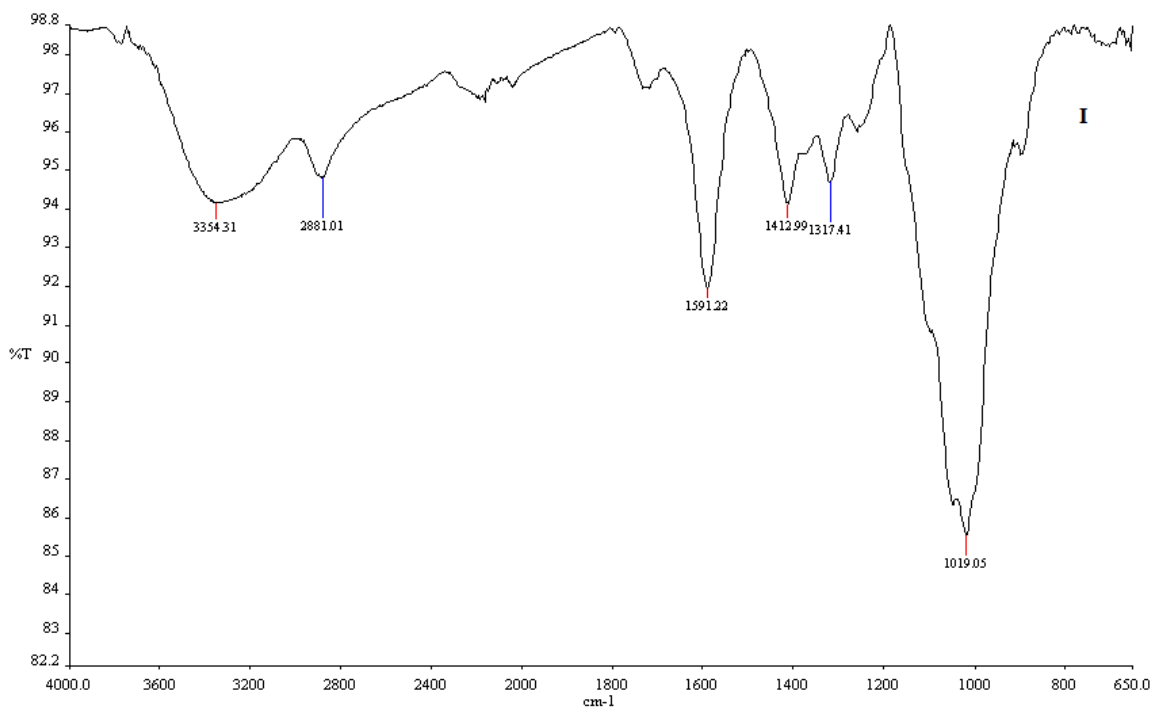


Figure 3.14 Typical IR spectrum of CCS (I) and a 1:1 binary mixture of TDF and CCS (II).

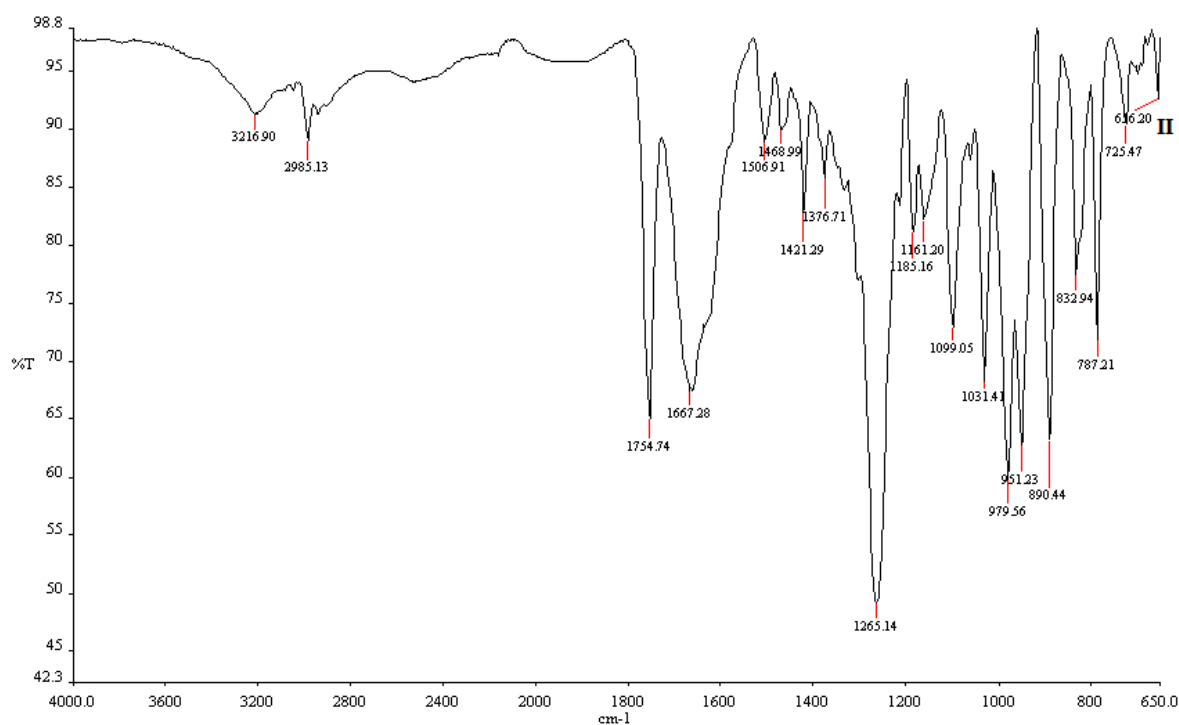
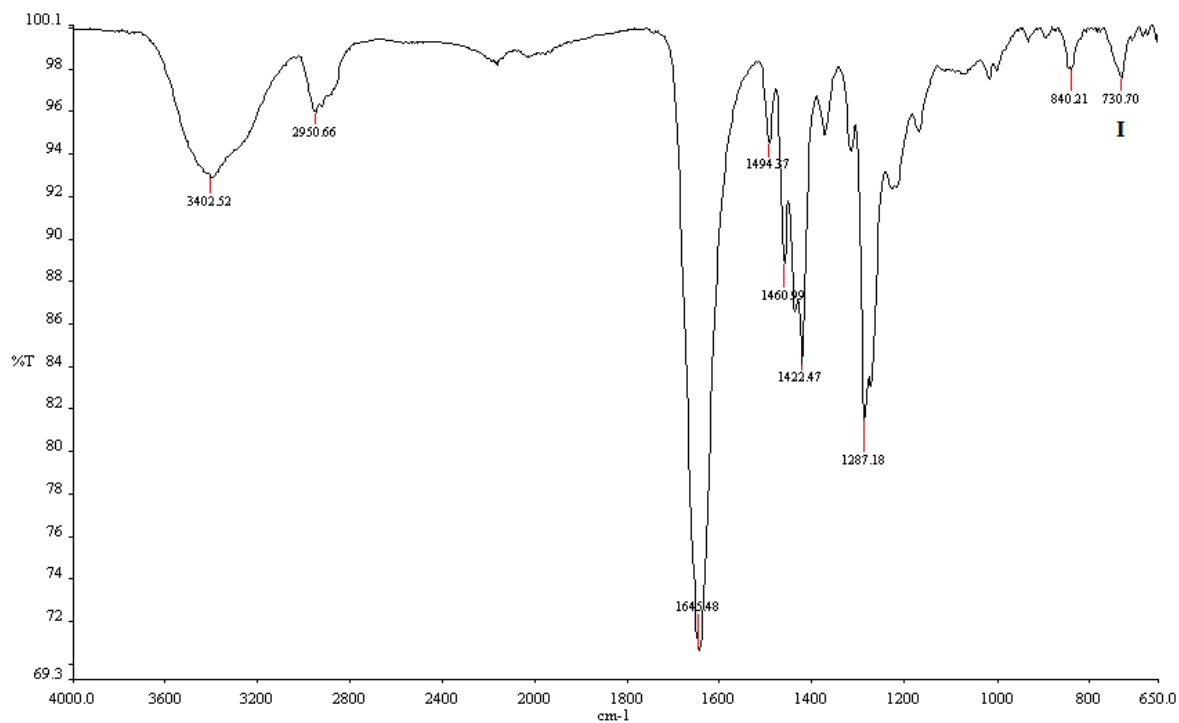


Figure 3.15 Typical IR spectrum of Kollidon® 30 (I) and a 1:1 binary mixture of TDF and Kollidon® (II).

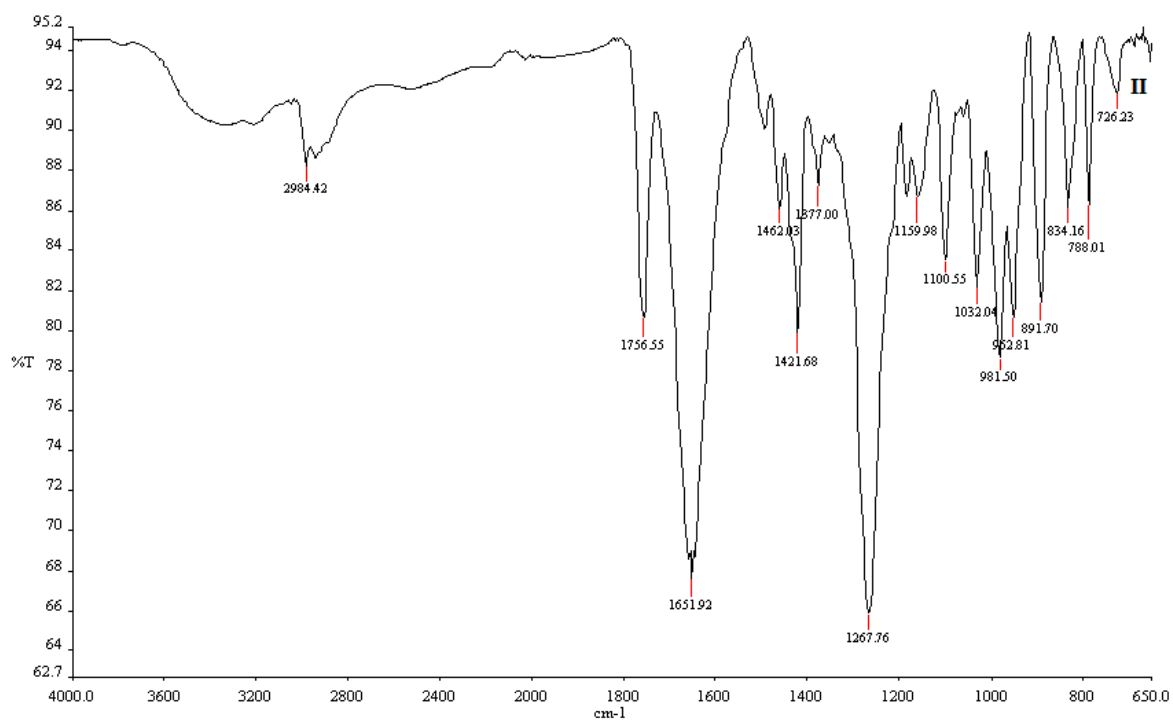
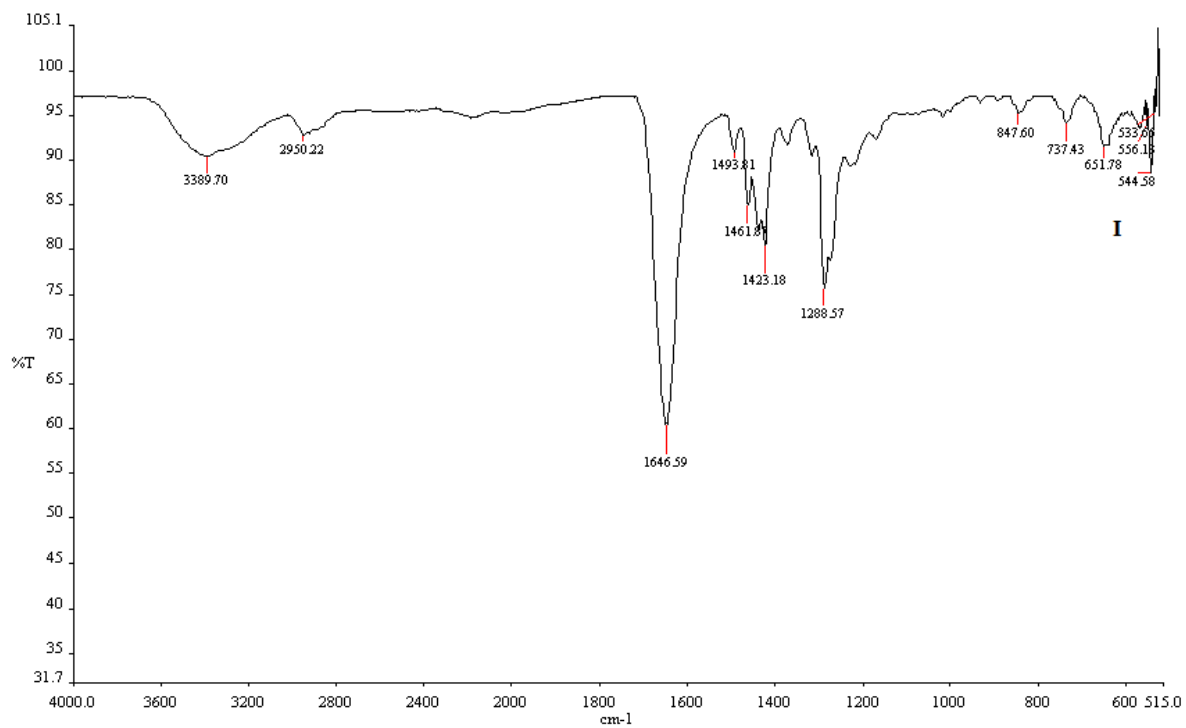


Figure 3.16 Typical IR spectrum of Kollidon® CL-M (I) and a 1:1 binary mixture of TDF and Kollidon® CL-M (II).

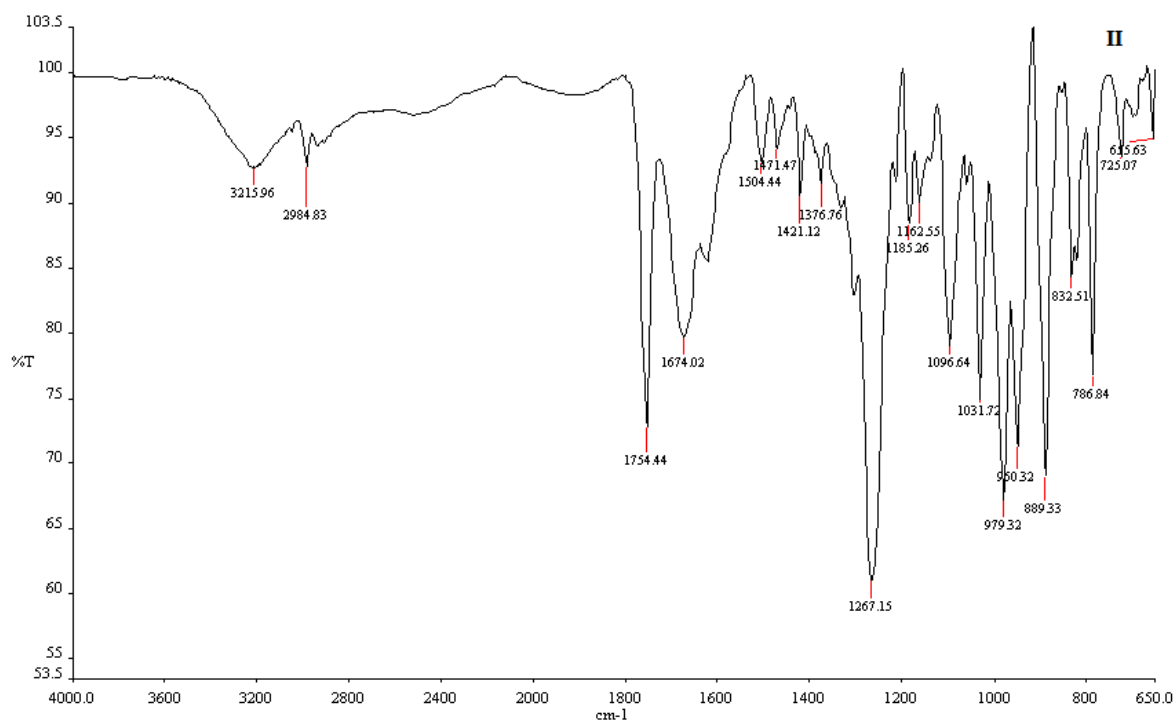
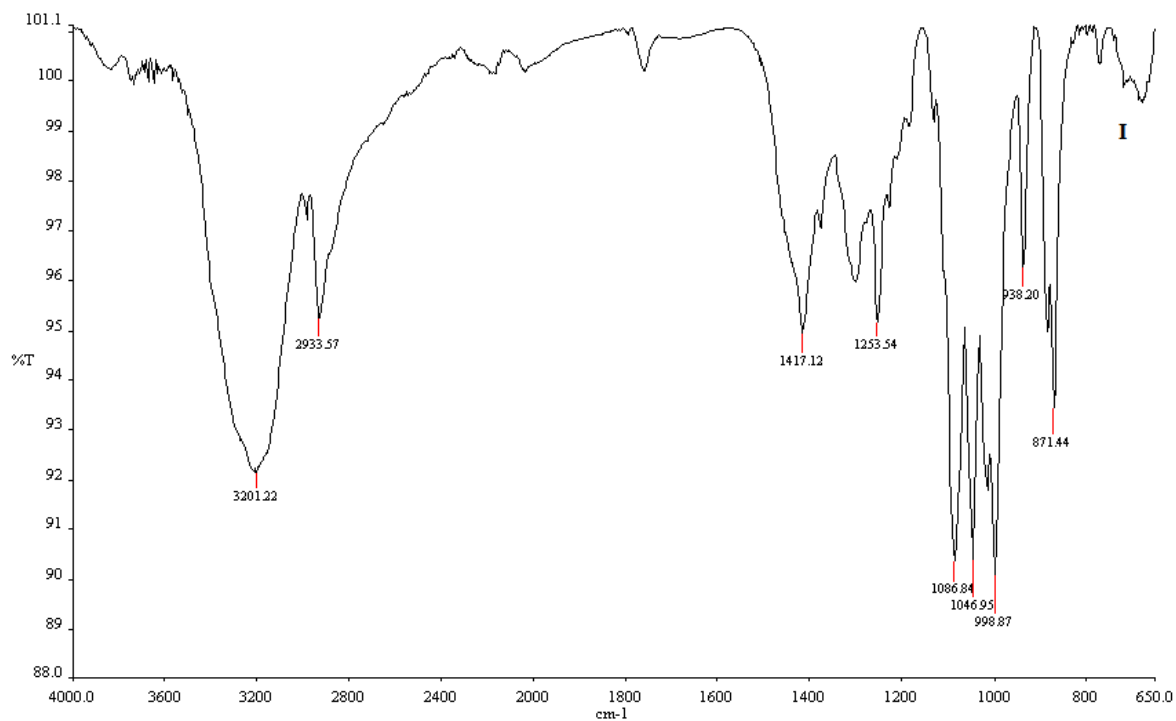


Figure 3.17 Typical IR spectrum of sorbitol (I) and 1:1 binary mixture of TDF and sorbitol (II).

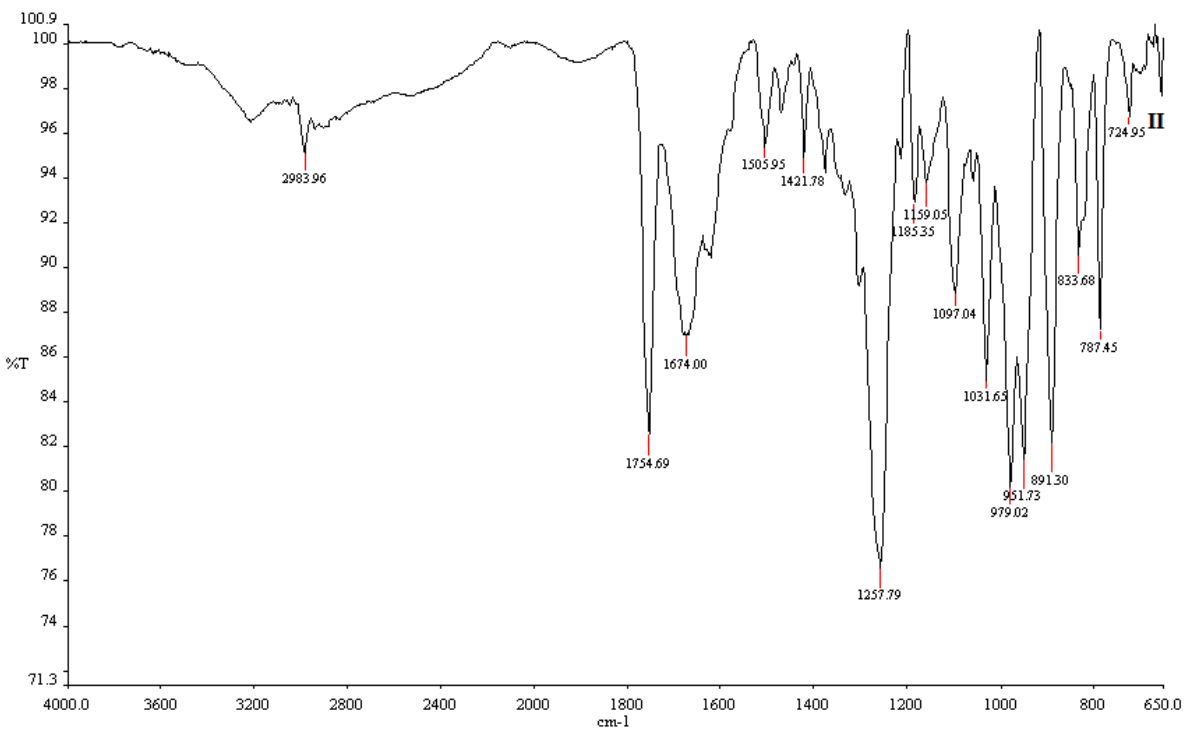
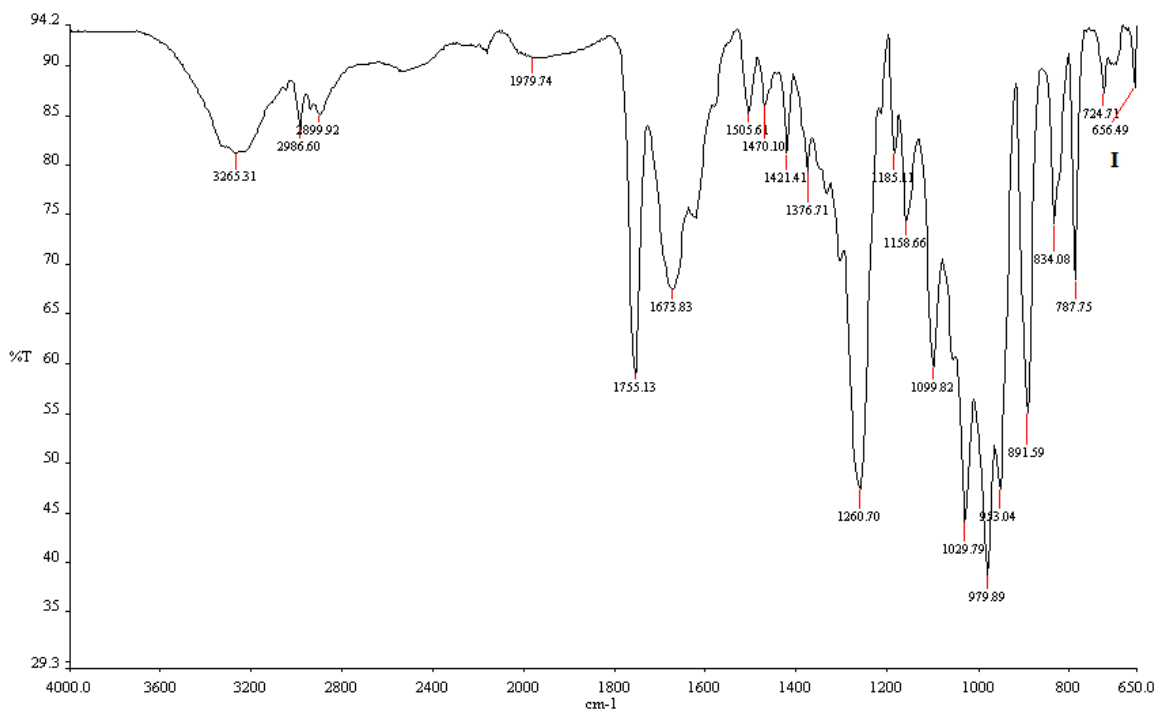


Figure 3.18 Typical IR spectrum of MCC (I) and a 1:1 binary mixture of TDF and MCC (II).

3.4 CONCLUSIONS

Preformulation studies are of vital importance during formulation development as they provide formulation scientists with relevant data to facilitate the prediction and behavior of a product during manufacture. Although the data offer no certainty, these studies form the foundation for building quality into pharmaceutical products.

The physical characteristics of MCC, CCS and Kollidon[®] CL-M established using SEM clearly confirm that the compounds possess the potential to exhibit suitable flowability and water retention properties as evidenced by the CI, HR and apparent sponge-like morphology of the materials. Furthermore SEM indicates that the particle size of all excipients and TDF are of similar size and range thereby ensuring that efficient powder blending is a likely result during processing which in turn would ensure product homogeneity.

DSC data revealed that no interactions were likely to occur between TDF and the excipients investigated and therefore no incompatibility reactions were expected during and following product manufacture. These findings were confirmed by IR analysis and no physical interaction between any of the excipients and TDF was observed or was likely to occur. DSC data revealed the existence of α and β -polymorphic forms of TDF as two enthalpy changes were observed in the DSC thermograms. The existence of two polymorphs is unlikely to result in incompatibility reactions and is further confirmed by the results of IR analysis.

The IR spectra for TDF revealed the presence of all characteristic peaks in 1:1 binary mixtures of TDF with each excipient. Therefore it can be concluded that TDF is compatible with all excipients tested and thermal analysis of TDF confirmed the stability of TDF under manufacturing conditions. The degradation temperature measured using DSC confirms that it is unlikely that manufacturing difficulties would arise during extrusion, spheronization and drying operations.

Significant data relating to the suitability for formulation and manufacture of TDF pellets with excipients tested have been generated and details of the manufacture of TDF pellets are reported in Chapter Four *vide infra*.

CHAPTER FOUR

FORMULATION DEVELOPMENT AND MANUFACTURE OF TENOFOVIR DISOPROXIL FUMARATE PELLETS

4.1 INTRODUCTION

4.1.1 Overview

Pharmaceutical dosage forms are drug delivery systems that are designed to deliver an API to the site of action. To achieve an optimal therapeutic response from any dosage form the API must be delivered at a rate and concentration that minimizes side-effects and maximizes therapeutic response for patients. Some common examples of well-established dosage forms include tablets, capsules, suppositories, parenterals and transdermal patches. The choice of a specific route of administration is dependent on a number of factors including but not limited to the nature of the API, site and onset of action, frequency of administration and age of the patient [84]. The oral route of administration is considered the most convenient route for drug delivery as it is adaptable, offers patient convenience and the most commonly used oral dosage forms include tablets and capsules [114, 115].

The use of multi-unit pellet systems (MUPS) in which delivery technologies are incorporated into capsules has increased over the years as they offer advantages for effective drug delivery [116]. MUPS containing granules, pellets or mini tablets were introduced in the early 1950s [117]. The production of MUPS is a useful strategy to control or modulate the release of an API as observed by the reproducibility of release profiles when compared to those generated when single unit dosage forms such as tablets are administered. The development of multi-particulate systems is a promising area of pharmaceutical research concerned with achieving a high level of control over the release rate of an API and offers flexibility for the adjustment of dose and release of that API [118, 119].

There are different approaches to pelletization and include extrusion and spheronization, layering, solution layering, spray congealing and direct pelletization [116].

4.1.2 Manufacture of multi-unit particulate systems (MUPS)

4.1.2.1 Pelletization by solution layering

Solution layering involves the deposition of successive layers of a solution of API and the components of a formulation onto a nucleus that may be manufactured from inert materials or from crystals or granules of the API. During the solution layering process all components of a formulation are dissolved in the application vehicle and therefore the solid content and the viscosity of the liquid to be applied are affected by this composition [120]. As the solution or suspension is sprayed onto the product bed, droplets of liquid impinge and spread evenly over the surfaces of the nuclei if the drying conditions and fluid dynamics of the process have been optimized. A drying phase follows and dissolved materials crystallize onto the surfaces of the nuclei to form solid bridges between the core material and initial layer of API in addition to subsequent layers of API or formulation that are added. The process continues until the desired number of layers of API and therefore the target potency for the pellets is realized [121, 122].

4.1.2.2 Direct pelletization

Direct pelletization involves mixing of a powder blend that is then moistened with a solvent and/or binder. The blend is subsequently set onto a smooth mobile surface that rotates at a set speed and through centrifugal motion, agglomerates are formed that become uniform round dense pellets over time [123, 124]. The pellets are then dried in a fluid bed drier and a schematic of the general process of direct pelletization is depicted in Figure 4.1.

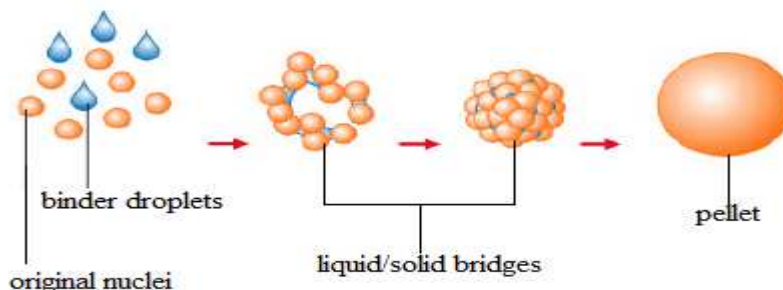


Figure 4.1 Schematic depicting the different stages of direct pelletization adapted from *Pellets: A general overview*[116]

4.1.2.3 Spray congealing

Spray congealing is a process in which an API is allowed to melt, disperse and/or dissolve in a hot melt comprised of a gum, wax or fatty acid material that is sprayed into an air chamber in which the air temperature is lower than the melting point of the formulation components in order to produce congealed spherical pellets [125, 126]. A critical requirement for any spray congealing process is that the formulation components have well-defined, sharp melting points or narrow melting zones. Consequently the number of excipients that a formulation scientist can select for this process is limited [127].

4.1.2.4 Extrusion and spheronization

Extrusion and spheronization is a multiple step process capable of making uniformly sized spherical particles that are referred to as pellets. The major advantage of extrusion and spheronization over other pelletization techniques is the ability of the process to ensure high drug loading without an excessive increase in particle size in an efficient and cost effective manner.

The first patent issued in the United States of America on the spheronization process was in 1964 using equipment known as a Marumerizer[®] [128]. This equipment is essentially similar to what is today, referred to as a spheronizer. This process gained recognition in 1970 when Conine and Hardley [129] outlined the actual steps involved in the extrusion and spheronization process. Reynolds [130] further provided a clear understanding of the mechanism(s) involved in the formation of spherical particles when using a spheronizer. Consequently with a greater understanding of the technique, formulation scientists recognized some of the potential advantages of using this approach to produce drug delivery technologies.

Extrusion- spheronization is a multi-step process that commences with dry mixing of an API with specific excipients, followed by wet granulation of the blend to produce a wet mass with appropriate plasticity that is extruded. The extrudate is then fed into a spheronizer fitted with an appropriate plate to produce spherical pellets after which the pellets are dried and screened to collect product of a pre-defined size distribution [131].

There are a number of varieties of extruders available but they can be generally classified as screw, gravity (sieve and basket) or piston fed (roll and ram) devices. The different types of

extruders available are depicted in Figure 4.2, and screw and gravity fed extruders are the primary types of extruder used in the pharmaceutical industry, whereas piston fed or ram extruders are most often used as research and development tools.

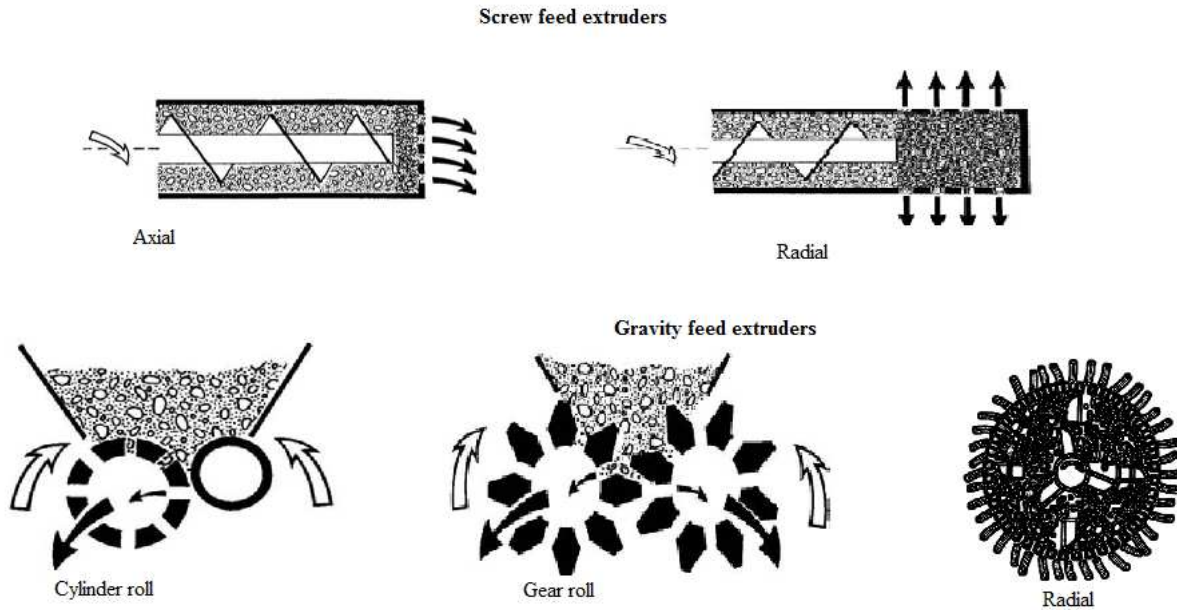


Figure 4.2 Extruders used for pellet manufacture adapted from *Pellets: A general overview*[116]

The primary variables in an extrusion process include feed rate, die opening diameter and length. In addition the fluid content of the granulate is critical since the properties of the resultant extrudate and subsequently the pellets are dependent on the plasticity, cohesiveness and lubricity of the wet mass [132]. The end-point of a granulation is also critical to ensuring that the wet mass has the appropriate plasticity and the determination of granulation end-point is further discussed in § 4.1.5, *vide infra*. The process variables and fluid content of a granulation determine the ultimate quality of an extrudate thereby also impacting the ultimate quality of pellets produced. An extrudate with extensive surface aberration will ultimately result in the production of poor quality pellets [132, 133]. The phenomenon of extrudate surface aberration is often referred to as shark skinning and this phenomenon is depicted in Figure 4.3. The presence of shark skinning is advantageous in facilitating the breakage of the extrudate during the spheronization process, however this is only true for certain types of extruders and this

phenomenon was found to hamper quality pellet production when ram extruders were used [134-136].

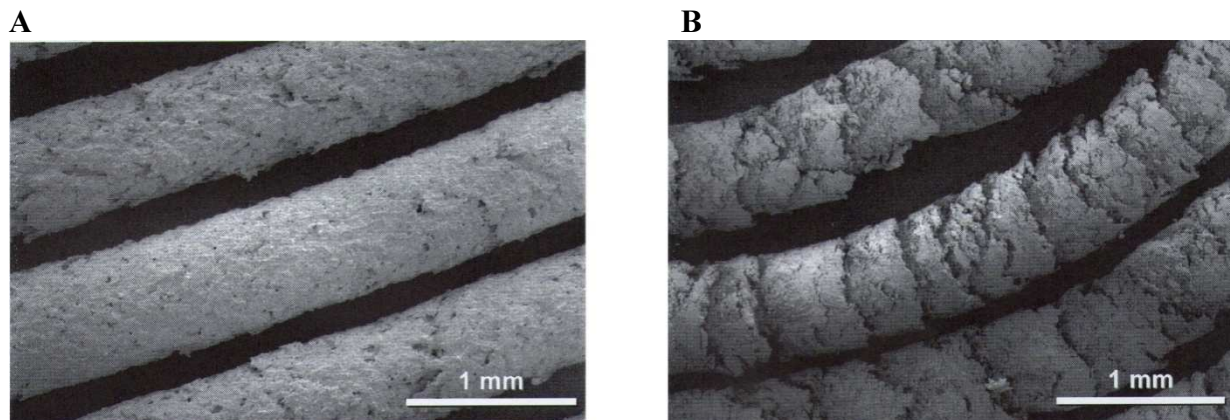


Figure 4.3 SEM images showing examples of a smooth extrudate (A) and an extrudate exhibiting shark skinning (B) adapted from *Pharmaceutical Extrusion Technology* [132]

The spheronization of materials is achieved using a spheronizer of which the primary working parts consist of a bowl and a rotating bottom plate or disk. Particle rounding is dependent on particle-particle and particle-disk interactions and in general two disk types are used *viz.*, either a radial or cross-hatched disk pattern as depicted in Figure 4.4.

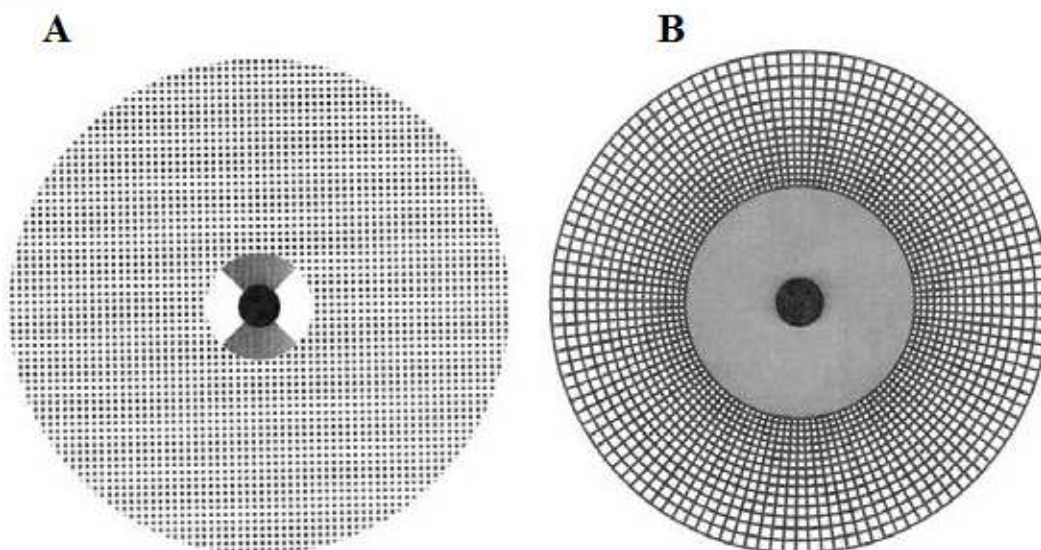


Figure 4.4 Two examples of spheronizer disk patterns *viz.*, cross-hatched (A) and radial (B)

Theoretically both types of plate should produce pellets of acceptable quality however some studies have shown that the rate of spheronization is more rapid when disks with radial patterns are used [137]. A number of proposals suggesting the mechanism of transformation of extrudate

from rod-shaped strands to spherical pellets in the spheronization chamber have been proposed [137-140]. At the beginning of the spheronization process when extrudate is loaded into the spheronizing chamber the mass is subjected to centrifugal forces that draw the material to the walls of the chamber. As the disk rotates there is a difference in particle velocity due to the varying location of particles in the chamber. As the particles move outwards towards the walls and the particles climb and fall onto the fast rotating disk the formation of a continuous flow of particles that appears as a rope-like mass as depicted in Figure 4.5 results. This phenomenon is a critical indicator of the quality of the extrudate that is produced and an over or under-wet extrudate results in particle movement without a rope-like motion and ultimately poor quality pellets are produced.

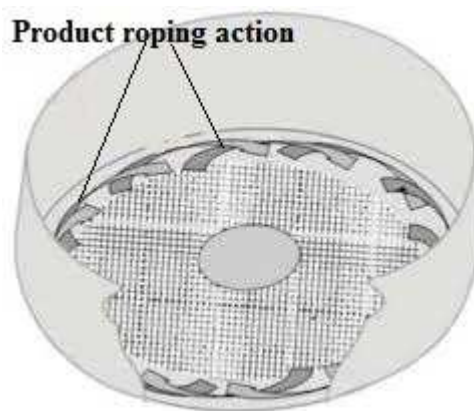


Figure 4.5 Characteristic rope-like formation observed during spheronization of extrudate adapted from Pellets: A general overview [116]

Two mechanisms have been proposed to describe the processes involved in transforming cylinder-shaped extrudate into spherical pellets. The formation of pellets is depicted, in part in Figure 4.6A and B. Rowe (Figure 4.6A) [138] described a transition in which almost cylindrical particles are first rounded and then form dumb-bell shaped particles that form ellipsoid-shaped materials prior to further shaping into spherical pellets. Baert *et al.*, (Figure 4.6B) [141] suggested that cylindrical particles initially deform into bent rod-shaped particles that are then twisted at the center to form a dumb-bell shape after which the dumb-bell shaped material splits at the center into two spherical shaped particles that have a single flat-side. The flat-sided spherical particles are then rounded to form spherical pellets during additional spheronization.

The exact process or mechanism by which shaping occurs may be composition dependent as both approaches are in agreement with particle-particle and particle-disk interactions that have been described when spherical pellets are formed.

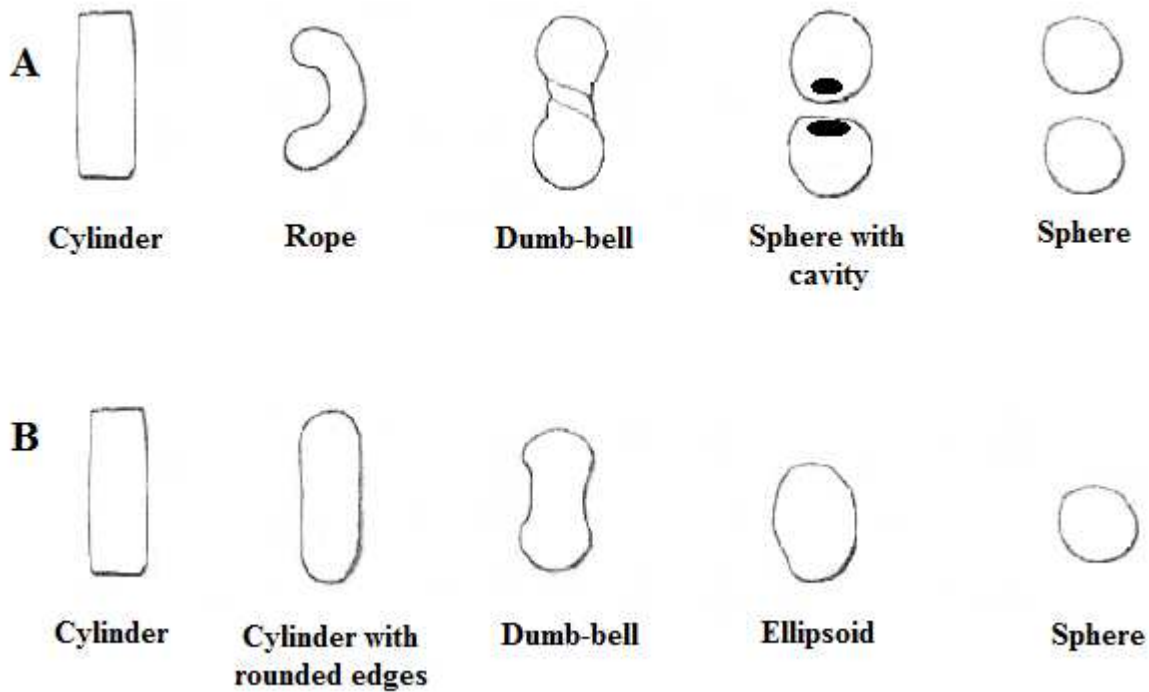


Figure 4.6 Graphic representation of the two models proposed to describe spheronization adapted from Pellets: A general overview [116]

A number of variables affect the spheronization process and include residence time in the spheronizer, disk speed, load size and chamber size of the spheronizer. Hasznos *et al.*, [142] reported that an increase in disk speed and residence time increased moisture loss during the spheronization process resulting in reduced extrudate plasticity that results in the formation of pellets that exist as deformed cylinders or dumb-bells (Figure 4.6B). However interaction between process variables may have a counter effect and an increase in load size may reduce moisture loss when the speed and residence time are increased. It has been suggested that the main variables affecting the shape of pellets include disk speed and residence time in the

spheronizer with high speeds and long residence times having been shown to produce more spherical-shaped particles [143].

The last step in the spheronization process requires drying of the pellets. Different approaches to drying include the use of tray, fluid bed and air drying. Tray drying is the slowest of these techniques and the use of fluid bed driers results in rapid drying since large volumes of material can be processed and high inlet air temperatures are used. Static tray drying is a slow process and introduces the possibility for an API to migrate to the surface of pellets and recrystallization of the API may occur. The more rapid the rate of drying in a fluid bed system minimizes the effects of migration an effect that is desirable since recrystallization may affect a number of the physical characteristics of particles and the dissolution rate of API particularly from controlled release formulations [144, 145].

4.1.3 Method of manufacture

The method of manufacture selected for the production of TDF pellets for inclusion into capsules was extrusion and spheronization due to the simplicity and cost effectiveness of this approach. The ability to achieve a high TDF loading is necessary to produce particles with a smaller mean size and therefore smaller sized capsules would be possible to deliver a specific dose. This in turn may result in better adherence, as patients would only need to take a single capsule. Pelletization using extrusion and spheronization is reproducible and pellets of uniform size and shape can be produced using commonly available excipients that are not excessively expensive.

4.1.4 Excipients

An excipient is a material that is used in a formulation to facilitate the manufacture of pharmaceutical dosage forms and ensure delivery of an API to the systemic circulation and/or site of action. Commonly used excipient types for extrusion and spheronization include but are not limited to binders, diluents, disintegrants, dissolution enhancers, solvents, flavourants, colourants, spheronization aids and anti-adherents.

4.1.4.1 Binders

Binders are adhesive materials that are incorporated in formulations to bind powders during pellet formation and to maintain pellet integrity following manufacture. Binders may be added to

a formulation as a solution or in powder form however addition using solutions is more efficient during the production of materials for extrusion. Initially liquid bridges hold powder particles together and as the binding liquid evaporates the binder precipitates and hardens to form the main bonding force in the materials. The physico-chemical properties of an API and the manufacturing process used have an impact on type of binder selected for inclusion in a formulation. In most cases the binder is usually applied from a solution in which the binder is used in a concentration range of between 2-10% w/w. However for poorly cohesive materials higher concentrations of binder may be required [146]. It is essential to optimize the amount of binder used so as to produce durable and non-friable pellets and ensure that the API is released at the desired rate. The selection of a binder and concentration thereof for use, is an important formulation variable to be investigated during development studies and commonly used binders for extrusion processes include gelatin, hydroxypropyl cellulose, methylcellulose, polyvinylpyrrolidone, sucrose and starch amongst others [147].

4.1.4.2 Diluents

Diluents are water soluble or insoluble materials that are included in pellet formulations to add bulk to products in which low doses of API are incorporated. A variety of diluents are available for use in pellet formulations and include sugars, starch and microcrystalline cellulose since these materials also facilitate pellet formation [148, 149]. The amount of diluent to be added is established by considering formulation and biopharmaceutical variables such as the desired dose, physical properties of the API and the manufacturing process to be used. Most pharmaceutical diluents are chemically compatible with most API however some materials are sensitive to changes in pH and should be used with appropriate diluents to facilitate the delivery of strongly acidic or basic molecules. When producing pellets by extrusion and spheronization the inert nature of excipients is important due to the high API to diluent ratio used in these technologies [150].

4.1.4.3 Disintegrants

Materials that are added to formulations to facilitate disintegration when the formulation comes into contact with liquids are classed as disintegrants. The purpose of disintegrant inclusion is to enhance dissolution of an API by ensuring that a large surface area of API is exposed to

dissolution fluids. Disintegrants counteract the effect(s) of binders and therefore the concentration of disintegrant to be used is determined in part, by the amount and type of binder used. Since the mechanism of disintegration involves moisture adsorption and/or swelling, prior to disruption of bonds that hold the dosage form together disintegrants must have considerable adsorptive and swelling properties to overcome the adhesive nature of binder(s) that may have been used. Some examples of disintegrants used in the manufacture of pellets include croscarmellose sodium, alginate and derivatives, crospovidone and sodium starch glycolate [151].

4.1.4.4 Surfactants

Dissolution enhancers are used in pellet formulations to improve the wettability of a product and to enhance dissolution rates of poorly soluble and hydrophobic compounds. Some examples of commonly used dissolution enhancers include sorbitol, sodium lauryl sulphate and non-ionic surfactants such as the polysorbates [152].

4.1.4.5 Spheronization aids

Spheronization aids are materials that are added to pellet formulations to facilitate the production of spherical pellets during the spheronization process. The materials confer plastic characteristics to formulations and impart binding properties that are essential for the production of pellets of suitable strength and integrity. The manufacture of rigid extrudate results in the production of dumb-bell shaped pellets with high levels of fine powders. Plastic extrudate without rigid characteristics tends to agglomerate and form excessively large pellets. To maintain a balance between rigidity and plasticity to ensure the production of pellets with appropriate characteristics, spheronization aids such as microcrystalline cellulose are used [153, 154]. Different types of microcrystalline cellulose have been studied to evaluate the impact on spheronization and it has been shown that individual physicochemical properties of materials are fundamental to produce pellets of the desired shape and size [155]. Other examples of spheronization aids that have been used for the manufacture of this type of product include polyvinylpyrrolidone, carrageenan, chitosan, pectinic acid, modified starches, sodium alginate and co-processed microcrystalline cellulose.

4.1.4.6 Separating agents

Separating agents are materials that adsorb onto surfaces and promote the separation of pellets into distinct units during the pelletization process. Inter-particulate adhesion as a result of surface charges formed during manufacture are a problem if the charge is not immediately dissipated by the addition of a liquid, as subsequent addition of binding agents may result in further adhesion and the production of large pellets [132].

4.1.4.7 Solvents

Different types of solvents have been used for wet granulation and include water, ethanol and isopropanol however due to safety concerns the use of organic liquids such as alcohol in pharmaceutical formulation and processing has diminished and the use of organic solvents has largely been replaced with aqueous based solvent systems. The granulation solvent ensures solvation of binders and wetting of powder blends that is important since the properties of the extrudate and the resulting pellets are dependent on the plasticity, cohesiveness and lubricity of the wet mass [132].

4.1.5 Wet granulation

Wet granulation approaches are used to produce granules and involve wetting of powder blends with a granulating fluid that is sprayed or poured onto the powder bed. The granulating fluid usually consists of a binder or wetting agent that is dissolved in an aqueous vehicle however, hydro-alcoholic solvents although dangerous have also been used when the API is susceptible to hydrolysis [138].

In order to produce the wet mass, a batch type mixer/granulator is generally used however any equipment that can produce a wet mass including continuous processors may be applied. Examples of batch-type processors include planetary, vertical or horizontal high shear and blade mixers [156]. The difference in granulation for extrusion and spheronization as compared to that for compression into tablets relate to the amount of granulating fluid required to produce the wet mass and the importance of achieving a uniform dispersion of the fluid in the powder blend for extrusion purposes. The amount of fluid needed to achieve pellets of uniform size and sphericity is greater than that required for a similar granulation intended for use in a tableting process.

Similarly the mixing time required to achieve granulating fluid uniformity is likely to be longer than that required for a tableting granulation [133, 157]. Over-granulation and the resulting dense particles produced are typically not of consequence for extrusion and spheronization as compared to the production of granules intended for compression. Torque rheometry has been used to characterize the deformation and flow characteristics of granulations used for extrusion-spheronization and it is a useful tool for identifying the rheological impact on formulation performance and process variations during the granulation process [158, 159].

Mixer torque rheometers are used for the characterization of wet powder masses regardless of their intended application. The mean torque and torque range or amplitude data can be used to assess the stages of a granulation procedure and the degree of spreading or interaction between formulation components. A schematic representation of the progressive stages of granule formation is depicted in Figure 4.7. Rowe and Parker [156, 160] reported that the torque range or amplitude of the rheometer were at a maximum when the wet mass reaches the funicular state of liquid saturation and voids and liquid bridges are present in the wet powder mass. The mean torque reflected on a rheometer will be at a maximum when the wet mass is at the capillary state of granulation and the largest number of capillary bridges exists between the granulating fluid and substrate materials. The difference in the relative positions of the two torque values *viz.*, mean torque and torque range indicates the degree of binder/substrate interaction or spreading and the larger the difference between the two values, the greater wetting and spreading of the granulation fluid has been achieved. Some studies have indicated that better wetting leads to the production of more spherical, smooth surfaced but large particles [133, 157, 161, 161, 162]. Mixer torque rheometry is still however a very expensive technique and thus formulation scientists still rely on older yet reliable squeeze and visual assessment methods for research purposes.

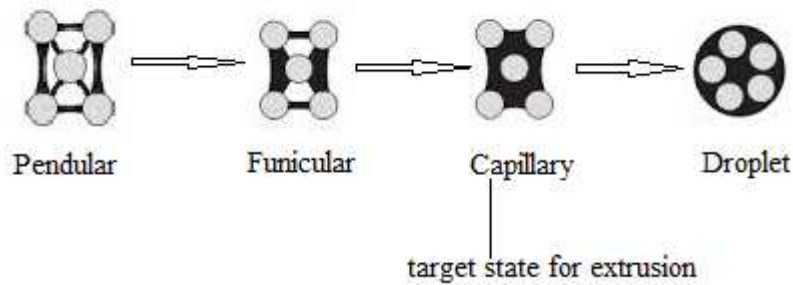


Figure 4.7 Schematic representation of granule formation adapted from *A new technique for the production of spherical particles*[130]

Granulation process variables such as the amount of granulating fluid and wet mass mixing time have a significant effect on the ultimate size of pellets that are produced using extrusion. At relatively low granulating fluid levels longer mixing times are required to distribute the fluid more effectively through the powders resulting in greater cohesive forces at granule surfaces that in turn result in a slight increase in the size of the pellet produced. In contrast when higher fluid levels are used, longer mixing times are necessary to distribute granulation fluids effectively within the pore structure of the particles, thereby reducing or eliminating the formation of over-wet surfaces whilst ensuring a sufficiently plastic mass is produced for extrusion. The effective distribution and reduction of surface water results in particles with a smaller mean and narrow size distribution [163].

4.1.6 Capsules

Capsules are solid dosage forms in which one or more API and inert ingredients are enclosed in a small shell or container usually made of gelatin. There are two types of gelatin capsules *viz.*, hard and soft. Hard capsules are two piece technologies consisting of a cap and body that take the form of small cylinders that are closed at one end and the cap fits over the open end of the longer piece that is the body. Capsules have several advantages including the ability to mask unpleasant taste and odor of API, easy administration, are slippery when moist thereby facilitating swallowing with water, require fewer excipients when compared to tablets, are economical to produce and the shells are physiologically inert and are digested in the gastrointestinal tract.

Capsules are available in many sizes to provide dosing flexibility and range in size from 000 (largest size) to 5 (smallest size). The weight capacity of a capsule is highly dependent on the

density of the fill material. The tapped density of a fill material is established and a capsule capacity table is used to determine the appropriate size of capsule to use which is usually the smallest size capsule that can be filled to eliminate void spaces.

Hard gelatin capsules were selected as the carrier technology for the pellets manufactured in these studies.

4.2 METHODS

4.2.1 Materials

TDF was purchased from Hetero Labs Limited (Jinnaram Mandal, India). Croscarmellose sodium (CCS), Kollidon[®] CL-M and sorbitol were purchased from BASF (Ludwigshafen, Germany). Avicel[®] PH102 (MCC) was donated by FMC Bio-polymer (Philadelphia, Pennsylvania, USA).

4.2.2 Manufacturing equipment

All raw materials were weighed using a Model PM4600 top-loading analytical balance with a sensitivity of 0.01g (Mettler Instruments, Zurich, Switzerland). Dry blending and wet granulation were undertaken using a Kenwood[®] FP693 planetary blender (Kenwood Ltd, Maraisburg, Gauteng, South Africa). A model 7521-001 Cole Palmer peristaltic pump (Cole Palmer Instruments Co., Barrinton, Illinois, USA) fitted with a spray gun was used for the addition of sterile water used as granulating fluid. The wet mass was extruded and spheronized using a Model 20 Caleva[®] extruder fitted with a 1 mm aperture sized radial screen and Caleva[®] MBS 250 spheronizer fitted with a cross hatched radial plate (Caleva Process Solution Ltd., Sturminster Newton, Dorset, United Kingdom). The pellets were dried in a STREA-1[™] Classic Aeromatic fluid bed drier (GEA Pharma Systems, Keerbaan, Wommelgem, Belgium).

4.2.3 Method of Manufacture

4.2.3.1 Manufacturing Procedure

The manufacture of pellets for inclusion in capsules was undertaken using wet granulation, extrusion and spheronization. MCC and Kollidon[®]CL-M were used as primary spheronization aids and CCS was included to ensure the rapid and immediate release of TDF from the pellets. Sorbitol was included as a dissolution enhancer and surface modifier to facilitate the production of smooth surfaced pellets. TDF loading was maintained at 75% w/w for all experiments. TDF and the excipients were dry blended for 20 minutes prior to granulation with water to produce an extrudable plastic mass. The granulation end point was determined using a hand squeeze test and visual inspection as only small experimental batches were to be produced.

The initial formulation was elucidated following evaluation of the literature reporting the manufacture of spheronized pellets. However the use of water and MCC PH101 as the only diluent and spheronization aid resulted in pellets that retarded TDF release from the pellets. Consequently the formulation was modified to ensure that rapid release of TDF could be achieved for this study.

Initially the mass was extruded at an extrusion speed of 30 rpm after which it was spheronized at 900 rpm for three minutes. The pellets were harvested and dried using a fluid bed drier with the inlet temperature maintained at 50°C and a target outlet temperature of 42°C. Air flow was maintained at 70m³/hr to avoid attrition of pellets and the production of fines at higher air flow speeds. An automatic 30 second blow back cycle was used to prevent fines build-up on each of the four nylon filter socks and ensure adequate air fluidization. The drying time was 35 min for all batches. A schematic representation of the method of manufacture is depicted in Figure 4.8.

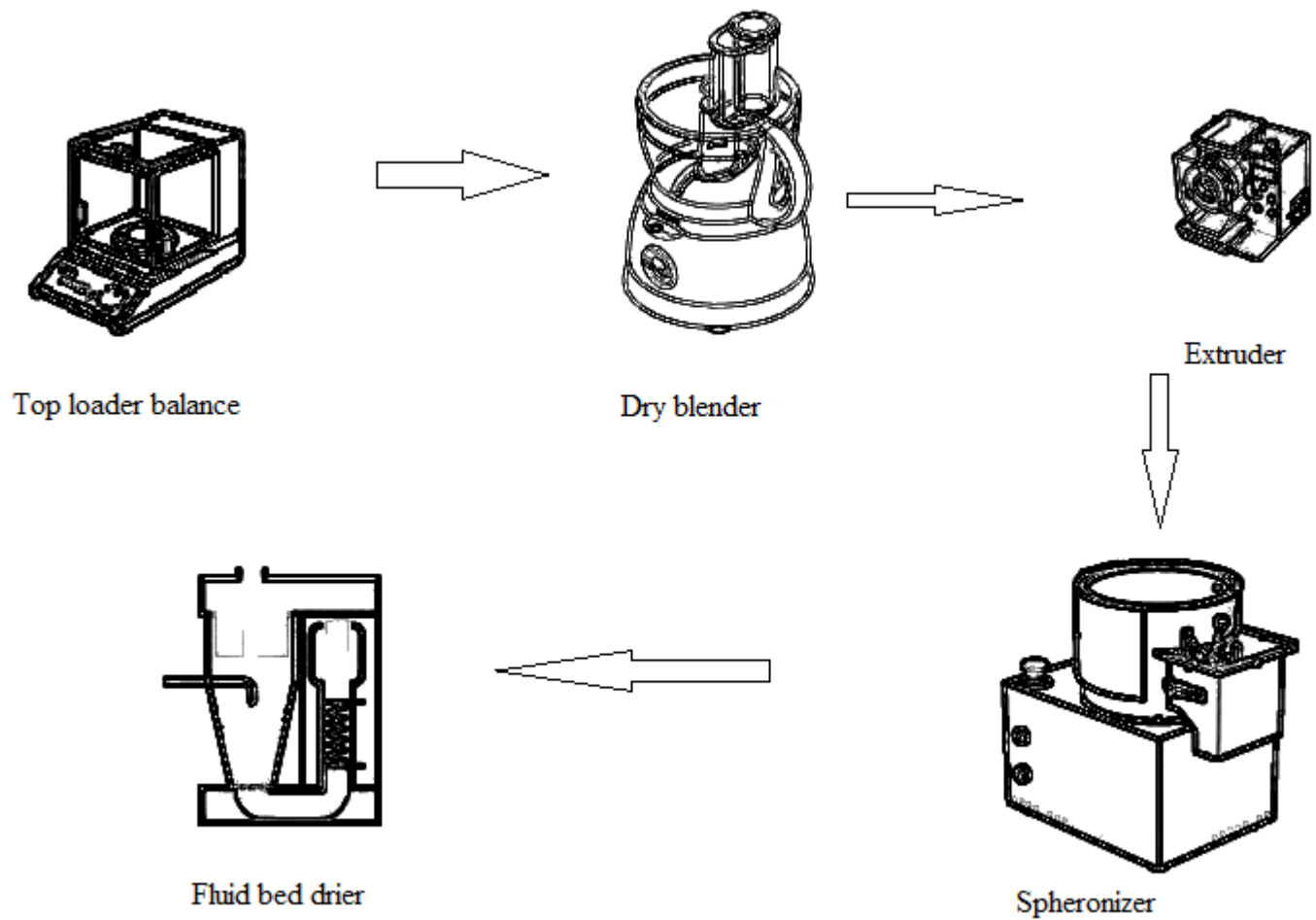


Figure 4.8 Method of manufacture of TDF pellets

The batch formulae used for the development and manufacture of pellets are summarized in Table 4.1.

Table 4.1 Formulae used for the manufacture of TDF pellets

BATCH	TDF % w/w	CCS % w/w	MCC %w/w	Sorbitol % w/w	Kollidon® CL-M % w/w
TDF 001	75	-	10	-	-
TDF 002	75	3	12	4	15
TDF 003	75	2	10	3	10
TDF 004	75	3	12	3	10
TDF 005	75	4	8	4	-
TDF 006	75	-	12	5	10
TDF 007	75	4	-	3	15
TDF 008	75	-	6	5	10
TDF 009	75	3	10	-	5
TDF 010	75	2	12	-	5

Following the manufacture of the initial formulations, Batch TDF 003 was selected for further optimization in respect of pellet shape and dissolution of TDF as it had better flow properties and TDF release was immediate. The success of the optimization procedure was evaluated by assessing the dissolution rate of TDF using the dissolution method described in § 4.2.5.3 *vide infra*.

The pellets were also evaluated by monitoring parameters such as size distribution, shape, % TDF released, density and flow properties.

4.2.3.2 Capsule filling

Control of the capsule filling process is essential to ensure dose uniformity and ultimately bioavailability, as bioavailability is affected by inadequate fill amounts. Capsule filling machines are commercially available but for small scale research purposes a manual hand filling process is usually used and this approach was used for the purposes of this study. A hand filling technique was devised to best suit capsule filling with the pellets produced by extrusion and spheronization. Quality control measures were also used to ensure adequate and precise capsule filling was achieved *viz.* weight uniformity, content uniformity and void volume measurement.

The effective dose of TDF established with reference to commercially available Viread[®] tablets was 300mg per day as a once daily dose. Consequently a pellet mass containing 300 mg TDF by weight was established using Equation 4.1.

$$\text{Capsule fill weight} = \frac{300 \times \% \frac{w}{w} \text{ of TDF in the formulation}}{75}$$

Equation 4.1

The tapped density of each batch was established and the highest value was used to determine the capsule size best to be used on the basis of fill volume. Therefore based on a tapped density of 0.57g/ml, size 0 capsules were selected as the most appropriate capsule size for pellet filling. A funnel made of sterile plastic tubing (Figure 4.9) was used to fill twenty capsules for each batch of pellets produced. Each batch was assayed (n=6) for quality control purposes and the results of these studies are summarized in Table 4.2 and reveal that filling was uniform and accurate.

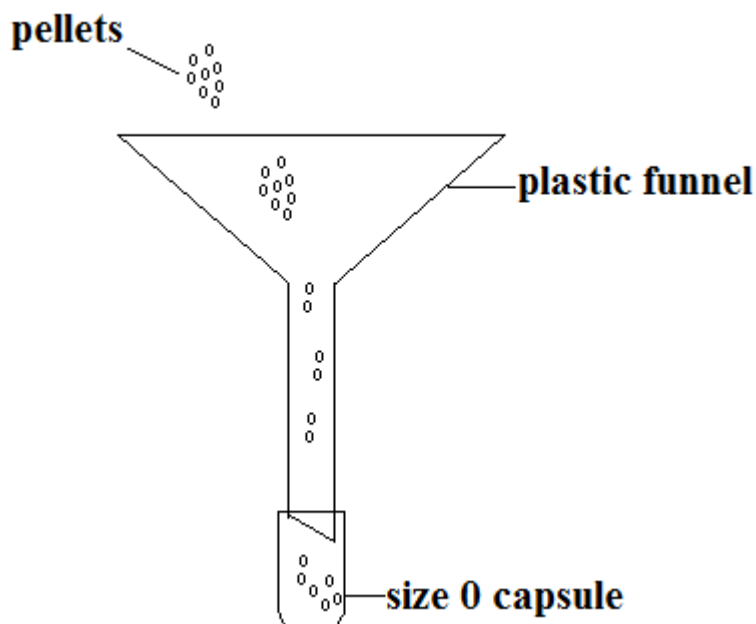


Figure 4.9 Schematic representation of capsule filling

Table 4.2 Capsule fill weight and assay results

Batch	Capsule fill weight (mg)	Assay %
TDF 001	340	97.12 ± 0.96
TDF 002	436	98.01 ± 1.12
TDF 003	400	99.33 ± 0.83
TDF 004	412	97.65 ± 0.67
TDF 005	364	98.01 ± 0.91
TDF 006	408	100.32 ± 1.26
TDF 007	388	-*
TDF 008	384	99.88 ± 2.82
TDF 009	372	99.35 ± 1.33
TDF 010	376	99.92 ± 1.58

*TDF 007 formulation composition didnot yield any pellets as the mass was not spheronizable.

Intra-batch variability was low with all SD values <5%. A shake test and visual assessment of the transparent filled capsules was made to ascertain if the void volume was appropriate to avoid attrition due to movement of pellets. The void volume was sufficient to limit excessive pellet movement.

4.2.4 Physical characterization of pellets

4.2.4.1 Size Analysis

The mean particle size of the pellets that were produced was measured by passing each batch of pellets through sieve screens with aperture sizes of 800 µm and 1250µm to harvest pellets that were in the target size range and the yield of pellets in this range was established using Equation 4.2.

$$\% Yield = \frac{\text{amount of pellets (800 – 1250}\mu\text{m)}g}{\text{total amount of pellets (g)}} \times 100$$

Equation 4.2

4.2.4.2 Sphericity

The sphericity of the pellets was evaluated using a Vega[®] Scanning Electron Microscope (Tescan, Vega LMU, Czechoslovakia Republic) and a relationship defined by Koo and Heng [164] that is used to determine pellet roundness. Batch samples were individually dusted onto a graphite plate and sputter coated with gold under vacuum for 30 minutes. The samples were

visualized at an accelerated voltage of 20 kV and pellet roundness was calculated using Equation 4.3.

$$R = \frac{0.9399P^2}{4\pi A}$$

Equation 4.3

Where,

R = roundness

P = perimeter of pellet image

A = area of pellet image

4.2.4.3 TDF release

Monitoring the percent TDF released over time is vital for quality control purposes and if used appropriately may be used to highlight potential bioavailability challenges from this formulation. *In vitro* dissolution testing was used to monitor the amount of TDF released to ensure that formulations that were manufactured released TDF as an immediate release dosage form.

Several dissolution apparatus have been described and include the rotating basket or USP Apparatus 1 and paddle or USP Apparatus 2. These instruments are simple, robust, can be readily standardized and as they are used worldwide, performance challenges and issues using these apparatus are generally well understood.

The earliest reference to dissolution was made by Noyes-Whitney in 1897 [165] and it has been suggested that the dissolution rate of solid substances is a function of the diffusion rate of drug through a very thin layer of saturated solution that forms instantaneously around a solid particle. Costa and Lobo [166] described dissolution as a process by which a solid of only fair solubility can enter into solution. Dissolution is a process whereby a solid particle immersed in a liquid undergoes two consecutive steps. Initially dissolution of the solid at an interface occurs to form a stagnant layer of a specific thickness around that particle. Further dissolution results in diffusion of solute molecules located in the stagnant layer to the bulk dissolution fluid. The initial step of the process is almost instantaneous and the subsequent step is slower and is often the rate limiting step for a dissolution processes and may impact drug absorption *in vivo*.

The dissolution of an API can be described by the Noyes-Whitney equation (Equation 4.4) which describes the dissolution of spherical particles, when the dissolution process is diffusion controlled and no chemical reaction is necessary to facilitate dissolution.

$$\frac{dC}{dt} = \frac{DA (C_s - C)}{h}$$

Equation 4.4

Where,

- dC/dt = rate of dissolution of drug particles
- D = diffusion coefficient of the API in solution in the gastrointestinal fluids
- A = surface area of the API particles in contact with the gastrointestinal fluids
- h = thickness of the diffusion layer around each particle
- C_s = saturation solubility of the API in solution in the stagnant or diffusion layer
- C = concentration of the API in the gastrointestinal fluids

Consequently the physicochemical properties of an API are an important factor to consider when dissolution of that material is investigated. Dissolution media are usually aqueous based fluids that may include a buffer or in rare cases only purified water is used [167]. Therefore the aqueous solubility of an API is a critical determinant in the rate of solution of bulk raw material. Additional factors that can impact the rate of solution of a molecule include particle size and crystalline state of the API. Furthermore several key properties of pharmaceutical products including type of dosage form, potency, mechanism of release and excipients used in the dosage form are also important factors to consider when designing, selecting and implementing a dissolution test method.

When developing a dissolution test procedure the impact of test parameters on dissolution rate must also be evaluated. The degree of agitation of the dissolution medium is one of the key factors that affect the dissolution of an API. To ensure the elimination of variability in the rate of API release from a delivery technology it is important that factors such as temperature, pH, in addition to the nature, composition and volume of dissolution medium to be used are adequately evaluated and controlled.

The USP requires that immediate release (IR) dosage forms release at least 85% API from a dosage unit into a dissolution medium maintained at $37\pm 0.5^{\circ}\text{C}$ within 45 min when using USP Apparatus 1 or 2 at agitation rates of 100 rpm or 50 rpm, respectively [167]. This is a general requirement and provides guidance for the development of acceptance criteria for the dissolution of an API from IR solid dosage forms. These specifications do not constitute an approach to the testing of a product that is alternative to that required in the monograph provided for that product. Nevertheless these criteria were used to set specifications for the TDF pellet formulations.

In vitro release studies of TDF pellet filled capsules was performed using USP Apparatus 2 (Hanson Research SR 8 PLUS , California, United States of America) fitted with an Autoplus™ Multifill™ and Maximizer Syringe Fraction Collector. Capsules were placed into six individual spiral capsule sinkers weighing 1.3g and 9.5 mm x 25 mm dimensional capacity (Hanson Research, California, United States of America). The capsules were dropped into the dissolution vessels that contained 900ml of vacuum degassed 0.1M HCl. The paddles were set to rotate at 50rpm and the temperature of the dissolution medium was maintained at $37\pm 0.5^{\circ}\text{C}$ for all studies. Aliquots (5ml) of the dissolution fluid were collected for analysis at 0, 5, 10, 20, 30 and 45 minutes following the commencement of testing. An equal volume of the dissolution medium was replaced after each sample had been collected. A 2.5ml aliquot of each sample was harvested using an electronic pipette (Boeckel and Co. GmbH, Hamburg, Germany) and transferred into a 5 ml A-grade volumetric flask followed by the addition of 700 μl of IS solution described in § 2.3.5, *vide infra*. The resultant solution was made up to volume using a solution of ACN and water in a ratio of 40:60 that had been filtered through a 0.22 μm Acrodisc® PSF syringe filter (Pall Corporation, Port Washington, New York, USA) prior to analysis. The samples were analyzed using the validated HPLC method that has been described in Chapter Two, *vide infra*.

4.2.4.4 Density

The bulk density of a material can be indicative of the packing properties of the particles that constitute the material and can be influenced by the diameter of the particles that make up that material. Loosely packed pellets have a greater arch strength due to the formation of bridges and are thus more resistant to flow than densely packed materials. The density of the pellets may

also affect capsule filling and most often pellets are filled into hard gelatin capsules volumetrically using automated capsule filling machines, however for this study hand filling was used as described in § 4.2.3.2, *vide infra*. If the density of the pellets varies significantly from batch to batch the potency of the finished capsules is likely to vary if less than required amount of TDF is delivered to site of action. Any significant variation in the density of pellets will also affect the determination of batch size for further manufacturing processes such as coating, capsule filling, or tableting if required.

The tapped density of the TDF pellets was determined using a Model SVM 203 (Erweka GmbH, Heuseastamm, Germany) tapped density tester at a rate of 220 taps per minute for 2 min. Approximately 20 g of pellets from each batch was filled into individual tared 100 ml graduated measuring cylinders. The bulk and tapped volumes, V_b and V_t were established and the test was performed in triplicate. The bulk and tapped densities were calculated using Equation 3.5.

4.2.4.5 Flow Properties

Carr's index (CI) was used to estimate the flow properties of the TDF pellets and was calculated using Equation 3.2. A Hausner ratio of < 1.25 indicates that powders are free flowing whereas a ratio > 1.25 indicates poor flow characteristics. The Hausner ratio for each batch was calculated following the estimation of CI for each batch using Equation 3.3. The Angle of Repose for each batch was also measured to estimate pellet flowability.

4.2.4.6 Assay

Twenty hard gelatin capsules that had been pre-filled with pellets containing an equivalent of 300 mg TDF were randomly selected and emptied into a mortar and then ground into a fine powder using a pestle. An aliquot of powder equivalent to the weight of the contents of one capsule (approximately 400 mg) was weighed using a Model AG 135 top loading analytical balance (Mettler Instruments[®], Zurich, Switzerland). The powder blend was transferred into a 100 ml A-grade volumetric flask and dissolved in an ACN: water solution in a ratio of 40:60 and sonicated for 5 minutes using a Model B-12 Ultrasonic bath (Branson Cleaning Equipment Co., Shelton, Connecticut, United States of America). The solution was then made up to volume with a solution of ACN: water (40:60) and filtered through ashless SS round filter paper (Schleicher and Schull GmbH, Postfach, Dassel, Germany) of 12 μm pore size and 125 mm in diameter. A 1

ml aliquot of the filtrate was transferred into a 100 ml A-grade volumetric flask and made up to volume with the ACN: water solution. Approximately 5ml of the solution was filtered through a 0.22 µm Acrodisc[®] PSF syringe filter (Pall Corporation, Port Washington, New York, USA) and an aliquot of 2 ml of the filtered solution was mixed with 2 ml of IS solution prior to analysis (n=3) using the validated HPLC method reported in Chapter 3.

4.3 RESULTS AND DISCUSSION

4.3.1 Physical properties of the pellets

A summary of the flow properties of the different batches that were manufactured and that were tested is summarized in Table 4.3.

Table 4.3 Flow properties of batches TDF 001 - 010

Batch number	CI	HR	AOR
TDF 001	5.41	1.06	23.96
TDF 002	12.71	1.06	30.47
TDF 003	5.31	1.05	22.89
TDF 004	11.13	1.05	25.73
TDF 005	4.76	1.05	31.42
TDF 006	4.76	1.05	23.10
TDF 007	_*	_*	_*
TDF 008	28.52	1.40	40.23
TDF 009	9.19	1.10	30.24
TDF 010	5.67	1.06	28.21

*TDF 007 formulation composition did not yield any pellets as the mass was not spheronizable

The flow properties of the pellets manufactured in these studies were assessed and the CI, AOR and HR for the pellet batches summarized in Table 4.3 suggest that batches TDF-001, TDF-003, TDF-004, TDF-006 and TDF-010 have better flow properties than other batches. There are many fundamental properties of solid particles that influence their flow properties such as particle size, particle size distribution, particles shape, surface texture and surface area. The inclusion of relatively low quantities of MCC and Kollidon[®] CL-M in batches TDF-001 and TDF-003 resulted in the need for less binder fluid (water) than that used for the manufacture of the other batches. The increased water content required for the granulations results in the production of pellets with varied pellet size that appeared to exhibit poor flow properties. The use of high concentrations of sorbitol in the formulation imparted a degree of tackiness to the granules with the result that the values for AOR were higher for batches TDF-002, TDF-005, TDF-008 and

TDF-009. The extrudate from batch TDF-007 lacked the required amount of plasticity that was necessary to break into short and uniform lengths of material that could be spheronized and therefore no viable spheres were produced. This can in part be attributed to the lack of MCC in that formulation that resulted in lower moisture uptake by the granulation resulting in a lack of lubricity when the mass was passed through the extruder screen also suggesting that the use of Kollidon[®]CL-M as the only spheronization aid is not sufficient for spheres of TDF manufactured using this approach. The porous nature of Kollidon[®] CL-M would be expected to aid in water uptake during wet granulation, however these results reveal that when used alone the material is unable to mimic the sponge-like effect exhibited by MCC resulting in the production of poor quality materials.

4.3.2 Physico-mechanical properties of the pellets

A summary of the physico-mechanical properties of the batches established during testing are summarized in Table 4.4.

Table 4.4 Physico-mechanical properties of batches TDF 001-008

Batch number	% yield (% between 0.8–1.25mm)	Roundness Value	Assay %
TDF 001	90.61	1.02	97.11
TDF 002	73.93	1.98	97.55
TDF 003	86.42	1.18	99.26
TDF 004	84.64	1.97	97.56
TDF 005	76.40	1.02	98.30
TDF 006	84.64	1.32	98.45
TDF 007	_*	_*	_*
TDF 008	56.45	1.99	99.12
TDF 009	67.50	1.96	99.10
TDF 010	68.33	1.78	101.16

*TDF 007 formulation composition did not yield any pellets as the mass was not spheronizable

An important characteristic of pellets is their sphericity and in this case this parameter was assessed using roundness as defined by Koo and Heng [164]. Batches TDF-001, TDF-003 and TDF-006 exhibited roundness values close to 1.0 suggesting these particles were close to perfect spheres. MCC has been used extensively as a spheronization aid since it promotes the tensile strength of a wet mass through auto-adhesion thereby resulting in better pellet shape and strength. Auto-adhesion is a term used to describe the strong bonds formed by the inter-diffusion of free polymer chain ends across particle–particle interfaces [116, 132]. Batches TDF-001 and

TDF-005 were formulated with MCC as the only spheronization aid and these batches exhibited the best shaped pellets that may be attributed to the fact that MCC imparts little resistance to the formation and shaping forces that materials are exposed to during the extrusion and spheronization process. The sponge-like effect that is evident when MCC is extruded contributes to the conforming effect observed when MCC is used as a spheronization aid [149, 152]. Batches TDF-002, TDF-004, TDF-008, TDF-009 and TDF-010 were manufactured with reduced amounts of MCC and included Kollidon®CL-M as an additional spheronization aid which may have increased the resistance of the formulation to the formation and shaping forces during extrusion and spheronization, thereby resulting in the production of irregular shaped pellets that is clearly indicated by the low values observed for roundness. The percent yield also indicates that when MCC is the only spheronization aid used or used in larger amounts, a greater number of pellets of the target size range are produced. The formulation for Batch TDF-007 was not suitable to produce viable spheres and the composition of this batch used only Kollidon®CL-M as the spheronization aid.

4.3.3 *In vitro* release of TDF

The amount of TDF released at 10 min and 45 min for all batches tested are listed in Table 4.5.

Table 4.5 Dissolution data for Batches TDF 001-008

Batch number	% TDF released at 10mins	% TDF released at 45mins
TDF 001	12.31	22.87
TDF 002	51.23	91.45
TDF 003	58.23	101.2
TDF 004	47.45	82.33
TDF 005	49.23	96.12
TDF 006	19.32	51.23
TDF 007	-*	-*
TDF 008	22.36	59.62
TDF 009	48.23	96.64
TDF 010	33.65	94.69

*TDF 007 formulation composition did not yield any pellets as the mass was not spheronizable.

Batches TDF-001, TDF-006 and TDF-008 released only 22.87%, 51.23% and 59.62% TDF respectively after 45 min in 0.1M HCl. These batches were formulated without a disintegrant and the pellets failed to disintegrate, therefore TDF release was slow and limited by diffusion of TDF from intact pellets with a low surface area. An SEM image of the surface of an intact TDF-001 pellet collected following dissolution is shown in Figure 4.9.

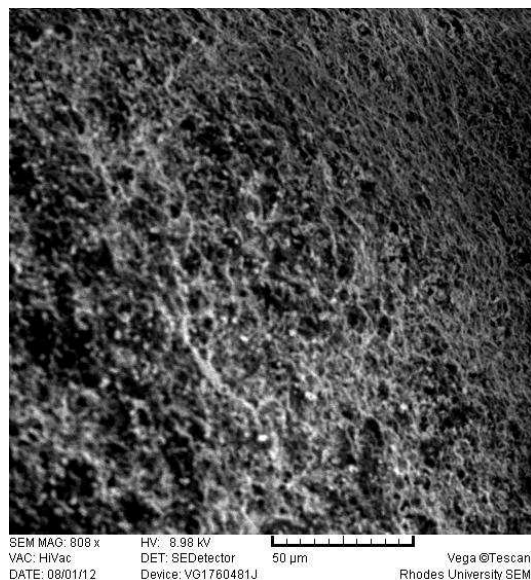


Figure 4.10 SEM image of the surface of a pellet from batch TDF-001 collected after 45 min of dissolution testing

The pellets did not disintegrate and the SEM scan reveals the presence of a porous surface that may permit TDF release that is limited by diffusion from the matrix. Batches TDF-006 and TDF-008 yielded slightly higher dissolution rates that can be attributed to the presence of Kollidon[®]CL-M and lower amounts of MCC in the formulation. These batches did not disintegrate as they did not contain CCS to aid disintegration. Kollidon[®] CL-M is a cross-linked polyvinyl pyrrolidone polymer with a physical structure that is highly porous as reported following surface morphology studies of Kollidon[®] CL-M (Chapter 3) thereby allowing faster diffusion of TDF from the pellets of batches TDF-006 and TDF-008 during dissolution testing. Since pellets from batches TDF-001, TDF-006 and TDF-008 did not disintegrate after dissolution for 45 min, they were harvested and air dried to establish the amount of TDF retained in the pellets. Assay values for these pellets are summarized in Table 4.6.

Table 4.6 Mass balance analysis of non-disintegrating pellets

Batch number	Assay %	Mass balance %
TDF 001	70.89	95.90
TDF 006	45.01	95.32
TDF 008	38.43	97.29

The results show that the assay values for the harvested pellets are similar to the amount of TDF remaining in the intact pellets with mass balance percentages above 95%. This suggests that dissolution of TDF from batches TDF-001, TDF-006 and TDF-008 seems to be dependent on diffusion.

TDF exhibits low aqueous solubility and therefore it is expected that the dissolution rate of the TDF from non-disintegrating spheres would be slow. The addition of a spheronization aid such as Kollidon[®] CL-M, a super disintegrant such as CCS and a wetting agent such as sorbitol to other batches increased the release of TDF exponentially with more than 85% TDF being released from batches TDF-002, TDF-003, TDF-005 and TDF-010 at 45 min. Batch TDF-003 exhibited a maximum amount of TDF released of 101.2% at 45 min.

4.4 CONCLUSIONS

The manufacture of pellets using extrusion and spheronization is challenging when a low-solubility API such as TDF is to be incorporated into the pellet formulation. In particular it is difficult to produce pellets with the appropriate shape, texture, flowability and release characteristics. The variability in physical characteristics is not an uncommon phenomenon with pellets especially if they are manufactured without the use of spheronization aids such as MCC that are essential for the production of a product that exhibits suitable physical characteristics. To date MCC remains the most frequently used excipient for the production of pellets using an extrusion spheronization process. Pellets manufactured using MCC are characterized by a narrow particle size distribution, high sphericity and exhibit appropriate mechanical properties. However when low solubility molecules such as TDF are manufactured using MCC based pellet formulations it is likely that prolonged release of the API will be observed as the pellets sometimes do not disintegrate due to the change in the internal characteristics of the technology. The objective of this project was to produce pellets that would exhibit an immediate release profile and therefore the formulations needed to include excipients that would facilitate the production and exhibit an appropriate *in vitro* release profile for TDF so as to meet the objectives set for this project.

Pellets containing TDF were successfully developed and manufactured using an extrusion and spheronization approach. The pellets were characterized by a narrow particle size distribution,

high degrees of sphericity, good flow properties and released TDF according the criteria set for immediate release dosage forms. The use of a co-spheronization aid and a super-disintegrant in the formulation was essential to ensure that the manufacture of an immediate release dosage form was achieved.

The pellets that were produced form the basis of a new TDF containing immediate release dosage form and the formulation was further optimized using Response Surface Methodology as described in Chapter 5 of this thesis.

CHAPTER FIVE

OPTIMIZATION OF A TDF PELLET FORMULATION USING RESPONSE SURFACE METHODOLOGY.

5.1 INTRODUCTION

Investigators perform experiments in all fields of enquiry in order to discover knowledge about a particular process or system. An experiment is defined as a test or series of tests in which changes are made to the input parameters of a process or system so as to establish their impact on outputs that are monitored [168].

To implement cost effective and efficient experimental strategies it is vital to reach an appropriate end-point in the shortest possible time through the efficient use of all resources. Quality by Design (QbD) has become an integral part of the formulation development process [169-171]. QbD is a systematic approach that is used by manufacturers throughout the formulation development process and commences with the identification of pre-defined objectives. Furthermore QbD emphasizes the need to develop product and process understanding based on preliminary experiments and a quality risk management approach [172, 173]. Design of Experiments (DOE) is a statistical methodology that is used in the QbD approach for formulation optimization and can be used to establish relationships, if any, between all input factors, *viz.* formulation and/or process parameters and final product performance characteristics. There has been an increase in the application of DOE approaches for pharmaceutical development, formulation composition and the optimization of processes [174, 175]. Furthermore DOE maybe used to generate mathematical models that can facilitate the production of graphical representations and describe the variability of responses of a system as a function of the input factors for that system. The use of a sequence of experiments designed to obtain an optimum response through statistical design and mathematical equations in the development and optimization of pharmaceutical formulations is defined as Response Surface Methodology (RSM) [176-180].

A schematic representation of the use of RSM in the optimization of pharmaceutical processes is depicted in Figure 5.1. The process is usually performed in five sequential steps, *viz.* initially using statistical design to establish a series of experiments, performing the experiments, collecting and analyzing data from the studies, obtaining a series of optimized input conditions

from mathematical models that describe the relationship between input variables and output responses and finally validating the optimized experimental parameters for the production of a system that produces the desired responses.

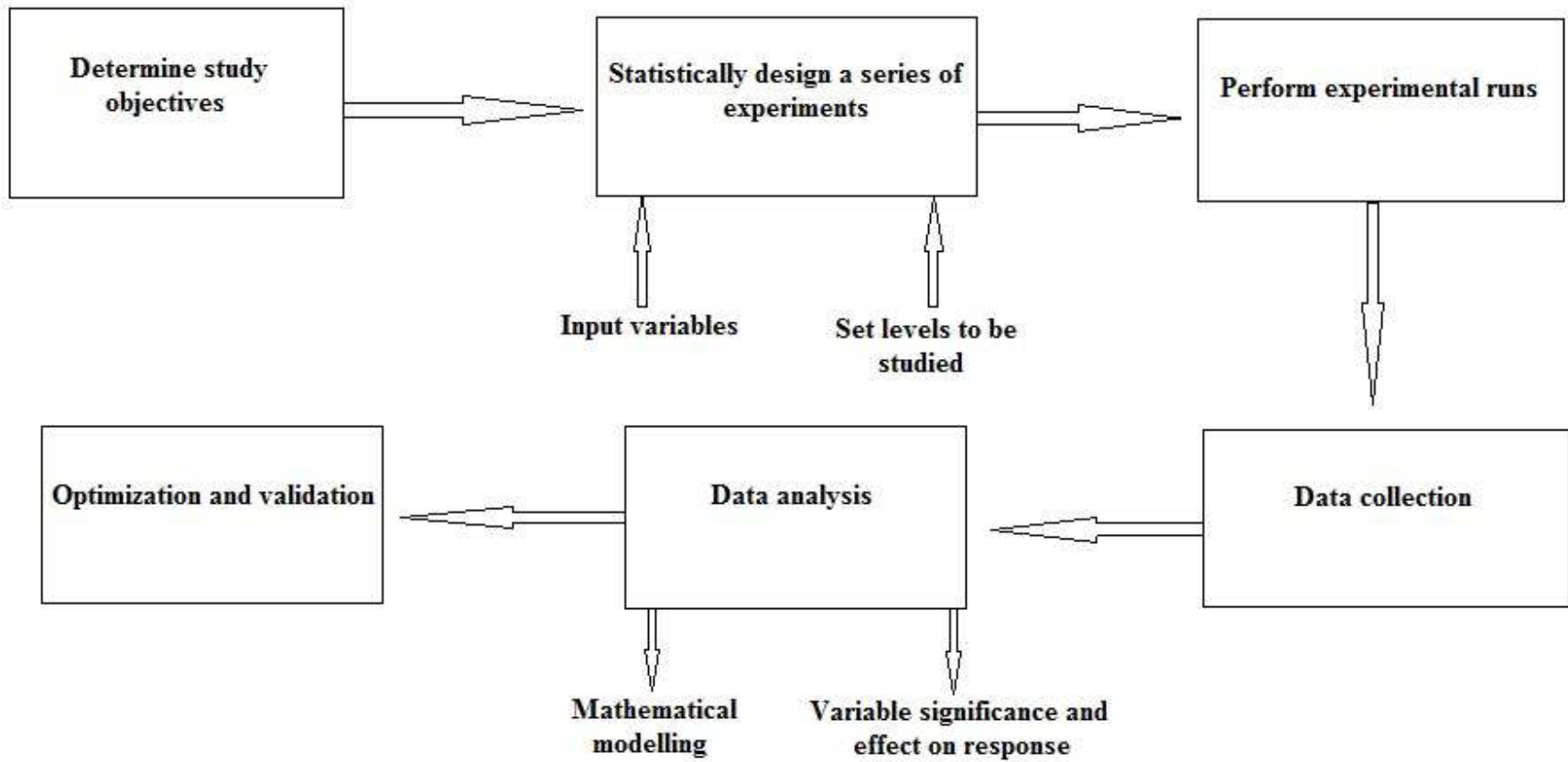


Figure 5.1 Process flow in DOE

5.2 EXPERIMENTAL DESIGN

5.2.1 Quantitative factors and the factor space

Continuous factors that exert an effect on a system and that can be described as a numerical value are defined as quantitative factors. Quantitative factors may be set at any value within pre-defined and/or prescribed limits [181, 182]. Examples of quantitative factors include but are not limited to the amount of liquid binder to be added to a granulation, the speed of the extruder, amount of excipients to be added and spheronization time. Therefore if the minimum and maximum extruder speed is 15 rpm and 35 rpm, the operating speed may be set at any value between 15 and 35 rpm. However quantitative factors may at times be set at discrete levels depending on the instrumentation used, for example the speed settings on a fixed scale granulator. With each natural variable linked to a quantitative factor an associated non-dimensional coded variable (X_i) can be assigned. This coding, also known as normalization is defined by transformation of natural variables and the level of the central value of the experimental domain is set to 0 whereas the levels of extreme values are set at ± 1 . The quantitative factors and the factor space for extruder speed and time are depicted in Figure 5.2.

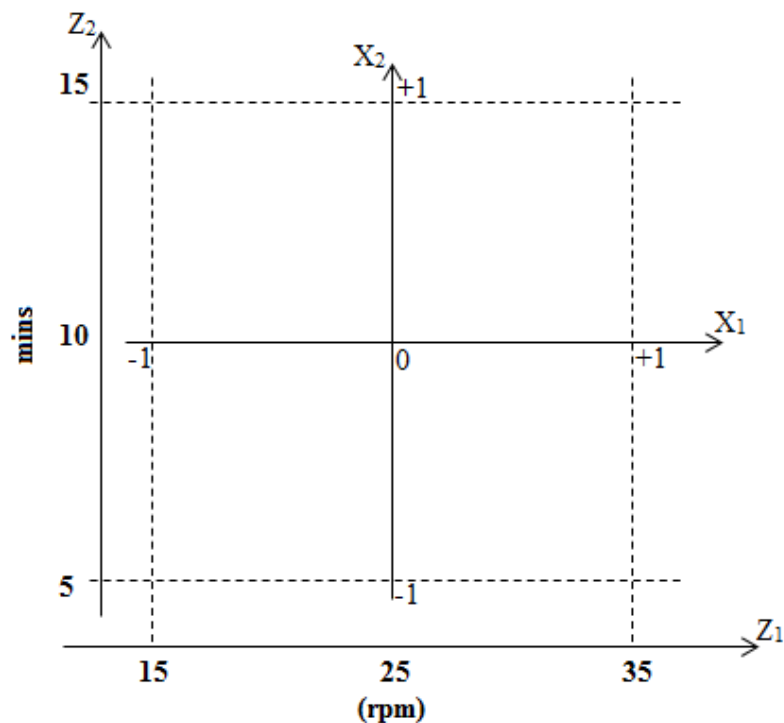


Figure 5.2 Quantitative factors and factor space for extruder speed and time.

The axes for variables such as extruder speed and extrusion time are labeled Z_1 and Z_2 and the axes for the corresponding coded variables are labeled X_1 and X_2 . The factor space covers an area that extends beyond it whereas the design space is the square enclosed by X_1 and $X_2 = \pm 1$.

Qualitative factors are discrete values and in the development of a pellet based product an example of this type of factor could include spheronizer disc type or the physico-chemical nature of the excipients used in the formulation. Response variables are measured properties that are outputs of a process and are sometimes referred to as dependent variables. The symbol for a measured response will be Y and the measured response for experiment i , is described by the function Y_i [183-187].

5.2.2 Mathematical models

Mathematical models are expressions that define the dependence of a response on independent input variables. Equations that describe the relationship between the responses and independent variables may be first, second or third order in nature depending on the manner in which the response variables react to changes of input variables.

Pharmaceutical systems are usually modeled by a linear function of independent variables and in this case the approximating function is a first order model that is mathematically depicted in Equation 5.1. In pharmaceutical systems that exhibit interactions between input factors and those that significantly affect response variables the data are modeled using a second order linear model that can be described using Equation 5.2.

$$y = \beta_0 + \beta_1x_1 + \beta_2x_2 + \dots + \varepsilon \quad \text{Equation 5.1}$$

$$y = \beta_0 + \beta_1x_1 + \beta_2x_2 + \beta_{12}x_1x_2 + \beta_{11}x_1^2 + \beta_{22}x_2^2 + \dots + \varepsilon \quad \text{Equation 5.2}$$

Where:

- y = predicted response
- x_i = input factors
- β_0 = intercept constant
- β_i = first order coefficient
- β_{ii} = second order coefficient
- β_{ij} = second order interaction coefficient

The response surface is represented graphically and the response is plotted against the levels of two input variables [188-191]. To visualize the shape of a response surface it is often portrayed as a two dimensional contour or three dimensional surface plot. In the contour plot the lines of a constant response are drawn in a plane for x_1 and x_2 and each contour corresponds to a particular height of the response surface. The values of the coefficients in the model are generated through multiple linear least squares regression analysis of empirical data. A coefficient with a positive value is indicative of a synergistic effect of the factors on the measured response whereas coefficients with a negative value indicate an antagonistic effect [192-194].

5.2.3 Optimization and validation

The use of DOE in pharmaceutical systems to identify input variables that significantly affect critical responses is well established [195-197]. The identification of significant input variables leads to the optimization of systems so as to yield pre-defined target responses. The determination of levels or the experimental domain that facilitates the production of a product that meets specifications for measured responses is achieved through the use of response surface plots. In practice a product or manufacturing process is rarely described by a single response variable but rather by a number of responses. Therefore the optimization of one response at a time may not lead to identification of the most appropriate values for other responses [188, 198-202]. In such cases optimization is redefined to reach satisfactory levels that require some degree of subjectivity in weighing up the relative importance of each factor. An example of this approach in formulation development would be the optimization of two responses in multi-particulate dosage forms manufactured using extrusion and spheronization where the percent yield of the process is more important than the visual appearance of pellets.

The validation of a formulation or process is necessary to produce documented evidence that the method performs as it is intended to and the desired outcomes are achieved with minimal error. Validation should always be performed to ensure that an optimized process is reproducible and can be used in different settings with the same result [188, 203, 204].

5.2.4 Response Surface Design

5.2.4.1 Taguchi orthogonal array

Taguchi proposed the use of an orthogonal array that is a fractional orthogonal design [180, 205]. These designs can be used to estimate the main effects in a process using a limited number of experiments and are not only applicable to two level factorial experiments but can also be used to investigate main effects when factors are used at more than two levels. The design can also be used to investigate the main effects for certain mixed level experiments where the factors included are not used at the same number of levels [206].

The primary focus of these studies was to make a product or process that was robust and for which variability that is inevitable over which there is little or no control. Two major tools used for the Taguchi approach include the use of an orthogonal array (OA) and signal to noise ratio. An OA is a matrix of numbers arranged in rows and columns and an example is summarized in Table 5.1.

Table 5.1 $L_9(3^4)$ orthogonal array

		Factors			
		A	B	C	D
Experiments	1	1	1	1	1
	2	1	2	2	2
	3	1	3	3	3
	4	2	1	2	3
	5	2	2	3	1
	6	2	3	1	2
	7	3	1	3	2
	8	3	2	1	3
	9	3	3	2	1

In this array the columns are mutually orthogonal and for any pair of columns all combinations of factors at all levels are present and occur with the same frequency. In this example there are four parameters *viz.*, A, B, C and D that are used at three levels. This type of array is a L9 design with the 9 representing nine rows, configurations or prototypes to be tested [205, 207, 208]. Specific test characteristics for each experiment are identified in the associated row of the table and the L9(3⁴) array results in the need for nine experiments to be performed in order to study four variables used at three levels. The number of columns of an array represents the maximum number of parameters that can be investigated using that array.

Assuming that a variable under investigation can have different values *viz.*, $v_1 \dots v_n$ and that a total of m experiments are to be conducted, the set of experiments is balanced with respect to the variable if $m = k_n$ for some integer k and each of the values, v_i , is tested in exactly k experiments.

An experiment is considered balanced if it is balanced with respect to each variable under investigation. For example in the L9 OA listed in Table 5.1 each of the column contains three levels *viz.*, 1, 2 and 3 for the factors assigned to that column [197]. The idea of balance ensures that equal chance is possible for each level of each variable and it is necessary to ensure that equal attention to combinations of multiple variables is assigned. Assuming that two variables *viz.*, A (values: $a_1 \dots a_n$) and B (values $b_1 \dots b_m$) are used, then the set of experiments is considered orthogonal if each pair-wise combination of values, (a_i, b_j) occurs in the same number of trials. For example in the L9 OA two factors with 3 levels combine in nine possible ways, *viz.*, 1,1, 1,2, 1,3, 2,1, 2,2, 2,3, 3,1, 3,2 and 3,3.

It is important to note that any two columns of an L9 OA have the same number of combinations and this is one of the features that provide orthogonality for all columns or factors. When two columns of an array are used to form combinations the same number of times and all columns provide the same number of tests under the first level of the factor and the same number of tests are conducted for the second level of the factor then the columns are balanced and orthogonal. Therefore all four columns of an L9 array are orthogonal to each other [205, 209]. In a Taguchi design the array is orthogonal indicating that the design is balanced and the factor levels are weighted equally. The real power in use of an OA is the ability to evaluate several input factors at the same time with a minimum number of experiments. This approach is considered efficient since large amounts of information can be gathered from a few trials [205, 208, 210, 211].

5.3 EXPERIMENTAL

5.3.1 Proposed design

The successful optimization of a product is dependent on selection of an appropriate formulation composition and identification and control of critical process parameters prior to and during manufacture of the product. The inclusion of appropriate and suitable excipients in amounts that facilitate manufacture and ensure performance is vital. Initial screening of suitable excipients for use in extrusion and spheronization was undertaken and is reported in Chapter 3, *vide infra*. An evaluation of the main, interactive and linear effects of the input and response variables was performed using a L18 Taguchi orthogonal array statistical design. The mathematical relationship between input variables and responses was established using Design Expert[®] Version 8.0.4 software (Stat-Ease Inc, Minneapolis, Minnesota, USA). The independent input variables selected included formulation and process parameters that were studied at three levels except for spheronizer residence time and blender speed that were studied at only two levels (Table 5.2). Batch TDF 003 manufactured using the formulation reported in § 4.2.4.1 was used as the starting point for the optimization process. All experimental batches were manufactured and assessed using the methodology described in Chapter 4, *vide infra*.

Table 5.2 Independent variables and levels investigated

INDEPENDENT VARIABLES	LEVELS		
	1	2	3
A - spheronizer residence time (min)	3	5	--
B - blender speed	LOW	HIGH	--
C - %w/w CCS	1	2	3
D - % w/w sorbitol	2	3	4
E - spheronizer speed (rpm)	650	850	1050
F - extruder speed (rpm)	15	25	35
G - % w/w MCC	8	10	12
H - % w/w Kollidon [®] CL-M	5	10	15

The actual values used for the implementation of the Taguchi L18 orthogonal array design of experiments approach are summarized in Table 5.3.

Table 5.3 Actual values used for experimental design

BATCH	VALUE							
	A min	B speed	C % w/w	D % w/w	E rpm	F rpm	G % w/w	H % w/w
TDF 011	5	HIGH	1	3	650	35	10	15
TDF 012	3	LOW	2	3	1050	25	10	10
TDF 013	5	HIGH	1	2	1050	35	12	10
TDF 014	3	HIGH	2	2	850	35	10	5
TDF 015	3	HIGH	3	3	650	15	12	10
TDF 016	5	LOW	3	3	1050	35	8	5
TDF 017	5	LOW	2	2	650	25	12	15
TDF 018	3	HIGH	1	3	850	25	12	5
TDF 019	3	HIGH	2	4	650	35	8	10
TDF 020	5	HIGH	2	3	850	15	8	15
TDF 021	3	LOW	3	4	850	35	12	15
TDF 022	3	LOW	1	2	650	15	8	5
TDF 023	3	HIGH	3	2	1050	15	10	15
TDF 024	5	LOW	1	4	850	15	10	10
TDF 025	5	HIGH	3	4	650	25	10	5
TDF 026	5	HIGH	3	2	850	25	8	10
TDF 027	3	HIGH	1	4	1050	25	8	15
TDF 028	5	HIGH	2	4	1050	15	12	5

The critical response values that were monitored included the percent pellets produced that were in the size range 0.8 - 1.25mm (R1), Carr's index (R2), Hausner ratio (R3), Angle of Repose (R4) % TDF released at 10 min (R5) % TDF released at 45 min (R6) and % TDF loaded into the pellets (R7). The constraints of the responses used in optimization studies are summarized in Table 5.4.

Table 5.4 Response values measured and constraints of response used for experimental design

Response Code	Name	Observations	Constraints
R1	% pellets in size range 0.8 - 1.25mm	18	Maximize
R2	Carr's index	18	5 > R7 < 5.5
R3	Hausner ratio	18	Minimize
R4	Angle of Repose	18	Minimize
R5	% TDF released at 10 min	18	50 > R5 < 65
R6	% TDF released at 45 min	18	Maximize
R7	% TDF loaded.	18	95 > R7 < 105

5.3.2 Statistical analysis

The significance of the model and model terms that were generated were analyzed by Analysis of Variance (ANOVA) type three (partial sum of squares) at a 5% level of significance using the statistical package, Design Expert[®] Version 8.0.4 Software(Stat-Ease Inc, Minneapolis, Minnesota, USA). The predicted residual error sum of squares (PRESS) was used to assess which of the input factors had a significant impact on the measured response(s). Predicted *versus* actual data diagnostic plots were used to determine the goodness of fit of the experimental data to the model and these results are listed in Appendix 2.

5.4 RESULTS AND DISCUSSION

5.4.1 Formulation Development

The L18 Taguchi orthogonal array design is an efficient optimization approach that does not use combinations of experiments for which all factors are used simultaneously at their highest or lowest levels. The L18 Taguchi orthogonal array design also avoids the need to generate data under extreme experimental conditions that is an approach used when the elimination of unsatisfactory data is necessary. A L18 Taguchi orthogonal array design was used to optimize the formulation and manufacture of TDF pellets produced by extrusion and spheronization. A total of 18 experiments were conducted using the designated design space and the response values observed are summarized in Table 5.5

Table 5.5 Responses observed following use of the Taguchi design

BATCH	RESPONSE VARIABLES						
	R1 % pellets 0.8 - 1.25 mm	R2 Carr's index	R3 Hausner ratio	R4 AOR/ °	R5 % TDF released 10 min	R6 % TDF released 45 min	R7 % TDF loaded
TDF 011	44.0	5.4	1.1	32.0	58	102	97.4
TDF 012	64.3	5.7	1.1	22.9	47	83	94.3
TDF 013	50.0	5.4	1.1	28.4	77	91	100.6
TDF 014	52.0	5.1	1.1	25.7	43	90	98.6
TDF 015	67.0	5.0	1.1	28.4	64	78	96.9
TDF 016	44.0	5.3	1.1	22.8	81	95	96.2
TDF 017	18.0	2.7	1.0	29.6	59	94	96.0
TDF 018	72.0	5.9	1.1	27.6	63	96	100.6
TDF 019	37.0	4.8	1.1	28.4	67	97	100.2
TDF 020	58.0	5.0	1.1	25.8	91	98	97.5
TDF 021	74.0	2.8	1.0	23.0	87	105	108.1
TDF 022	80.2	5.4	1.1	24.0	47	100	100.6
TDF 023	59.0	4.9	1.1	25.2	50	97	101.8
TDF 024	49.0	5.1	1.1	25.5	80	101	98.1
TDF 025	62.0	5.3	1.1	28.4	66	100	100.7
TDF 026	59.0	5.3	1.1	27.1	76	96	103.4
TDF 027	15.0	4.8	1.1	30.5	52	103	104.2
TDF 028	45.0	5.1	1.1	28.1	92	110	106.5

5.4.2 Model fitting and statistical analysis

ANOVA and the Regression Coefficient (R^2) were used to statistically analyze the data reported in Table 5.5. In addition normal plots of residuals, externally studentized residuals, Box-Cox plots, interaction and 3-dimensional plots were used to describe these data. The model(s) that best described the data were selected for use in the optimization process. Results were analyzed and used to establish experimental parameters to achieve target performance levels. In order to establish measures for significant responses ANOVA was used at a 5% level of significance and the data are summarized in Table 5.6.

Table 5.6 ANOVA data at 5% level of significance

Response	PRESS	Sum of squares	DF	Mean Square	F-value	p-value prob > F	Significance
R1	5203.67	1989.62	3	663.21	2.87	0.0737	Not significant
R2	11.06	5.97	3	1.99	4.43	0.0217	Significant
R3	0.010	0.013	5	0.0027	7.20	0.0025	Significant
R4	89.68	68.66	3	22.89	6.11	0.0071	Significant
R5	4183.02	1422.47	2	711.24	3.83	0.0412	Significant
R6	581.25	722.11	5	144.42	6.71	0.0033	Significant
R7	189.10	101.55	2	50.77	5.80	0.0136	Significant

The data summarized in Table 5.6 reveal that Carr's index, Hausner ratio, Angle of Repose, % TDF released at 10 min, % TDF released at 45 min and % TDF drug loaded were significant however the percent of pellets that were in the size range 0.8 – 1.25 mm was not a significant response. Importance levels were assigned to each response for the optimization process and were based on the defined target objectives for this study and the core responses % TDF loaded and % TDF released at 45 min were used for further numerical optimization. These two responses are further discussed in detail and the data for other significant responses have been included in Appendix 2 for completeness.

5.5 Response Surface Modeling

5.5.1 % TDF released at 45 min

The impact of formulation and process variables on the % TDF released at 45 min (R6) from the pellets was investigated using RSM to establish and identify which of the input variables have a significant impact on this response. A half-normal plot (Figure 5.3) can be used to identify significant effects and large and/or significant values are located above 70% probability. Evaluation of the half-normal plot reveals that the % w/w sorbitol (D) and % w/w Kollidon[®] CL-M (B) are two formulation variables that have a significant impact on this response. Spheronization time (A) was the only process variable that affected the % TDF released at 45 minutes. ANOVA was used to determine which, if any of the other input variables had a significant effect on the % TDF released at 45 minutes and the ANOVA data are reported in Table 5.7.

Design-Expert® Software
% release at 45 mins

▲ Error estimates

Shapiro-Wilk test

W-value = 0.928

p-value = 0.563

A: spheronization time.

B: BLENDER SPEED

C: % Croscarmellose-Na

D: % sorbitol

E: spheroniser speed

F: extruder speed

G: % MCC

H: % Kollidon CL-M

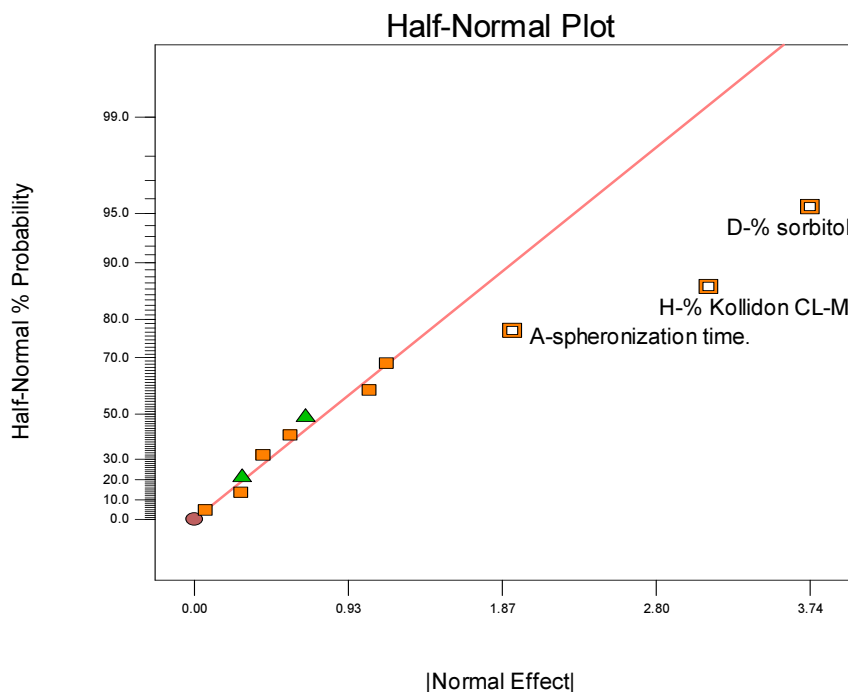


Figure 5.3 Half-normal plot depicting input variable effects on response R6

The data reveal that the model is significant as the effect of % w/w Kollidon[®] CL-M (H) and % w/w sorbitol (D) result in p-values <0.05 indicating that these input parameters have a significant effect on the % TDF released. The impact of spheronization time and other input variables are negligible on % TDF released at 45 minutes.

Table 5.7 ANOVA results for % TDF released at 45 min

Source	Sum of Squares	DF	Mean Square	F Value	p-value Prob > F	
Model	722.11	5	144.42	6.71	0.0033	significant
A-spheronization time.	80.22	1	80.22	3.73	0.0775	
D-% w/w sorbitol	369.78	2	184.89	8.59	0.0048	
H-% w/w Kollidon [®] CL-M	272.11	2	136.06	6.32	0.0133	
Residual	258.33	12	21.53			
Cor Total	980.44	17				

The % w/w sorbitol included in the formulation was expected to have an impact on the rate and extent of TDF release from the pellets. The % w/w Kollidon[®] CL-M affects the disintegration properties of pellets as they make contact with dissolution media and therefore is expected to have a significant effect on the % TDF released at 45 min.

The effect of % w/w sorbitol and % w/w Kollidon[®] CL-M on this response can be mathematically expressed using the linear relationship described in Equation 5.3

$$R6 = +96.44 - 1.78 * D[1] - 4.44 * D[2] + 2.06 * H[1] - 5.44 * H[2]$$

Equation 5.3

The equation, reported in terms of coded factors, can be used to make predictions about the response for specific levels of each factor. By default the high levels of the factors used are coded as +1 and the low levels are coded as -1. The coded equation is useful for identifying the relative impact of factors on responses through comparison of the coefficients for each factor [212, 213]. Coefficients that are associated with more than one factor represent an interaction effect between input variables or factors. The adequacy of the model can also be investigated by examining the residuals for data reduction. Externally studentized residuals are used to measure the number of standard deviations that separate actual and predicted values. A normal probability plot of residuals is then used to evaluate the data generated and a linear trend in the plot confirms that the data follows a normal distribution and defines, in part, the character of the residuals. The normal plot of residuals for the % TDF released at 45 minutes is depicted in Figure 5.4 and reveals that the plot follows a linear trend indicating that the residuals are normally distributed [214].

Design-Expert® Software
% release at 45 mins

Color points by value of
% release at 45 mins:

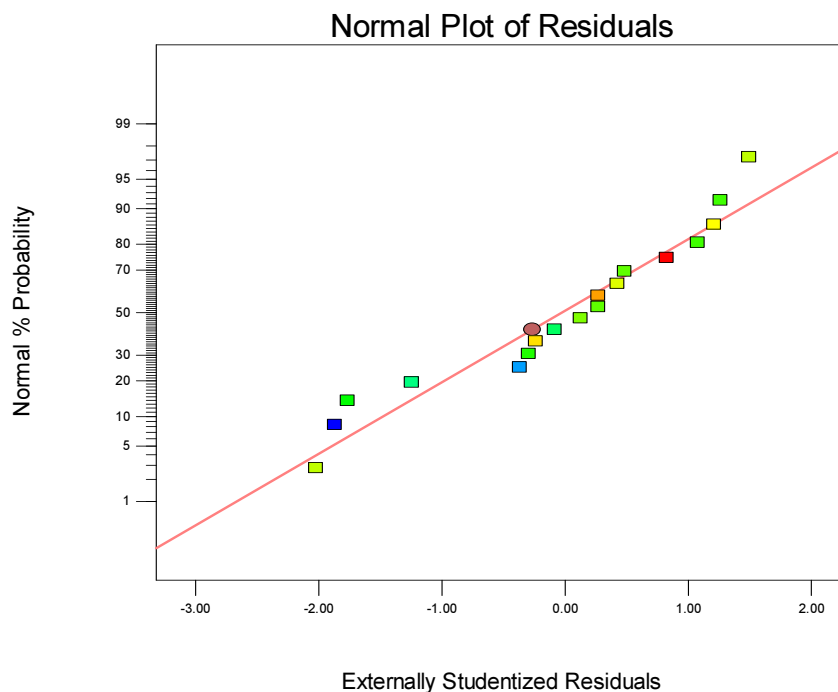


Figure 5.4 Normal plot of residuals for % TDF released at 45 min

A scatter plot of the externally studentized residuals and predicted responses can be used to determine the adequacy of a model. The plot should generally show random scatter that would suggest that the variance of the original observations is constant for all response values [214]. A funnel-shaped pattern is observed if the variance of the response depends on the mean level of % TDF released. Therefore an investigation of the adequacy of a model is undertaken to provide an indication if transformation of the model for the response variable of interest is necessary. The transformation of data may be required in order to enhance the applicability and usefulness of a model and these data are usually presented using a Box-Cox plot (Figure 5.5). These plots provide a guideline for selecting the correct power law transformation for the data. A recommended transformation is based on the best lambda value plotted as a green line that is found at the minimum point of a curve generated from the natural log of the sum of squares of the residuals. If the 95% confidence interval around lambda includes 1 that is represented by a blue line then a specific transformation is not recommended. Consequently the data are therefore located approximately in the best possible region of the parabola [188, 215-222].

Design-Expert® Software
% release at 45 mins

Lambda
Current = 1
Best = 3
Low C.I. =
High C.I. =

Recommend transform:
None
(Lambda = 1)

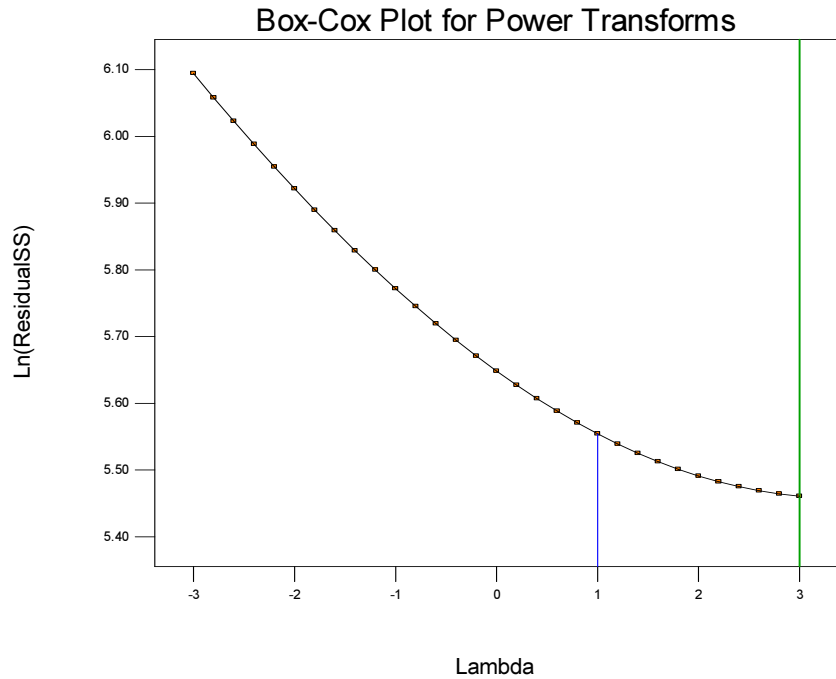


Figure 5.5 Box-Cox Plot for Power Transformation for % TDF released at 45 min

The externally studentized residuals plot for the % TDF released at 45 minutes is depicted in Figure 5.6. This plot represents the residuals *versus* ascending predicted response values for these data and permits evaluation of an assumption of constant variance. This approach also permits the detection of outliers in the data. Data points that fall outside the red lines are data points that are not well fitted to the current model [188, 223-227] and reflect that the observed value or model used may be wrong. However the externally studentized residuals plot reveals that the data are generally scattered and no obvious outliers are observed suggesting that data transformation was not required.

Design-Expert® Software
% release at 45 mins

Color points by value of
% release at 45 mins:

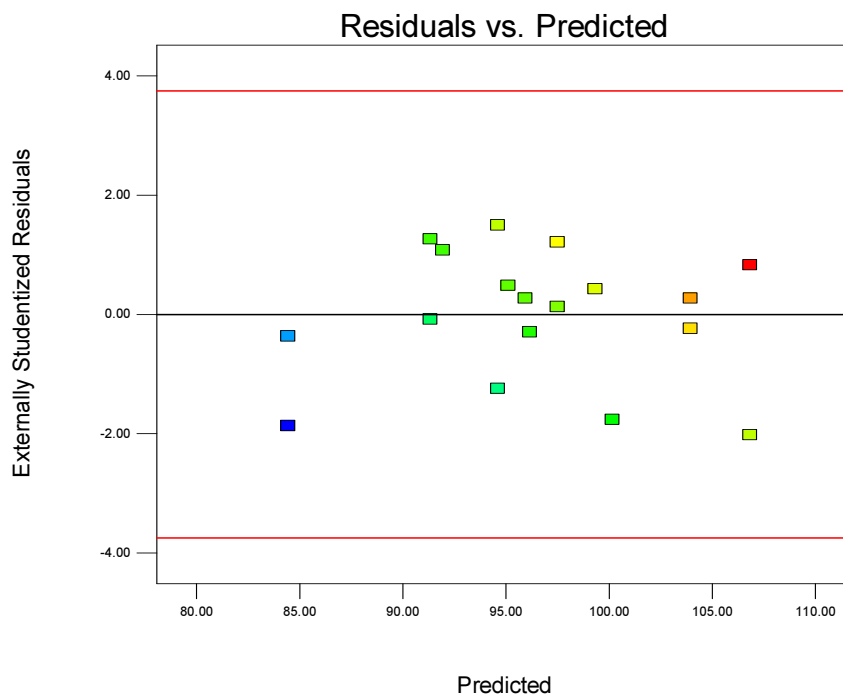


Figure 5.6 Plot of externally studentized residuals vs. predicted responses for % TDF released at 45 min.

One Factor Effects plots are used to depict linear effects of changing the level of a single factor at a time. The plot is constructed by predicting the responses for low (-1) and high (+1) levels of a factor and the "I beam" range symbols on the effect plot are established through least significant difference (LSD) calculations performed at the 95 % confidence level. If the LSD bars do not overlap, it can be assumed that the points are significantly different from each other. One Factor Effect Plots for % TDF released at 45 minutes vs. % w/w sorbitol and % w/w Kollidon® CL-M are depicted in Figures 5.7 and 5.8. The plots reveal that there is a direct correlation between the % TDF released at 45 min and the % w/w sorbitol and % w/w Kollidon® CL-M used in the formulation.

Design-Expert® Software
 Factor Coding: Actual
 % release at 45 mins (%)
 ● Design Points

X1 = D: % sorbitol

Actual Factors
 A: spherization time. = 3
 B: BLENDER SPEED = LOW
 C: % Croscarmellose-Na = 1%
 E: spheroniser speed = 650
 F: extruder speed = 15
 G: % MCC = 8
 H: % Kollidon CL-M = 5%

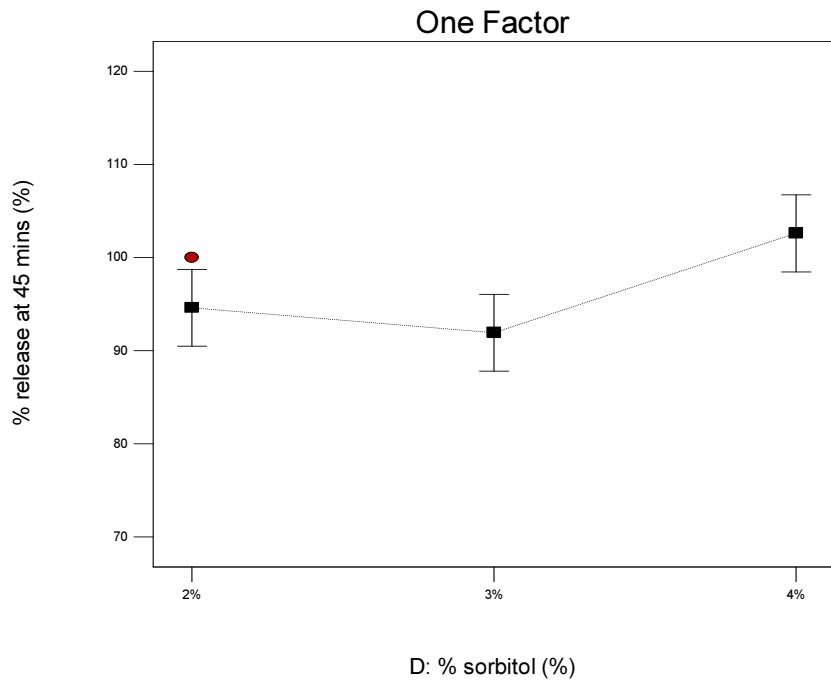


Figure 5.7 One Factor Effects Plot for % TDF released at 45 minutes vs. % w/w sorbitol

Design-Expert® Software
 Factor Coding: Actual
 % release at 45 mins (%)
 ● Design Points

X1 = H: % Kollidon CL-M

Actual Factors
 A: spherization time. = 3
 B: BLENDER SPEED = LOW
 C: % Croscarmellose-Na = 1%
 D: % sorbitol = 2%
 E: spheroniser speed = 650
 F: extruder speed = 15
 G: % MCC = 8

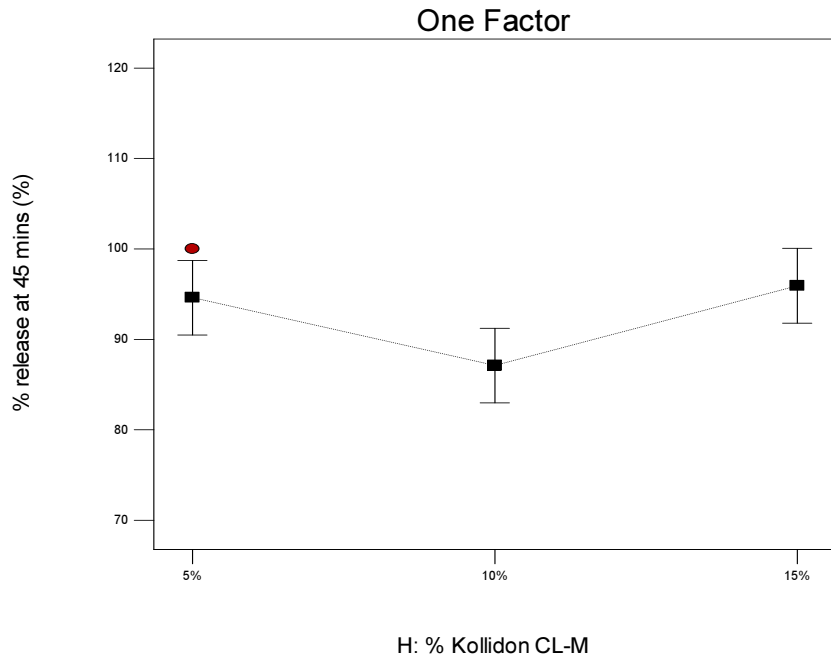


Figure 5.8 One Factor Effects Plot for % TDF released at 45 minutes vs. %w/w Kollidon® CL-M

An increase in the amount of each excipient used in the formulation is expected to increase the % TDF released as sorbitol is a dissolution enhancer and Kollidon® CL-M should increase pellet disintegration. However a dip in the plots is observed as the amount of each excipient is

increased and this may be attributed to an interaction between input parameters that are not evaluated when using a Taguchi screening design or can be partially explained by a lack of blend homogeneity. In order to further investigate such interactive effects a model such as Box-Behnken or Central Composite Design that are able to predict interactions should be used to reveal any interactive and individual parameter effects.

Three dimensional graphs are a projection of contour plots that allow for the spread points to be defined. The plots in Figures 5.9 and 5.10 display the effect of % w/w Kollidon[®] CL-M, % w/w sorbitol and spheronization time on the % TDF released at 45mins.

Design-Expert[®] Software
 Factor Coding: Actual
 % release at 45 mins (%)
 ● Design points above predicted value

X1 = H: % Kollidon CL-M
 X2 = A: spheronization time.

Actual Factors
 B: BLENDER SPEED = LOW
 C: % Croscarmellose-Na = 1%
 D: % sorbitol = 2%
 E: spheroniser speed = 650
 F: extruder speed = 15
 G: % MCC = 8

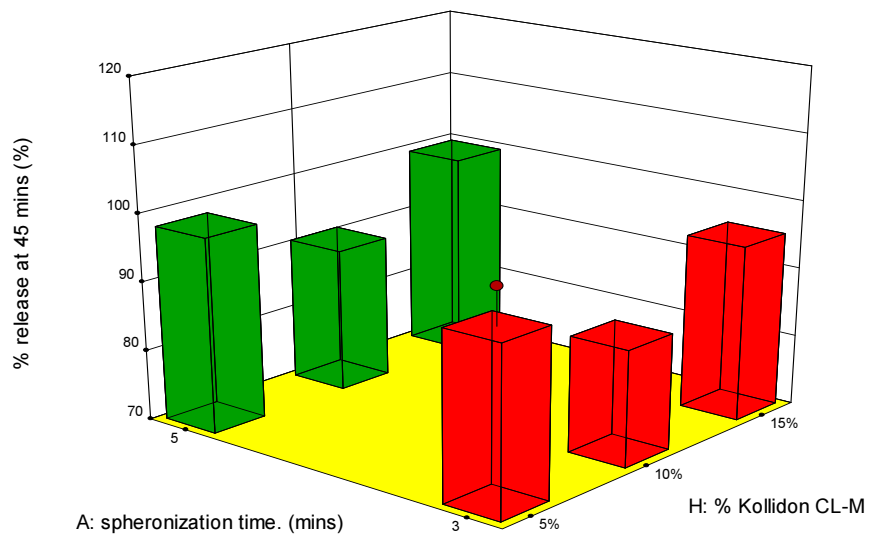


Figure 5.9 3-D plot of the effect of % w/w Kollidon[®] CL-M on % TDF released at 45 min.

The data in Figure 5.9 reveal that an increase in the amount of Kollidon[®] CL-M used with an increase in spheronization time results in an increase in the % TDF released at 45 min. An increase in the amount of Kollidon[®] CL-M would increase the rate of disintegration of pellets due to the popcorn-like structure of the product. An increase in the spheronization time and amount of Kollidon[®] CL-M used improves the sphericity of the pellets thereby increasing the surface area that is in contact with the dissolution medium resulting in a further increase in the % TDF released.

The same phenomenon is observed when an increased amount of sorbitol is used with longer spheronization times since sorbitol enhances dissolution rates by improving pellet surface morphology thereby increasing the surface area of the pellet that is in contact with the dissolution medium.

Design-Expert® Software
 Factor Coding: Actual
 % release at 45 mins (%)
 ● Design points above predicted value

X1 = D: % sorbitol
 X2 = A: spheronization time.

Actual Factors
 B: BLENDER SPEED = LOW
 C: % Croscarmellose-Na = 1%
 E: spheroniser speed = 650
 F: extruder speed = 15
 G: % MCC = 8
 H: % Kollidon CL-M = 5%

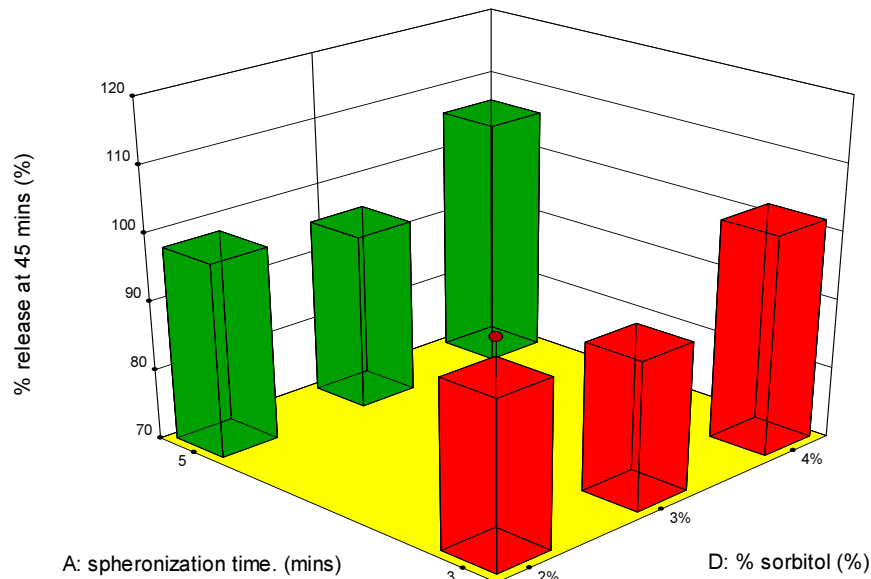


Figure 5.10 3-D plot of the effect of % w/w sorbitol on % TDF released at 45 min

An assessment of the data collected suggests that high amounts of Kollidon® CL-M and sorbitol used in conjunction with long spheronization times would result in a more rapid dissolution rate for TDF at the same time as enhancing the shape and surface morphology of the pellets. However the Taguchi orthogonal array design fails to identify interactions between input parameters and other factorial design models are required to elucidate the effect of interactions between process and formulation parameters.

5.5.2 % TDF loaded

The impact of formulation and process variables on the % TDF loaded (R7) was investigated using RSM to determine which input variable(s) may have a significant impact on this response. The half-normal plot reveals that the % w/w sorbitol (D) is the major formulation variable that affects the TDF loading. ANOVA analysis (Table 5.8) revealed a p-value < 0.05 for % w/w sorbitol confirming that this is a significant input variable.

Table 5.8 ANOVA results for % TDF loaded

Source	Sum of Squares	DF	Mean Square	F Value	p-value Prob > F	
Model	101.55	2	50.77	5.80	0.0136	significant
D-% w/w sorbitol	101.55	2	50.77	5.80	0.0136	
Residual	131.32	15	8.75			
Cor Total	232.87	17				

The effect of sorbitol content on response R7 can be mathematically described using a linear equation as shown in Equation 5.4

$$R7 = +100.9 + 0.072 * D[1] - 2.94 * D[2]$$

Equation 5.4

It is evident that sorbitol has an overall synergistic effect on the loading of TDF into the pellets. However the One Factor Effects plot (Figure 5.11) reveals an initial drop in TDF loading up to 3% w/w sorbitol followed by a gradual and linear increase thereafter. The Taguchi design fails to take into account interactions between process and formulation parameters and therefore the dip in % w/w TDF loading cannot be adequately explained but may be explained, in part by a lack of blend heterogeneity during batch to batch manufacture. Sorbitol assists with pellet rounding and improved surface morphology and is therefore expected to facilitate TDF incorporation into the pellets thereby increasing loading. However the opposite is observed when sorbitol content is increased from 2% w/w to 3% w/w. Therefore further optimization using other models that account for input variable interactions is necessary.

Design-Expert® Software
 Factor Coding: Actual
 drug load (%)
 ● Design Points

X1 = D: % sorbitol

Actual Factors
 A: spheronization time. = 3
 B: BLENDER SPEED = LOW
 C: % Croscarmellose-Na = 1%
 E: spheroniser speed = 650
 F: extruder speed = 15
 G: % MCC = 8
 H: % Kollidon CL-M = 5%

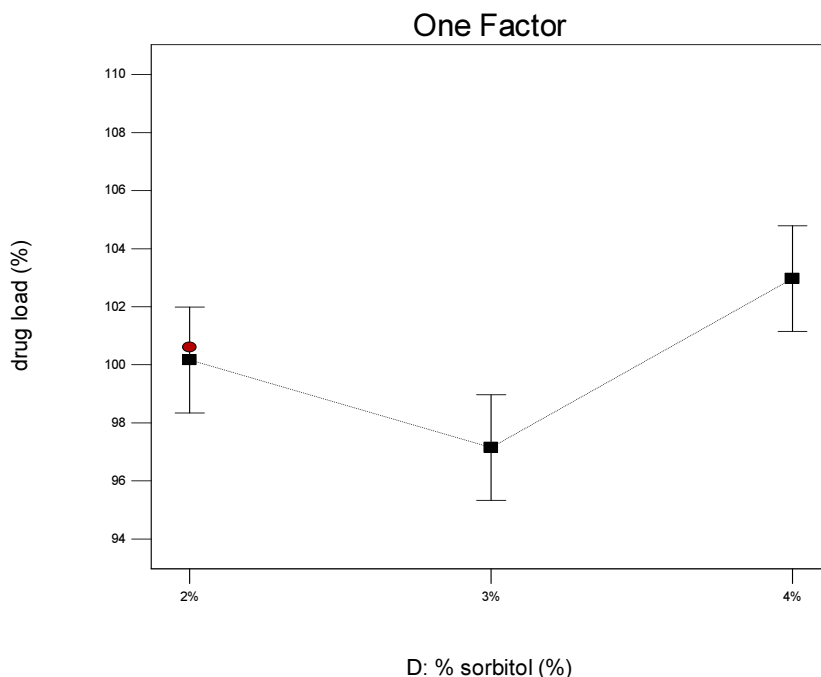


Figure 5.11 One Factor Effects Plot for % TDF loaded vs. % w/w sorbitol

5.5.3 Formulation optimization

Following an evaluation of RSM data generated following the analysis of the pellets manufactured using a L18 Taguchi orthogonal array, numerical optimization was used for the development of an optimized formulation that would ensure that the responses observed met pre-defined specifications for the pellets and that TDF was formulated in an immediate release dosage form. The constraints and responses listed in Table 5.4 were used for this purpose. The predicted response values and respective factor compositions for these studies are summarized in Table 5.9.

Table 5.9 Input variables and predicted responses.

Factor composition		Predicted response	
Spheronizer residence time (min)	3	% pellets of 0.8 - 1.25 mm	50.3
Blender speed	HIGH	Carr's index	5.4
% w/w CCS	1	Hausner ratio	1.1
% w/w sorbitol	4	Angle of Repose	26.9°
Spheronizer speed (rpm)	850	% TDF released at 10 min	57.7
Extruder speed (rpm)	15	% TDF released at 45 min	95.1
% w/w MCC	12	% TDF loaded.	102.9
% w/w Kollidon® CL-M	10		

Ramp plots (Figure 5.12) were used to provide a graphical view of the optimal solution for each parameter and the optimum factor settings are designated by red dots whereas the optimum expected responses are displayed in blue. The over-all desirability score is also displayed in these plots and is reported in the range between 0 and 1. Consequently the optimum solution is one that records the highest desirability score. The selected solution had a desirability score of 0.128 and experimental results generated using the optimum solution conditions are summarized in Table 5.10. A comparison of the observed and predicted responses was performed to establish the accuracy of the model.

Table 5.10 *Experimental and predicted responses for prediction of the optimized formulation.*

Response	Experimental value	Predicted value	Percent prediction error
% pellets of 0.8 - 1.25 mm	49.1	50.3	2.44
Carr's index	5.1	5.4	5.88
Hausner ratio	1.1	1.1	0.00
Angle of Repose	25.5	26.9	5.49
% TDF released at 10 min	63.1	57.7	8.56
% TDF released at 45 min	97.8	95.1	2.76
% TDF loaded	100.2	102.9	2.69

The actual responses observed for the optimized formulation are in close agreement with the predicted responses and the error of prediction summarized in Table 5.10 is < 10% in all cases. The percent prediction error is low for all responses indicating that the model is accurate.

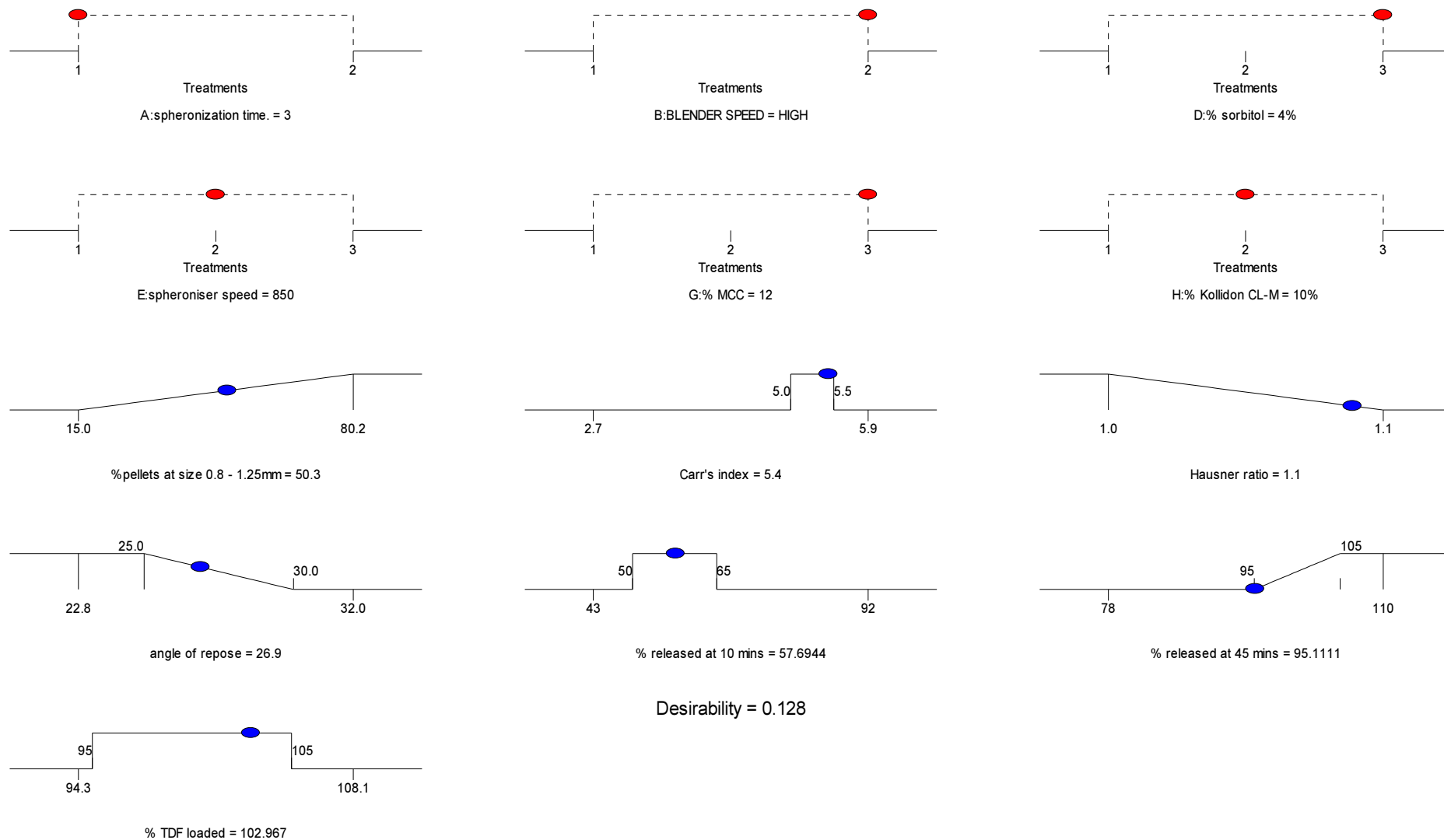


Figure 5.12 Ramp plots used for numerical optimization of input variables and target responses

The dissolution profiles for TDF released from the pellets produced using the optimized formulation compared to commercially available tablets are depicted in Figure 5.13.

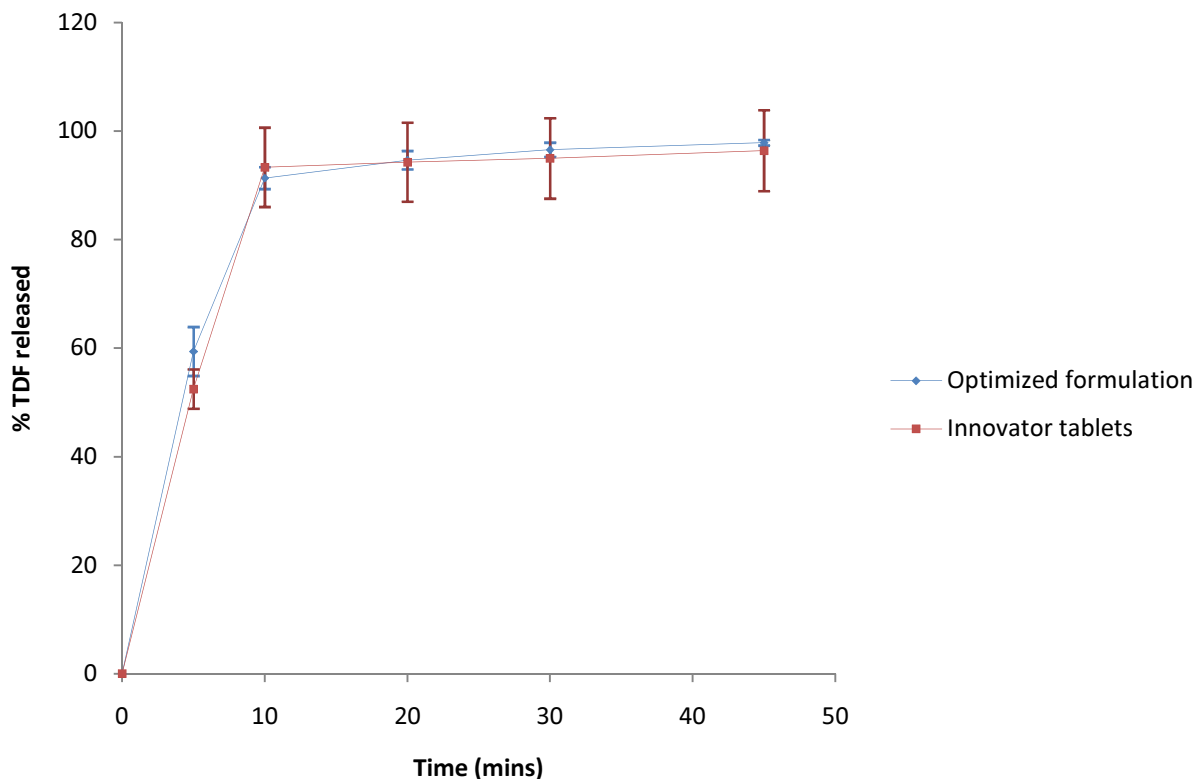
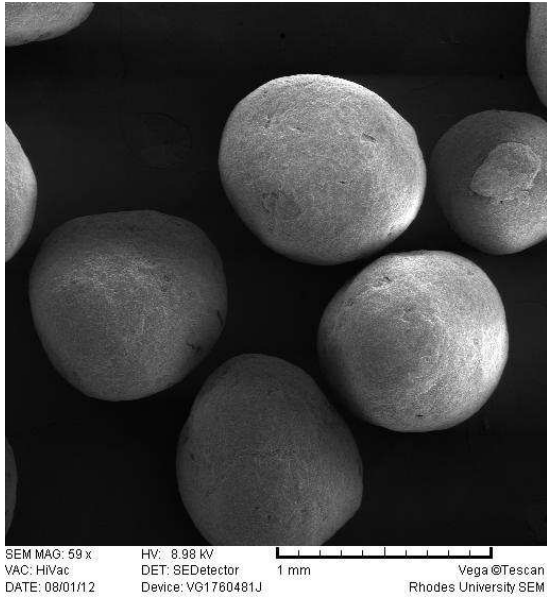


Figure 5.13 Dissolution profile of TDF from the optimized formulation and innovator tablets

The *in vitro* dissolution profile for TDF from the optimized formulation reveals that the optimized formulation is an immediate release dosage form and meets the compendial limits of at least 85% TDF released within 45 minutes of the commencement of testing. The formulation shows a similar release profile to the commercially available TDF tablet formulation.

The surface morphology and shape of the pellets following SEM imaging are depicted in Figures 5.14 and 5.15. The pellets that were manufactured exhibited excellent sphericity with a resultant value for roundness of 1.24. The pellets all exhibited a smooth surface with the presence of few craters and surface distortions evident. The physical features observed comply with the objectives that were set for the production of pellets i.e. smooth particles with a high degree of sphericity that exhibited good flow properties.

(I)



(II)

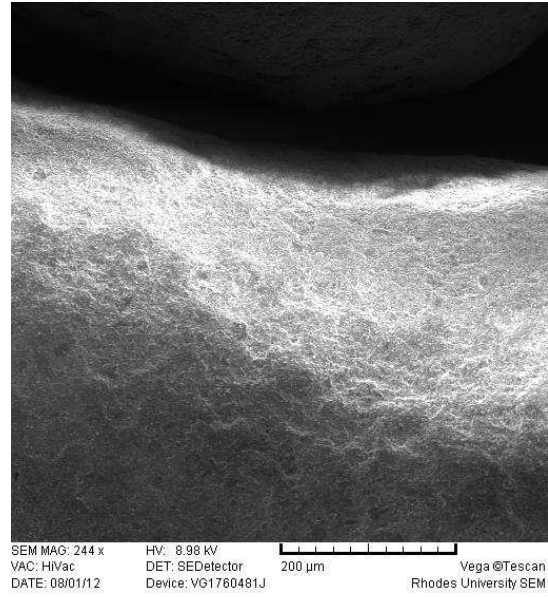


Figure 5.14 SEM image showing pellet shape (I) and pellet surface morphology (II)

5.6 CONCLUSIONS

Response Surface Methodology has many applications in the development and optimization of pharmaceutical systems, including the optimization of formulations, manufacturing processes and analytical methods. However the application of RSM requires accurate, precise and reproducible experimental conditions to be used for the generation of reliable data. Therefore the potential wide application of RSM is limited due to the sensitivity of this technique to experimental variability [180, 188, 228-231].

The benefits of using RSM for formulation optimization is that more than one input factor or variable can be investigated at a time and therefore large amounts of information can be generated with fewer experiments thereby ensuring a more efficient process with respect to time and cost is undertaken. An added advantage of this approach is that mathematical relationships generated for the models that are developed provide the formulation scientist with an indication of whether the effect(s) between factors are synergistic or antagonistic in nature.

There are several statistical design approaches that use RSM. A Taguchi orthogonal array design was selected for this optimization process since fewer experiments are required to generate data

for the same number of factors to be investigated when compared to other statistical approaches such as Central Composite (CCD) and Box-Behnken(BBD) designs uses lesser experimental runs and thus becomes faster and more economical [56, 232].

The process and formulation variables that were selected as input variables for evaluation included spheronizer residence time, blender speed, spheronizer speed, extruder speed, amount of CCS, sorbitol, MCC and Kollidon[®] CL-M for their impact on two significant responses *viz.*, % TDF loading and % TDF released at 45 min.

ANOVA analysis and 3-D graphs were plotted and clearly demonstrated the impact of the input variables on the % TDF released at 45 min and the % TDF loaded into the pellets. The amount of sorbitol and Kollidon[®] CL-M were the only significant variables that affected the % TDF released at 45 min. Kollidon[®] CL-M and sorbitol exhibited an overall synergistic effect on the *in vitro* release of TDF. However One Factor Effects plots revealed an initial dip in the release rate of TDF as the amount of the excipients were increased and this phenomenon can be attributed to interactive effects between factors that are not taken into account when the Taguchi design model is applied. Consequently further optimization may be required and would necessitate the use of a full factorial design model such as CCD that can account for input variable interaction(s).

Despite shortcomings the Taguchi approach permitted the identification of significant factors in the formulations investigated. The predicted optimum formulation was manufactured met pre-determined specifications. With the aid of mathematical modeling it was established that an optimized TDF pellet formulation required 75% w/w TDF, 1.0% w/w CCS, 4.0% w/w sorbitol, 12% w/w MCC and 10% w/w Kollidon[®] CL-M. The pellets were produced using an extruder speed of 15 rpm, a spheronizer speed of 850 rpm, a spheronization time of 3 minutes and blending was required to be achieved with blender speed set at the high level.

An optimized TDF containing pellet dosage form has been successfully developed and manufactured using experimental design and RSM

CHAPTER SIX

CONCLUSIONS

Pellets produced by extrusion and spheronization have several advantages over conventional drug delivery systems. This approach to produce spherical particles with a high loading capacity for API without producing extensively large particles is valuable in providing an alternate approach to produce novel technologies. Furthermore the extrusion and spheronization process facilitates the production of particles of uniform size with a narrow size distribution, that exhibit good flow properties in a relatively simple and cost effective manner. Pellets in which different API are loaded can be blended and filled into a single-unit dosage form that facilitates the delivery of two or more chemically compatible or incompatible API at the same time. Pellets offer a therapeutic advantage as they exhibit a low potential for irritation of the GIT, more uniform API absorption and greater bioavailability. Another major advantage of extrusion and spheronization is that it is a high throughput process that is associated with low production cost and may be used as a semi-continuous process. With the increasing cost of therapy for the treatment of chronic conditions such as HIV/AIDS that have reached epidemic proportions the WHO millennium development goals aimed to achieve universal access to treatment for HIV/AIDS at the lowest cost possible. Therefore in line with these goals the use of extrusion and spheronization to produce pellets of TDF may result in the production of medicines at reduced cost as the process is a high throughput with fewer process variables that can adversely affect the production process. Although the initial cost of equipment needed is high processing is cheaper and therefore only the setup costs determine the total cost to production. Consequently a TDF pellet formulation manufactured by extrusion and spheronization was developed, manufactured and assessed in these studies.

An HPLC method was developed for the quantitation of TDF in dosage forms and validated in accordance with ICH guidelines. The method was found to be sensitive, accurate, precise and linear over the concentration range of 1 – 180 µg/ml. The precision and accuracy of the HPLC method was confirmed by use of % RSD and % bias and the results reveal that these parameters were < 3% in all cases. The method is selective and stability indicating and can be used for the quantitation of TDF in dosage forms in the presence of excipients and for the separation of degradation products. Analysis was achieved using a validated RP-HPLC method using a 5µm

Phenomenex[®] Luna[®], C₁₈ (2)150 x 4.60 mm i.d stationary phase with a mobile phase of ACN: water in a 40:60 % v/v ratio at a flow rate of 0.9 ml min⁻¹. The injection volume was maintained at 10 µl and sample detection was achieved using a UV detection system at a wavelength of 259 nm and a 0.1 AUFS sensitivity setting. System suitability tests *viz.*, resolution and peak tailing factor were undertaken throughout the development and validation of the HPLC method to ensure that the results generated were appropriate and that performance of the method was continually monitored during analysis.

Preformulation studies are important in formulation development activities as they provide formulation scientists with data to facilitate the production of a quality dosage form and permits the product development team to anticipate the behavior of some materials during product manufacture. Although the data generated offers no certainty in respect of interactions these studies form the foundation of building quality into a pharmaceutical product. The physical characteristics of MCC, CCS and Kollidon[®] CL-M were assessed using SEM and clearly confirmed that the compounds were likely to flow adequately. The flowability was also evaluated by establishing the Angle of Repose, CI and HR for the materials. Furthermore SEM analysis established that the particle size of all excipients and API were within a narrow range suggesting that blend homogeneity could be achieved following blending and that the size-reduction of the materials was not necessary.

DSC data demonstrated that no interaction between TDF and the excipients used was likely to occur and therefore long term incompatibilities were not expected to be observed. These findings were confirmed using IR analysis and no physical interaction was observed between the excipients and TDF. DSC data also revealed the existence of α and β -polymorphic forms of TDF as two enthalpy changes were observed on the thermograms generated during analysis of the API. The existence of two polymorphs is unlikely to result in an incompatibility and this was confirmed by IR analysis. The IR spectra generated for TDF and 1:1 binary mixtures of TDF and excipients revealed that the characteristic peaks for TDF were present in all mixtures and it can be concluded that TDF is likely to be compatible with all excipients tested. Thermal analysis of TDF also confirmed that TDF was likely to be stable during manufacture and the degradation temperature observed using DSC confirmed that degradation of TDF during manufacture was unlikely. Whilst it is unlikely that incompatibilities would occur between TDF and the excipients

used in these studies, long term stability studies on the final product must be conducted to ensure that this is the case.

Extrusion and spheronization was used to produce TDF pellets, as a high TDF load in a small dosage form using a simple production approach were part of the objectives of this study. The formulation of pellets using extrusion and spheronization is challenging when a poorly soluble API such as TDF is to be incorporated into pellets to produce an appropriate shape, texture, flowability and TDF release characteristics from the pellets. The variation in physical characteristics and the slow release of TDF is not an uncommon phenomenon when producing pellets, particularly if spheronization aids such as MCC only, are used in the formulation. To date MCC remains the most frequently used excipient for the production of pellets by extrusion and spheronization based on its good binding properties that provide cohesiveness to a wetted mass containing MCC. Furthermore it is able to adsorb and retain a large quantity of water due to a large surface area and high internal porosity and therefore facilitation of extrusion, improved wet mass plasticity and enhanced spheronization are possible. Furthermore control of the movement of water through the plastic mass prevents phase separation during extrusion or spheronization. Due to these properties MCC containing pellets manufactured by extrusion and spheronization are characterized by a narrow particle size distribution, high sphericity, smooth surface properties and exhibit a high density. However when poorly soluble molecules are loaded into pellets manufactured with MCC only there is a tendency to exhibit prolonged release that is in part due to the lack of disintegration of pellets. MCC facilitates water uptake into pellets, however swelling effects are insufficient to break the spherical shape apart leading to diffusion control of release of the TDF through an intact matrix resulting in prolonged release. The objective of this project was to produce pellets that would result in immediate release of TDF and therefore the use of excipients that would enhance TDF release were also included in the formulation.

The initial prototype formulation was established following a literature review of formulae used for the manufacture of pellets. However the use of water and MCC as the only diluent and spheronization aid resulted in retarded release of TDF from the pellets. Consequently the formulation was modified to ensure that rapid release of TDF could be achieved. A co-blended composition of MCC and Kollidon[®] CL-M was used to enhance release. In addition, CCS and

sorbitol were also included in the test formulation. The aim of initial formulation development studies was to maintain as high a loading of TDF as possible whilst using the lowest amount of MCC that would produce pellets of the quality defined by the study objectives. The amount of TDF was maintained at 75% w/w for initial formulation development studies and 10 batches of pellets were manufactured with different amounts of MCC, Kollidon[®] CL-M, CCS and sorbitol and the data suggests that Batches TDF-001, TDF-003, TDF-004, TDF-006 and TDF-010 had better flow properties than other batches. The inclusion of relatively low quantities of MCC and Kollidon[®] CL-M in Batches TDF-001 and TDF-003 resulted in the need for less water than that used for the manufacture of the remaining batches. The increased water content required for the granulations resulted in the production of pellets with varied pellet size that appeared to exhibit poor flow properties. Batches TDF-002, TDF-004, TDF-008, TDF-009 and TDF-010 were manufactured with reduced amounts of MCC and included Kollidon[®] CL-M which may have increased the resistance of the formulation to the formation and shaping forces involved during extrusion and spheronization, thereby resulting in the production of irregular shaped pellets that is clearly indicated by the values observed for roundness compared to batches with higher roundness values. Batches TDF-001, TDF-006 and TDF-008 released only 22.87%, 51.23% and 59.62% TDF respectively after 45 min in 0.1M HCl. These batches were formulated without a disintegrant and the pellets failed to disintegrate thus TDF release was slower. TDF exhibits low aqueous solubility and therefore it is expected that dissolution rates will be slow. The addition of Kollidon[®] CL-M, CCS and sorbitol to other batches increased the release of TDF exponentially with more than 85% TDF being released from Batches TDF-002, TDF-003, TDF-005 and TDF-010 at 45 min. Batch TDF-003 exhibited a maximum amount of TDF released of 101.2% at 45 min. Some of the batches produced at this stage of the research process met all requirements for quality of TDF pellets which included the production of pellets with high sphericity over a narrow particle size distribution, smooth surface properties, high density and immediate release characteristics. Following evaluation of the initial products a single formulation, *viz.*, Batch TDF-003 was selected for further optimization using DOE.

DOE is a statistical approach that has become a popular tool in the pharmaceutical industry to optimize formulation composition, analytical methods and manufacturing processes as it allows for the investigation of several input factors at the same time and avoids the tedious and

traditional “modification of one variable at a time” approach. Consequently solutions to problems can be readily distilled in a short time period.

The results of optimization studies revealed that the response for % TDF released at 45 min and % TDF loaded were the most significant factors affected by process parameters and the formulation composition. Specifically these responses were strongly dependent on the levels of sorbitol and Kollidon[®] CL-M used in the formulation of the pellets. Although the results of evaluating the models generated suggest that interactive effects of process variables may exist, they could not be categorically identified as the Taguchi screening design used for the optimization process does not permit elucidation of interactive effects. Therefore it would be necessary to conduct further optimization studies using either a partial or full factorial statistical design approach to establish if any interactions do in fact, exist.

A numerical optimization approach using a desirability function was used to predict a formulation composition that would produce pellets that exhibited responses that fell within pre-determined specifications or limits. A formulation composition that included 75% w/w TDF, 1% w/w CCS, 4% w/w sorbitol, 12% w/w MCC and 10% w/w Kollidon[®] CL-M was predicted as the optimum composition. The manufacturing parameters predicted required the use of an extruder speed of 15 rpm, a spheronizer speed of 850 rpm, a spheronization time of 3 minutes and use of the blender with the speed set at the maximum level. The predicted response values were in close agreement with the experimentally derived values and the average percent prediction error (PPE) was < 9% for all responses measured, indicating that the model was adequate for the prediction of values for measured responses.

Size 0 capsules were filled manually and quality control for intra-batch variability was conducted using the assay value and capsule fill weight to ascertain uniform fill across batches. Intra-batch variability was low with a maximum relative standard deviation < 5% observed in all cases. The hard gelatin capsules dissolve rapidly and did not hinder the dissolution rate of TDF and are therefore adequate carriers for this IR dosage form.

A pellet dosage form of TDF has been developed and manufactured by use of extrusion and spheronization. The manufacturing process was optimized and the impact of changes in formulation composition on dosage form performance was evaluated using DOE. In addition

RSM was used to optimize the pellet formulation with respect to physical characteristics, TDF loading and *in vitro* release.

Future studies in respect of this technology must necessarily include stability testing to assess potential changes in the quality of TDF alone and in the dosage form under the influence of different temperature and humidity conditions to establish long term chemical stability and physical performance of the dosage form. Further optimization of the formulation using partial or full factorial designs that can identify the interactive effect(s) of process and formulation variables on product attributes and performance should also be performed.

APPENDIX 1

Batch record summaries

RHODES UNIVERSITY

FACULTY OF PHARMACY, GRAHAMSTOWN, SOUTH AFRICA

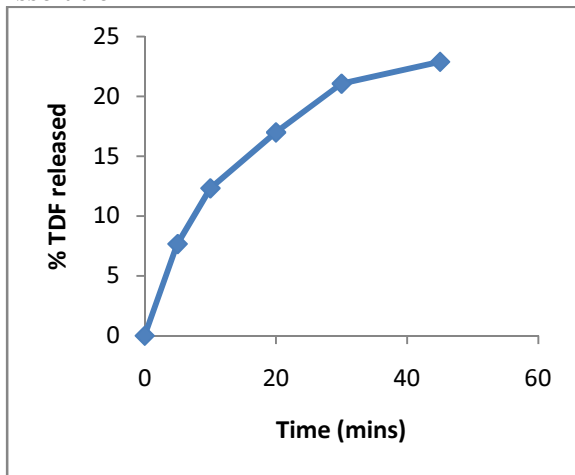
BATCH SUMMARY

Formulator:	Tawanda Dube	Batch Size	250g
Product :	TDF Pellets	Temperature	21.4°C
Batch ID:	TDF-001	Humidity	42%
Production Date	16-01-2012		

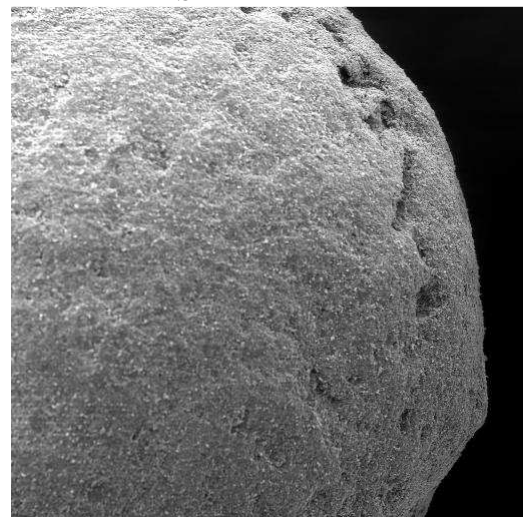
Material	Amount added	Production	Model
TDF	75%	Extruder	Caleva Extruder 20
Kollidon CL-M	-	Spheronizer	Caleva MBS 250
Sorbitol	-	Dryer	STREA-1 Aeromatic fluid bed dryer
CCS	-	Analysis	
MCC PH-102	10%	SEM	Tescan, VEGA LMU
Water	137ml	Dissolution	Hanson Research SR 8 PLUS

Process Parameters	Value
Blender speed	High
Extruder speed	30
Spheronizer speed	900 rpm
Spheronizer resident time	3 min

Dissolution



SEM



SEM MAG: 257 x HV: 10.00 kV 200 μm Vega ©Tescan
VAC: HiVac DET: SEDetector
DATE: 08/01/12 Device: VG1760481J Rhodes University SEM

AOR : 23.96

HR : 1.06

CI : 5.41

COMMENTS: Spherical pellets, retarded TDF release.

RHODES UNIVERSITY

FACULTY OF PHARMACY, GRAHAMSTOWN, SOUTH AFRICA

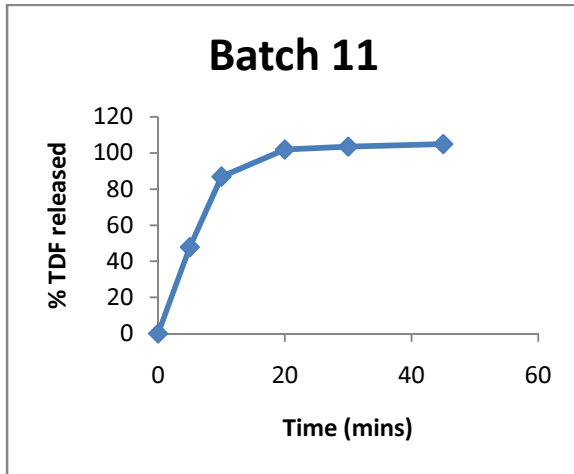
BATCH SUMMARY

Formulator	Tawanda Dube	Batch Size	250g
Product	TDF Pellets	Temperature	21.9°C
Batch ID	TDF-002	Humidity	42%
Production Date	16-01-2012		

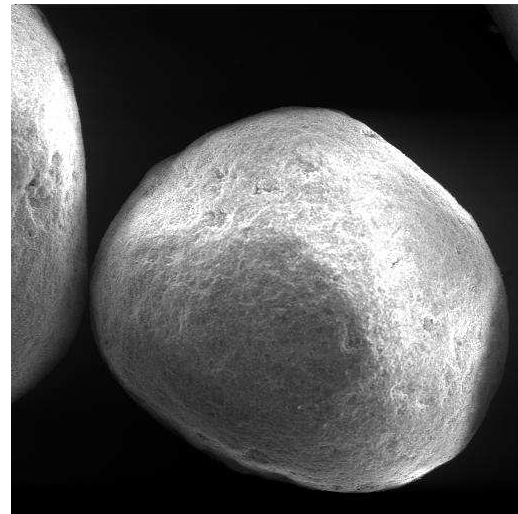
Material	Amount added	Production	Model
TDF	75%	Extruder	Caleva Extruder 20
Kollidon CL-M	15%	Spheronizer	Caleva MBS 250
Sorbitol	4%	Dryer	STREA-1 Aeromatic fluid bed dryer
CCS	3%	Analysis	
MCC PH-102	12%	SEM	Tescan, VEGA LMU
Water	137ml	Dissolution	Hanson Research SR 8 PLUS

Process Parameters	Value
Blender speed	High
Extruder speed	30
Spheronizer speed	900 rpm
Spheronizer resident time	3 min

Dissolution



SEM



SEM MAG: 143 x HV: 8.98 kV
 VAC: HiVac DET: SEDetector 500 µm Vega ©Tescan
 DATE: 08/01/12 Device: VG1760481J Rhodes University SEM

AOR : 30.47
HR : 1.06
CI : 12.71

COMMENTS: Large size variability, smooth surface.

RHODES UNIVERSITY

FACULTY OF PHARMACY, GRAHAMSTOWN, SOUTH AFRICA

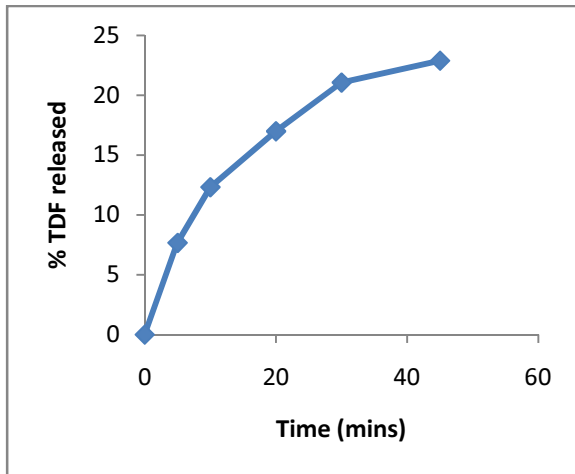
BATCH SUMMARY

Formulator	Tawanda Dube	Batch Size	250g
Product	TDF Pellets	Temperature	21.6°C
Batch ID	TDF-003	Humidity	41%
Production Date	16-01-2012		

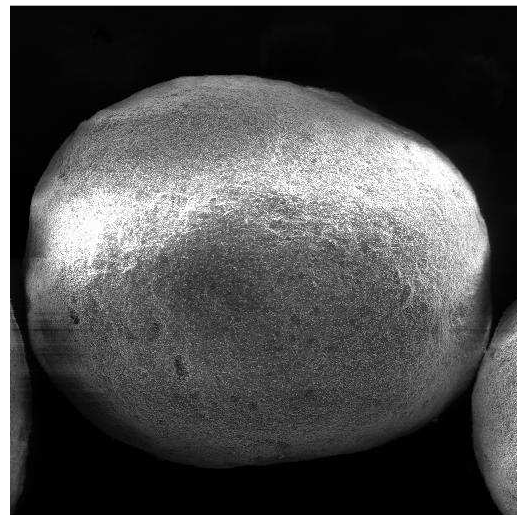
Material	Amount added	Production	Model
TDF	75%	Extruder	Caleva Extruder 20
Kollidon CL-M	10%	Spheronizer	Caleva MBS 250
Sorbitol	3%	Dryer	STREA-1 Aeromatic fluid bed dryer
CCS	2%	Analysis	
MCC PH-102	10%	SEM	Tescan, VEGA LMU
Water	137ml	Dissolution	Hanson Research SR 8 PLUS

Process Parameters	Value
Blender speed	High
Extruder speed	30
Spheronizer speed	900 rpm
Spheronizer resident time	3 min

Dissolution



SEM



SEM MAG: 126 x HV: 10.00 kV
 YAC: HiVac DET: SEDetector 500 μm Vega ©Tescan
 DATE: 08/01/12 Device: VG1760481J Rhodes University SEM

AOR : 22.89
HR : 1.05
CI : 5.31

COMMENTS: Irregular shape, immediate TDF release.

RHODES UNIVERSITY

FACULTY OF PHARMACY, GRAHAMSTOWN, SOUTH AFRICA

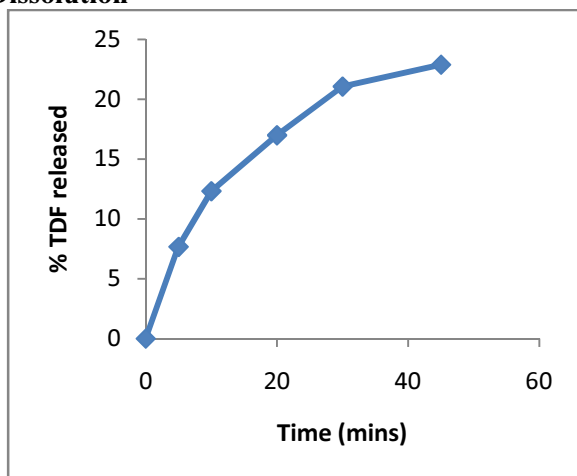
BATCH SUMMARY

Formulator	Tawanda Dube	Batch Size	250g
Product	TDF Pellets	Temperature	21.8°C
Batch ID	TDF-004	Humidity	42%
Production Date	16-01-2012		

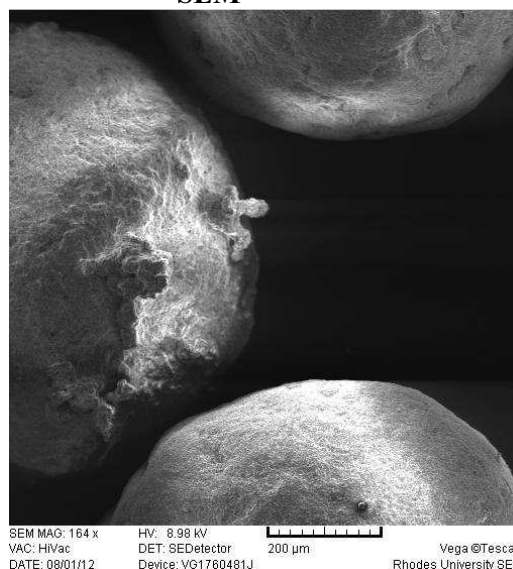
Material	Amount added	Production	Model
TDF	75%	Extruder	Caleva Extruder 20
Kollidon CL-M	10%	Spheronizer	Caleva MBS 250
Sorbitol	3%	Dryer	STREA-1 Aeromatic fluid bed dryer
CCS	3%	Analysis	
MCC PH-102	12%	SEM	Tescan, VEGA LMU
Water	137ml	Dissolution	Hanson Research SR 8 PLUS

Process Parameters	Value
Blender speed	High
Extruder speed	30
Spheronizer speed	900 rpm
Spheronizer resident time	3 min

Dissolution



SEM



AOR : 25.73
HR : 1.05
CI : 11.13

COMMENTS: Rough surface with craters, rapid TDF release

RHODES UNIVERSITY

FACULTY OF PHARMACY, GRAHAMSTOWN, SOUTH AFRICA

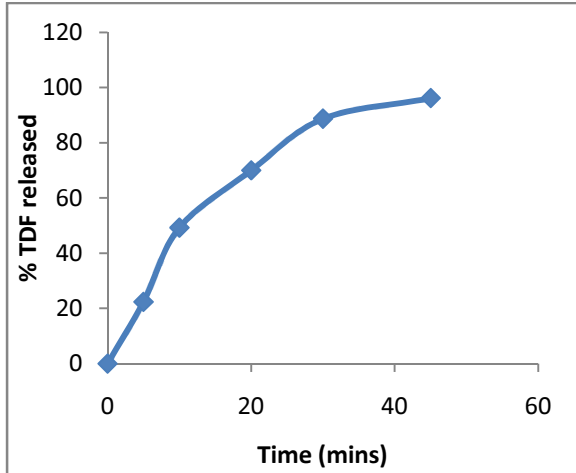
BATCH SUMMARY

Formulator	Tawanda Dube	Batch Size	250g
Product	TDF Pellets	Temperature	21.8°C
Batch ID	TDF-005	Humidity	42%
Production Date	16-01-2012		

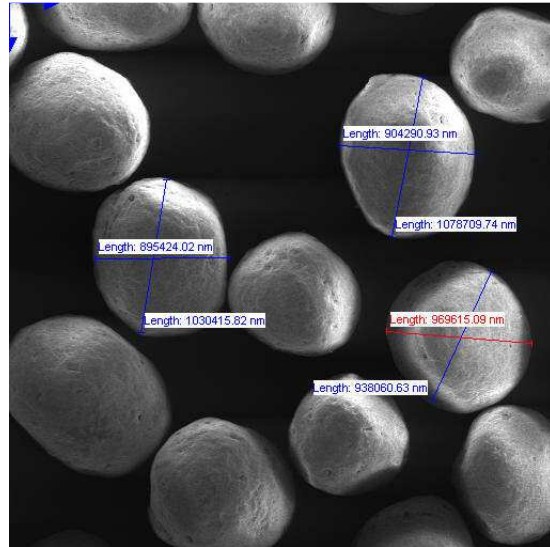
Material	Amount added	Production	Model
TDF	75%	Extruder	Caleva Extruder 20
Kollidon CL-M	0%	Spheronizer	Caleva MBS 250
Sorbitol	4%	Dryer	STREA-1 Aeromatic fluid bed dryer
CCS	4%	Analysis	
MCC PH-102	8%	SEM	Tescan, VEGA LMU
Water	137ml	Dissolution	Hanson Research SR 8 PLUS

Process Parameters	Value
Blender speed	High
Extruder speed	30
Spheronizer speed	900 rpm
Spheronizer resident time	3 min

Dissolution



SEM



AOR : 31.42
HR : 1.05
CI : 4.76

COMMENTS: Good flow properties, large size variation.

RHODES UNIVERSITY

FACULTY OF PHARMACY, GRAHAMSTOWN, SOUTH AFRICA

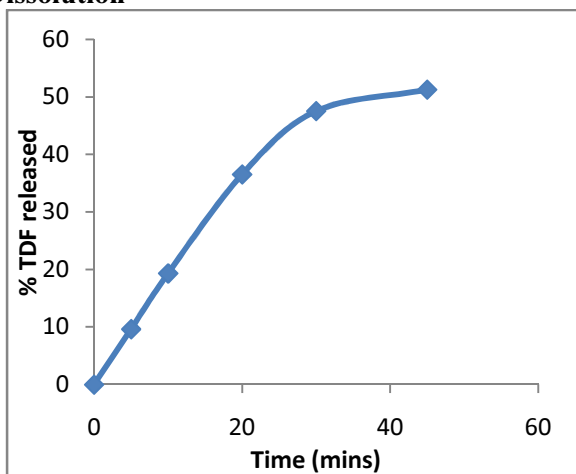
BATCH SUMMARY

Formulator	Tawanda Dube	Batch Size	250g
Product	TDF Pellets	Temperature	21.8°C
Batch ID	TDF-006	Humidity	42%
Production Date	16-01-2012		

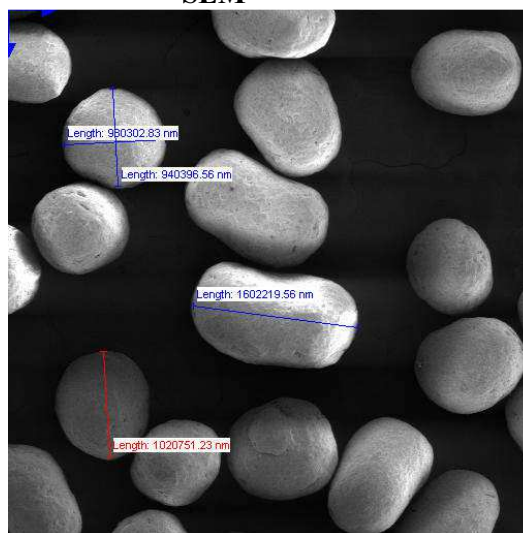
Material	Amount added	Production	Model
TDF	75%	Extruder	Caleva Extruder 20
Kollidon CL-M	10%	Spheronizer	Caleva MBS 250
Sorbitol	5%	Dryer	STREA-1 Aeromatic fluid bed dryer
CCS	0%	Analysis	
MCC PH-102	12%	SEM	Tescan, VEGA LMU
Water	137ml	Dissolution	Hanson Research SR 8 PLUS

Process Parameters	Value
Blender speed	High
Extruder speed	30
Spheronizer speed	900 rpm
Spheronizer resident time	3 min

Dissolution



SEM



AOR : 23.10
HR : 1.05
CI : 4.76

COMMENTS: Retarded TDF release, irregular shape.

RHODES UNIVERSITY

FACULTY OF PHARMACY, GRAHAMSTOWN, SOUTH AFRICA

BATCH SUMMARY

Formulator	Tawanda Dube	Batch Size	250g
Product	TDF Pellets	Temperature	21.8°C
Batch ID	TDF-007	Humidity	42%
Production Date	16-01-2012		

Material	Amount added	Production	Model
TDF	75%	Extruder	Caleva Extruder 20
Kollidon CL-M	15%	Spheronizer	Caleva MBS 250
Sorbitol	3%	Dryer	STREA-1 Aeromatic fluid bed dryer
CCS	4%	Analysis	
MCC PH-102	0%	SEM	Tescan, VEGA LMU
Water	137ml	Dissolution	Hanson Research SR 8 PLUS

Process Parameters	Value
Blender speed	High
Extruder speed	30
Spheronizer speed	900 rpm
Spheronizer resident time	3 min

AOR : --

HR : --

CI : --

COMMENTS: No product obtained

RHODES UNIVERSITY

FACULTY OF PHARMACY, GRAHAMSTOWN, SOUTH AFRICA

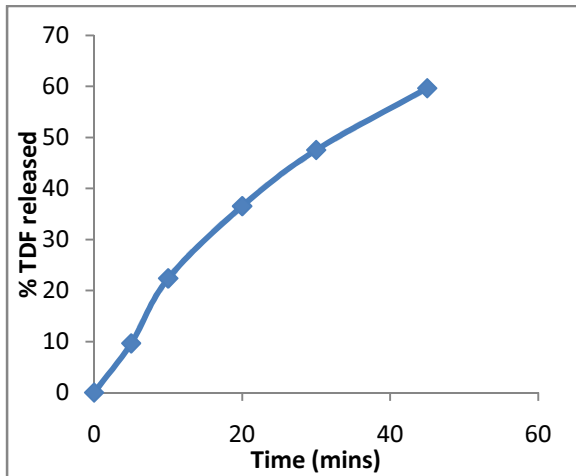
BATCH SUMMARY

Formulator	Tawanda Dube	Batch Size	250g
Product	TDF Pellets	Temperature	21.8°C
Batch ID	TDF-008	Humidity	42%
Production Date	16-01-2012		

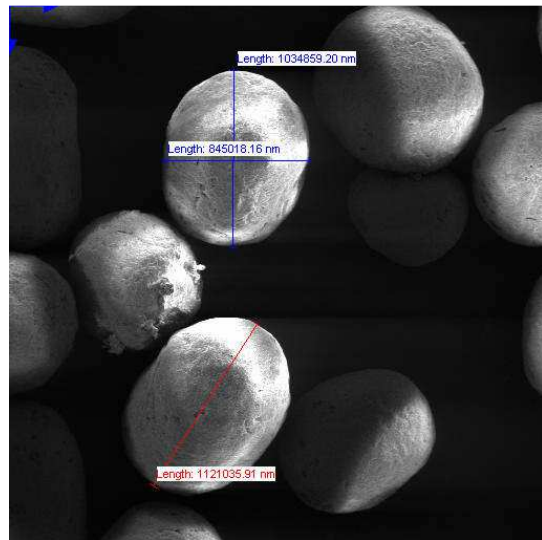
Material	Amount added	Production	Model
TDF	75%	Extruder	Caleva Extruder 20
Kollidon CL-M	10%	Spheronizer	Caleva MBS 250
Sorbitol	5%	Dryer	STREA-1 Aeromatic fluid bed dryer
CCS	0%	Analysis	
MCC PH-102	6%	SEM	Tescan, VEGA LMU
Water	137ml	Dissolution	Hanson Research SR 8 PLUS

Process Parameters	Value
Blender speed	High
Extruder speed	30
Spheronizer speed	900 rpm
Spheronizer resident time	3 min

Dissolution



SEM



AOR : 40.23
HR : 1.40
CI : 28.52

COMMENTS: Retarded TDF release, rough pellet surface

RHODES UNIVERSITY

FACULTY OF PHARMACY, GRAHAMSTOWN, SOUTH AFRICA

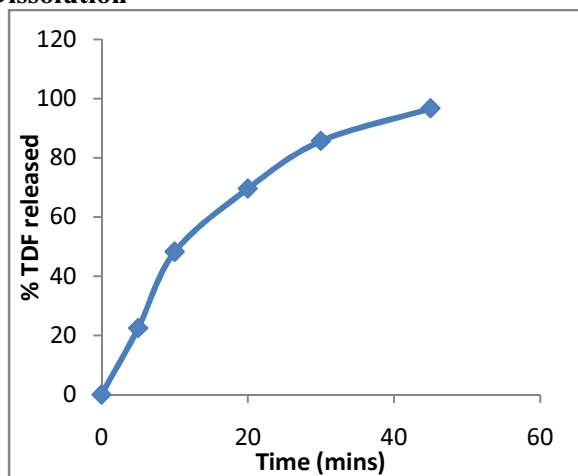
BATCH SUMMARY

Formulator	Tawanda Dube	Batch Size	250g
Product	TDF Pellets	Temperature	21.8°C
Batch ID	TDF-009	Humidity	42%
Production Date	16-01-2012		

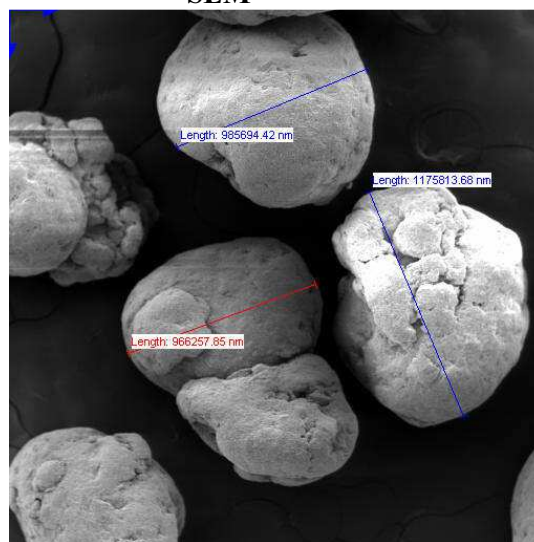
Material	Amount added	Production	Model
TDF	75%	Extruder	Caleva Extruder 20
Kollidon CL-M	5%	Spheronizer	Caleva MBS 250
Sorbitol	0%	Dryer	STREA-1 Aeromatic fluid bed dryer
CCS	3%	Analysis	
MCC PH-102	10%	SEM	Tescan, VEGA LMU
Water	137ml	Dissolution	Hanson Research SR 8 PLUS

Process Parameters	Value
Blender speed	High
Extruder speed	30
Spheronizer speed	900 rpm
Spheronizer resident time	3 min

Dissolution



SEM



AOR : 30.24
HR : 1.10
CI : 9.19

COMMENTS: Irregular shape, rough surface.

RHODES UNIVERSITY

FACULTY OF PHARMACY, GRAHAMSTOWN, SOUTH AFRICA

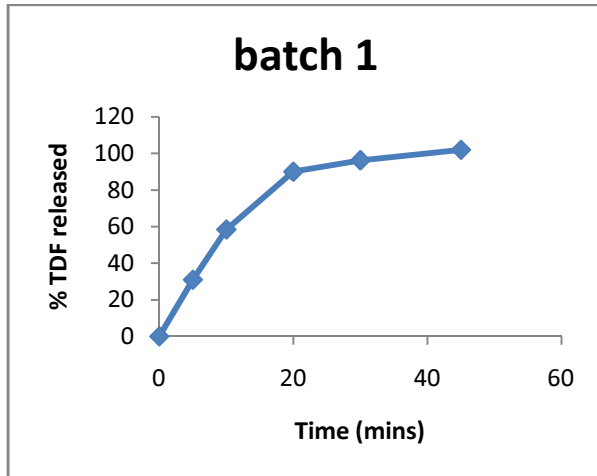
BATCH SUMMARY

Formulator	Tawanda Dube	Batch Size	250g
Product	TDF Pellets	Temperature	17.9°C
Batch ID	TDF-010	Humidity	51%
Production Date	23-03-2012		

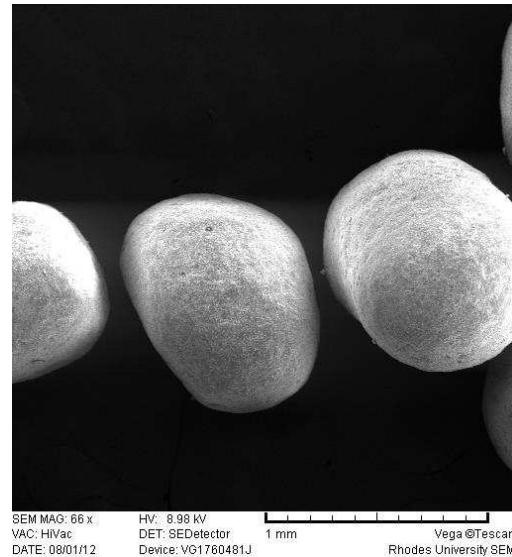
Material	Amount added	Production	Model
TDF	75%	Extruder	Caleva Extruder 20
Kollidon CL-M	5%	Spheronizer	Caleva MBS 250
Sorbitol	2%	Dryer	STREA-1 Aeromatic fluid bed dryer
CCS	1%	Analysis	
MCC PH-102	8%	SEM	Tescan, VEGA LMU
Water	120ml	Dissolution	Hanson Research SR 8 PLUS

Process Parameters	Value
Blender speed	Low
Extruder speed	15 rpm
Spheronizer speed	650 rpm
Spheronizer resident time	3 min

Dissolution



SEM



AOR : 28.21
HR : 1.06
CI : 5.67

COMMENTS: Immediate TDF release, smooth surface

RHODES UNIVERSITY

FACULTY OF PHARMACY, GRAHAMSTOWN, SOUTH AFRICA

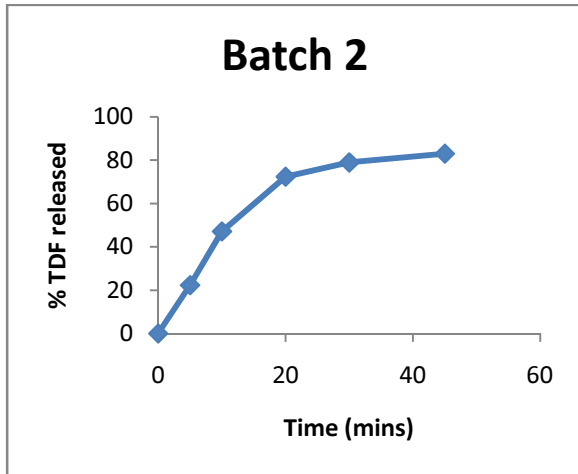
BATCH SUMMARY

Formulator	Tawanda Dube	Batch Size	250g
Product	TDF Pellets	Temperature	18.1°C
Batch ID	TDF-011	Humidity	52%
Production Date	23-03-2012		

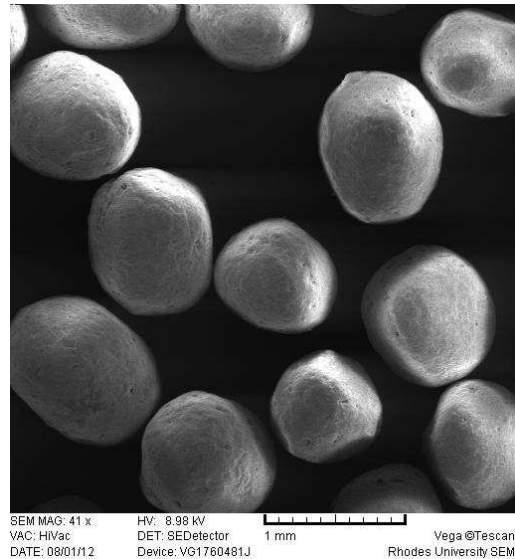
Material	Amount added	Production	Model
TDF	75%	Extruder	Caleva Extruder 20
Kollidon CL-M	10%	Spheronizer	Caleva MBS 250
Sorbitol	3%	Dryer	STREA-1 Aeromatic fluid bed dryer
CCS	2%	Analysis	
MCC PH-102	10%	SEM	Tescan, VEGA LMU
Water	120ml	Dissolution	Hanson Research SR 8 PLUS

Process Parameters	Value
Blender speed	Low
Extruder speed	25 rpm
Spheronizer speed	1050 rpm
Spheronizer resident time	3 min

Dissolution



SEM



AOR : 23.96
HR : 1.05
CI : 5.41

COMMENTS: Large size variation, smooth surface.

RHODES UNIVERSITY

FACULTY OF PHARMACY, GRAHAMSTOWN, SOUTH AFRICA

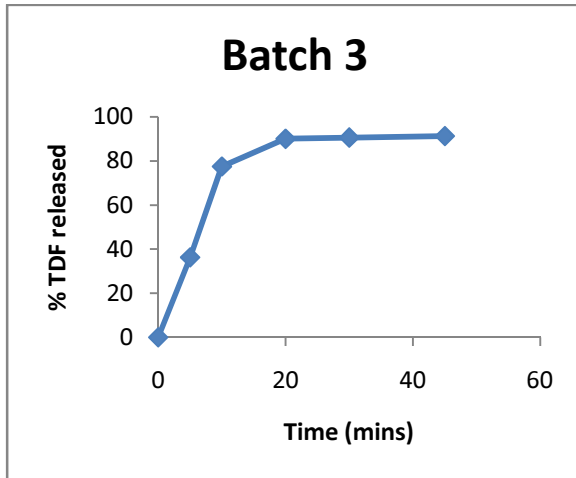
BATCH SUMMARY

Formulator	Tawanda Dube	Batch Size	250g
Product	TDF Pellets	Temperature	18.2°C
Batch ID	TDF-012	Humidity	52%
Production Date	23-03-2012		

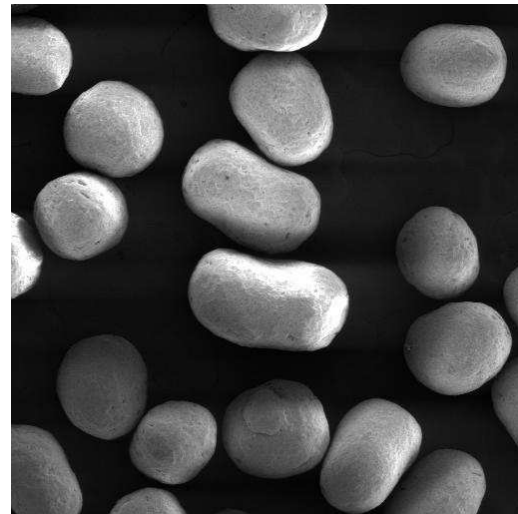
Material	Amount added	Production	Model
TDF	75%	Extruder	Caleva Extruder 20
Kollidon CL-M	15%	Spheronizer	Caleva MBS 250
Sorbitol	4%	Dryer	STREA-1 Aeromatic fluid bed dryer
CCS	3%	Analysis	
MCC PH-102	12%	SEM	Tescan, VEGA LMU
Water	120ml	Dissolution	Hanson Research SR 8 PLUS

Process Parameters	Value
Blender speed	Low
Extruder speed	35 rpm
Spheronizer speed	850 rpm
Spheronizer resident time	3 min

Dissolution



SEM



SEM MAG: 29 x Hv: 8.98 kV
 VAC: HiVac DET: SEDetector 2 mm Vega ©Tescan
 DATE: 08/01/12 Device: VG1760481J Rhodes University SEM

AOR : 22.89
HR : 1.06
CI : 5.71

COMMENTS: Irregular shaped pellets.

RHODES UNIVERSITY

FACULTY OF PHARMACY, GRAHAMSTOWN, SOUTH AFRICA

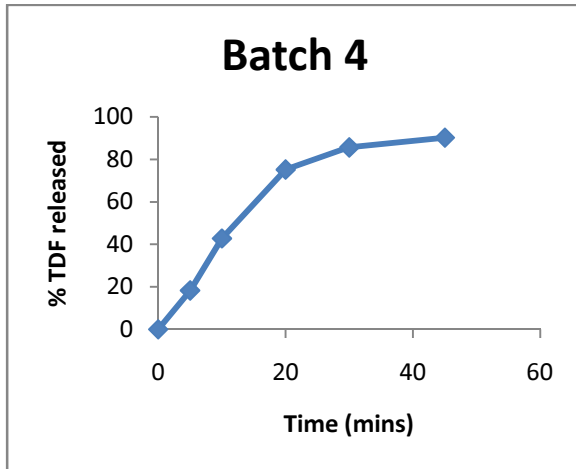
BATCH SUMMARY

Formulator	Tawanda Dube	Batch Size	250g
Product	TDF Pellets	Temperature	18.1°C
Batch ID	TDF-013	Humidity	52%
Production Date	23-03-2012		

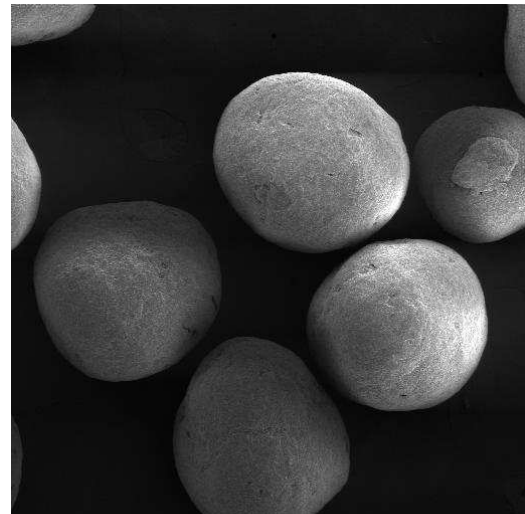
Material	Amount added	Production	Model
TDF	75%	Extruder	Caleva Extruder 20
Kollidon CL-M	5%	Spheronizer	Caleva MBS 250
Sorbitol	3%	Dryer	STREA-1 Aeromatic fluid bed dryer
CCS	1%	Analysis	
MCC PH-102	12%	SEM	Tescan, VEGA LMU
Water	120ml	Dissolution	Hanson Research SR 8 PLUS

Process Parameters	Value
Blender speed	High
Extruder speed	25 rpm
Spheronizer speed	850 rpm
Spheronizer resident time	3 min

Dissolution



SEM



SEM MAG: 59 x HV: 8.98 kV
 VAC: HiVac DET: SEDetector 1 mm
 DATE: 08/01/12 Device: VG1780481J Vega ©Tescan
 Rhodes University SEM

AOR : 22.95
HR : 1.03
CI : 2.78

COMMENTS: Good shape and smooth surface.

RHODES UNIVERSITY

FACULTY OF PHARMACY, GRAHAMSTOWN, SOUTH AFRICA

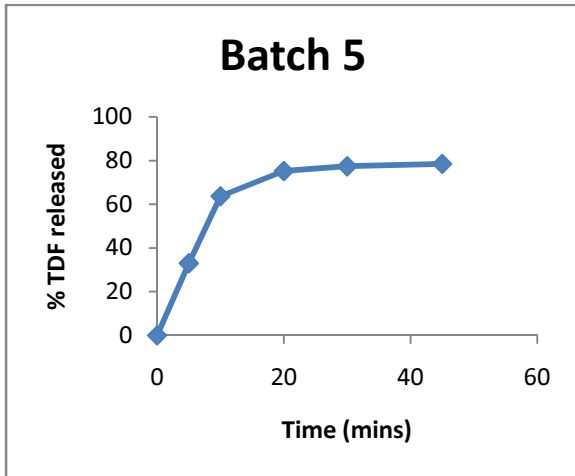
BATCH SUMMARY

Formulator	Tawanda Dube	Batch Size	250g
Product	TDF Pellets	Temperature	18.1°C
Batch ID	TDF-014	Humidity	52%
Production Date	23-03-2012		

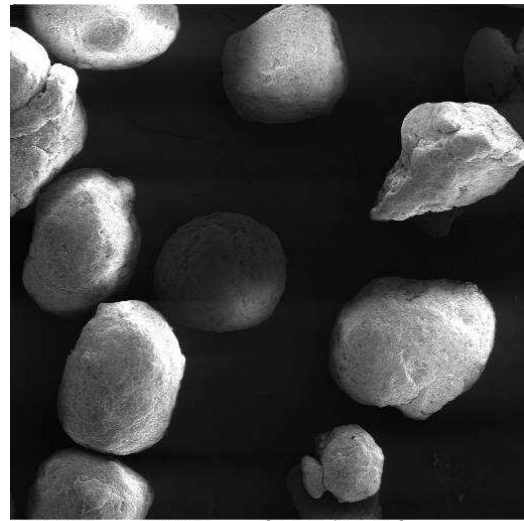
Material	Amount added	Production	Model
TDF	75%	Extruder	Caleva Extruder 20
Kollidon CL-M	10%	Spheronizer	Caleva MBS 250
Sorbitol	4%	Dryer	STREA-1 Aeromatic fluid bed dryer
CCS	2%	Analysis	
MCC PH-102	8%	SEM	Tescan, VEGA LMU
Water	120ml	Dissolution	Hanson Research SR 8 PLUS

Process Parameters	Value
Blender speed	High
Extruder speed	35 rpm
Spheronizer speed	650 rpm
Spheronizer resident time	3 min

Dissolution



SEM



SEM MAG: 39 x HV: 8.98 kV
 VAC: HiVac DET: SEDetector 1 mm Vega ©Tescan
 DATE: 08/01/12 Device: VG1760481J Rhodes University SEM

AOR : 27.60
HR : 1.06
CI : 5.88

COMMENTS: Irregular shape, retarded release, rough surface.

RHODES UNIVERSITY

FACULTY OF PHARMACY, GRAHAMSTOWN, SOUTH AFRICA

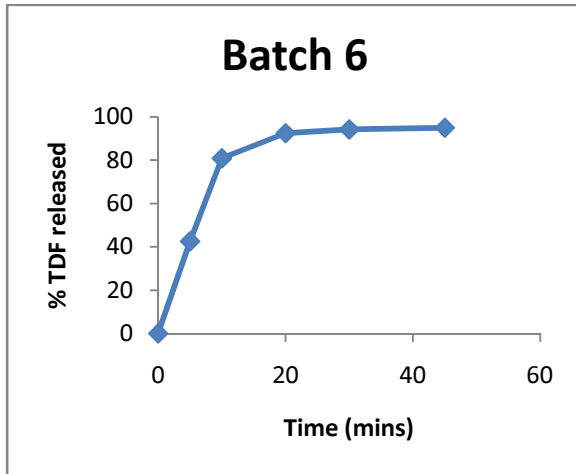
BATCH SUMMARY

Formulator	Tawanda Dube	Batch Size	250g
Product	TDF Pellets	Temperature	18.0°C
Batch ID	TDF-015	Humidity	52%
Production Date	23-03-2012		

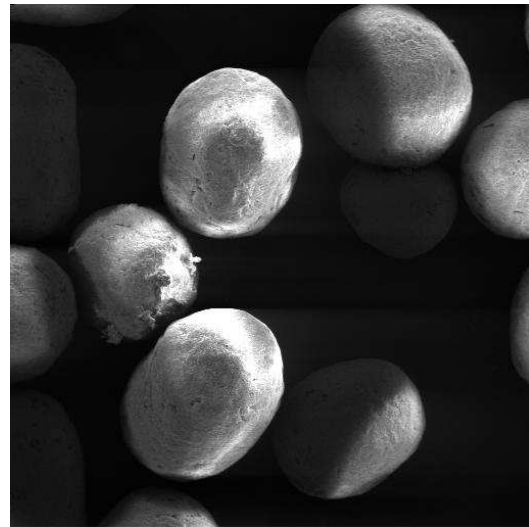
Material	Amount added	Production	Model
TDF	75%	Extruder	Caleva Extruder 20
Kollidon CL-M	15%	Spheronizer	Caleva MBS 250
Sorbitol	2%	Dryer	STREA-1 Aeromatic fluid bed dryer
CCS	3%	Analysis	
MCC PH-102	10%	SEM	Tescan, VEGA LMU
Water	120ml	Dissolution	Hanson Research SR 8 PLUS

Process Parameters	Value
Blender speed	High
Extruder speed	15 rpm
Spheronizer speed	1050 rpm
Spheronizer resident time	3 min

Dissolution



SEM



SEM MAG: 48x HV: 8.98 kV
 VAC: HiVac DET: SEDetector 1 mm Vega ©Tescan
 DATE: 08/01/12 Device: VG1780481J Rhodes University SEM

AOR : 28.42
HR : 1.05
CI : 4.76

COMMENTS: Immediate release profile, rough surface.

RHODES UNIVERSITY

FACULTY OF PHARMACY, GRAHAMSTOWN, SOUTH AFRICA

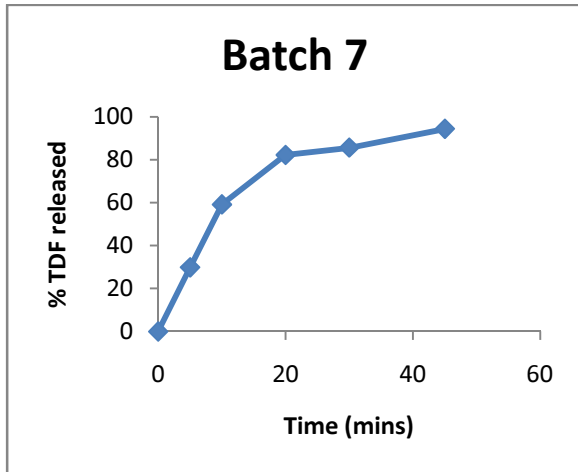
BATCH SUMMARY

Formulator	Tawanda Dube	Batch Size	250g
Product	TDF Pellets	Temperature	17.9°C
Batch ID	TDF-016	Humidity	56%
Production Date	23-03-2012		

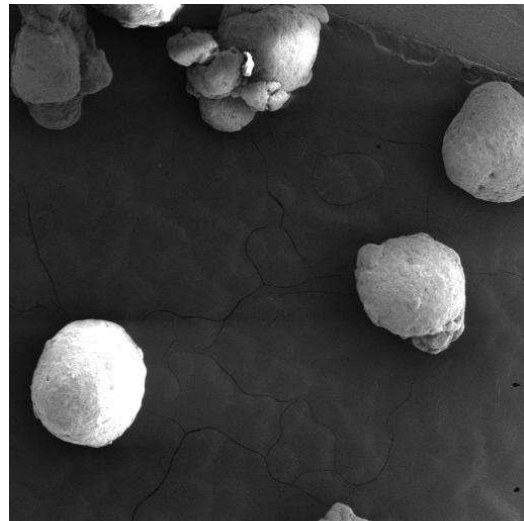
Material	Amount added	Production	Model
TDF	75%	Extruder	Caleva Extruder 20
Kollidon CL-M	15%	Spheronizer	Caleva MBS 250
Sorbitol	4%	Dryer	STREA-1 Aeromatic fluid bed dryer
CCS	1%	Analysis	
MCC PH-102	8%	SEM	Tescan, VEGA LMU
Water	120ml	Dissolution	Hanson Research SR 8 PLUS

Process Parameters	Value
Blender speed	High
Extruder speed	15 rpm
Spheronizer speed	1050 rpm
Spheronizer resident time	3 min

Dissolution



SEM



SEM MAG: 33 x HV: 8.98 kV
 VAC: HVac DET: SEDetector 2 mm Vega ©Tescan
 DATE: 08/01/12 Device: VG1760481J Rhodes University SEM

AOR : 25.20
HR : 1.05
CI : 4.88

COMMENTS: Agglomerated pellets with rough surface.

RHODES UNIVERSITY

FACULTY OF PHARMACY, GRAHAMSTOWN, SOUTH AFRICA

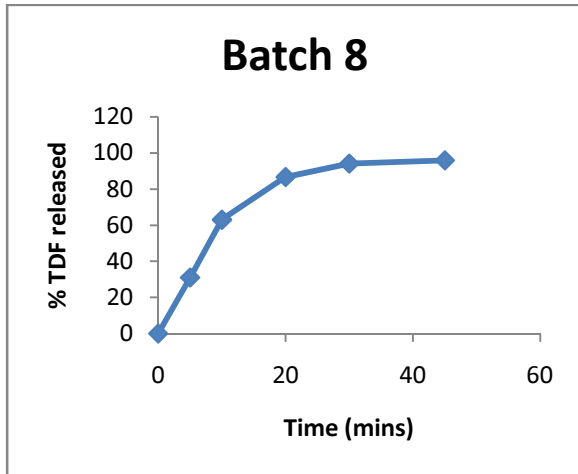
BATCH SUMMARY

Formulator	Tawanda Dube	Batch Size	250g
Product	TDF Pellets	Temperature	21.2°C
Batch ID	TDF-017	Humidity	41%
Production Date	24-03-2012		

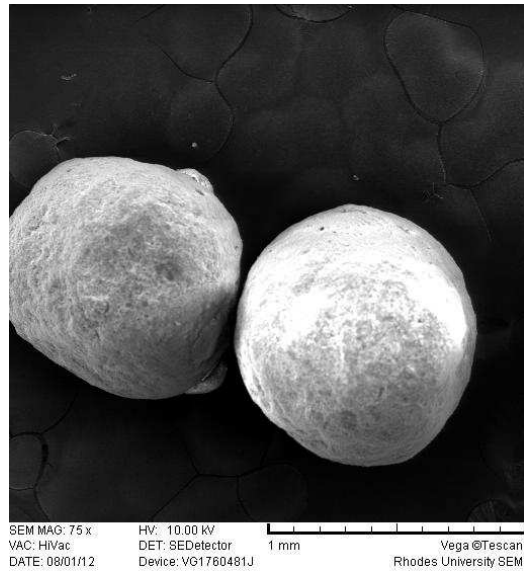
Material	Amount added	Production	Model
TDF	75%	Extruder	Caleva Extruder 20
Kollidon CL-M	5%	Spheronizer	Caleva MBS 250
Sorbitol	2%	Dryer	STREA-1 Aeromatic fluid bed dryer
CCS	2%	Analysis	
MCC PH-102	10%	SEM	Tescan, VEGA LMU
Water	120ml	Dissolution	Hanson Research SR 8 PLUS

Process Parameters	Value
Blender speed	High
Extruder speed	35 rpm
Spheronizer speed	850 rpm
Spheronizer resident time	3 min

Dissolution



SEM



AOR : 30.47
HR : 1.05
CI : 4.76

COMMENTS: Smooth spherical pellets.

RHODES UNIVERSITY

FACULTY OF PHARMACY, GRAHAMSTOWN, SOUTH AFRICA

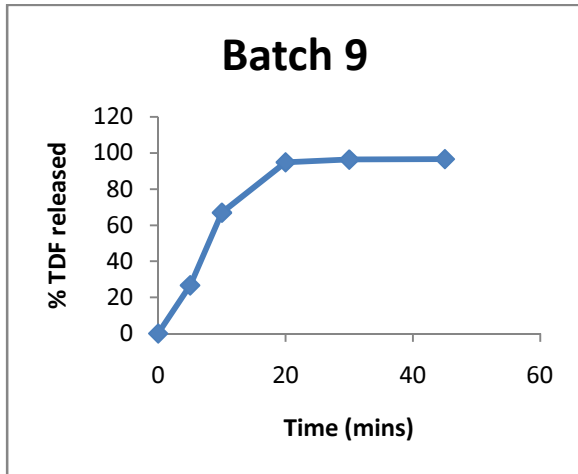
BATCH SUMMARY

Formulator	Tawanda Dube	Batch Size	250g
Product	TDF Pellets	Temperature	22°C
Batch ID	TDF-018	Humidity	40%
Production Date	24-03-2012		

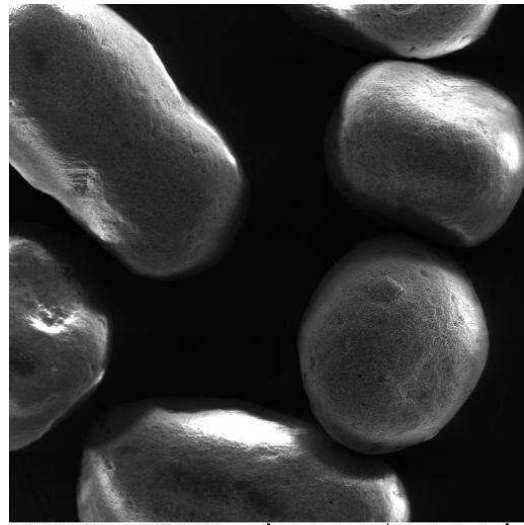
Material	Amount added	Production	Model
TDF	75%	Extruder	Caleva Extruder 20
Kollidon CL-M	10%	Spheronizer	Caleva MBS 250
Sorbitol	3%	Dryer	STREA-1 Aeromatic fluid bed dryer
CCS	3%	Analysis	
MCC PH-102	12%	SEM	Tescan, VEGA LMU
Water	120ml	Dissolution	Hanson Research SR 8 PLUS

Process Parameters	Value
Blender speed	High
Extruder speed	15 rpm
Spheronizer speed	650 rpm
Spheronizer resident time	3 min

Dissolution



SEM



SEM MAG: 70 x HV: 10.00 kV
 VAC: HVac DET: SEDetector 1 mm Vega ©Tescan
 DATE: 08/01/12 Device: VG1780481J Rhodes University SEM

AOR : 25.73
HR : 1.05
CI : 5.13

COMMENTS: Elongated irregular pellets.

RHODES UNIVERSITY

FACULTY OF PHARMACY, GRAHAMSTOWN, SOUTH AFRICA

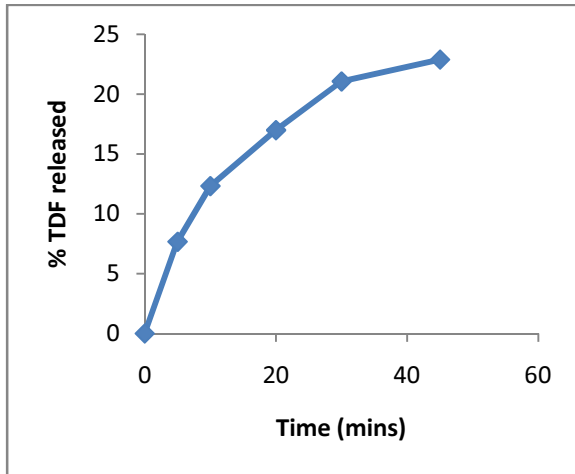
BATCH SUMMARY

Formulator	Tawanda Dube	Batch Size	250g
Product	TDF Pellets	Temperature	22.1°C
Batch ID	TDF-019	Humidity	40%
Production Date	24-03-2012		

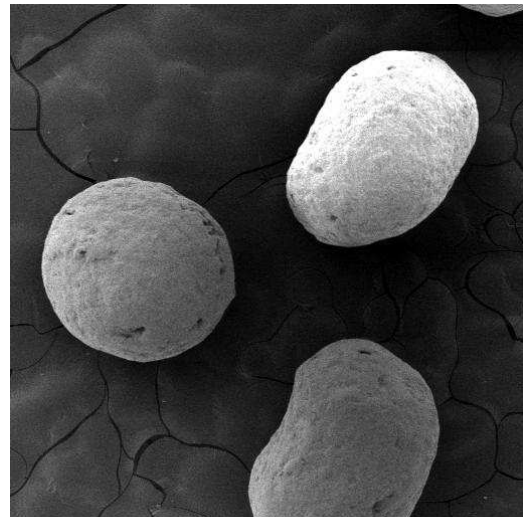
Material	Amount added	Production	Model
TDF	75%	Extruder	Caleva Extruder 20
Kollidon CL-M	10%	Spheronizer	Caleva MBS 250
Sorbitol	4%	Dryer	STREA-1 Aeromatic fluid bed dryer
CCS	1%	Analysis	
MCC PH-102	10%	SEM	Tescan, VEGA LMU
Water	120ml	Dissolution	Hanson Research SR 8 PLUS

Process Parameters	Value
Blender speed	Low
Extruder speed	15 rpm
Spheronizer speed	850 rpm
Spheronizer resident time	3 min

Dissolution



SEM



SEM MAG: 52 x HV: 10.00 kV
 VAC: HiVac DET: SEDetector 1 mm Vega ©Tescan
 DATE: 08/01/12 Device: VG1760481J Rhodes University SEM

AOR : 28.42
HR : 1.05
CI : 5.00

COMMENTS: Smooth surface, large size variations.

RHODES UNIVERSITY

FACULTY OF PHARMACY, GRAHAMSTOWN, SOUTH AFRICA

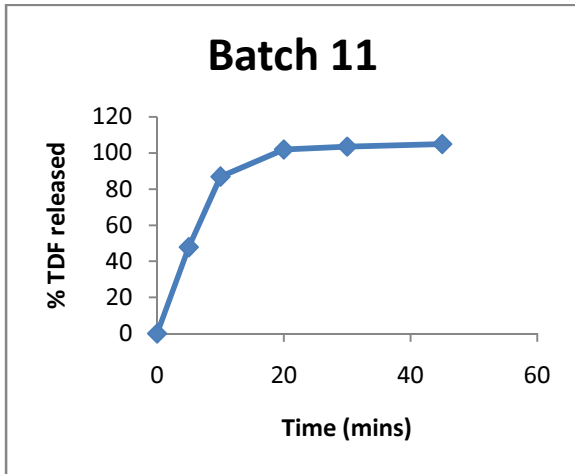
BATCH SUMMARY

Formulator	Tawanda Dube	Batch Size	250g
Product	TDF Pellets	Temperature	22°C
Batch ID	TDF-020	Humidity	41%
Production Date	24-03-2012		

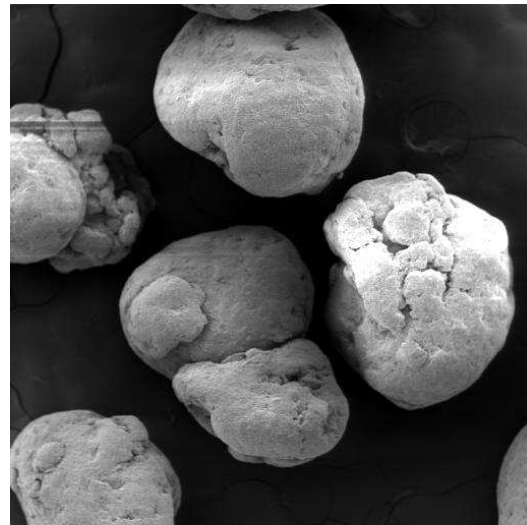
Material	Amount added	Production	Model
TDF	75%	Extruder	Caleva Extruder 20
Kollidon CL-M	15%	Spheronizer	Caleva MBS 250
Sorbitol	2%	Dryer	STREA-1 Aeromatic fluid bed dryer
CCS	2%	Analysis	
MCC PH-102	12%	SEM	Tescan, VEGA LMU
Water	120ml	Dissolution	Hanson Research SR 8 PLUS

Process Parameters	Value
Blender speed	Low
Extruder speed	25 rpm
Spheronizer speed	650 rpm
Spheronizer resident time	5 min

Dissolution



SEM



SEM MAG: 58 x HV: 10.00 kV
 VAC: HiVac DET: SEDetector 1 mm Vega ©Tescan
 DATE: 08/01/12 Device: VG1760481J Rhodes University SEM

AOR : 25.46
HR : 1.05
CI : 5.13

COMMENTS: Rough surface with craters.

RHODES UNIVERSITY

FACULTY OF PHARMACY, GRAHAMSTOWN, SOUTH AFRICA

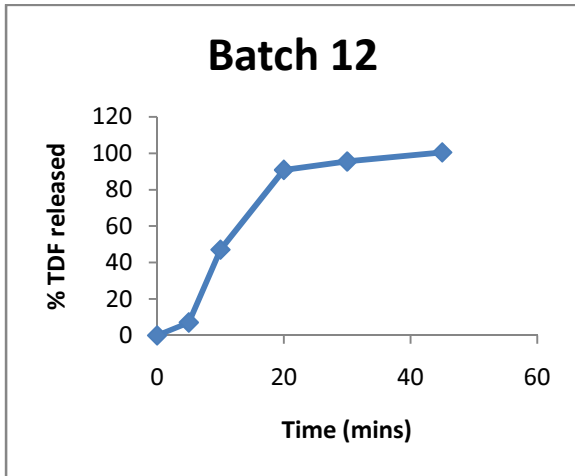
BATCH SUMMARY

Formulator	Tawanda Dube	Batch Size	250g
Product	TDF Pellets	Temperature	21.8°C
Batch ID	TDF-021	Humidity	40%
Production Date	24-03-2012		

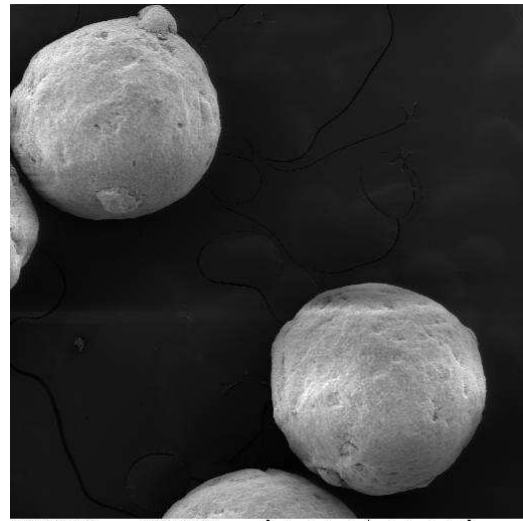
Material	Amount added	Production	Model
TDF	75%	Extruder	Caleva Extruder 20
Kollidon CL-M	5%	Spheronizer	Caleva MBS 250
Sorbitol	3%	Dryer	STREA-1 Aeromatic fluid bed dryer
CCS	3%	Analysis	
MCC PH-102	8%	SEM	Tescan, VEGA LMU
Water	120ml	Dissolution	Hanson Research SR 8 PLUS

Process Parameters	Value
Blender speed	Low
Extruder speed	35 rpm
Spheronizer speed	1050 rpm
Spheronizer resident time	5 min

Dissolution



SEM



SEM MAG: 59 x HV: 10.00 kV
 VAC: HiVac DET: SEDetector 1 mm Vega ©Tescan
 DATE: 08/01/12 Device: VG1760481J Rhodes University SEM

AOR : 29.60
HR : 1.03
CI : 2.70

COMMENTS: Rough surface with craters and agglomerated fines.

RHODES UNIVERSITY

FACULTY OF PHARMACY, GRAHAMSTOWN, SOUTH AFRICA

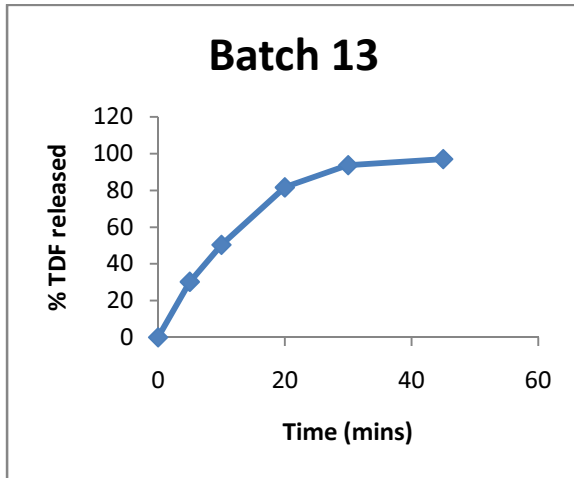
BATCH SUMMARY

Formulator	Tawanda Dube	Batch Size	250g
Product	TDF Pellets	Temperature	22°C
Batch ID	TDF-022	Humidity	41%
Production Date	24-03-2012		

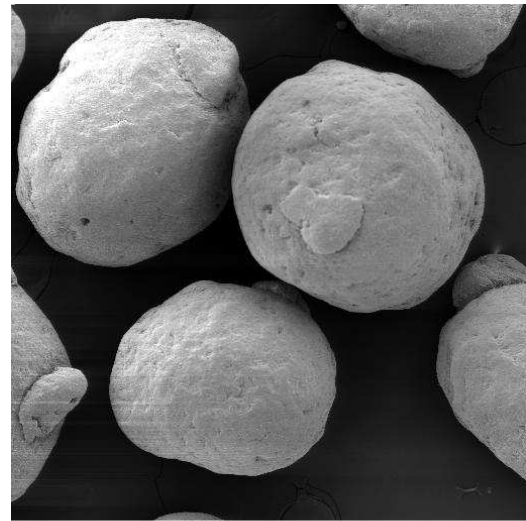
Material	Amount added	Production	Model
TDF	75%	Extruder	Caleva Extruder 20
Kollidon CL-M	10%	Spheronizer	Caleva MBS 250
Sorbitol	2%	Dryer	STREA-1 Aeromatic fluid bed dryer
CCS	1%	Analysis	
MCC PH-102	12%	SEM	Tescan, VEGA LMU
Water	120ml	Dissolution	Hanson Research SR 8 PLUS

Process Parameters	Value
Blender speed	High
Extruder speed	35 rpm
Spheronizer speed	1050 rpm
Spheronizer resident time	5 min

Dissolution



SEM



SEM MAG: 65 x HV: 10.00 kV
 VAC: HiVac DET: SEDetector 1 mm Vega ©Tescan
 DATE: 08/01/12 Device: VG1760481J Rhodes University SEM

AOR : 22.83
HR : 1.06
CI : 5.26

COMMENTS: Rough pellet surface , irregular shape.

RHODES UNIVERSITY

FACULTY OF PHARMACY, GRAHAMSTOWN, SOUTH AFRICA

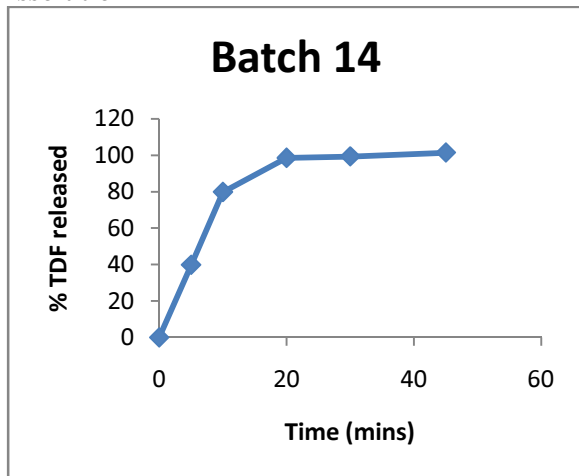
BATCH SUMMARY

Formulator	Tawanda Dube	Batch Size	250g
Product	TDF Pellets	Temperature	21.8°C
Batch ID	TDF-023	Humidity	40%
Production Date	24-03-2012		

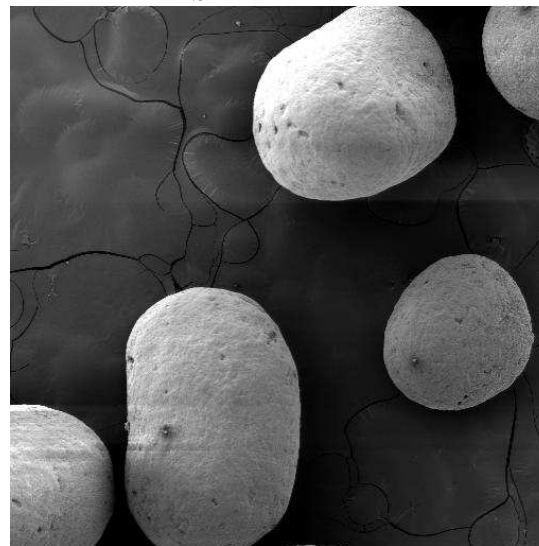
Material	Amount added	Production	Model
TDF	75%	Extruder	Caleva Extruder 20
Kollidon CL-M	15%	Spheronizer	Caleva MBS 250
Sorbitol	3%	Dryer	STREA-1 Aeromatic fluid bed dryer
CCS	2%	Analysis	
MCC PH-102	8%	SEM	Tescan, VEGA LMU
Water	120ml	Dissolution	Hanson Research SR 8 PLUS

Process Parameters	Value
Blender speed	High
Extruder speed	15 rpm
Spheronizer speed	850 rpm
Spheronizer resident time	5 min

Dissolution



SEM



SEM MAG: 50 x HV: 10.00 kV
 VAC: HiVac DET: SEDetector 1 mm Vega ©Tescan
 DATE: 08/01/12 Device: VG1760481J Rhodes University SEM

AOR : 28.42
HR : 1.06
CI : 5.41

COMMENTS: Elongated shapes and smooth surface.

RHODES UNIVERSITY

FACULTY OF PHARMACY, GRAHAMSTOWN, SOUTH AFRICA

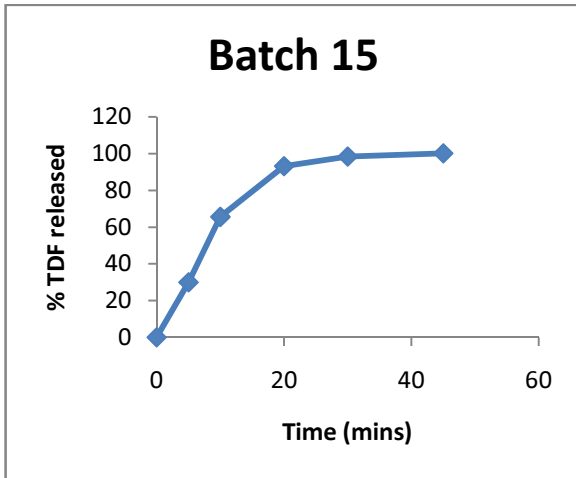
BATCH SUMMARY

Formulator	Tawanda Dube	Batch Size	250g
Product	TDF Pellets	Temperature	21.8°C
Batch ID	TDF-024	Humidity	40%
Production Date	24-03-2012		

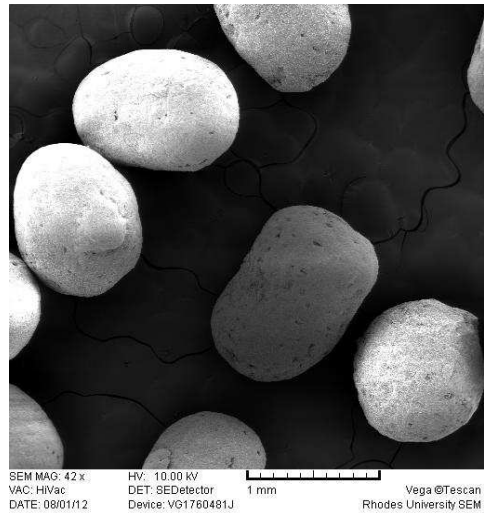
Material	Amount added	Production	Model
TDF	75%	Extruder	Caleva Extruder 20
Kollidon CL-M	5%	Spheronizer	Caleva MBS 250
Sorbitol	4%	Dryer	STREA-1 Aeromatic fluid bed dryer
CCS	3%	Analysis	
MCC PH-102	10%	SEM	Tescan, VEGA LMU
Water	120ml	Dissolution	Hanson Research SR 8 PLUS

Process Parameters	Value
Blender speed	High
Extruder speed	25 rpm
Spheronizer speed	650 rpm
Spheronizer resident time	5 min

Dissolution



SEM



AOR : 25.84
HR : 1.05
CI : 5.00

COMMENTS: Agglomerated fines on surface.

RHODES UNIVERSITY

FACULTY OF PHARMACY, GRAHAMSTOWN, SOUTH AFRICA

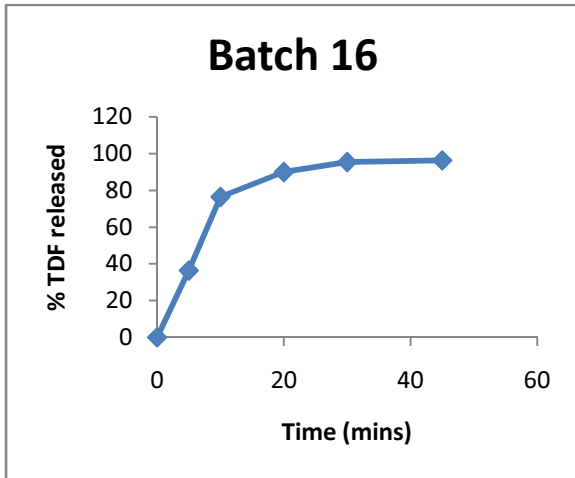
BATCH SUMMARY

Formulator	Tawanda Dube	Batch Size	250g
Product	TDF Pellets	Temperature	22°C
Batch ID	TDF-025	Humidity	40%
Production Date	24-03-2012		

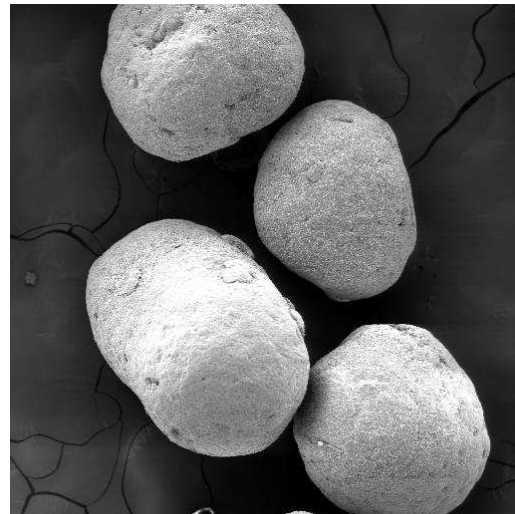
Material	Amount added	Production	Model
TDF	75%	Extruder	Caleva Extruder 20
Kollidon CL-M	15%	Spheronizer	Caleva MBS 250
Sorbitol	3%	Dryer	STREA-1 Aeromatic fluid bed dryer
CCS	1%	Analysis	
MCC PH-102	10%	SEM	Tescan, VEGA LMU
Water	120ml	Dissolution	Hanson Research SR 8 PLUS

Process Parameters	Value
Blender speed	High
Extruder speed	650 rpm
Spheronizer speed	35 rpm
Spheronizer resident time	5 min

Dissolution



SEM



SEM MAG: 59 x HV: 10.00 kV
 VAC: HiVac DET: SEDetector 1 mm Vega ©Tescan
 DATE: 08/01/12 Device: VG1760481J Rhodes University SEM

AOR : 28.42
HR : 1.06
CI : 5.26

COMMENTS: Irregular shapes, rough surfaces.

RHODES UNIVERSITY

FACULTY OF PHARMACY, GRAHAMSTOWN, SOUTH AFRICA

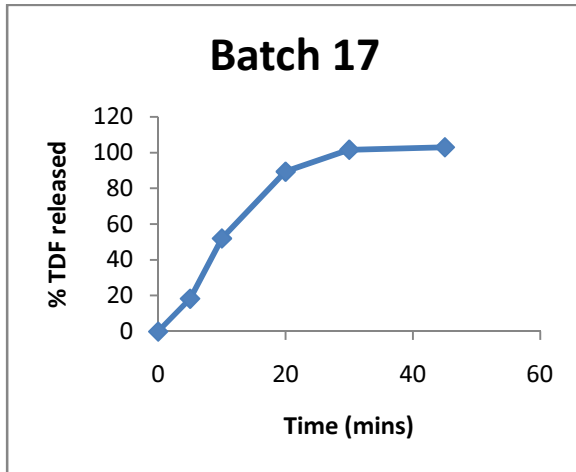
BATCH SUMMARY

Formulator	Tawanda Dube	Batch Size	250g
Product	TDF Pellets	Temperature	21.7°C
Batch ID	TDF-026	Humidity	41%
Production Date	24-03-2012		

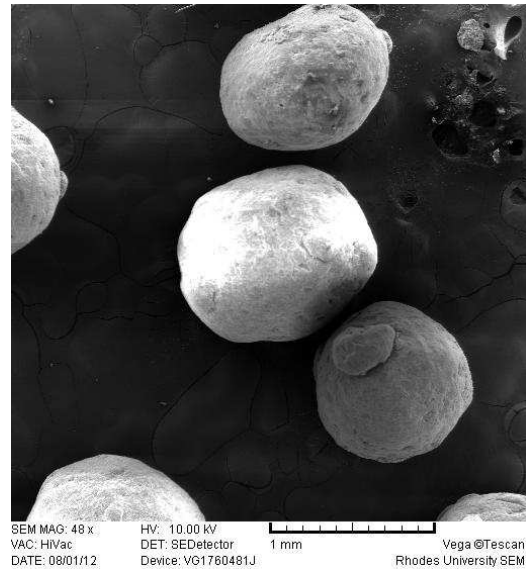
Material	Amount added	Production	Model
TDF	75%	Extruder	Caleva Extruder 20
Kollidon CL-M	5%	Spheronizer	Caleva MBS 250
Sorbitol	4%	Dryer	STREA-1 Aeromatic fluid bed dryer
CCS	2%	Analysis	
MCC PH-102	12%	SEM	Tescan, VEGA LMU
Water	120ml	Dissolution	Hanson Research SR 8 PLUS

Process Parameters	Value
Blender speed	High
Extruder speed	15 rpm
Spheronizer speed	1050 rpm
Spheronizer resident time	5 min

Dissolution



SEM



AOR : 32.01
HR : 1.06
CI : 5.41

COMMENTS: Surface agglomeration, irregular shape.

RHODES UNIVERSITY

FACULTY OF PHARMACY, GRAHAMSTOWN, SOUTH AFRICA

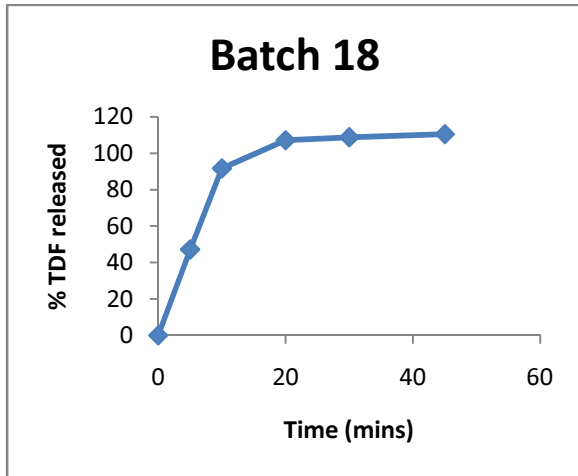
BATCH SUMMARY

Formulator	Tawanda Dube	Batch Size	250g
Product	TDF Pellets	Temperature	21.2°C
Batch ID	TDF-027	Humidity	40%
Production Date	24-03-2012		

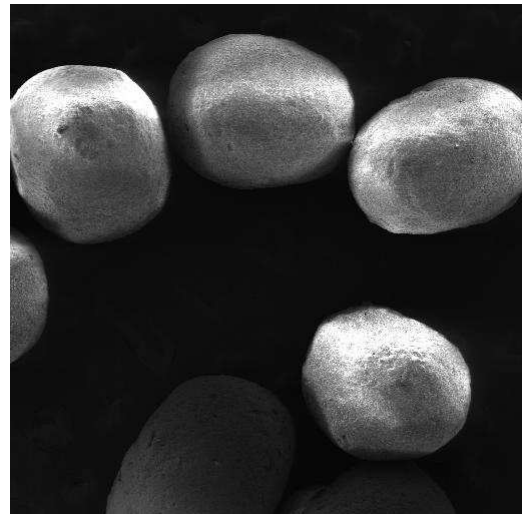
Material	Amount added	Production	Model
TDF	75%	Extruder	Caleva Extruder 20
Kollidon CL-M	10%	Spheronizer	Caleva MBS 250
Sorbitol	2%	Dryer	STREA-1 Aeromatic fluid bed dryer
CCS	3%	Analysis	
MCC PH-102	8%	SEM	Tescan, VEGA LMU
Water	120ml	Dissolution	Hanson Research SR 8 PLUS

Process Parameters	Value
Blender speed	High
Extruder speed	25 rpm
Spheronizer speed	850 rpm
Spheronizer resident time	5 min

Dissolution



SEM



SEM MAG: 49x HV: 10.00 kV
 VAC: HiVac DET: SEDetector
 DATE: 08/01/12 Device: VG1760481J 1 mm Vega ©Tescan
 Rhodes University SEM

AOR : 28.07
HR : 1.05
CI : 5.13

COMMENTS: Smooth surface, irregular shape

RHODES UNIVERSITY

FACULTY OF PHARMACY, GRAHAMSTOWN, SOUTH AFRICA

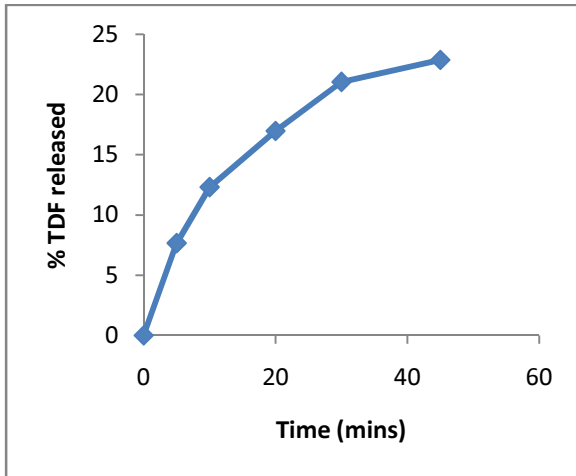
BATCH SUMMARY

Formulator	Tawanda Dube	Batch Size	250g
Product	TDF Pellets	Temperature	21.7°C
Batch ID	TDF-028	Humidity	41%
Production Date	24-03-2012		

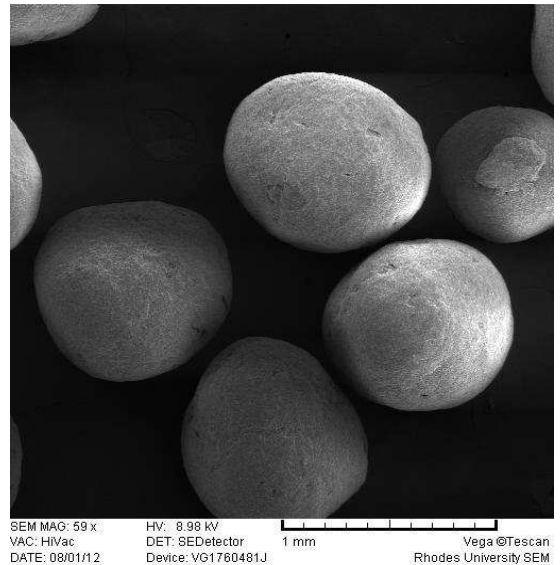
Material	Amount added	Production	Model
TDF	75%	Extruder	Caleva Extruder 20
Kollidon CL-M	10%	Spheronizer	Caleva MBS 250
Sorbitol	4%	Dryer	STREA-1 Aeromatic fluid bed dryer
CCS	1%	Analysis	
MCC PH-102	12%	SEM	Tescan, VEGA LMU
Water	120ml	Dissolution	Hanson Research SR 8 PLUS

Process Parameters	Value
Blender speed	High
Extruder speed	15 rpm
Spheronizer speed	850 rpm
Spheronizer resident time	3 min

Dissolution



SEM



AOR : 27.07
HR : 1.06
CI : 5.26

COMMENTS: Smooth, spherical pellets and immediate release profile.

APPENDIX 2

Response Surface Methodology Statistics

% YIELD (SIZE 0.8 – 1.25mm)

Table A2.1 ANOVA data for the Response Surface Linear Model for % Yield

Source	Sum of Squares	DF	Mean Square	F Value	p-value Prob> F	
Model	1989.62	3	663.21	2.87	0.0737	not significant
A-spheronization time.	1100.03	1	1100.03	4.77	0.0465	
B-BLENDER SPEED	42.25	1	42.25	0.18	0.6752	
AB	1482.25	1	1482.25	6.43	0.0238	
Residual	3229.78	14	230.70			
Cor Total	5219.41	17				

Design-Expert® Software
%pellets at size 0.8 - 1.25mm

Color points by value of
%pellets at size 0.8 - 1.25mm:

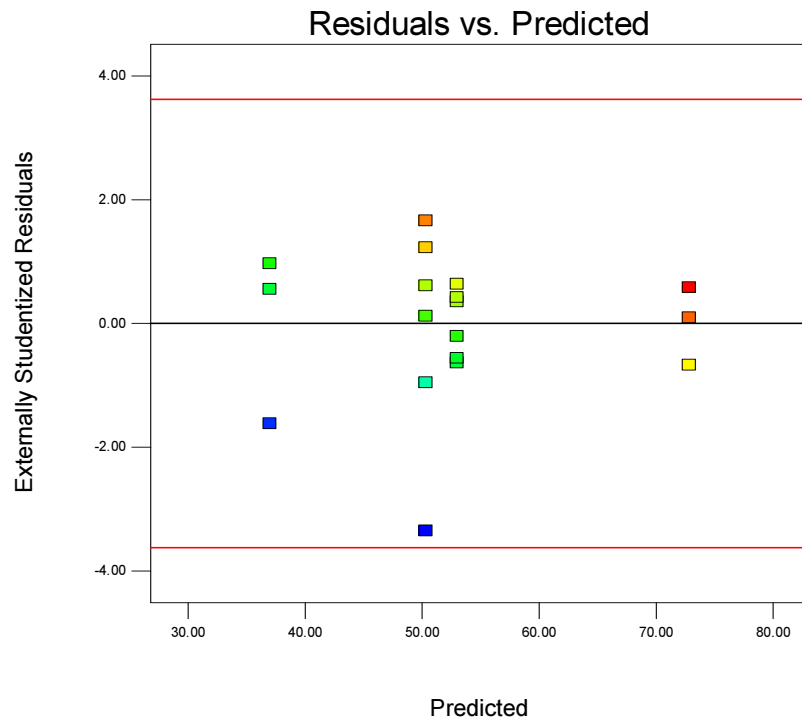


Figure A2.1 Residuals versus Predicted plot for % yield

Design-Expert® Software
%pellets at size 0.8 - 1.25mm

Lambda
Current = 1
Best = 1.99
Low C.I. = 0.77
High C.I. = 3.42

Recommend transform:
None
(Lambda = 1)

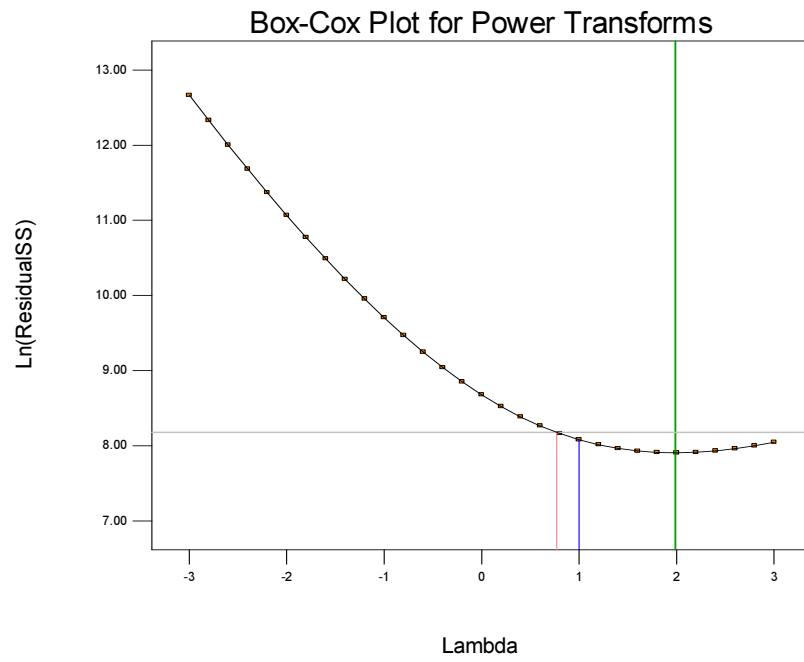


Figure A2.2 Box-Cox plot for % yield

CARR's INDEX

Table A2.2 ANOVA data for Response Surface Linear Model for Carr's Index

Source	Sum of Squares	df	Mean Square	F Value	p-value Prob> F	
Model	5.97	3	1.99	4.43	0.0217	significant
B-BLENDER SPEED	1.78	1	1.78	3.96	0.0664	
H-% Kollidon CL-M	4.19	2	2.09	4.67	0.0280	
Residual	6.28	14	0.45			
Cor Total	12.24	17				

Design-Expert® Software
carr's index

Color points by value of
carr's index
5.9
2.7

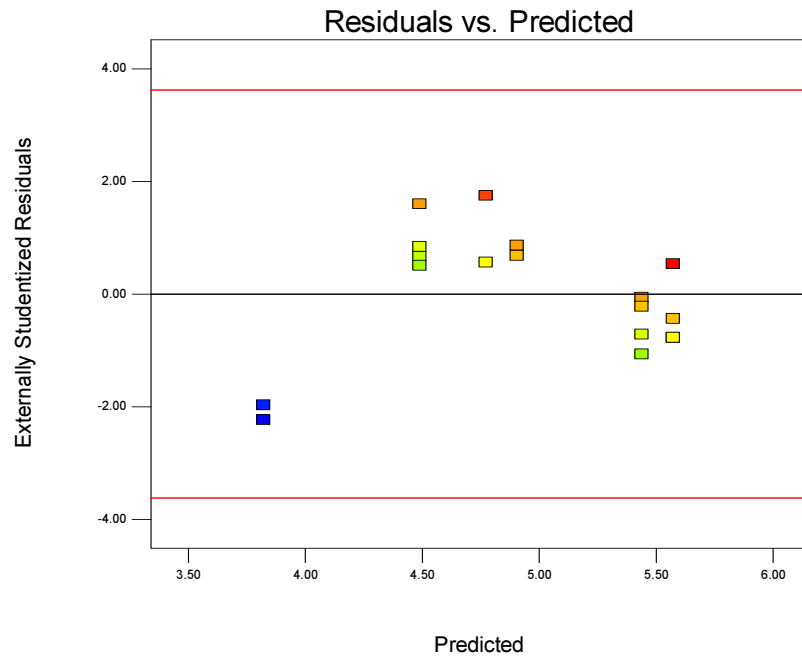


Figure A2.3 Residuals versus Predicted plot for Carr's Index

Design-Expert® Software
carr's index

Lambda
Current = 1
Best = 3
Low C.I. =
High C.I. =

Recommend transform:
None
(Lambda = 1)

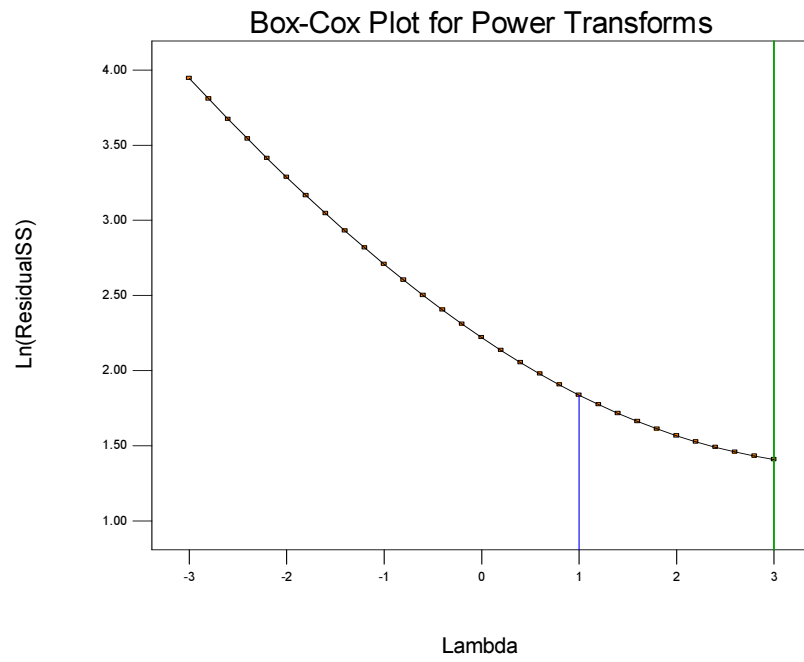


Figure A2.4 Box-Cox plot for Carr's Index

HAUSNER RATIO

Table A2.3 ANOVA for Response Surface Linear Model for Hausner ratio

Source	Sum of Squares	df	Mean Square	F Value	p-value Prob> F	
Model	0.013	5	2.667E-003	7.20	0.0025	significant
B-BLENDER SPEED	4.444E-003	1	4.444E-003	12.00	0.0047	
G-% MCC	4.444E-003	2	2.222E-003	6.00	0.0156	
H-% Kollidon CL-M	4.444E-003	2	2.222E-003	6.00	0.0156	
Residual	4.444E-003	12	3.704E-004			
Cor Total	0.018	17				

Design-Expert® Software
hausner ratio

Color points by value of
hausner ratio:

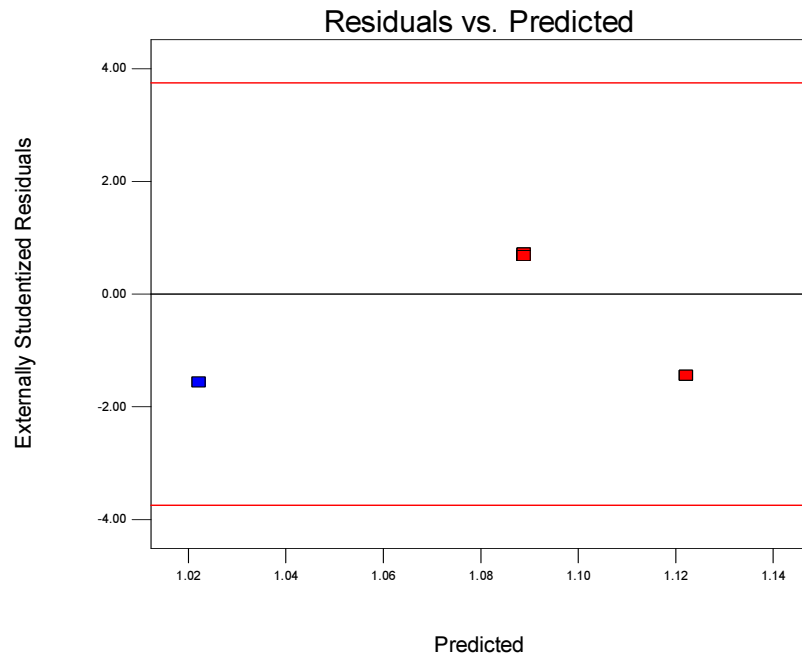


Figure A2.5 Residuals versus. Predicted plot for Hausner ratio

Design-Expert® Software
hausner ratio

Lambda
Current = 1
Best = 3
Low C.I. =
High C.I. =

Recommend transform:
None
(Lambda = 1)

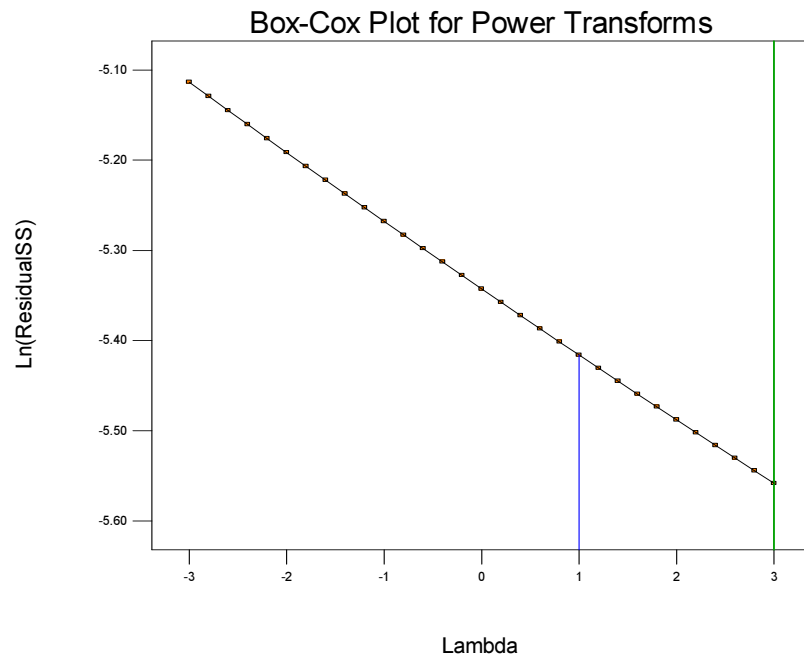


Figure A2.6 Box-Cox plot for Hausner ratio

ANGLE OF REPOSE

Table A2.4 ANOVA data for Response Surface Linear Model for Angle of Repose

Source	Sum of Squares	df	Mean Square	F Value	p-value Prob> F	
Model	68.66	3	22.89	6.11	0.0071	significant
B-BLENDER SPEED	44.44	1	44.44	11.86	0.0040	
E-spheroniser speed	24.21	2	12.11	3.23	0.0702	
Residual	52.47	14	3.75			
Cor Total	121.12	17				

Design-Expert® Software
angle of repose

Color points by value of
angle of repose:

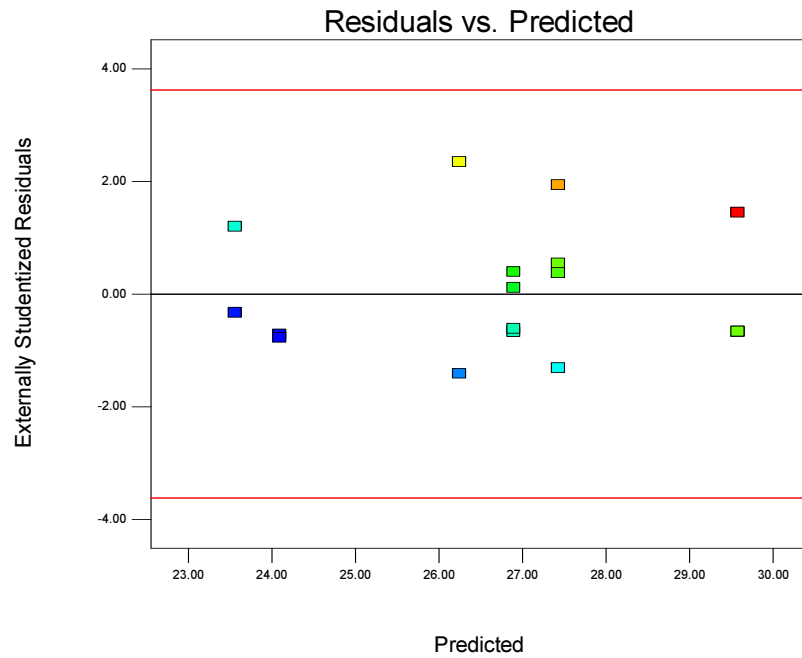


Figure A2.7 Residuals versus. Predicted plot for Angle of Repose

Design-Expert® Software
angle of repose

Lambda
Current = 1
Best = -0.92
Low C.I. = -6.05
High C.I. = 4.21

Recommend transform:
None
(Lambda = 1)

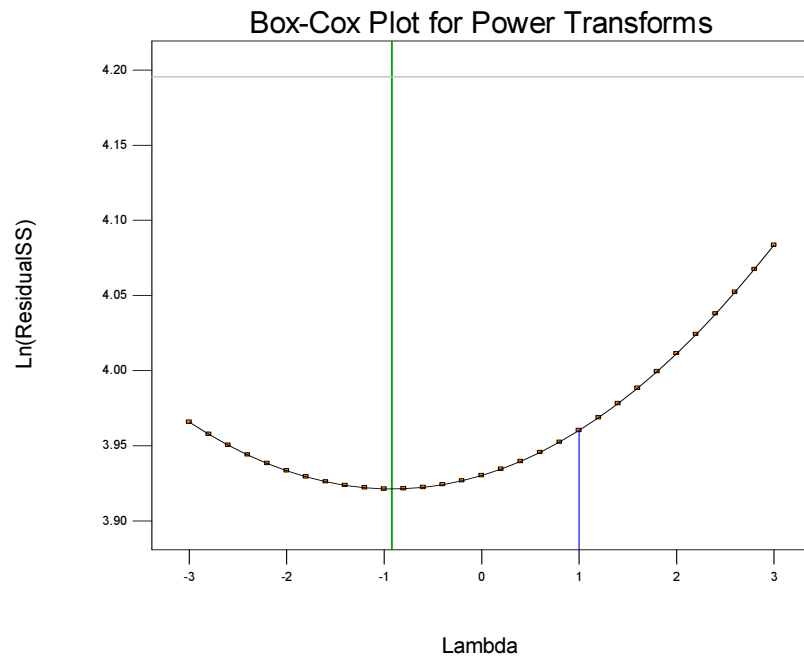


Figure A2.8 Box-Cox plot for Angle of Repose

% TDF RELEASED AT 10 MIN

Table A2.5 ANOVA data for Response Surface Linear Model for % TDF released at 10 min

Source	Sum of Squares	df	Mean Square	F Value	p-value Prob> F	
Model	1422.47	2	711.24	3.83	0.0452	significant
A-spheronization time.	1422.22	1	1422.22	7.66	0.0143	
B-BLENDER SPEED	0.25	1	0.25	1.347E-003	0.9712	
Residual	2783.53	15	185.57			
Cor Total	4206.00	17				

Design-Expert® Software
% release at 10 mins

Color points by value of
% release at 10 mins:

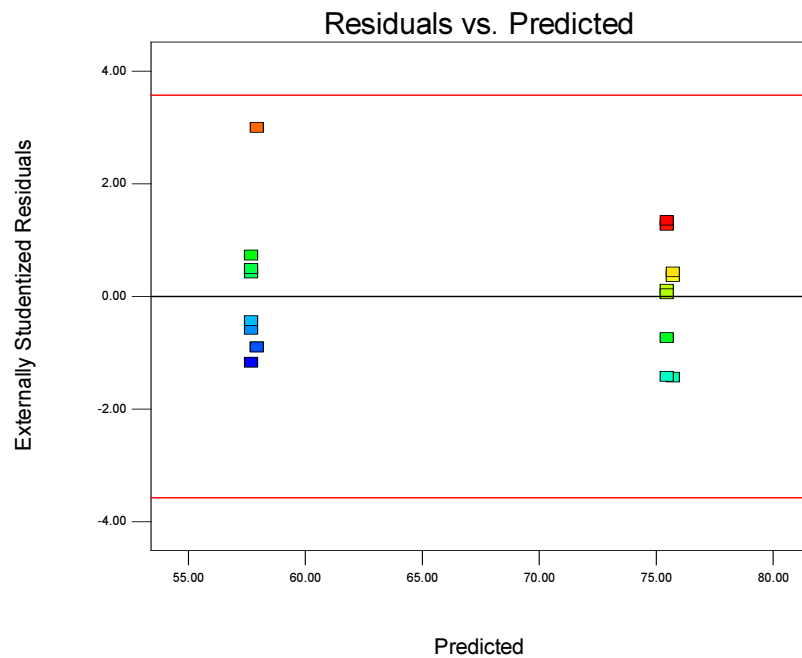


Figure A2.9 Residuals versus. Predicted plot for % TDF released at 10 min

Design-Expert® Software
% release at 10 mins

Lambda
Current = 1
Best = 0.11
Low C.I. = -2.15
High C.I. = 2.47

Recommend transform:
None
(Lambda = 1)

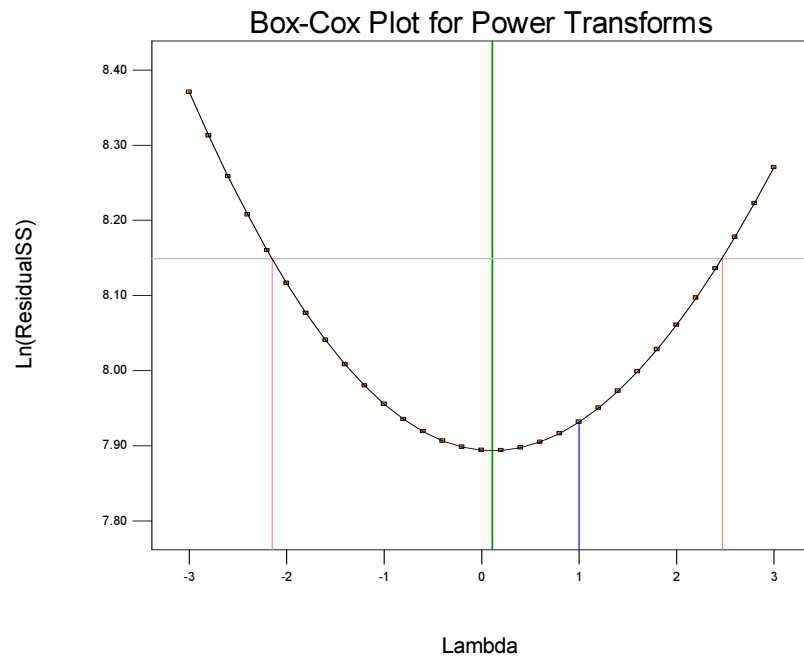


Figure A2.10 Box-Cox plot for % TDF released at 10 min

REFERENCES

1. R. A. Weiss, "How does HIV cause AIDS?," *Science*, Vol. 260, No. 5112, 1993, pp. 1273-1279.
2. S. D. Lawn, "AIDS in Africa: the impact of coinfections on the pathogenesis of HIV-1 infection," *Journal of Infection*, Vol. 48, No. 1, 2004, pp. 1-12.
3. J. Stover, "Can we reverse the HIV/AIDS pandemic with an expanded response?," *Lancet*, Vol. 360, 2002, pp. 73-77.
4. M. Nijhuis, N. M. van Maarseveen, J. Verheyen, and C. A. Boucher, "Novel mechanisms of HIV protease inhibitor resistance," *Current Opinion HIV AIDS*, Vol. 3, No. 6, 2008, pp. 627-632.
5. T. Antoniou, L. Y. Park-Wyllie, and A. L. Tseng, "Tenofovir: a nucleotide analog for the management of human immunodeficiency virus infection," *Pharmacotherapy*, Vol. 23, 2003, pp. 29-43.
6. B. P. Kearney, J. F. Flaherty, and J. Shah, "Tenofovir disoproxil fumarate: clinical pharmacology and pharmacokinetics," *Clinical Pharmacokinetics*, Vol. 43, 2004, pp. 595-612.
7. A. M. M. S. Williams and J. M. H. P. F. Fortunak. "Process development of the anti-retroviral drug, Tenofovir". pp 1-85. 12-6-2010. Howard University, proquest dissertations and theses.
8. WHO, "Scaling up antiretroviral therapy in resource-limited settings: Treatment guidelines for a public health approach," 2003.
9. WHO, "New WHO Recommendations: Antiretroviral therapy for adults and adolescents," 2009.
10. J. E. Gallant, J. A. Winston, and E. DeJesus, "The 3-year renal safety of a tenofovir disoproxil fumarate vs. a thymidine analogue-containing regimen in antiretroviral-naive patients," *AIDS*, Vol. 22, 2008, pp. 2155-2163.
11. T. Delahunty, L. Bushman, B. Robbins, and C. V. Fletcher, "The simultaneous assay of tenofovir and emtricitabine in plasma using LC/MS/MS and isotopically labeled internal standards," *Journal of Chromatography B-Analytical Technologies in the Biomedical and Life Sciences*, Vol. 877, No. 20-21, 2009, pp. 1907-1914.
12. A. S. Zidan, C. Spinks, J. Fortunak, M. Habib, and M. A. Khan, "Near-Infrared Investigations of Novel Anti-HIV Tenofovir Liposomes," *Aaps Journal*, Vol. 12, No. 2, 2010, pp. 202-214.

13. "South African Medicines Formulary". Rossiter, D. 9, pp 331-336. 10-10-2010. Health and Medical Publishing Group of the South African Medical Association. Blockman, M. 1-1-2012.
14. E. Ribera, M. Tuset, M. Martin, and E. del Cacho, "Characteristics of antiretroviral drugs," *Enfermedades Infecciosas y Microbiologia Clinica*, Vol. 29, No. 5, 2011, pp. 362-391.
15. H. Izzedine, C. Isnard-Bagnis, and J. S. Hulot, "Renal safety of tenofovir in HIV treatment-experienced patients," *AIDS*, Vol. 18, 2004, pp. 1074-1076.
16. K. Wever, M. A. van Agtmael, and A. Carr, "Incomplete Reversibility of Tenofovir-Related Renal Toxicity in HIV-Infected Men," *Journal of Acquired Immune Deficiency Syndrome*, Vol. 55, 2010, pp. 78-81.
17. M. E. Haverkort, B. W. van der Spek, P. Lips, W. A. Slieker, R. Ter Heine, A. D. Huitema, and W. Bronsveld, "Tenofovir-induced Fanconi syndrome and osteomalacia in two HIV-infected patients: Role of intracellular tenofovir diphosphate levels and review of the literature," *Scandinavian Journal of Infectious Diseases*, Vol. 43, No. 10, 2011, pp. 821-826.
18. M. D. Gitman, D. Hirschwerk, C. H. Baskin, and P. C. Singhal, "Tenofovir-induced kidney injury," *Expert Opinion on Drug Safety*, Vol. 6, No. 2, 2007, pp. 155-164.
19. H. Izzedine, V. Thibault, M. A. Valantin, G. Peytavin, L. Schneider, and Y. Benhamou, "Tenofovir/probenecid combination in HIV/HBV-coinfected patients: how to escape Fanconi syndrome recurrence?," *AIDS*, Vol. 24, No. 7, 2010, pp. 1078-1079.
20. P. Miaillhes, M. A. Trabaud, P. Pradat, B. Lebouche, M. Chevallier, P. Chevallier, F. Zoulim, and C. Trepo, "Impact of highly active antiretroviral therapy (HAART) on the natural history of hepatitis B virus (HBV) and HIV coinfection: relationship between prolonged efficacy of HAART and HBV surface and early antigen seroconversion," *Clinical Infectious Diseases*, Vol. 45, 2007, pp. 624-632.
21. M. Crane, B. Oliver, G. Matthews, A. Avihingsanon, S. Ubolyam, V. Markovska, J. J. Chang, G. J. Dore, P. Price, K. Visvanathan, M. French, K. Ruxrungtham, and S. R. Lewin, "Immunopathogenesis of hepatic flare in HIV/hepatitis B virus (HBV)-coinfected individuals after the initiation of HBV-active antiretroviral therapy," *Journal of Infectious Diseases*, Vol. 199, 2009, pp. 974-981.
22. "Updated US Public Health Service guidelines for the management of occupational exposures to HBV, HCV, and HIV and recommendations for post exposure prophylaxis," *MMWR Recomm Rep*, Vol. 50, No. RR-11, 2001, pp. 1-52.
23. T. Weberschock, P. Gholam, E. Hueter, K. Flux, and M. Hartmann, "Long-term Efficacy and Safety of Once-daily Nevirapine in Combination with Tenofovir and Emtricitabine in the Treatment of HIV-infected Patients: A 72-week Prospective Multicenter Study (TENOR-Trial)," *European Journal of Medical Research*, Vol. 14, 2009, pp. 516-519.

24. S. Pujari, A. Dravid, N. Gupte, K. Joshix, and V. Bele, "Effectiveness and Safety of Generic Fixed-Dose Combination of Tenofovir/Emtricitabine/Efavirenz in HIV-1-Infected Patients in Western India," *Journal of International AIDS Society*, Vol. 10, 2008, pp. 196.
25. R. Ter Heine, A. D. R. Huitema, R. S. Jansen, P. H. M. Smits, E. C. M. van Gorp, J. F. P. Wagenaar, J. H. Beijnen, and J. W. Mulder, "Prolonged exposure to tenofovir monotherapy 1 month after treatment discontinuation because of tenofovir-related renal failure," *Antiviral Therapy*, Vol. 14, No. 2, 2009, pp. 299-301.
26. J. M. Irizarry-Alvarado, J. P. Dwyer, L. M. Brumble, S. Alvarez, and J. C. Mendez, "Proximal tubular dysfunction associated with tenofovir and didanosine causing Fanconi syndrome and diabetes insipidus: a report of 3 cases," *AIDS Read*, Vol. 19, 2009, pp. 114-121.
27. S. Rodriguez-Novoa, P. Labarga, and V. Soriano, "Predictors of kidney tubular dysfunction in HIV-infected patients treated with tenofovir: a pharmacogenetic study," *Clinical Infectious Diseases*, Vol. 48, 2009, pp. e108-e116.
28. I. Gilead Sciences, "**Product Monograph: Tenofovir disoproxil fumarate (Viread)**," 2012, http://www.gilead.ca/pdf/ca/viread_pm_english.pdf [cited 2 October 2012].
29. E. D. Deeks and C. M. Perry, "Efavirenz/Emtricitabine/Tenofovir Disoproxil Fumarate Single-Tablet Regimen (Atripla (R)) A Review of its Use in the Management of HIV Infection," *Drugs*, Vol. 70, No. 17, 2010, pp. 2315-2338.
30. I. Cassetti, J. V. Madruga, J. M. Suleiman, A. Etzel, L. Zhong, A. K. Cheng, and J. Enejosa, "The safety and efficacy of tenofovir DF in combination with lamivudine and efavirenz through 6 years in antiretroviral-naive HIV-1-infected patients," *HIV Clinical Trials*, Vol. 8, 2007, pp. 164-172.
31. B. P. Kearney, J. R. Sayre, J. F. Flaherty, S. S. Chen, S. Kaul, and A. K. Cheng, "Drug-drug and drug-food interactions between tenofovir disoproxil fumarate and didanosine," *Journal of Clinical Pharmacology*, Vol. 45, No. 12, 2005, pp. 1360-1367.
32. T. Cihlar, A. S. Ray, and G. Laflamme, "Molecular assessment of the potential for renal drug interactions between tenofovir and HIV protease inhibitors," *Antiviral Therapy*, Vol. 12, 2007, pp. 267-272.
33. A. M. Taburet, C. Piketty, C. Chazallon, I. Vincent, L. Gerard, V. Calvez, F. Clavel, J. P. Aboulker, and P. M. Girard, "Interactions between atazanavir-ritonavir and tenofovir in heavily pretreated human immunodeficiency virus-infected patients," *Antimicrobial Agents and Chemotherapy*, Vol. 48, No. 6, 2004, pp. 2091-2096.
34. M. C. Gagnieu, M. El Barkil, J. M. Livrozet, L. Cotte, P. Mialhes, A. Boibieux, J. Guitton, and M. Tod, "Population Pharmacokinetics of Tenofovir in AIDS Patients," *Journal of Clinical Pharmacology*, Vol. 48, No. 11, 2008, pp. 1282-1288.

35. A. E. Zimmermann, T. Pizzoferrato, J. Bedford, A. Morris, R. Hoffman, and G. Braden, "Tenofovir-associated acute and chronic kidney disease: a case of multiple drug interactions," *Clinical Infectious Diseases*, Vol. 42, 2006, pp. 283-290.
36. W. Stohr, D. Back, D. Dunn, C. Sabin, A. Winston, R. Gilson, D. Pillay, T. Hill, J. Ainsworth, B. Gazzard, C. Leen, L. Bansi, M. Fisher, C. Orkin, J. Anderson, M. Johnson, P. Easterbrook, S. Gibbons, and S. Khoo, "Factors influencing lopinavir and atazanavir plasma concentration," *Journal of Antimicrobial Chemotherapy*, Vol. 65, No. 1, 2010, pp. 129-137.
37. H. Izzedine, V. Launay-Vacher, V. Jullien, G. Aymard, C. Duvivier, and G. Deray, "Pharmacokinetics of tenofovir in haemodialysis," *Nephrology Dialysis Transplantation*, Vol. 18, No. 9, 2003, pp. 1931-1933.
38. S. Benaboud, D. Hirt, O. Launay, E. Pannier, G. Firtion, E. Rey, N. Bouazza, F. Foissac, H. Chappuy, S. Urien, and J. M. Treluyer, "Pregnancy-Related Effects on Tenofovir Pharmacokinetics: a Population Study with 186 Women," *Antimicrobial Agents and Chemotherapy*, Vol. 56, No. 2, 2012, pp. 857-862.
39. L. M. Mofenson and U. P. H. S. T. F. Centers for Disease Control and Prevention, "U.S. Public Health Service Task Force recommendations for use of antiretroviral drugs in pregnant HIV-1-infected women for maternal health and interventions to reduce perinatal HIV-1 transmission in the United States," *MMWR Recommendation Report*, Vol. 51, No. RR-18, 2002, pp. 1-38.
40. D. Nurutdinova, N. F. Onen, E. Hayes, K. Mondy, and E. T. Overton, "Adverse Effects of Tenofovir Use in HIV-Infected Pregnant Women and their Infants," *Annals of Pharmacotherapy*, Vol. 42, No. 11, 2008, pp. 1581-1585.
41. L. Levin, L. Henry-Reid, D. A. Murphy, L. Peralta, M. Sarr, Y. Ma, A. S. Rogers, and Adolescent Medicine HIV/AIDS Research Network, "Incident pregnancy rates in HIV infected and HIV uninfected at-risk adolescents," *Journal of Adolescent Health*, Vol. 29, No. 3 Suppl, 2001, pp. 101-108.
42. D. Hirt, S. Urien, D. K. Ekouevi, E. Rey, E. Arrive, S. Blanche, C. mani-Bosse, E. Nerrienet, G. Gray, M. Kone, S. K. Leang, J. McIntyre, F. Dabis, and J. M. Treluyer, "Population Pharmacokinetics of Tenofovir in HIV-1-Infected Pregnant Women and Their Neonates (ANRS 12109)," *Clinical Pharmacology & Therapeutics*, Vol. 85, No. 2, 2009, pp. 182-189.
43. P. L. Anderson, J. J. Kiser, E. M. Gardner, J. E. Rower, A. Meditz, and R. M. Grant, "Pharmacological considerations for tenofovir and emtricitabine to prevent HIV infection," *Journal of Antimicrobial Chemotherapy*, Vol. 66, No. 2, 2011, pp. 240-250.
44. UNAIDS/WHO, "AIDS Epidemic Update: Special Report on HIV Prevention," 2005.
45. WHO Department of HIV/AIDS and UNAIDS. "Short-term priorities for antiretroviral drug optimization". pp 1-16. 8-8-2011.

46. WHO, "Antiretroviral therapy for HIV infection in adults and adolescents: towards universal access. Recommendations for a public health approach," 2006.
47. WHO/UNAIDS/UNICEF, "Towards Universal Access: Scaling up priority HIV/AIDS interventions in the health sector. Progress report 2009," 2009.
48. WHO. "The strategic use of antiretrovirals to help end the HIV epidemic". pp 1-54. 7-1-2012.
49. WHO Department of HIV/AIDS and UNAIDS. "The treatment 2.0 framework for action: catalysing the next phase of treatment, care and support". pp 1-32. 9-12-2011. WHO.
50. David G.Watson, *Pharmaceutical Analysis*, 2 ed., Elsevier Churchill Livingstone, Glasgow, 2005, pp. 1-373.
51. "The Pharmacopeia of the United States of America". [15], pp 802. 1-1-1955. Rockville, MD, United States Pharmacopeia Convention, Inc. 1-1-2012.
52. "The United States Pharmacopeia". 19th[23rd rev], pp 1206. 1-1-1975. Rockville, MD, The United States Pharmacopeial Convention.
53. John A.Adamovics, *Chromatographic analysis of pharmaceuticals*, 1 ed., Vol. 49, Marcel Dekker, Inc., New York, 1990, pp. 3-627.
54. R.J.Hamilton and P.A.Sewell, *Introduction to high performance liquid chromatography*, 2 ed., Chapman and Hall, New York, 1977, pp. 1-247.
55. Lloyd R.Snyder, Joseph J.Kirkland, and Joseph L.Glajch, *Practical HPLC method development*, 2nd ed., Vol. 1, John Wiley & Sons, Inc. 1997.
56. Loti David King'ori. "The development and assessment of a fixed dose combination tablet of ranitidine and metronidazole.". pp 1-300. 1-1-2011. Grahamstown, South Africa, Rhodes University. 1-1-2012.
57. "British Pharmacopeia". [2], pp 676-690. 1-2-2002. London, British Pharmacopoeia Commission Office.
58. S.Sentenac, C.Fernandez, A.Thuillier, P.Lechat, and G.Aymard, "Sensitive determination of tenofovir in human plasma samples using reversed-phase liquid chromatography," *JOURNAL OF CHROMATOGRAPHY B*, Vol. 793, 2003, pp. 317-324.
59. V.Jullien, J.M.Treluyer, G.Pons, and E.Rey, "Determination of tenofovir in human plasma by high-performance chromatography with spectrofluorimetric detection.," *JOURNAL OF CHROMATOGRAPHY B*, Vol. 785, 2002, pp. 377-381.
60. J. F. Guo, F. H. Meng, L. Li, B. H. Zhong, and Y. M. Zhao, "Development and Validation of an LC/MS/MS Method for the Determination of Tenofovir in Monkey Plasma," *Biological & Pharmaceutical Bulletin*, Vol. 34, No. 6, 2011, pp. 877-882.

61. N Appala Raju and Shabana Begum, "Simultaneous RP-HPLC Method for the Estimation of the Emtricitabine, Tenofovir Disoproxil Fumerate and Efavirenz in Tablet Dosage Forms," 2008, pp. 522-525,
http://rjptonline.org/RJPT_%20Vol1%284%29/50.pdf [cited 7 May 2012].
62. S.Havele and S.Dhaneshwar, "Stress Studies of Tenofovir Disoproxil Fumarate by HPTLC in Bulk Drug and Pharmaceutical Formulation," *Scientific World Journal*, Vol. 2012, No. 1, 2012, pp. 1-6.
63. Center for Drug Evaluation and Research Control. "Validation of Chromatographic methods". 3. 201. Rockville, FDA.
64. M. J. Green, "A Practical guide to Analytical method Validation," *Analytical Chemistry*, Vol. 68, 1996, pp. 305A-309A.
65. Ludwig Huber. "Validation of Analytical Methods and Procedures". 5-3-2012. Rockville, FDA. 5-3-2012.
66. "General Chapter 1225, Validation of compendial methods," *United States Pharmacopeia 30, National Formulary 25*, 2007 ed. The United States Pharmacopeial Convention, Inc., Rockville, Md., USA, 2007.
67. I. Taverniers, M. De Loose, and E. Van Bockstaele, "Trends in quality in the analytical laboratory. II. Analytical method validation and quality assurance," *Trends in Analytical Chemistry*, Vol. 23, No. 8, 2004, pp. 535-552.
68. World Health Organization, *WHO Expert Committee on Specifications for Pharmaceutical Preparations: Fortieth Report*, World Health Organization 2006.
69. D. Barends, J. Dressman, J. Hubbard, H. Junginger, R. Patnaik, J. Polli, and S. Stavchansky, "MULTISOURCE (GENERIC) PHARMACEUTICAL PRODUCTS: GUIDELINES ON REGISTRATION REQUIREMENTS TO ESTABLISH INTERCHANGEABILITY DRAFT REVISION," 2005.
70. European medicines agency. "Validation of Analytical Procedures: Definitions and Methodology Q2 (R1)". 1995. London, European Medicines Agency.
71. "ICH harmonized tripartite guideline - stability testing of new drug substances and products Q1A". R2[R2]. 1-6-2003.
72. Chung Chow Chan, "ANALYTICAL METHOD VALIDATION: PRINCIPLES AND PRACTICES," 2012, http://www.pharmaquality.com/Media/PublicationsArticle/Pgs28-31_ChapterPDF.pdf [cited 3 May 2012].
73. FDA. "FDA ORA laboratory procedure: Laboratory Guide to Method Validation". 1.6, pp 1-19. 1-25-2012. FDA.

74. C. Kumkumian and L. Linda. "Validation of chromatographic methods". pp 1-33. 1-11-1994. Rockville, CDER.
75. G. S. Clarke, "The validation of analytical methods for drug substances and drug products in UK pharmaceutical laboratories," *Journal of Pharmaceutical and Biomedical Analysis*, Vol. 12, No. 5, 1994, pp. 643-652.
76. D. Ashenafi, V. Chintam, D. van Veghel, S. Dragovic, J. Hoogmartens, and E. Adams, "Development of a validated liquid chromatographic method for the determination of related substances and assay of tenofovir disoproxil fumarate," *Journal of Separation Science*, Vol. 33, No. 12, 2010, pp. 1708-1716.
77. S. Jayadev, K. Manikanta, B. S. Sundar, and V. J. Rao, "Simultaneous Estimation of Lamivudine and Tenofovir Disoproxil Fumarate by RP-HPLC in the Pharmaceutical Dosage Form," *Asian Journal of Chemistry*, Vol. 23, No. 4, 2011, pp. 1683-1686.
78. R. Sharma and K. Mehta, "Simultaneous Spectrophotometric Estimation of Tenofovir Disoproxil Fumarate and Lamivudine in Three Component Tablet Formulation Containing Efavirenz," *Indian Journal of Pharmaceutical Sciences*, Vol. 72, No. 4, 2010, pp. 527-530.
79. v. Raghuvver, "A Validated RP-HPLC Method for Estimation of Tenofovir Disoproxil Fumarate in Tablet Dosage Form and its Stress Degradation Studies," *Journal of Pharmacy Research TM (New Journal BioMedRx; Vol 4, No 12 (2011): Review & Research articles*, 2012.
80. V. P. Choudhari, S. R. Parekar, S. G. Chate, P. D. Bharande, R. R. Singh, and B. S. Kuchekar, "Development and Validation of UV-Visible Spectrophotometric Baseline Manipulation Method for Simultaneous Quantitation of Tenofovir Disoproxil Fumarate and Emtricitabine in Pharmaceutical Dosage Form," *Journal of Spectroscopy*, 2013.
81. Jens T. Carstensen, "Preformulation studies," *Modern Pharmaceutics*, edited by Gilbert S Banker and Christopher T Rhodes, 4th ed. Marcel Dekker AG, Wisconsin, 2002, pp. 175-194.
82. L. M. Augsburger and S. W. Hoag, *Pharmaceutical Dosage Forms*, 3 ed., Vol. 1, Informa Health Care, Chicago USA, 2008, pp. 440-470.
83. S. Ahuja and S. Scypinski, *Handbook of Modern Pharmaceutical Analysis*, Vol. 3, Academic Press, London, 2001, pp. 172-173.
84. H. G. Brittain, "Pharmaceutical Preformulation and Formulation," *Pharmaceutical Development & Technology*, Vol. 14, No. 5, 2009, pp. 565.
85. L. Obregon, A. Realpe, and C. Velazquez, "Mixing fo granular materials, part II: Effect of particle size under periodic shear," *Powder Technology*, Vol. 210, 2010, pp. 193-200.

86. K. Prasad and L. Wan, "Measurement of the particle size of tablet excipients with the aid of video recording," *Pharmaceutical research*, Vol. 4, No. 6, 1987, pp. 503-509.
87. H. M. Massaranduba Santos, F. J. Baptista Veiga, M. E. Tavares De Pina, and J. J. M. Simões De Sousa, "Production of pellets by pharmaceutical extrusion and spheronisation, Part I. Evaluation of technological and formulation variables," *Revista Brasileira de Ciências Farmacêuticas/Brazilian Journal of Pharmaceutical Sciences*, Vol. 40, No. 4, 2004, pp. 455-470.
88. J. J. Sousa, A. Sousa, F. Podczeczek, and J. M. Newton, "Factors influencing the physical characteristics of pellets obtained by extrusion-spheronization," *International Journal of Pharmaceutics*, Vol. 232, No. 1-2, 2002, pp. 91-106.
89. R. I. Mahato, "Biopharmaceutical and physiological consideration," *Pharmaceutical Dosage Forms and Drug Delivery*, 2007, pp. 29-48.
90. J. C. Ramirez-Dorronsoro, R. B. Jacko, and D. O. Kildsig, "Chargeability measurement of selected pharmaceutical dry powders to assess their electrostatic charge control capabilities," *AAPS PharmSciTech [electronic resource]*, Vol. 4, No. 7, 2006, pp. E1-E9.
91. H. A. Lieberman, L. Leon, and J. B. Schwartz, *Pharmaceutical Dosage Forms: Tablets*, 2 ed., Vol. 1, Marcel Dekker, New York, 1989.
92. c. Lau, "Preformulation studies," *Separation Science and Technology Handbook of Modern Pharmaceutical Analysis*, edited by Satinder Ahuja and Stephen Scypinski, Volume 3 ed. Academic Press, 2001, pp. 173-233.
93. E. C. Abdullah and D. Geldart, "The use of bulk density measurements as flowability indicators," *Powder Technology*, Vol. 102, No. 2, 1999, pp. 151-165.
94. D. Geldart, E. C. Abdullah, and A. Verlinden, "Characterisation of dry powders," *Powder Technology*, Vol. 190, No. 1, 2009, pp. 70-74.
95. E. Emery, J. Oliver, T. Pugsley, J. Sharma, and J. Zhou, "Flowability of moist pharmaceutical powders," *Powder Technology*, Vol. 189, No. 3, 2009, pp. 409-415.
96. E. Horosanskaia, A. Seidel-Morgenstern, and H. Lorenz, "Investigation of Drug Polymorphism: Case of Artemisinin," *Thermochimica Acta*, No. 0, 2009.
97. U. J. Griesser, M. E. Auer, and A. Burger, "Micro-thermal analysis, FTIR- and Raman-microscopy of (R,S)-proxiphylline crystal forms," *Microchemical Journal*, Vol. 65, No. 3, 2000, pp. 283-292.
98. K. P. Shadangi and K. Mohanty, "Kinetic study and thermal analysis of the pyrolysis of non-edible oilseed powders by thermogravimetric and differential scanning calorimetric analysis," *Renewable Energy*, Vol. 63, No. 0, 2014, pp. 337-344.

99. T. Wang, A. Dorner-Reisel, and E. Müller, "Thermogravimetric and thermokinetic investigation of the dehydroxylation of a hydroxyapatite powder," *Journal of the European Ceramic Society*, Vol. 24, No. 4, 2004, pp. 693-698.
100. C. A. Strydom, Q. I. Roode, and J. H. Potgieter, "Thermogravimetric and X-ray powder diffraction analysis of precipitator dust from a rotating lime kiln," *Cement and Concrete Research*, Vol. 26, No. 8, 1996, pp. 1269-1276.
101. C. Schick, "2.31 - Calorimetry," *Polymer Science: A Comprehensive Reference*, edited by K. Matyjaszewski and M. Müller Elsevier, Amsterdam, 2012, pp. 793-823.
102. G. W. H. Höhne, "High pressure differential scanning calorimetry on polymers," *Thermochimica Acta*, Vol. 332, No. 2, 1999, pp. 115-123.
103. R. +. Sellin, J. M. Clacens, and C. Coutanceau, "A thermogravimetric analysis/mass spectroscopy study of the thermal and chemical stability of carbon in the Pt/C catalytic system," *Carbon*, Vol. 48, No. 8, 2010, pp. 2244-2254.
104. L. Harding, S. Qi, G. Hill, M. Reading, and D. Q. M. Craig, "The development of microthermal analysis and photothermal microspectroscopy as novel approaches to drug excipient compatibility studies," *International Journal of Pharmaceutics*, Vol. 354, No. 1-2, 2008, pp. 149-157.
105. T. Selzer, M. Radau, and J. +. Kreuter, "Use of isothermal heat conduction microcalorimetry to evaluate stability and excipient compatibility of a solid drug," *International Journal of Pharmaceutics*, Vol. 171, No. 2, 1998, pp. 227-241.
106. R. K. Verma and S. Garg, "Selection of excipients for extended release formulations of glipizide through drug-excipient compatibility testing," *Journal of Pharmaceutical and Biomedical Analysis*, Vol. 38, No. 4, 2005, pp. 633-644.
107. B. Tiúá, A. Fuliá, G. Bandur, E. Marian, and D. Tiúá, "Compatibility study between ketoprofen and pharmaceutical excipients used in solid dosage forms," *Journal of Pharmaceutical and Biomedical Analysis*, Vol. 56, No. 2, 2011, pp. 221-227.
108. P. Mura, A. Manderioli, G. Bramanti, S. Furlanetto, and S. Pinzauti, "Utilization of differential scanning calorimetry as a screening technique to determine the compatibility of ketoprofen with excipients," *International Journal of Pharmaceutics*, Vol. 119, No. 1, 1995, pp. 71-79.
109. R. Chadha and S. Bhandari, "Drug excipient compatibility screening Role of thermoanalytical and spectroscopic techniques," *Journal of Pharmaceutical and Biomedical Analysis*, Vol. 87, No. 0, 2014, pp. 82-97.
110. FMC biopolymer and FMC Europe NV. "Material safety data sheet Avicel® PH 102 Microcrystalline Cellulose". 9004-34-6[9004-34-6/9], pp 1-9. 1-31-2008. PA, USA. 1-31-2008.

111. FMC biopolymer and FMC Europe NV. "Material data safety sheet Ac-Di-Sol® SD-711 Crosscarmellose Sodium". 7481-65-7[7481-65-7/10], pp 1-8. 2-5-2005. PA, USA. 2-5-2005.
112. BASF Aktiengesellschaft Fine Chemicals Division. "Soluble polyvinylpyrrolidone (Povidone Ph.Eur, USP, JP) for the pharmaceutical industry". 2[MEMP-030730e-01]. 1-1-2004. Ludwigshafen Germany, BASF. 1-1-2004.
113. Merck, "Material safety data D-sorbitol," Vol. 1, No. 1 2008, pp. 1-15, http://www.chemicalbook.com/ProductMSDSDetailCB7183649_EN.htm [cited 5 August 2012].
114. Gibaldi M, *Biopharmaceutics and clinical pharmacokinetics*, 3 ed., Vol. 1, Lea and Febiger, Philadelphia, 1984.
115. Kaynak MS, Kas SH, and Oner L, "Formulation of controlled release Glipizide pellets using pan coating method," *Hacettepe Univeristy. Journal of Faculty of Pharmacy*, Vol. 1, 2005, pp. 93-106.
116. Ghebre-Sellassie, *Pellets: A general overview. Pharmaceutical Pelletization Technology*, 1 ed., Vol. 1, Marcel Dekker 1989.
117. Shaji J, Chadawar V, and Talwalkar P, "Multiparticulate Drug Delivery System," *The Indian Pharmacist*, Vol. 6, No. 60, 2007, pp. 21-28.
118. Dashora K and Saraf S, "Development of sustained release multicomponent microparticulate system of Diclofenac sodium and Tizanidine hydrochloride," *International Journal of Pharmaceutics*, Vol. 1, 2008, pp. 98-105.
119. Roy P and Shahiwala A, "Review: Multiparticulate formulation approach to pulsatile drug delivery: Current perspectives," *Journal of Controlled release formulations*, Vol. 1, No. 134, 2009, pp. 74-80.
120. Thoma K and Ziegler I, "The pH independent release of fenoldopam from pellets with insoluble film coats," *European Journal of Pharmaceutical Sciences*, Vol. 1, No. 46, 1998, pp. 105-113.
121. Claudio N, Rita C, Elisabetta E, Alberto G, Alessandro S, Carlo V, and Enea M, "Influence of the formulation and process parameters on pellet production by powder layering technique," *AAPS PharmSciTech [electronic resource]*, Vol. 1, No. 2, 2000, pp. 1-12.
122. Melia C, Washington N, and Wilson GC, *Multiparticulate Controlled Release Oral Dosage Forms*, 1 ed., Scottish Academic Press Ltd 1994.
123. Jose S, Dhanya K, Cinu TA, and Aleykutti NA, "Multiparticulate system for colon targeted delivery of ondansetron," *Indian Journal of Pharmaceutical Science*, No. 20, 2010, pp. 58-64.

124. Padhee K, Chowdhary KA, Pattnaik S, Sahoo SK, and Pathak N, "Design and development of Multiple-Unit, Extended release drug delivery system of Verapamil HCl by Pelletization Technique," *International Journal of Drug Development and Research*, Vol. 3, No. 3, 2011, pp. 118-125.
125. Handa AK, Kerudi AV, and Bhalla HL, "Development and evaluation of ethylcellulose coated controlled release pellets," *Indian Journal of Pharmaceutical Science*, Vol. 2, No. 62, 2000, pp. 147-153.
126. Gandhi BR, Badgujar BP, and Kasliwal AV, "Development and *in-vitro* evaluation of multiparticulate system using novel coating material for controlled drug delivery system," *International Journal of Pharmaceutics*, Vol. 3, No. 3, 2011, pp. 96-99.
127. F. Podczeck, S. R. Rahman, and J. M. Newton, "Evaluation of a standardised procedure to assess the shape of pellets using image analysis," *International Journal of Pharmaceutics*, Vol. 192, No. 2, 1999, pp. 123-138.
128. Nakahara. "U.S. Patent". [3.277.520]. 1-10-1996.
129. Conine JW and Hadley HR, "Preparation of small solid pharmaceutical spheres," *Drug Cosmet Ind*, Vol. 1, No. 106, 1970, pp. 38-41.
130. Reynolds AD, "A new technique for the production of spherical particles," *Manufacturing Chemical Aerosols News*, Vol. 1, No. 41, 1970, pp. 40-43.
131. Newton JM, "The preparation of spherical granules by extrusion/spheronization," *STP Pharma*, Vol. 1, No. 6, 1990, pp. 396-398.
132. Ghebre-Sellassie and Martin C, *Pharmaceutical Extrusion technology*, 1 ed., Vol. 1, Marcel Dekker, Inc 2003.
133. Jalal IM, Malinowski HJ, and Smith WE, "Tablet granulations composed of sphericalshaped particles," *Journal of Pharmaceutical science*, Vol. 1, No. 61, 1972, pp. 1466-1468.
134. Hellen L, Yliruusi J, Mercku P, and Kristoffersson E, "Process variables of instant granulator and spheronizer: I. Physical properties of granules, extrudate and pellets," *International Journal of Pharmaceutics*, Vol. 1, No. 96, 1993, pp. 197-204.
135. Ojile JE, Macfarlane CB, and Selkirk AB, "Drug distribution during massing and its effect on dose uniformity in granules," *International Journal of Pharmaceutics*, Vol. 1, No. 10, 1982, pp. 99-107.
136. Kleinebudde P and Linder H, "Experiments with a twin-screw extruder using a single-step granulation/extrusion process," *International Journal of Pharmaceutics*, Vol. 1, No. 94, 1993, pp. 49-58.

137. Erkobini DF, Fiore SA, Wheatley Ta, and Davan T. "The effect of various process and formulation variables on the quality of spheres produced by extrusion/spheronization. Poster presentation". 1-1-1991. AAPS National Meeting. 3-2-2012.
138. Harrison PJ, Newton JM, and Rowe RC, "The characterization of wet powder masses suitable for extrusion/spheronization," *Journal of Pharmaceutics and Pharmacology*, Vol. 1, No. 37, 1985, pp. 686-691.
139. R. Gandhi, C. L. Kaul, and R. Panchagnula, "Extrusion and spheronization in the development of oral controlled- release dosage forms," *Pharmaceutical Science and Technology Today*, Vol. 2, No. 4, 1999, pp. 160-170.
140. O'Connor RE, Holinez J, and Schwartz JB, "Spheronization: I. Processing and evaluation of spheres prepared from commercially available excipients," *American Journal of Pharmacy*, Vol. 1, No. 156, 1984, pp. 80-87.
141. Baert L, Remon JP, Elbers JAC, and Van Bommel EMG, "Comparison between a gravity feed extruder and a twin screw extruder," *International Journal of Pharmaceutics*, Vol. 1, No. 99, 1993, pp. 7-12.
142. Hasznos L, Langer I, and Gyarmathy M, "Some factors influencing pellet characteristics made by an extrusion/spheronization process: Part I. Effects on size characteristics and moisture content decrease of pellets," *Drug Development and Industrial Pharmacy*, Vol. 1, No. 18, 1992, pp. 409-437.
143. Hellen L and Yliruusi J, "Process variables of instant granulator and spheronizer: III. Shape and shape distribution of pellets," *International Journal of Pharmaceutics*, Vol. 1, No. 96, 1993, pp. 217-223.
144. Bataille B, Ligarski K, Jacob M, Thomas C, and Duru C, "Study of the influence of spheronization and drying condition on the physico-mechanical properties of neutral spheroids containing Avicel PH-101 and lactose," *Drug Development and Industrial Pharmacy*, Vol. 1, No. 19, 1993, pp. 653-671.
145. Dyer AM, Khan KA, and Aulton ME, "Effect of the drying method on the mechanical and drug release properties of pellets prepared by extrusion," *Drug Development and Industrial Pharmacy*, Vol. 1, No. 20, 1994, pp. 3045-3068.
146. Newton JM, Chow AK, and Jeewa KB, "The effect of excipient source on spherical granules made by extrusion/spheronization," *Pharmaceutical Development & Technology*, Vol. 1, No. 10, 1992, pp. 52-58.
147. Funck JAB, Schwartz JB, Reilly WJ, and Ghali ES, "Binder effectiveness for beads with high drug levels," *Drug Development and Industrial Pharmacy*, Vol. 1, No. 17, 1991, pp. 1143-1156.

148. Linder H and Kleinebudde P, "Use of powdered cellulose for the production of pellets by extrusion/spheronization," *Journal of Pharmaceutics and Pharmacology*, Vol. 1, No. 46, 1994, pp. 2-7.
149. K. E. Fielden, *Extrusion and Spheronization of Microcrystalline, Cellulose and Lactose Mixtures* 1987.
150. Fielden KE, Newton JM, and Rowe RC, "The influence of lactose particle size on the spheronization of extrudate processed by a ram extruder," *International Journal of Pharmaceutics*, Vol. 1, No. 81, 1992, pp. 205-224.
151. P. Kleinebudde, "Shrinking and swelling properties of pellets containing microcrystalline cellulose and low substituted hydroxypropylcellulose: I. Shrinking properties," *International Journal of Pharmaceutics*, Vol. 109, No. 3, 1994, pp. 209-219.
152. Law MFL and Deast PB, "Use of hydrophilic polymers with microcrystalline cellulose to improve extrusion-spheronization," *European Journal of Pharmaceutics and Biopharmaceutics*, Vol. 1, No. 45, 1998, pp. 57-65.
153. Rowe R and Iles C, "Spheronization systems downsized for research," *Manufacturing Chemistry*, Vol. 1, No. 11, 1995, pp. 35-37.
154. Wan LS, Heng PW, and Liew CV, "Spheronization conditions on shape and size," *International Journal of Pharmaceutics*, Vol. 1, No. 96, 1993, pp. 59-63.
155. Rowe RC, "Spheronization: a novel pill-making process?," *Pharmaceutical Development & Technology*, Vol. 1, No. 6, 1985, pp. 119-123.
156. Harrison PJ, Newton JM, and Rowe RC, "The application of capillary rheometry to the extrusion of wet masses," *Journal of Pharmaceutical science*, Vol. 1, No. 35, 1987, pp. 235-242.
157. W. F. Sakr, M. A. Ibrahim, F. K. Alanazi, and A. A. Sakr, "Upgrading wet granulation monitoring from hand squeeze test to mixing torque rheometry," *Saudi Pharmaceutical Journal*, Vol. 20, No. 1, 2012, pp. 9-19.
158. Hicks DC and Freese HL, "Extrusion and Spheronization Equipment," *Pharmaceutical Pelletization Technology*, edited by Ghebre-Sellassie, 1 ed. Marcel Dekker, New York, 1989, pp. 71-100.
159. Harrison PJ, Newton JM, and Rowe RC, "Flow defects in wet powder masses," *Journal of Pharmacy and Pharmacology*, Vol. 1, No. 37, 1984, pp. 81-83.
160. Rowe RC and Parker MD, "Mixer Torque Rheometry: an update," *Pharmaceutical Development & Technology*, Vol. 1, No. 3, 1994, pp. 74-82.

161. Parker MD, Rowe RC, and Upjohn NG, "Mixer Torque Rheometry: a method of quantifying the consistency of wet granulations," *Pharmaceutical Development & Technology*, Vol. 1, No. 2, 1990, pp. 50-62.
162. M. Fonteyne, A. L. Fussell, J. Vercruysse, C. Vervaet, J. P. Remon, C. Strachan, T. Rades, and B. T. De, "Distribution of binder in granules produced by means of twin screw granulation," *Int.J.Pharm.*, Vol. 462, No. 1-2, 2014, pp. 8-10.
163. Millili GP and Schwartz JB, "The strength of microcrystalline cellulose pellets: the effect of granulating with water/ethanol mixtures," *Drug Development and Industrial Pharmacy*, Vol. 1, No. 16, 1990, pp. 1411-1426.
164. Koo O.M and Heng PW, "The influence of microcrystalline cellulose grade on shape and shape distributions of pellets produced by extrusion-spheronization," *Chemical pharmacy Journal*, Vol. 1, No. 49, 2001, pp. 1383-1387.
165. Aulton M, *Dissolution and solubility*, "Pharmaceutics: the science of dosage form design", 2 ed., Vol. 1, Churchill Livingstone, Edinburgh, 2002, pp. 15-32.
166. P. Costa and J. M. Sousa Lobo, "Modeling and comparison of dissolution profiles," *European Journal of Pharmaceutical Sciences*, Vol. 13, No. 2, 2001, pp. 123-133.
167. FDA and CDER. "Guidance for Industry Immediate Release Solid Oral Dosage Forms Scale-Up and Postapproval Changes: Chemistry, Manufacturing, and Controls, In Vitro Dissolution Testing, and In Vivo Bioequivalence Documentation". 1[5], pp 1-54. 1-11-1995.
168. "Quality by design: new trends from the First Annual National Symposium on Health Care Interior Design," *Hosp.Strategy.Rep.*, Vol. 1, No. 8, 1989, pp. 5-7.
169. S. Adam, D. Suzzi, C. Radeke, and J. G. Khinast, "An integrated Quality by Design (QbD) approach towards design space definition of a blending unit operation by Discrete Element Method (DEM) simulation," *Eur.J.Pharm.Sci.*, Vol. 42, No. 1-2, 2011, pp. 106-115.
170. B. Aksu, B. T. De, S. Folestad, J. Ketolainen, H. Linden, J. A. Lopes, M. M. de, W. Oostra, J. Rantanen, and M. Weimer, "Strategic funding priorities in the pharmaceutical sciences allied to Quality by Design (QbD) and Process Analytical Technology (PAT)," *Eur.J.Pharm.Sci.*, Vol. 47, No. 2, 2012, pp. 402-405.
171. L. L. Chaves, A. C. Vieira, S. H. Reis, B. Sarmiento, and D. C. Ferriera, "Quality By Design: Discussing And Assessing The Solid Dispersions Risk," *Curr.Drug Deliv.*, 2014.
172. A. Baldinger, L. Clerdent, J. Rantanen, M. Yang, and H. Grohgan, "Quality by design approach in the optimization of the spray-drying process," *Pharm.Dev.Technol.*, Vol. 17, No. 4, 2012, pp. 389-397.

173. J. K. de Kruif, J. Khoo, R. Bravo, and M. Kuentz, "Novel quality by design tools for concentrated drug suspensions: surface energy profiling and the fractal concept of flocculation," *J.Pharm.Sci.*, Vol. 102, No. 3, 2013, pp. 994-1007.
174. R. K. Deshmukh and J. B. Naik, "Aceclofenac microspheres: Quality by design approach," *Mater.Sci.Eng C.Mater.Biol.Appl.*, Vol. 36, 2014, pp. 320-328.
175. J. Djuris, D. Medarevic, M. Krstic, Z. Djuric, and S. Ibric, "Application of quality by design concepts in the development of fluidized bed granulation and tableting processes," *J.Pharm.Sci.*, Vol. 102, No. 6, 2013, pp. 1869-1882.
176. J. Huang, C. Goolcharran, and K. Ghosh, "A Quality by Design approach to investigate tablet dissolution shift upon accelerated stability by multivariate methods," *Eur.J.Pharm.Biopharm.*, Vol. 78, No. 1, 2011, pp. 141-150.
177. H. M. Ibrahim, T. A. Ahmed, M. D. Hussain, Z. Rahman, A. M. Samy, A. A. Kaseem, and M. T. Nutan, "Development of meloxicam in situ implant formulation by quality by design principle," *Drug Dev.Ind Pharm.*, Vol. 40, No. 1, 2014, pp. 66-73.
178. J. Kushner, B. A. Langdon, I. Hicks, D. Song, F. Li, L. Kathiria, A. Kane, G. Ranade, and K. Agarwal, "A Quality-by-Design Study for an Immediate-Release Tablet Platform: Examining the Relative Impact of Active Pharmaceutical Ingredient Properties, Processing Methods, and Excipient Variability on Drug Product Quality Attributes," *J.Pharm.Sci.*, 2013.
179. E. A. Abd, A. C. Ward, and J. Glassey, "Response surface methodology for optimising the culture conditions for eicosapentaenoic acid production by marine bacteria," *J.Ind Microbiol.Biotechnol.*, Vol. 40, No. 5, 2013, pp. 477-487.
180. M. Ashengroph, I. Nahvi, and J. Amini, "Application of Taguchi Design and Response Surface Methodology for Improving Conversion of Isoeugenol into Vanillin by Resting Cells of *Psychrobacter* sp. CSW4," *Iran J.Pharm.Res.*, Vol. 12, No. 3, 2013, pp. 411-421.
181. R. Bala, S. Khanna, and P. K. Pawar, "Formulation and optimization of fast dissolving intraoral drug delivery system for clobazam using response surface methodology," *J.Adv.Pharm.Technol.Res.*, Vol. 4, No. 3, 2013, pp. 151-159.
182. J. Batra, D. Beri, and S. Mishra, "Response Surface Methodology Based Optimization of beta-Glucosidase Production from *Pichia pastoris*," *Appl.Biochem.Biotechnol.*, Vol. 172, No. 1, 2014, pp. 380-393.
183. M. Dabhi, M. Gohel, R. Parikh, N. Sheth, and S. Nagori, "Formulation development of ambroxol hydrochloride soft gel with application of statistical experimental design and response surface methodology," *PDA.J.Pharm.Sci.Technol.*, Vol. 65, No. 1, 2011, pp. 20-31.

184. L. B. Delf, M. Jelvehgari, P. Zakeri-Milani, and H. Valizadeh, "Statistical Optimization of Oral Vancomycin-Eudragit RS Nanoparticles Using Response Surface Methodology," *Iran J.Pharm.Res.*, Vol. 11, No. 4, 2012, pp. 1001-1012.
185. S. Dey, S. Pramanik, and A. Malgope, "Formulation and optimization of sustained release Stavudine microspheres using response surface methodology," *ISRN.Pharm.*, Vol. 2011, 2011, pp. 627623.
186. S. S. Dey and K. C. Dora, "Optimization of the production of shrimp waste protein hydrolysate using microbial proteases adopting response surface methodology," *J.Food Sci.Technol.*, Vol. 51, No. 1, 2014, pp. 16-24.
187. S. Dubey, A. Singh, and U. C. Banerjee, "Response surface methodology of nitrilase production by recombinant Escherichia coli," *Braz.J.Microbiol.*, Vol. 42, No. 3, 2011, pp. 1085-1092.
188. "Retraction notice to "Study of the filtration performance of a plain wave fabric filter using response surface methodology" [J. Hazard. Mater. 176 (2010) 559-568]," *J.Hazard.Mater.*, Vol. 182, No. 1-3, 2010, pp. 946.
189. A. A. Elsaid Ali, M. Taher, and F. Mohamed, "Microencapsulation of alpha-mangostin into PLGA microspheres and optimization using response surface methodology intended for pulmonary delivery," *J.Microencapsul.*, Vol. 30, No. 8, 2013, pp. 728-740.
190. F. N. Engmann, Y. Ma, H. Zhang, L. Yu, and N. Deng, "The application of response surface methodology in studying the effect of heat and high hydrostatic pressure on anthocyanins, polyphenol oxidase, and peroxidase of mulberry (*Morus nigra*) juice," *J.Sci.Food Agric.*, 2014.
191. S. Ghanbarzadeh, H. Valizadeh, and P. Zakeri-Milani, "Application of response surface methodology in development of sirolimus liposomes prepared by thin film hydration technique," *Bioimpacts.*, Vol. 3, No. 2, 2013, pp. 75-81.
192. P. C. Giordano, H. D. Martinez, A. A. Iglesias, A. J. Beccaria, and H. C. Goicoechea, "Application of response surface methodology and artificial neural networks for optimization of recombinant *Oryza sativa* non-symbiotic hemoglobin 1 production by *Escherichia coli* in medium containing byproduct glycerol," *Bioresour.Technol.*, Vol. 101, No. 19, 2010, pp. 7537-7544.
193. G. Goswami, S. Chakraborty, S. Chaudhuri, and D. Dutta, "Optimization of process parameters by response surface methodology and kinetic modeling for batch production of canthaxanthin by *Dietzia maris* NIT-D (accession number: HM151403)," *Bioprocess.Biosyst.Eng*, Vol. 35, No. 8, 2012, pp. 1375-1388.
194. N. Hatambeygi, G. Abedi, and M. Talebi, "Method development and validation for optimised separation of salicylic, acetyl salicylic and ascorbic acid in pharmaceutical formulations by hydrophilic interaction chromatography and response surface methodology," *J.Chromatogr.A*, Vol. 1218, No. 35, 2011, pp. 5995-6003.

195. J. Koenig, "Does process excellence handcuff drug development?," *Drug Discov.Today*, Vol. 16, No. 9-10, 2011, pp. 377-381.
196. V. Nekkanti, A. Marwah, and R. Pillai, "Media milling process optimization for manufacture of drug nanoparticles using design of experiments (DOE)," *Drug Dev.Ind Pharm.*, 2013.
197. R. Periasamy and T. Palvannan, "Optimization of laccase production by *Pleurotus ostreatus* IMI 395545 using the Taguchi DOE methodology," *J.Basic Microbiol.*, Vol. 50, No. 6, 2010, pp. 548-556.
198. S. Honary, P. Ebrahimi, and R. Hadianamrei, "Optimization of particle size and encapsulation efficiency of vancomycin nanoparticles by response surface methodology," *Pharm.Dev.Technol.*, Vol. 19, No. 8, 2014, pp. 987-998.
199. J. K. Im, M. K. Kim, and K. D. Zoh, "Optimization of photolysis of diclofenac using a response surface methodology," *Water Sci.Technol.*, Vol. 67, No. 4, 2013, pp. 907-914.
200. P. Kanmani, R. S. Kumar, N. Yuvaraj, K. A. Paari, V. Pattukumar, and V. Arul, "Application of response surface methodology in the optimisation of a growth medium for enhanced natural preservative bacteriocin production by a probiotic bacterium," *Nat.Prod.Res.*, Vol. 26, No. 16, 2012, pp. 1539-1543.
201. S. M. Khamanga and R. B. Walker, "The use of response surface methodology in the evaluation of captopril microparticles manufactured using an oil in oil solvent evaporation technique," *J.Microencapsul.*, Vol. 29, No. 1, 2012, pp. 39-53.
202. S. Kokkinidou and D. G. Peterson, "Response surface methodology as optimization strategy for reduction of reactive carbonyl species in foods by means of phenolic chemistry," *Food Funct.*, Vol. 4, No. 7, 2013, pp. 1093-1104.
203. G. Y. Li, M. Zhong, Z. D. Zhou, Y. D. Zhong, P. Ding, and Y. Huang, "Formulation optimization of chelerythrine loaded O-carboxymethylchitosan microspheres using response surface methodology," *Int.J.Biol.Macromol.*, Vol. 49, No. 5, 2011, pp. 970-978.
204. H. Li, S. Zhou, Y. Sun, and J. Lv, "Application of response surface methodology to the advanced treatment of biologically stabilized landfill leachate using Fenton's reagent," *Waste Manag.*, Vol. 30, No. 11, 2010, pp. 2122-2129.
205. M. V. Ghica, M. G. Albu, L. Popa, and S. Moisescu, "Response surface methodology and Taguchi approach to assess the combined effect of formulation factors on minocycline delivery from collagen sponges," *Pharmazie*, Vol. 68, No. 5, 2013, pp. 340-348.
206. G. Singh, R. S. Pai, and V. K. Devi, "Response surface methodology and process optimization of sustained release pellets using Taguchi orthogonal array design and central composite design," *J.Adv.Pharm.Technol.Res.*, Vol. 3, No. 1, 2012, pp. 30-40.

207. M. S. Venkata and R. M. Venkateswar, "Optimization of critical factors to enhance polyhydroxyalkanoates (PHA) synthesis by mixed culture using Taguchi design of experimental methodology," *Bioresour. Technol.*, Vol. 128, 2013, pp. 409-416.
208. M. S. Venkata, K. Sirisha, R. R. Sreenivasa, and P. N. Sarma, "Bioslurry phase remediation of chlorpyrifos contaminated soil: process evaluation and optimization by Taguchi design of experimental (DOE) methodology," *Ecotoxicol. Environ. Saf.*, Vol. 68, No. 2, 2007, pp. 252-262.
209. S. V. Mohan and P. C. Mouli, "Assessment of aerosol (PM10) and trace elemental interactions by Taguchi experimental design approach," *Ecotoxicol. Environ. Saf.*, Vol. 69, No. 3, 2008, pp. 562-567.
210. H. Assemi, M. Rezapanah, R. Vafaei-Shoushtari, and A. Mehrvar, "Modified artificial diet for rearing of tobacco budworm, *Helicoverpa armigera*, using the Taguchi method and Derringer's desirability function," *J. Insect Sci.*, Vol. 12, 2012, pp. 100.
211. O. Canli, G. E. Tasar, and M. Taskin, "Inulinase production by *Geotrichum candidum* OC-7 using migratory locusts as a new substrate and optimization process with Taguchi DOE," *Toxicol. Ind Health*, Vol. 29, No. 8, 2013, pp. 704-710.
212. M. A. Khan, R. Hamid, M. Ahmad, M. Z. Abdin, and S. Javed, "Optimization of culture media for enhanced chitinase production from a novel strain of *Stenotrophomonas maltophilia* using response surface methodology," *J. Microbiol. Biotechnol.*, Vol. 20, No. 11, 2010, pp. 1597-1602.
213. S. A. Sayyad, B. P. Panda, S. Javed, and M. Ali, "Optimization of nutrient parameters for lovastatin production by *Monascus purpureus* MTCC 369 under submerged fermentation using response surface methodology," *Appl. Microbiol. Biotechnol.*, Vol. 73, No. 5, 2007, pp. 1054-1058.
214. M. M. Zulkali, A. L. Ahmad, and N. H. Norulakmal, "Oryza sativa L. husk as heavy metal adsorbent: optimization with lead as model solution," *Bioresour. Technol.*, Vol. 97, No. 1, 2006, pp. 21-25.
215. J. Ma, R. Guan, X. Chen, Y. Wang, Y. Hao, X. Ye, and M. Liu, "Response surface methodology for the optimization of beta-lactoglobulin nano-liposomes," *Food Funct.*, 2014.
216. Y. Ma, Y. Zhang, S. Zhao, Y. Wang, S. Wang, Y. Zhou, N. Li, H. Xie, W. Yu, Y. Liu, W. Wang, and X. Ma, "Modeling and optimization of membrane preparation conditions of the alginate-based microcapsules with response surface methodology," *J. Biomed. Mater. Res. A*, Vol. 100, No. 4, 2012, pp. 989-998.
217. B. Maiti, A. Rathore, S. Srivastava, M. Shekhawat, and P. Srivastava, "Optimization of process parameters for ethanol production from sugar cane molasses by *Zymomonas mobilis* using response surface methodology and genetic algorithm," *Appl. Microbiol. Biotechnol.*, Vol. 90, No. 1, 2011, pp. 385-395.

218. H. R. Masoumi, M. Basri, A. Kassim, D. K. Abdullah, Y. Abdollahi, S. S. bd Gani, and M. Rezaee, "Statistical optimization of process parameters for lipase-catalyzed synthesis of triethanolamine-based esterquats using response surface methodology in 2-liter bioreactor," *ScientificWorldJournal.*, Vol. 2013, 2013, pp. 962083.
219. A. T. Nair, A. R. Makwana, and M. M. Ahammed, "The use of response surface methodology for modelling and analysis of water and wastewater treatment processes: a review," *Water Sci.Technol.*, Vol. 69, No. 3, 2014, pp. 464-478.
220. P. Paiga and C. erue-Matos, "Response surface methodology applied to SPE for the determination of ibuprofen in various types of water samples," *J.Sep.Sci.*, Vol. 36, No. 19, 2013, pp. 3220-3225.
221. N. Razzaghi-Asl, A. Ebadi, N. Edraki, A. Mehdipour, S. Shahabipour, and R. Miri, "Response surface methodology in docking study of small molecule BACE-1 inhibitors," *J.Mol.Model.*, Vol. 18, No. 10, 2012, pp. 4567-4576.
222. S. Ren, H. Mu, F. Alchaer, A. Chtatou, and A. Mullertz, "Optimization of self nanoemulsifying drug delivery system for poorly water-soluble drug using response surface methodology," *Drug Dev.Ind Pharm.*, Vol. 39, No. 5, 2013, pp. 799-806.
223. F. Monajjemzadeh, H. Hamishehkar, P. Zakeri-Milani, A. Farjami, and H. Valizadeh, "Design and optimization of sustained-release divalproex sodium tablets with response surface methodology," *AAPS PharmSciTech*, Vol. 14, No. 1, 2013, pp. 245-253.
224. I. M. Moorthy and R. Baskar, "Statistical modeling and optimization of alkaline protease production from a newly isolated alkalophilic Bacillus species BGS using response surface methodology and genetic algorithm," *Prep.Biochem.Biotechnol.*, Vol. 43, No. 3, 2013, pp. 293-314.
225. M. H. Muhamad, A. Sheikh, Sr., A. B. Mohamad, R. R. Abdul, and A. A. Hasan Kadhum, "Application of response surface methodology (RSM) for optimisation of COD, NH₃-N and 2,4-DCP removal from recycled paper wastewater in a pilot-scale granular activated carbon sequencing batch biofilm reactor (GAC-SBBR)," *J.Environ.Manage.*, Vol. 121, 2013, pp. 179-190.
226. M. Polak-Berecka, A. Wasko, M. Kordowska-Wiater, Z. Targonski, and A. Kubik-Komar, "Application of response surface methodology to enhancement of biomass production by Lactobacillus rhamnosus E/N," *Braz.J.Microbiol.*, Vol. 42, No. 4, 2011, pp. 1485-1494.
227. M. Rajabi, M. Kamalabadi, M. R. Jamali, J. Zolgharnein, and N. Asanjarani, "Application of response surface methodology for optimization of ionic liquid-based dispersive liquid-liquid microextraction of cadmium from water samples," *Hum.Exp.Toxicol.*, Vol. 32, No. 6, 2013, pp. 620-631.

228. A. Arasteh, M. Habibi-Rezaei, A. Ebrahim-Habibi, and A. A. Moosavi-Movahedi, "Response surface methodology for optimizing the bovine serum albumin fibrillation," *Protein J.*, Vol. 31, No. 6, 2012, pp. 457-465.
229. Q. Y. Zhang, W. W. Zhou, Y. Zhou, X. F. Wang, and J. F. Xu, "Response surface methodology to design a selective co-enrichment broth of *Escherichia coli*, *Salmonella* spp. and *Staphylococcus aureus* for simultaneous detection by multiplex PCR," *Microbiol. Res.*, Vol. 167, No. 7, 2012, pp. 405-412.
230. C. Zhao, Z. Zheng, J. Zhang, D. Wen, and X. Tang, "Adsorption characteristics of ammonium exchange by zeolite and the optimal application in the tertiary treatment of coking wastewater using response surface methodology," *Water Sci. Technol.*, Vol. 67, No. 3, 2013, pp. 619-627.
231. L. C. Zhao, J. Liang, W. Li, K. M. Cheng, X. Xia, X. Deng, and G. L. Yang, "The use of response surface methodology to optimize the ultrasound-assisted extraction of five anthraquinones from *Rheum palmatum* L," *Molecules.*, Vol. 16, No. 7, 2011, pp. 5928-5937.
232. A. F. Fauzee, S. M. Khamanga, and R. B. Walker, "The impact of manufacturing variables on in vitro release of clobetasol 17-propionate from pilot scale cream formulations," *Drug Dev. Ind Pharm.*, 2013.